

**PLEIOTROPIC RELATIONSHIPS AMONG MEASURES OF
BONE MINERAL DENSITY, BONE GEOMETRY, LEAN
MUSCLE MASS AND FAT MASS**

by

Ryan L. Minster

B.S., University of Pittsburgh, 1998

M.S.I.S., University of Pittsburgh, 2003

Submitted to the Graduate Faculty of
the Graduate School of Public Health in partial fulfillment
of the requirements for the degree of
Doctor of Philosophy

University of Pittsburgh

2011

UNIVERSITY OF PITTSBURGH
GRADUATE SCHOOL OF PUBLIC HEALTH

This dissertation was presented

by

Ryan L. Minster

It was defended on

June 10, 2011

and approved by

Candace M. Kammerer, Ph.D.
Associate Professor, Department of Human Genetics
Graduate School of Public Health, University of Pittsburgh

M. Michael Barmada, Ph.D.
Associate Professor, Department of Human Genetics
Graduate School of Public Health, University of Pittsburgh

Robert E. Ferrell, Ph.D.
Professor, Department of Human Genetics
Graduate School of Public Health, University of Pittsburgh

Daniel E. Weeks, Ph.D.
Professor, Departments of Human Genetics & Biostatistics
Graduate School of Public Health, University of Pittsburgh

Joseph M. Zmuda, Ph.D., M.P.H.
Assistant Professor, Departments of Epidemiology & Human Genetics
Graduate School of Public Health, University of Pittsburgh

Dissertation Director: Candace M. Kammerer, Ph.D.
Associate Professor, Department of Human Genetics
Graduate School of Public Health, University of Pittsburgh

Copyright © by Ryan L. Minster

2011

**PLEIOTROPIC RELATIONSHIPS AMONG MEASURES OF BONE MINERAL DENSITY,
BONE GEOMETRY, LEAN MUSCLE MASS AND FAT MASS**

Ryan L. Minster, PhD

University of Pittsburgh, 2011

Osteoporosis, sarcopenia and changes in fat distribution with age increase risk of fractures, affect quality of life, and are of major public health significance. Investigations into the genetic architecture of endophenotypes of these conditions could lead to better prediction of who is at greatest risk as well as revealing targets for therapies to delay disease onset or diminish their effects on afflicted individuals. Covariation among these conditions may be due to pleiotropy, although little is known about the specific genes involved. I explored relationships among twenty-two measures of arm and leg bone mineral density and geometry, arm and leg lean mass and arm and leg fat mass using data from two populations of Afro-Caribbeans from the island of Tobago: a sample of 1,937 unrelated men aged ≥ 40 years and a set of 470 men and women aged ≥ 18 years in seven extended pedigrees (mean family size = 67). I also performed genomewide association (GWA) studies of lumbar spine and femoral neck bone mineral density (BMD) and fractures in an older (aged ≥ 70 years) population of European and African Americans ($n = 1,663$ and $1,139$ respectively). Hierarchical and principal component (PC) analysis revealed three clusters: (1) a “geometry group” that comprises mostly bone geometry traits and lean mass (PC1); (2) a “density group” that comprises mostly BMD traits (PC2); and (3) a “fat mass group” that comprises measures of fat mass (PC3). Estimates of residual heritability ranged from 0.206 to 0.763 ($p < 0.007$ for all traits). Linkage analysis revealed significant evidence ($\text{LOD} > 3.3$) for quantitative trait loci (QTLs) on two chromosomes: 10q for PC1 and tibial periosteal circumference and 21q for PC3 and arm fat mass. GWA analyses of BMD and fractures in European and African Americans revealed several dozen potential candidate loci with suggestive levels of significance ($p \leq 5 \times 10^{-6}$), the most promising of which is *SLC4A7* on

3q24.1, a sodium bicarbonate cotransporter expressed in osteoclasts. Thus, I present evidence for specific QTLs with pleiotropic effects on multiple body composition traits, as well as loci associated with areal BMD and fracture risk. Additional analyses of these regions could reveal genes that jointly influence susceptibility to osteoporosis, sarcopenia and obesity.

Keywords: pleiotropy, osteoporosis, sarcopenia, bone mineral density, fractures, GWAS, linkage analysis.

TABLE OF CONTENTS

PREFACE	xx
1.0 INTRODUCTION	1
1.1 PUBLIC HEALTH SIGNIFICANCE	1
1.2 ENDOPHENOTYPES	3
1.2.1 Measures of bone quality	3
1.2.2 Measures of muscle quality	5
1.2.3 Measures of adiposity	5
1.3 GENETIC EPIDEMIOLOGY OF BONE QUALITY, MUSCLE QUALITY AND ADIPOSIY	6
1.3.1 Heritability, QTLs & Candidate Genes Influencing Bone Quality Traits . . .	6
1.3.2 Heritability, QTLs & Candidate Genes Influencing Muscle Quality Traits .	8
1.3.3 Heritability, QTLs & Candidate Genes Influencing Adiposity Traits	8
1.4 SOURCES OF COVARIATION	9
1.4.1 Developmental & Homeostatic	9
1.4.2 Mechanical	10
1.4.3 Genetic	11
1.5 STUDY APPROACH AND METHODOLOGY	12
1.5.1 Study populations	12
1.5.2 Traits	13
1.5.2.1 <i>Bone, muscle and fat traits</i>	13
1.5.2.2 <i>Covariates</i>	15
1.5.3 Genetic Markers	16

1.5.3.1	<i>Linkage markers</i>	16
1.5.3.2	<i>Association markers</i>	16
1.5.4	Statistical Methods	17
1.5.4.1	<i>Phenotype analyses – Specific Aim 1</i>	17
1.5.4.2	<i>Heritability – Specific Aim 2</i>	19
1.5.4.3	<i>Genomewide linkage analyses – Specific Aim 2</i>	20
1.5.4.4	<i>Genomewide association analyses – Specific Aim 3</i>	21
1.5.4.5	<i>Genomewide association analyses – Specific Aim 4</i>	23
1.6	SPECIFIC AIMS	24
2.0	PHENOTYPE CHARACTERIZATION IN AFRO-CARIBBEAN MEN	26
2.1	INTRODUCTION	26
2.2	METHODS	27
2.2.1	Study Populations	27
2.2.2	Phenotypes	28
2.2.3	Statistical Analyses	28
2.2.4	Genetic Analysis	29
2.3	RESULTS	30
2.3.1	Subject Characteristics	30
2.3.2	Hierarchical Clustering Analysis	33
2.3.3	Principal Component Analysis	33
2.3.4	Heritability	35
2.4	DISCUSSION	42
3.0	GENOMEWIDE LINKAGE STUDY IN AFRO-CARIBBEANS	44
3.1	INTRODUCTION	44
3.2	METHODS	45
3.2.1	Study Population	45
3.2.2	Phenotypes	46
3.2.3	Markers	46
3.2.4	Statistical Analyses	47
3.2.5	Genetic Analysis	47

3.3	RESULTS	48
3.3.1	Subject Characteristics	48
3.3.2	Univariate Linkage Analysis	48
3.3.3	Bivariate Genetic Correlation and Linkage Analyses	49
3.4	DISCUSSION	53
3.4.1	10q26.3–qter	56
3.4.2	21pter–q21.1	56
3.4.3	Other Suggestive QTLs	56
3.4.4	General Conclusion	57
4.0	GENOMEWIDE ASSOCIATION STUDY IN EUROPEAN AMERICANS	58
4.1	INTRODUCTION	58
4.2	METHODS	59
4.2.1	Study Population	59
4.2.2	Bone Mineral Density	59
4.2.3	Fractures	60
4.2.4	Genotyping and Imputation	60
4.2.5	Statistical Analysis	61
	4.2.5.1 <i>Association analysis methods</i>	61
	4.2.5.2 <i>Statistical power</i>	62
	4.2.5.3 <i>Replication and fine mapping</i>	62
4.3	RESULTS	63
4.3.1	Subject Characteristics	63
4.3.2	Genomewide Association Analysis of Bone Mineral Density	63
4.3.3	Genomewide Association Analysis of Fracture Risk	69
4.3.4	Replication of GEFOS Results	73
4.4	DISCUSSION	77
4.4.1	Association with Bone Mineral Density	77
4.4.2	Association with Fracture Incidence	83
4.4.3	Replication of Prior GEFOS Results	84
	4.4.3.1 <i>CTNNB1 (β-catenin)</i>	84

4.4.3.2	<i>ESR1 (estrogen receptor 1)</i>	85
4.4.3.3	<i>TNFRSF11B (tumor necrosis factor receptor superfamily, member 11b; osteoprotegerin)</i>	85
4.4.4	General Conclusions	85
5.0	GENOMEWIDE ASSOCIATION STUDY IN AFRICAN AMERICANS	87
5.1	INTRODUCTION	87
5.2	METHODS	88
5.2.1	Study Population	88
5.2.2	Phenotype Definitions	88
5.2.3	Genotyping and Imputation	89
5.2.4	Statistical Analyses	89
5.2.4.1	<i>Association analysis methods</i>	89
5.2.4.2	<i>Power to detect genomewide association in the HealthABC African American cohort</i>	90
5.2.4.3	<i>Replication and fine mapping</i>	90
5.3	RESULTS	90
5.3.1	Subject Characteristics	90
5.3.2	Genomewide Association Analysis of Bone Mineral Density	92
5.3.3	Replication of Results from European American GWAS	93
5.3.4	Identification of Potential Candidate Genes under Linkage Peaks	98
5.4	DISCUSSION	98
5.4.1	Association with Bone Mineral Density	98
5.4.2	Replication of Potential Candidate Loci from Association Analyses of BMD in European Americans	100
5.4.2.1	<i>SLC4A7 (solute carrier family 4, sodium bicarbonate cotransporter, member 7)</i>	100
5.4.2.2	<i>Identification of QTLs from Linkage Analyses in Afro-Caribbeans</i>	100
5.4.3	General Conclusions	101
6.0	CONCLUSIONS	102
6.1	SUMMARY OF MAJOR RESULTS	103

6.2	STRENGTHS AND LIMITATIONS	105
6.3	FUTURE DIRECTIONS	106
6.3.1	Validation	106
6.3.2	Fine Mapping	106
6.3.3	Functional Assessment	107
6.3.4	Data Mining	108
6.4	PUBLIC HEALTH SIGNIFICANCE	108
	APPENDIX A. ABBREVIATIONS	110
	APPENDIX B. TOBAGO FAMILY HEALTH STUDY PEDIGREES	113
	APPENDIX C. LINKAGE PLOTS	121
	APPENDIX D. QUANTILE–QUANTILE PLOTS	131
	APPENDIX E. MANHATTAN PLOTS	135
	APPENDIX F. SNPS WITH SUGGESTIVE <i>P</i> VALUES	140
	APPENDIX G. LOCUS PLOTS OF BMD IN EUROPEAN AMERICANS	150
	APPENDIX H. LOCUS PLOTS OF FRACTURE RISK IN EUROPEAN AMERICANS	158
	APPENDIX I. LOCUS PLOTS OF 1000 GENOMES REPLICATION ANALYSIS	164
	APPENDIX J. LOCUS PLOTS OF BMD IN AFRICAN AMERICANS	170
	BIBLIOGRAPHY	177

LIST OF TABLES

1.1	Study Populations	13
1.2	Endophenotypes Examined in This Study	14
2.1	Tobago Characteristics	31
2.2	Tobago Phenotypes	32
2.3	Hierarchical Clustering Groups	35
2.4	Tobago Men Principal Components	38
2.5	Tobago Families Heritabilities	40
3.1	Univariate LOD Scores	49
3.2	Genetic Correlations — Lean Muscle and Fat Mass	53
3.3	Bivariate LOD Scores on 21pter–q21.1	54
3.4	Genetic Correlations — PC1	55
4.1	HealthABC Population Characteristics	64
4.2	European American BMD Analyses	65
4.3	BMD Loci – European Americans	68
4.4	European American Fracture Analyses	72
4.5	Fracture Loci – European Americans	75
4.6	Replication Analysis of GEFOS BMD SNPs in HealthABC	76
5.1	HealthABC Population Characteristics	91
5.2	African American BMD Analyses	92
5.3	BMD Loci – African Americans	95
A1	Abbreviations	110
F1	FNBMDB Pooled Hits – European Americans	140

F2	FNBMD Men Hits – European Americans	142
F3	FNBMD Women Hits – European Americans	144
F4	LSBMD Pooled Hits – European Americans	145
F5	LSBMD Men Hits – European Americans	145
F6	LSBMD Women Hits – European Americans	145
F7	All Fx Pooled Hits – European Americans	146
F8	All Fx Men – European Americans	146
F9	All Fx Women – European Americans	146
F10	NV Fx Pooled Hits – European Americans	147
F11	NV Fx Men Hits – European Americans	147
F12	NV Fx Women Hits – European Americans	148
F13	FNBMD Pooled Hits – African Americans	148
F14	LSBMD Pooled Hits – African Americans	149

LIST OF FIGURES

2.1	Phenotypic Correlations in TBHS participants	34
2.2	Phenotypic Correlations in TBHS participants (age \geq 60)	36
2.3	Phenotypic Correlations in TBHS participants (age $<$ 60)	37
2.4	First Three Principal Components of Phenotypes in TBHS participants	39
2.5	Tobago Families Residual Heritabilities	41
3.1	Chromosome 1 Univariate QTL	50
3.2	Chromosome 10 Univariate QTLs	50
3.3	Chromosome 12 Univariate QTLs	51
3.4	Chromosome 17 Univariate QTL	51
3.5	Chromosome 20 Univariate QTL	52
3.6	Chromosome 21 Univariate QTLs	52
3.7	Chromosome 21 Bivariate QTLs	54
4.1	QQ Plot FNBMD Pooled	66
4.2	QQ Plot LSBMD Pooled	66
4.3	Manhattan Plot FNBMD Pooled	67
4.4	Manhattan Plot LSBMD Pooled	67
4.5	Association between FNBMD and HapMap SNPs around <i>rs11717372</i> (3p24.1) . . .	70
4.6	Association between FNBMD and 1000 Genomes SNPs around <i>rs11717372</i> (3p24.1)	71
4.7	QQ Plot All Fractures Pooled	72
4.8	QQ Plot Non-Vert. Fractures Pooled	72
4.9	Manhattan Plot All Fractures Pooled	74
4.10	Manhattan Plot Non-Vertebral Fractures Pooled	74

4.11	Association between LSBMD and 1000 Genomes SNPs around <i>CTNNB1</i> (3p22.1) . . .	78
4.12	Association between FNBMD and 1000 Genomes SNPs around <i>ESR1</i> (6q25.1) . . .	79
4.13	Association between FNBMD and 1000 Genomes SNPs around <i>TNFRSF11B</i> (8q24.12)	80
5.1	QQ Plot FNBMD Pooled	93
5.2	QQ Plot LSBMD Pooled	93
5.3	Manhattan Plot FNBMD Pooled-Gender – African Americans	94
5.4	Manhattan Plot LSBMD Pooled-Gender – African Americans	94
5.5	Association between LSBMD and HapMap SNPs around <i>rs10501203</i> (11p12) . . .	96
5.6	Association between FNBMD and HapMap SNPs around <i>rs11717372</i> (3p24.1) . . .	97
5.7	African American LSBMD – 10q26.3qter	99
B1	Pedigree 1	114
B2	Pedigree 2	115
B3	Pedigree 3	116
B4	Pedigree 4	117
B5	Pedigrees 5 and 7	118
B6	Pedigree 6	119
B7	Pedigree 8	120
C1	Radius Length	121
C2	Tibia Length	121
C3	Arm Lean Muscle Mass	122
C4	Leg Lean Muscle Mass	122
C5	Arm Fat Mass	122
C6	Leg Fat Mass	123
C7	4% Radius Total Area	123
C8	4% Tibia Total Area	123
C9	4% Radius Trabecular Bone Mineral Density	124
C10	4% Tibia Trabecular Bone Mineral Density	124
C11	33% Radius Cortical Area	124
C12	33% Tibia Cortical Area	125
C13	33% Radius Cortical Bone Mineral Density	125

C14	33% Tibia Cortical Bone Mineral Density	125
C15	33% Radius Cortical Thickness	126
C16	33% Tibia Cortical Thickness	126
C17	33% Radius Periosteal Circumference	126
C18	33% Tibia Periosteal Circumference	127
C19	33% Radius Endosteal Circumference	127
C20	33% Tibia Endosteal Circumference	127
C21	66% Total Bone Mineral Density	128
C22	66% Tibia Cortical Bone Mineral Density	128
C23	Principal Component 1	128
C24	Principal Component 2	129
C25	Principal Component 3	129
C26	Principal Component 4	129
C27	Principal Component 5	130
C28	Principal Component 6	130
C29	Principal Component 7	130
D1	QQ Plot FNBMD European American Men	131
D2	QQ Plot FNBMD European American Women	131
D3	QQ Plot LSBMD European Americans Men	132
D4	QQ Plot LSBMD European Americans Women	132
D5	QQ Plot All Fractures European American Men	132
D6	QQ Plot All Fractures European American Women	132
D7	QQ Plot Non-Vertebral Fractures European American Men	133
D8	QQ Plot Non-Vertebral Fractures European American Women	133
D9	QQ Plot FNBMD African American Men	133
D10	QQ Plot FNBMD African American Women	133
D11	QQ Plot LSBMD African American Men	134
D12	QQ Plot LSBMD African American Women	134
E1	Manhattan Plot for FNBMD in European American Men	136
E2	Manhattan Plot for FNBMD in European American Women	136

E3	Manhattan Plot for LSBMD in European American Men	137
E4	Manhattan Plot for LSBMD in European American Women	137
E5	Manhattan Plot for All Fractures in European American Men	138
E6	Manhattan Plot for All Fractures in European American Women	138
E7	Manhattan Plot for Non-Vertebral Fractures in European American Men	139
E8	Manhattan Plot for Non-Vertebral Fractures in European American Women	139
G1	European American BMD – <i>rs2054993</i>	150
G2	European American BMD – <i>rs13010707</i>	150
G3	European American BMD – <i>rs6718108</i>	151
G4	European American BMD – <i>rs11717372</i>	151
G5	European American BMD – <i>rs9813487</i>	151
G6	European American BMD – <i>rs10804984</i>	151
G7	European American BMD – <i>rs2973839</i>	152
G8	European American BMD – <i>rs3909479</i>	152
G9	European American BMD – <i>rs318373</i>	152
G10	European American BMD – <i>rs736004</i>	152
G11	European American BMD – <i>rs1397005</i>	153
G12	European American BMD – <i>rs10954649</i>	153
G13	European American BMD – <i>rs13252590</i>	153
G14	European American BMD – <i>rs12114940</i>	153
G15	European American BMD – <i>rs278530</i>	154
G16	European American BMD – <i>rs12309051</i>	154
G17	European American BMD – <i>rs12578256</i>	154
G18	European American BMD – <i>rs640960</i>	154
G19	European American BMD – <i>rs17382033</i>	155
G20	European American BMD – <i>rs1113590</i>	155
G21	European American BMD – <i>rs16962904</i>	155
G22	European American BMD – <i>rs957029</i>	155
G23	European American BMD – <i>rs11076239</i>	156
G24	European American BMD – <i>rs2962454</i>	156

G25	European American BMD – <i>rs2190800</i>	156
G26	European American BMD – <i>rs8109254</i>	156
G27	European American BMD – <i>rs331360</i>	157
G28	European American BMD – <i>rs11795763</i>	157
H1	European American Fracture Risk – <i>rs7567544</i>	158
H2	European American Fracture Risk – <i>rs7575679</i>	158
H3	European American Fracture Risk – <i>rs9654002</i>	159
H4	European American Fracture Risk – <i>rs6809471</i>	159
H5	European American Fracture Risk – <i>rs6849590</i>	159
H6	European American Fracture Risk – <i>rs17688188</i>	159
H7	European American Fracture Risk – <i>rs9368834</i>	160
H8	European American Fracture Risk – <i>rs2329399</i>	160
H9	European American Fracture Risk – <i>rs288746</i>	160
H10	European American Fracture Risk – <i>rs4840583</i>	160
H11	European American Fracture Risk – <i>rs10096579</i>	161
H12	European American Fracture Risk – <i>rs10979528</i>	161
H13	European American Fracture Risk – <i>rs2296734</i>	161
H14	European American Fracture Risk – <i>rs2607894</i>	161
H15	European American Fracture Risk – <i>rs17100963</i>	162
H16	European American Fracture Risk – <i>rs7164422</i>	162
H17	European American Fracture Risk – <i>rs12955627</i>	162
H18	European American Fracture Risk – <i>rs4073740</i>	162
H19	European American Fracture Risk – <i>rs2983097</i>	163
H20	European American Fracture Risk – <i>rs4893537</i>	163
I1	1000 Genomes – <i>rs7524102</i> (<i>ZBTB40</i>)	164
I2	1000 Genomes – <i>rs1430742</i> (<i>GPR177</i>)	164
I3	1000 Genomes – <i>rs11898505</i> (<i>SPTBN1</i>)	165
I4	1000 Genomes – <i>rs87938</i> (<i>CTNNB1</i>)	165
I5	1000 Genomes – <i>rs1471403</i> (<i>MEPE</i>)	165
I6	1000 Genomes – <i>rs1366594</i> (<i>MEF2C</i>)	165

I7	1000 Genomes – <i>rs2504063 (ESR1)</i>	166
I8	1000 Genomes – <i>rs1524058 (STARD3NL)</i>	166
I9	1000 Genomes – <i>rs7781370 (FLJ42280)</i>	166
I10	1000 Genomes – <i>rs2062377 (TNFRSF11B)</i>	166
I11	1000 Genomes – <i>rs7117858 (SOX6)</i>	167
I12	1000 Genomes – <i>rs16921914 (DCDC5)</i>	167
I13	1000 Genomes – <i>rs7932354 (ARHGAP1)</i>	167
I14	1000 Genomes – <i>rs599083 (LRP5)</i>	167
I15	1000 Genomes – <i>rs2016266 (SP7)</i>	168
I16	1000 Genomes – <i>rs9533090 (AKAP11)</i>	168
I17	1000 Genomes – <i>rs10048146 (FOXL1)</i>	168
I18	1000 Genomes – <i>rs228769 (HDAC5)</i>	168
I19	1000 Genomes – <i>rs9303521 (CRHR1)</i>	169
I20	1000 Genomes – <i>rs884205 (TNFRSF11A)</i>	169
J1	African American BMD – <i>rs2281415</i>	170
J2	African American BMD – <i>rs13408008</i>	170
J3	African American BMD – <i>rs6712733</i>	171
J4	African American BMD – <i>rs10937334</i>	171
J5	African American BMD – <i>rs7794562</i>	171
J6	African American BMD – <i>rs10216608</i>	171
J7	African American BMD – <i>rs16939006</i>	172
J8	African American BMD – <i>rs2279986</i>	172
J9	African American BMD – <i>rs2813457</i>	172
J10	African American BMD – <i>rs12241361</i>	172
J11	African American BMD – <i>rs16935728</i>	173
J12	African American BMD – <i>rs12417203</i>	173
J13	African American BMD – <i>rs11605876</i>	173
J14	African American BMD – <i>rs10501203</i>	173
J15	African American BMD – <i>rs10894988</i>	174
J16	African American BMD – <i>rs2305709</i>	174

J17	African American BMD – <i>rs758641</i>	174
J18	African American BMD – <i>rs17745091</i>	174
J19	African American BMD – <i>rs9898716</i>	175
J20	African American BMD – <i>rs16967627</i>	175
J21	African American BMD – <i>rs12607377</i>	175
J22	African American BMD – <i>rs10412883</i>	175
J23	African American BMD – <i>rs10404733</i>	176
J24	African American BMD – <i>rs2834247</i>	176

PREFACE

This research project could not have been done without the extraordinary support of many people. I am so grateful to everyone who has supported me over the years, and I would like to acknowledge a few in particular.

First I would like to thank the participants, staff, investigators, collaborators and funding sources of the Tobago Bone Health Study; the Tobago Family Health Study; the Dynamics of Health, Aging and Body Composition Study; and the Genetic Factors for Osteoporosis Consortium for allowing me to be a part of these research projects.

I would also like to thank the faculty, staff, students and alumni of the Departments of Human Genetics, Epidemiology and Biostatistics for their insights and companionship. In particular I'd like to acknowledge Ilyas Kamboh, Yeşim Demirci and my colleagues from their labs—especially Purnima Desai Sundar, Qi Chen, Cara Nestlerode, Erin Luedeking-Zimmer, Birgit Suppé, Jessica Figgins, Lauren Burns and Farah Khalifa—who gave me my first opportunity to work in this field thirteen years ago. I would like to recognize Dan Weeks and Anne Newman who have given me the chance to work on their grants and expand my repertoire in human genetics and epidemiology.

I would like to thank my colleagues in the Kammerer lab—Allison Kuipers, John Shaffer, Xiaojing Wang, Hu Li, Ankur Mukherjee, Laura Yerges-Armstrong, Jatinder Singh and Amy Dressen—for their intellectual engagement and camaraderie.

I'm also grateful to Kyu-Ha Kim, Kyōki Roberts and the late Wei Si, special teachers who helped find clarity when I was feeling lost, and to the late Alec Stewart and the University Honors College, who offered me the scholarship seventeen years ago that brought me to the University of Pittsburgh and forever altered the course of my life.

Utmost thanks goes to the members of my dissertation committee: Candy Kammerer, Dan Weeks, Joe Zmuda, Mike Barmada and Bob Ferrell. It has been a pleasure to study with them. My

committee chair and advisor, Candy, has been a tremendous guide through this project, with a kind heart, keen intellect, avid curiosity and plain-spoken frankness that makes her a joy to work with. She is truly a gift to her students.

To my parents, Mike and Karen Minster, who have been with me from my very beginning and have allowed me the crazy freedom to find my own path, I am so grateful. They have always been there, quietly, for me, and I could not be where I am without them.

Finally, I would like to express my gratitude to my husband, Anthony Roscoe. His support, encouragement, patience and love have sustained me throughout this project and throughout my time as a student. I cannot have asked for a better partner on this journey. Where will the next fifteen years take us?

May this work benefit all beings.

1.0 INTRODUCTION

1.1 PUBLIC HEALTH SIGNIFICANCE

Osteoporosis, sarcopenia and changes in body fat distribution are complex, age-related conditions that result from the effects of genes and environmental factors. Osteoporosis is a common degenerative disorder of the skeleton that affects aging women and men worldwide. It is characterized by reduced bone mass and deteriorated bone microarchitecture. In the United States, approximately 4–6 million women and 1–2 million men over the age of 50 (that is, 13%–18% of women over 50 and 3%–6% of men over 50) have osteoporosis. An additional 13–17 million women and 8–13 million men (that is 37%–50% of women and 28%–50% of men) have the associated condition osteopenia, low bone mineral density, which is considered a precursor to osteoporosis [Looker et al. 1997].

The decreased bone mass and degraded bone structure increase the risk of fractures with a concomitant increase in morbidity and mortality. An estimated 2 million fractures were attributed to osteoporosis in 2005, of which nearly 300,000 are fractures of the hip. It is projected that fractures due to this disorder will increase to 3 million per year by 2025 [Burge et al. 2007]. Worldwide, for 2000, the estimated incidence of osteoporotic fractures was 9 million, with 56.2 million people living with fracture-related disability and a total of 5.8 million disability-adjusted life-years lost due to this condition [Johnell and Kanis 2006].

Fractures in the elderly often result in loss of independence and a decline in quality of life; 20% of those who suffer a hip fracture and were ambulatory prior to injury require long-term care post-fracture. Just 15% of hip fracture patients can walk unaided six months post-fracture [National Osteoporosis Foundation 2008]. More than a quarter of hip fracture patients die within a year of injury [van Staa et al. 2001]. The economic burden of treatments is significant. For 2005 the estimated cost

of treating incident fractures in the United States is estimated to be \$16.9 billion and is predicted to rise to \$25.3 billion by 2025 [Burge et al. 2007].

Muscle tissue quality and mass also decline with age. This phenomenon, called sarcopenia, or muscle wasting, has traditionally been defined by low muscle mass, typically greater than two standard deviations (SD; a table of abbreviations can be found in Appendix A) below the young adult mean [Baumgartner et al. 1998]. However, because loss of muscle mass is not strictly equivalent to age-related degeneration in muscle function [Clark and Manini 2008], the definition has been expanded to additionally require low muscle function, as measured by strength or performance, with cutoffs dependent on the clinical tools used to measure them [Cruz-Jentoft et al. 2010]. For instance an individual with a skeletal muscle mass index two standard deviations below the adult mean and a gait speed of ≤ 0.8 m/s would be classified as sarcopenic. This condition affects 19%–23% of women and 24%–27% of men over the age of 64 [Iannuzzi-Sucich et al. 2002; Chien et al. 2008] and 31% and 53% of women and men over the age of 80 [Iannuzzi-Sucich et al. 2002]. Because of the known relationship between bone strength and mechanical stress, sarcopenia may account for part of the age-related reduction in bone mass [Pearson and Lieberman 2004].

The distribution of fat tissue changes with age; in particular fat deposition increases in the skeletal muscle tissue and bone marrow [Kuk et al. 2009]. The increased fat deposition in the muscle tissue is thought to contribute to sarcopenia [Karasik and Kiel 2008] and in the bone marrow to osteoporotic fracture risk [Wehrli et al. 2000]. Visser et al. [2002] found that reduced muscle attenuation—indicative of increased intramuscular fat—was associated with lower leg physical function independently of total body fat and muscle area. Additionally, it has been observed that increases in body mass index (BMI) have been associated with reduced risk of hip fractures [Schott et al. 1998; De Laet et al. 2005] as well as increases in bone mineral density, suggesting that increased adiposity has a protective effect against osteoporosis [Beck et al. 2009]. However, other studies have reported increased risks of limb fractures in obese adults [e.g., Gnudi et al. 2009].

To date, considerable research has been done to identify genetic and environmental factors influencing osteoporosis, sarcopenia and body fat distribution separately. However, our current knowledge of development, as well as results from epidemiological studies, indicate that a common set of genetic and environmental factors may influence all three tissue types (details are described below). Identification of pleiotropic relationships among bone, muscle and fat traits could lead to a

greater understanding of the mechanisms involved in the growth, maintenance, dysregulation and senescence of the musculoskeletal and adipose systems. For example, although osteoporosis can develop as the result of hormonal disorders or prolonged use of glucosteroids, in most cases the bone mass loss and structural deterioration appear to be a component of organismal senescence. The Haversian remodeling that occurs as part of adult bone maintenance is altered as a result of disease, accumulated microtrauma, and decline in muscle input via mechanical loading [Karasik and Kiel 2008]. Studies of the relationships between these systems could reveal insights that lead to the development of new therapies to prevent, delay the onset of or mitigate the effects of osteoporosis, sarcopenia and changes in fat distribution.

Because osteoporosis, sarcopenia and changes in fat distribution are complex, relatively late-onset traits, many studies have been performed using underlying endophenotypes of these conditions, including loss of bone quality, loss of muscle quality and adiposity. An endophenotype is a biological marker, highly associated with an illness or disorder, that could conceivably serve as a intermediate between genotype and gross phenotype. For example, bone mineral density often serves as an endophenotype for osteoporosis. However endophenotypes may also be complex traits to quantify, and there is no one single measure that can completely capture the total complexity. Some of the surrogates for osteoporosis, sarcopenia and age-related changes in fat are briefly explored below.

1.2 ENDOPHENOTYPES

1.2.1 Measures of bone quality

Detection and diagnosis of osteoporosis is usually accomplished by dual-energy x-ray absorptiometry (DXA), which determines bone mineral density (BMD) by measuring the absorption of x-rays by the subject's bones. As BMD increases, so does the absorption of the radiation by the bone tissue. BMD can be measured at various skeletal sites. Hip BMD (right or left proximal femur) is one of the main predictive risk factors for osteoporosis [Black et al. 1992]. The World Health Organization's (WHO) diagnostic criteria for osteoporosis are based upon BMD. The International Society of Clin-

ical Densitometry recommends, as a standard, BMD measurement at the spine and the hip [Leib et al. 2004].

Osteopenia is defined as the condition of having a BMD value between 1 and 2.5 standard deviations (SD) below the mean in young adults; whereas osteoporosis is defined as having a BMD value < 2.5 SD below the reference mean [Kanis et al. 1994; World Health Organization 1994]. DXA BMD measurements can be taken at various sites in the body, and it is unilateral measurement at the hip (right or left proximal femur) that is the standard within the WHO criteria. Most genetic studies of osteoporosis and BMD have been of femoral neck and lumbar spine BMD [e.g., Pocock et al. 1987; Harris et al. 1998; Xiong et al. 2009].

Bone mineral density can also be measured by peripheral quantitative computed tomography (pQCT). pQCT uses multiple cross-sectional x-ray scans to construct a volumetric model of bone mineral density distribution, while DXA measures areal density. Areal BMD can be confounded by bone size, and so tends to be over-estimated in large bones [Carter et al. 1992]. pQCT also enables the dissection of the bone into its trabecular and cortical components (the spongy bone typical of bone ends or epiphyses, and the compact bone typical of the shaft or diaphysis, respectively) and provides measures of bone mineral density and bone mineral content for them. It also provides metrics of bone geometry such as periosteal circumference, endosteal circumference and trabecular and cortical area. Recent studies have begun to explore measurements by this method [e.g., Wang et al. 2007b; Yerges et al. 2009].

Other densitometric measures include speed of sound as measured by quantitative ultrasound (QUS) (at distal radius, diaphyseal tibia, calcaneus), broadband ultrasound attenuation by QUS (at calcaneus) [Karasik et al. 2004; Moayyeri et al. 2009] and bone mineral content as measured by single photon densitometer (at forearm) [Pocock et al. 1987].

Bone geometry can also contribute to bone strength. It is often measured by DXA, and more recently by pQCT. Metrics available from DXA scans include length, width, cross-sectional area, subperiosteal width, buckling ratio, cortical thickness and section modulus of the femoral neck; width, cross-sectional area, subperiosteal width, center of mass, area moment of inertia and section modulus of the femoral shaft; femoral neck–shaft angle; pelvic axis length; and femoral head, calcar and medulla width [Koller et al. 2001; Karasik et al. 2009]. Another measure of bone geometry is

cortical index, the ratio of combined cortical thickness to bone diameter, of metacarpal bones, which can be obtained from x-ray films [Karasik et al. 2000; Ginsburg et al. 2001].

A final common measure of bone quality is the main clinical manifestation of osteoporosis: fracture. Total fractures, wrist fracture and vertebral fractures are often examined in studies, and both fracture prevalence and incidence have been considered [Deng et al. 2001; Stykarsdottir et al. 2008].

Bone quality is a function of bone mineral content and density, macroarchitecture or geometry such as bone angle and cortical thickness and microarchitecture such as lattice structure in the trabecular bone and osteon structure in cortical bone. No particular measure captures the picture of bone quality completely, and methods that incorporate information from multiple assessments of the bone quality could prove fruitful.

1.2.2 Measures of muscle quality

Muscle biopsy is most accurate in assessing sarcopenia and muscle quality, but is not practical for large research studies. Lower leg lean mass as measured by DXA has been considered a reliable surrogate for muscle quality [Visser et al. 1998a; Broadwin et al. 2001; Visser et al. 2002; Huygens et al. 2004; Karasik et al. 2009]. However, it has also been reported that loss of isokinetic knee extensor strength was about three times greater than loss of leg lean mass as measured by DXA in individuals ages 70–79 [Goodpaster et al. 2006], suggesting that mass may not be a complete indicator of muscle strength. Other measures of muscle mass and quality include total lean body mass as assessed by DXA [Goodpaster et al. 2006], thigh muscle cross-sectional area and muscle attenuation (a measure of fat infiltration) as assessed by computed tomography (CT) [Goodpaster et al. 2006], percentage of body mass as assessed by bioelectrical impedance analysis [Broadwin et al. 2001] and specific torque (strength per unit mass) as measured by dynamometer [Goodpaster et al. 2006].

1.2.3 Measures of adiposity

Obesity, or excess body fat, which is not an age-related condition per se, is defined by the body mass index (BMI), the ratio of weight and squared height in metric units, and so BMI is a common substitute for adiposity [Thorleifsson et al. 2008]. An individual is categorized as obese when his

or her BMI ≥ 30 kg/m². Other measures of adiposity found in the literature include obesity as a dichotomous trait [Meyre et al. 2009]; waist–hip ratio; waist circumference [Lindgren et al. 2009]; hip circumference [Polašek et al. 2009]; brachial circumference [Polašek et al. 2009]; total body fat mass as measured by DXA [Hsu et al. 2005]; percentage of fat mass as measured by bioelectric impedance analysis [Broadwin et al. 2001]; intra-abdominal fat as measured by magnetic resonance imaging (MRI); visceral fat area and volume, subcutaneous fat area and volume [Norris et al. 2009], and muscle attenuation (a measure of fat infiltration) as measured by CT [Goodpaster et al. 2006]; and the ratio of visceral to subcutaneous fat area [Norris et al. 2009].

1.3 GENETIC EPIDEMIOLOGY OF BONE QUALITY, MUSCLE QUALITY AND ADIPOSITY

1.3.1 Heritability, Quantitative Trait Loci & Candidate Genes Influencing Bone Quality Traits

Studies of bone mineral density and content, bone geometry and fracture risk have indicated that these traits have large genetic components of the phenotypic variance. In general, heritability of areal BMD ranges from 0.54 to 0.92 across multiple skeletal sites, for men and women and for different ethnic groups [Pocock et al. 1987; Karasik et al. 2004; Wang et al. 2007b]. Similarly, heritability of volumetric BMD ranges from 0.29 to 0.73 [Wang et al. 2007b], and measures of bone geometry range between 0.58 and 0.83 [Koller et al. 2001].

Given the moderate to high heritability of areal BMD and bone geometry traits, many linkage studies using data on sibling pairs and families have been performed and numerous quantitative trait loci (QTLs) have been detected [e.g., Koller et al. 2000, 2001; Deng et al. 2002; Peacock et al. 2005; Shen et al. 2005; Xiong et al. 2006; Demissie et al. 2007]. Two meta-analyses of genomewide linkage studies have been conducted [Lee et al. 2006; Ioannidis et al. 2007], and they reported three putative QTLs on 1p13–q23 [Ioannidis et al. 2007], 9q31–q33 [Ioannidis et al. 2007] and 16pter–p12.3 [Lee et al. 2006]. There has been little consistency among the QTLs identified by the various studies, and these studies have not identified a specific gene or polymorphism that influences bone

quality with one exception: *LRP5* (low density lipoprotein receptor–related protein 5), a gene in the Wnt-signaling pathway [Johnson et al. 1997; Koay et al. 2004; Ferrari et al. 2004]

Many candidate gene association studies have been conducted on bone quality traits to further pinpoint specific involved genes and have produced mixed results. Nonetheless, effects of several candidate genes, such as *LRP5*, *ESR1* (estrogen receptor 1) and *BMP2* (bone morphogenetic protein 2) on bone quality phenotypes have been replicated. Recent meta-analyses of genomewide association studies (GWAS or GWA studies) across multiple populations have both replicated previous candidate genes results, such as *LRP5* [Richards et al. 2008], *ESR1* [Styrkarsdottir et al. 2008], *TNFRSF11B* (tumor necrosis factor receptor superfamily, member 11b; osteoprotegerin) [Styrkarsdottir et al. 2008; Richards et al. 2008] and *TNFSF11* (tumor necrosis factor ligand superfamily, member 11; receptor activator of nuclear factor κ B ligand; or RANKL) [Styrkarsdottir et al. 2008], and expanded the list of potential genes, such as *ADAMTS18* (a disintegrin-like and metallopeptidase domain-containing protein 8) and *TGFBR3* (transforming growth factor, β receptor III) [Xiong et al. 2009], involved in these phenotypes. GWAS performed on five large populations of individuals of European ancestry (total $n = 19,195$) has revealed a total of 20 loci influencing lumbar spine BMD and femoral neck BMD as measured by DXA [Rivadeneira et al. 2009]. Of these 20 loci, seven—*ZBTB40* (zinc finger and bric à brac–tramtrack–broad-complex domain containing 40), *ESR1*, *TNFRSF11B*, *LRP5*, *SP7* (Sp7 transcription factor; osterix; or OSX), *TNFSF11* and *TNFRSF11A* (tumor necrosis factor receptor superfamily member 11a; receptor activator of nuclear factor κ B; or RANK)—were previously identified candidate genes [Styrkarsdottir et al. 2008, 2009; Richards et al. 2008]. Thus the GWA studies have revealed additional molecular pathways that may influence BMD and subsequently, fracture risk.

A more complete accounting of candidate gene results can be found at the Human Genome Epidemiology (HuGE) Navigator (hugenavigator.net) [Yu et al. 2008] or at the National Center for Biotechnology Information's (NCBI) Association Results Browser (www.ncbi.nlm.nih.gov/projects/gapplusprev/sgap_plus.htm). A catalog of genomewide association study results is maintained by the Office of Population Genetics at the National Human Genome Research Institute (NHGRI) at genome.gov/gwastudies. However, neither candidate gene studies nor genomewide association studies have revealed any genes that account for more than a small fraction of the total phenotypic variance.

1.3.2 Heritability, Quantitative Trait Loci & Candidate Genes Influencing Muscle Quality Traits

Lean muscle mass has substantial genetic contributions; the heritability of lean body mass has been estimated to range from 0.6 to 0.8 in Australian female twins [Seeman et al. 1996], and from 0.7 to 0.9 in brothers [Huygens et al. 2004]. Another study, of leg lean mass in Afro-Caribbean men and women revealed a lower heritability of 0.18–0.23 [Prior et al. 2007]. Linkage analyses using twins, nuclear families and sibling pairs have found multiple quantitative trait loci [Arden and Spector 1997; Hsu et al. 2005; Blain et al. 2006; Livshits et al. 2007]. As yet, the genes underlying variation in muscle mass traits remain largely unknown. To date just one genomewide association study of lean mass has been conducted, which produced a promising candidate gene, *TRHR* (thyrotropin-releasing hormone receptor), in a European American discovery sample with replication in two further European American samples and a Han Chinese sample [Liu et al. 2009a].

1.3.3 Heritability, Quantitative Trait Loci & Candidate Genes Influencing Adiposity Traits

The heritabilities of adiposity measures, such as BMI and fat mass have been estimated to be quite high: estimates for BMI range from 0.2 to 0.8 [Maes et al. 1997], and estimates for fat mass range from 0.63 to 0.71 [Hsu et al. 2005]. Myriad genomewide linkage analyses have been performed, such that, by 2005, 253 quantitative trait loci for fat measures have been reported with 52 regions observed in multiple studies. Significant associations with obesity, BMI, body weight, body composition or fat distribution have been reported for 127 candidate genes [Rankinen et al. 2006].

Subsequent whole-genome association studies have replicated several of these genes, such as *PPARG* (peroxisome proliferator-activated receptor γ) [Fox et al. 2007], *ADIPOQ* (adiponectin) [Fox et al. 2007; Ling et al. 2009] and *MC4R* (melanocortin receptor 4) [Loos et al. 2008; Willer et al. 2008; Thorleifsson et al. 2008; Meyre et al. 2009; Heard-Costa et al. 2009]. One novel gene reported by genomewide association studies is *FTO* (*Fat*so homolog or *fat* mass and *obesity*-associated) [Peters et al. 1999], which has been replicated across fifteen genomewide association studies [Frayling et al. 2007; Scuteri et al. 2007; Hinney et al. 2007; Loos et al. 2008; Willer et al. 2008; Thorleifsson et al. 2008; Meyre et al. 2009; Cho et al. 2009; Cotsapas et al. 2009; Heard-Costa et al. 2009; Scherag et al. 2010; Speliotes et al. 2010; Wan et al. 2010; Dorajoo et al. 2011; Wang et al. 2011].

1.4 SOURCES OF COVARIATION

Epidemiological studies have shown that there is correlation between bone-, muscle- and fat-related measures of body composition. As noted above, it has been suggested that obesity may have a protective effect against osteoporosis [Beck et al. 2009]. Indeed, BMI is used in the WHO FRAX algorithm for determining 10-year fracture risk when hip BMD is unavailable. Body weight is considered a strong predictor of bone mass in both men and women [Glauber et al. 1995]. Studies have shown that high body fat and high body mass index are associated with greater muscle mass [Visser et al. 1998a,b] as well as increased fat infiltration into the muscle [Kelley et al. 1991; Ryan and Nicklas 1999]. Finally, a strong, positive correlation between muscle strength and bone mass is well documented [Karasik and Kiel 2008].

There is evidence of ethnic differences in the relationship between fat and muscle traits. A comparison of muscle attenuation in African American and European American women revealed that the African American women had lower muscle attenuation, indicating more fat infiltration. A comparison in men revealed no such difference [Visser et al. 2002].

Both muscle mass and body fat percentage are associated with total body BMD in women, whereas in men, muscle mass but not body fat is positively associated with BMD [Visser et al. 1998b]. In another study, fat mass and BMD were correlated ($r = 0.48$) in premenopausal women, but again not in men [Reid et al. 1992].

There are multiple potential mechanisms behind the covariation in bone, muscle and fat traits. These include coordinated patterns of development, intertwined homeostasis, mechanical effects and, of particular interest here, genetic effects.

1.4.1 Developmental & Homeostatic

The diverse lineages of bone, muscle and fat tissue descend from the same germ layer in embryonic development and from the same multipotent stromal cells—mesenchymal stem cells—during later organismal maintenance. The signaling pathways that allocate the stem cells to osteogenesis, myogenesis and adipogenesis are complex, and it is difficult to conceive of how variation in an element of those pathways would not cause covariant effects. For example, bone morphogenetic protein 2

(BMP2), a member of the transforming growth factor- β super-family, plays a role in the differentiation of the stem cells. Its presence at high levels promotes osteo- or chondrogenesis and inhibits myogenesis; at low levels, it promotes adipogenesis. This control is achieved by regulating the expression of transcription factors such as MyoD and myogenin (muscle), Runx2 (bone) and PPAR γ (fat) [Devaney et al. 2009].

During adult maintenance, the mesenchymal stem cells are present in multiple tissues, such as bone marrow, periosteum, local soft tissues, vasculature and in circulation [Barry and Murphy 2004]. It has been hypothesized that osteoblastogenesis need not solely arise from differentiation of marrow and periosteal stem cells, but could come from other local tissues [Schindeler et al. 2009]. Not only does muscle tissue serve as a potential alternative source of precursor cells, it may improve prognosis in recovery from fracture injuries. In rats, fracture repair is delayed where there is no muscle apposite the fracture site [Utvåg et al. 2002]. Additional evidence of the presence of osteoprogenitors in muscle tissue comes from examination of heterotrophic ossification—the formation of bone within muscle tissue—an aspect of fibrodysplasia ossificans progressiva. This disorder arises from mutation in *ACVR1*, a bone morphogenetic protein receptor, that leads to dysregulation of BMP signaling, such that soft tissue injury results in tissue ossification [Shore et al. 2006; Billings et al. 2007].

In addition to the protective effect of obesity on osteoporosis even in non-weight-bearing bones, evidence of the non-mechanical relationships between bone and fat comes from a study that showed that osteocalcin, an osteoblast-specific protein, can stimulate adiponectin production in adipocytes, which is associated with increased insulin sensitivity [Lee et al. 2007]. Conversely, there is evidence that leptin, produced by fat cells, influences bone growth, size and remodeling [Thomas and Burguera 2002].

1.4.2 Mechanical

Another potential source of trait covariation is mechanical. The mechanostat theory proposes that bone strength adapts primarily in response to muscle load on the bones [Frost 2003]. As muscles grow stronger, they generate more strain, to which the bones respond by growing stronger, above and beyond the usual remodeling. Conversely, in activities such as space flight, when mechanical

strains are minimized, there is profound bone degeneration [Graebe et al. 2004]. It is estimated that 40% of bone strength is due to mechanical use [Frost and Schönau 2000]. So while much of the correlation is likely mechanical, or environmental, the physiological response to these environmental stressors must be regulated by a biological mechanism in bone that could be subject to variation by genetic factors [Karasik and Kiel 2008].

Obesity-induced mechanical loading seems to be a contributing factor in the positive relationship between fat mass and BMD. Indeed, at weight-bearing sites, most of the effect seems to be due to mechanical loading. At non-weight-bearing sites, adiposity is more important, possibly due to metabolic factors [Glauber et al. 1995]. However, the strength of this effect may differ between men and women, and some studies have observed the association in women but not men [Thomas and Burguera 2002].

1.4.3 Genetic

Evidence of a genetic source to muscle, bone and fat covariation abounds, although it is not always consistent [Nguyen et al. 1998]. Substantial genetic correlations have been reported between lean body mass and BMD and bone geometry, with correlations ranging from 0.28 to 0.72 [Sun et al. 2006; Videman et al. 2007]. Genetic correlations between leg lean mass and hip geometry in another study ranged from 0.087 to 0.454 [Karasik et al. 2009]. Potential QTLs influencing pairs of traits have also been identified by bivariate linkage analysis. Analyses have identified loci linked to both leg lean mass and bone geometry [Karasik et al. 2009], lean body mass and BMD [Wang et al. 2007d], body fat mass and BMD (with loci specific to women and to men identified) [Tang et al. 2007], and body fat mass and body lean mass (again with male- and female-specific loci suggested) [Zhao et al. 2008]. There is evidence that variation in at least one gene specifically, *BMP2*, is pleiotropic. Variation in a 3' post-transcriptional regulatory motif of *BMP2* has been associated with effects on subcutaneous fat volume and lean mass in directions consistent with its hypothesized effects on mesenchymal stem cell differentiation [Devaney et al. 2009]. Also, given the allometric demands of the mechanical system, which must maintain the relationship between the size and growth of a component to the size and growth of the organism, it is expected that gross muscle and bone morphology has evolved to covary to keep the system functioning [Churchill 1996].

1.5 STUDY APPROACH AND METHODOLOGY

The overall goal of this project was to assess whether variation in bone, lean mass and fat mass traits are influenced by variation in a similar set of genes and/or environmental factors. To achieve this overall goal, I first determined the phenotypic relationships among these trait categories and derive multivariate endophenotypes within and between categories in a population of African ancestry (the Tobago Bone Health Study). Second, I determined the heritability of these traits and endophenotypes using data on families with African ancestry (the Tobago Family Health Study). Third, I used linkage analyses to determine whether QTLs influence one or more traits among these categories within these families. Finally, I performed GWA studies on two bone traits (lumbar spine and femoral neck BMD) and two measures of fractures in a group of European- and African-ancestry individuals for whom data on BMD, fractures and > 2.6 million genotypes are available. These results were compared and contrasted with each other. Because I was also interested in whether possible genetic and environmental covariation among the trait categories differs between men and women, the GWAS analyses were also performed in men and women separately. A brief discussion of the study populations, the traits, genetic markers and the statistical and genetic methods that were used to address these specific goals are described below.

1.5.1 Study populations

I used data from three study populations: the Tobago Bone Health Study; the Tobago Family Health Study; and the Dynamics of Health, Aging and Body Composition Study. These populations were selected for several reasons: (1) phenotypic and genotypic data were already available; (2) relationships among phenotypes and genotypes could be assessed using a variety of family- and population-based approaches; and (3) potential similarities and differences between ethnic groups could be assessed.

A brief summary of the available populations and the genetic data available for them can be found in Table 1.1.

The Tobago Bone Health Study (TBHS) arose from the collection of DXA and pQCT scans of individuals recruited for the Tobago Prostate Cancer Survey, a longitudinal study of prostate cancer prevalence in Tobagonian men aged 40 years or older. Tobago is one of the two main islands that

Table 1.1: Study Populations

Study	Relationships	Nationality	Ancestry	<i>n</i>		Genotypes
				Women	Men	
Tobago Bone Health	unrelated	Tobago	African	—	1,937	sporadic
Tobago Family Health	7 pedigrees	Tobago	African	284	186	6,000 (linkage panel)
Dynamics of Health, Aging	unrelated	U.S.A.	African	651	488	2.6 million
& Body Composition	unrelated	U.S.A.	European	784	879	3.0 million

make up the Republic of Trinidad and Tobago off the coast of Venezuela in the southern Caribbean. The ancestry of the Tobago population has been estimated to be approximately 94% African, 5% European and 1% Native American [Miljkovic-Gacic et al. 2005]. For this study I examined the data from 1,937 unrelated men of African descent—individuals who report four grandparents of African ancestry.

The unrelated men from TBHS served as potential probands for the Tobago Family Health Study (TFS). Individuals with the largest families were recruited first. In all, seven families of African descent were collected for a total of 470 individuals—284 women and 186 men. Family sizes are 153, 97, 96, 49, 28, 26 and 21 (mean family size = 67.14). Generations per family ranged from four to seven. Reported relationships include 365 parent–offspring, 473 full siblings, 104 grandparent–grandchild, 1,099 avuncular, 89 half-siblings and 1,364 cousins. Pedigrees can be found in Appendix B.

The Dynamics of Health, Aging and Body Composition Study (HealthABC) is a longitudinal study of African American and European American men and women. Data are available for 2,802 individuals—1,139 African Americans and 1,663 European Americans—between the ages of 68 and 80. The individuals were drawn equally from two sites: Pittsburgh, Pennsylvania, and Memphis, Tennessee.

1.5.2 Traits

1.5.2.1 Bone, muscle and fat traits I examined twenty-two phenotypes in this study (Table 1.2). These phenotypes are available for the Tobago Men and the Tobago Families. I analyzed lumbar spine and femoral neck BMD in the HealthABC participants. A few traits related to body composi-

tion, such as body mass index, standing height and total fat mass, were not included in the current analyses because (1) they were highly collinear with another trait, (2) they were a linear modification of one of the traits of interest or (3) they were a trait of which another trait was a component. For example, periosteal circumference and total area are simple linear transformations of each other, so only the circumference was included. On the other hand, tibia length is a component of standing height; therefore the component trait, tibia length, was retained.

Table 1.2: Endophenotypes Examined in This Study

Arm	Leg
Radius length (mm)	Tibia length (mm)
Lean mass (g)	Lean mass (g)
Fat mass (g)	Fat mass (g)
<i>at 4% radius</i>	<i>at 4% tibia</i>
Total area (mm ²)	Total area (mm ²)
Trabecular BMD (mg/cm ³)	Trabecular BMD (mg/cm ³)
<i>at 33% radius</i>	<i>at 33% tibia</i>
Cortical area (mm ²)	Cortical area (mm ²)
Cortical BMD (mg/cm ³)	Cortical BMD (mg/cm ³)
Cortical thickness (mm)	Cortical thickness (mm)
Periosteal circumference (mm)	Periosteal circumference (mm)
Endosteal circumference (mm)	Endosteal circumference (mm)
	<i>at 66% tibia</i>
	Total BMD (mg/cm ³)
	Cortical BMD (mg/cm ³)

For the Tobago participants, the length of the tibia is measured from the medial malleolus to the medial condyle of the tibia, and forearm length was measured from the olecranon to the styloid process of the ulna. Arm and leg lean and fat mass were measured by whole body DXA using a QDR 4500W densitometer (Hologic, Bedford, MA, USA). Scans were analyzed with the software QDR 8.26a. The remaining sixteen traits were determined by pQCT. Single axial tomographic slices of the distal epiphyseal and diaphyseal radius and tibia were scanned using an XCT 2000 densitometer (StraTec Medizintechnik, Pforzheim, Germany) according to standardized measurement and analysis procedures. Measurements were taken at 4% and 33% of the length of the bone proximal to the distal endplate to assess trabecular and cortical bone respectively. Additional measurements were also taken at 66% of the tibia. Image processing was performed using StraTec software version 5.5E. All 4% scans were analyzed using identical parameters for contour-finding trabecular

bone compartments. All 33% scans were analyzed using identical parameters to determine the volumetric BMD of cortical bone compartments.

For HealthABC participants, areal bone mineral density was measured using DXA at the proximal femur and the whole body. Measurements were taken using a QDR 4500A (software version 9.03; Hologic, Bedford, MA, USA). Femoral neck BMD (FNBMD) was derived from the femoral neck subregion of the proximal femur scan, and lumbar spine BMD (LSBMD) was derived from the lumbar spine subregion of the whole body scan. Quality assurance procedures were employed at both study sites to ensure scanner reliability and identical scan protocols. To assess longitudinal performance of the scanners, an anthropometric spine phantom was scanned daily, and a hip phantom, weekly [Cauley et al. 2007].

1.5.2.2 Covariates Demographic characteristics, medical history and lifestyle habits were ascertained by questionnaire at the clinical sites. Subjects were classified as current smokers (yes/no); individuals who had smoked < 100 cigarettes over their lifetime were classified as nonsmokers. Data on alcohol consumption was also obtained by questionnaire (drinks/week). Subjects were asked whether a doctor or other healthcare provider had ever informed them that they had arthritis, diabetes, hypertension or cardiovascular disease. Hypertension was defined as a diastolic blood pressure exceeding 90 mmHg, systolic blood pressure exceeding 140 mmHg or currently taking blood pressure medication. Diabetes was defined as fasting glucose level > 126 mg/dl or currently taking diabetes medication.

I initially considered age, age squared, sex, age \times sex, age squared \times sex, current smoking status, current alcohol use, parity, menopause status, vitamin D use, diabetes and arthritis as covariates for the heritability models of the phenotypes from the Tobago Bone Health Study and Tobago Family Study. Covariates were evaluated using variance-components models that take into account the nonindependence of family members. After considering the effect size of each potential covariate in those models, age, age squared and sex were retained to be tested in all models, and menopause status was included in the models of cortical BMD. Age, age squared and sex were screened for inclusion in the model using a retention threshold of $\alpha = 0.1$.

For the analyses of BMD in the HealthABC participants, age, age squared, weight, clinical site and ancestry principal components (PCs) were used as covariates consistent with models employed

by the other studies participating a meta-analysis of FNBMD and LSBMD. For the analyses of fractures in the HealthABC populations, age, age squared, weight, standing height, clinical site and ancestry PCs were included as covariates. Sex was also included as a covariate when fractures in men and women were analyzed together.

1.5.3 Genetic Markers

1.5.3.1 Linkage markers A single-nucleotide polymorphism (SNP) linkage panel of 6,090 SNPs [Infinium HumanLinkage-12 Assay (Illumina)] was genotyped on the TFS participants. This panel covers 93.2% of the genome, and the assays were performed by the University of Pittsburgh Core Genetics Laboratory. We performed quality control measures and excluded SNPs (1) with a call rate $< 90\%$, (2) not in Hardy–Weinberg equilibrium ($p < 0.001$) and (3) with a minor allele frequency < 0.05 . The Markov chain Monte Carlo algorithm as implemented in LOKI [Heath 1997] was employed to calculate the multipoint identity-by-descent (MIBD) estimates, and these MIBDs were used in multipoint linkage analyses (described below). LOKI is unable to process SNP at interval of less than one centimorgan so a subset of 1,516 of these markers at intervals > 1 cM were used to calculate multipoint identity-by-descent (MIBD).

All of the markers that passed the initial quality control procedures were used to verify relationships among the TFS members. Cotterman's k 's, which reflect allele-sharing between individuals, were calculated for every pair of participants using RELPAIR [Boehnke and Cox 1997; Epstein et al. 2000] and compared to the hypothetical allele-sharing for the relationships as reported. Putative erroneous relationships were examined and corrected, and relationships that could not be conclusively categorized were removed.

1.5.3.2 Association markers For all subjects in HealthABC, genotyping of genetic markers was performed by the Center for Inherited Disease Research (CIDR) using the Illumina Human1M-Duo BeadChip system. Samples were removed from the data if the sample failed overall ($< 97\%$ SNPs genotyped), if the chromosome sex did not match the reported sex or if first-degree relatedness was detected using the SNP data. SNPs were removed if the SNP had a minor allele frequency (MAF) $< 1\%$, was called with $< 97\%$ success, or had a Hardy–Weinberg equilibrium (HWE) test p value $<$

10^{-6} . A total of 1,151,215 autosomal SNPs were successfully genotyped in 1,663 European American individuals and were carried forward to imputation.

Imputation was performed using MACH 1.0.16 [Li et al. 2010b] and the HapMap II phased haplotypes [Frazer et al. 2007] as the reference. Genotypes were available for 914,263 SNPs based on the HapMap CEPH (Centre d'Étude du Polymorphisme Humain) reference panel (rel. 22, b36). A total of 2,543,887 genotyped and imputed autosomal SNPs were ultimately available for analysis as part of the "HapMap SNP" set. A total of 40,949 chromosome X SNPs were successfully genotyped in all European Americans subjects. An additional 40,818 SNPs were imputed using a method similar to that used for the autosomes for a total of 81,767 X chromosome SNPs. The chromosome X SNPs were included in the HapMap SNP set for a total of 2,625,654 SNPs. The HapMap imputation was performed by Yongmei Liu and Kurt Lohman of Wake Forest University.

A second set of genotyped and imputed SNPs was prepared from the 1.2 million successfully genotyped SNPs and 1,663 subjects using the 1000 Genomes reference haplotypes (June 2010 release) [Abecasis et al. 2010]. A total of 6,858,264 genotyped and imputed autosomal SNPs were available as part of the "1000 Genomes SNP" set. The 1000 Genomes imputation was performed by Michael Nalls at the National Institutes of Health.

1.5.4 Statistical Methods

1.5.4.1 Phenotype analyses – Specific Aim 1 *Overall questions: What are the phenotypic relationships among measures of bone mineral density and geometry, lean mass and fat mass at multiple skeletal sites? Do these relationships vary by age?*

There are several ways to assess phenotypic relationships among a set of measures. I employed two in my project: hierarchical clustering and principal components analysis. These methods of elucidating phenotype relationships should be performed on samples of unrelated individuals as the strong correlations between family members can introduce excessive covariance that not representative of the population from which the sample is drawn.

Cluster analysis [Tryon 1939] is a method for grouping data into meaningful 'clusters' based upon the structure of the data. The particular type of clustering that I employed to examine structure in the body composition phenotypes is agglomerative hierarchical clustering. Hierarchical clus-

tering organizes the data into a tree structure, or dendrogram, based on similarities between the observations, such that more similar observations are closer together in the dendrogram. The Euclidean distance metric was the pairwise Pearson product-moment correlation coefficient between each pair of traits. The complete linkage (or furthest neighbor) method was used to determine the proximity of the clusters, where the distance d between two elements x and y in clusters \mathcal{A} and \mathcal{B} is $\max\{d(x, y) : x \in \mathcal{A}, y \in \mathcal{B}\}$ [Sørensen 1948; Everitt et al. 2001]. Unsupervised clustering algorithms such as this have the advantage of using the information in the data itself to determine the clusters, rather than potentially biased group assignment by a human [Tan et al. 2005]. However, while this method can elucidate data structure, it does not provide interpretation [Hill and Lewicki 2007]. Complete linkage clustering is useful if the data reflects groups that cluster together in non-elongated clusterings, but is inappropriate if the clusterings are elongated [Hill and Lewicki 2007]. This clustering was accomplished using `hclust()` as implemented in R. The resulting dendrograms were plotted adjacent to heatmaps of the matrix of the pairwise correlations using `heatmap()`. Dendrograms and heatmaps were created and compared for phenotypes from TBHS.

Principal components analysis is a method for orthogonalizing or decorrelating collinear data to elucidate underlying structure among the data. The data's dimensions are recast along new axes using linear combinations such that each of the new dimensions, or principal components, maximally explains a dimension of the variance and is orthogonal to all the other dimensions. The principal components are subsequently ordered by decreasing variance. Those new dimensions with the smallest variances can be excluded, thereby allowing the retention of information from all traits while reducing the number of dimensions. Principal components analysis was performed in R using `prcomp()`, which generates the component loadings and enumerates the component variances. All traits were scaled and centered prior to this analysis. The principal components themselves were generated using `predict()`. Those first n principal components that explain at least 80% of the variance were retained for further analysis. Principal components were generated for the traits from TBHS. The principal components for TFS, used in heritability and linkage analyses, were generated using the TFS phenotypes and the TBHS loadings.

1.5.4.2 Heritability – Specific Aim 2 Overall questions: What are the genetic relationships among measures of bone mineral density and geometry, lean mass and fat mass? Are they heritable? Is there evidence of pleiotropy?

Genetic relationships among the traits were explored using two standard methods of calculating the portions of the variance of the traits and covariance between the traits that is genetic: heritability and genetic correlation, respectively.

Heritability (h^2) is the fraction of the phenotypic variance that is genetic ($h^2 = \sigma_G^2/\sigma_P^2$). The residual heritability (h_r^2) is the portion of the phenotypic variance, less the variance attributable to known environmental factors (σ_E^2) such as age and sex, that is genetic [$h_r^2 = \sigma_G^2/(\sigma_P^2 - \sigma_E^2)$]. The heritability and residual heritability were estimated by partitioning the phenotypic variance (σ_P^2) into three components: that attributable to additive genetic factors (σ_G^2), that attributable to known environmental factors (σ_E^2) and that attributable to unknown genetic and environmental factors. The additive genetic variance is estimated using the kinships of the individuals in the pedigrees and the variance between them. The statistical significance of the covariates and heritabilities is calculated using the likelihood ratio test, comparing models with and without the parameter in question. A threshold of $\alpha = 0.1$ was used to determine which covariates to retain in the model. The heritability analysis was accomplished using SOLAR 4.2.0 [Almasy and Blangero 1998a]. Potential covariates were assessed based on previous evidence of their involvement [Wang et al. 2007c]. Age, age squared, sex, sex \times age, sex \times age squared, smoking status, alcohol consumption, pregnancy status, menopause status, vitamin D supplement use, diabetes status and arthritis status were considered initially as known environmental factors in the analysis. The variance due to known environmental factors was compared in models with and without covariates which may be subject to pleiotropy with the study phenotypes; this allowed assessment of their impact on the model. Heritabilities were calculated using the traits and pedigrees from TFS.

High heritabilities in each of two traits and a high degree of phenotypic correlation do not necessarily mean that a high degree of genetic correlation is also present [Chen et al. 2009]. However, genetic correlation can be derived from a decomposition of the phenotypic correlation (ρ_P) into genetic (ρ_G) and environmental (ρ_E) components. The relationship between ρ_P , ρ_G and ρ_E is given by

$$\rho_P = \rho_G \sqrt{h_{r1}^2} \sqrt{h_{r2}^2} + \rho_E \sqrt{1 - h_{r1}^2} \sqrt{1 - h_{r2}^2}.$$

This genetic correlation could be due a gene or set of genes affecting both traits, i.e. pleiotropy; similarly the environmental correlation reflects how two phenotypes are co-affected by the same (unmeasured) environmental factors. As with heritability, the genetic correlations are estimated using the kinships of the individuals and the variance–covariances between them.

Heritabilities and genetic correlations have been traditionally been estimated using family data because the relationships between the individuals of whom the observations are taken are known. However, some recent studies have indicated that given the recent plethora of marker information available on individuals in a population, examination of the shared markers can illuminate distant relationships among them and so allow calculation of these statistics in “unrelated” individuals or even facilitating the construction of pedigrees [Lee et al. 2008; Purcell et al. 2009; Riester et al. 2009].

1.5.4.3 Genomewide linkage analyses – Specific Aim 2 *Overall questions: Do specific quantitative trait loci influence individual or joint measures of bone mineral density and geometry, lean mass and fat mass in individuals with African ancestry?*

To explore whether specific genes influenced my phenotypes individually, jointly or both, I conducted genomewide linkage analyses (GWLS). Linkage analysis has been a powerful tool in genetics for many years and is carried out with family data because of the necessity of following transmission of common markers between family members with similar traits. Linkage analysis’ strengths lie in the use of familial relationships and the linkages of transmitted markers with traits. It does not rely on the identity of a specific allele for detection of a linked locus. It is robust to population substructure because the relationships between the individuals are known and indeed are part of the model. However, it does require the collection of large families, and only regions that are strongly linked to the quantitative trait can be detected, that is, the presumed QTL must have a relatively large effect. When such a region is detected, the genomic region under the linkage peak can contain hundreds of genes. One way to identify potential QTLs is to perform association analyses of genes under the linkage peaks. GWA analyses can also be used as an agnostic approach to identify common polymorphisms that influence traits.

Multipoint linkage analysis, like heritability analysis, uses variance components methods, extending them to include the effect of presumed quantitative trait loci (σ_{QTL}^2) as a component of the genetic variance (σ_G^2). Multipoint identity-by-descent probabilities are estimated for all relative pairs

at every marker using a Markov chain Monte Carlo method [Heath 1997]. The QTL effect is estimated using maximum likelihood methods based on the expected covariance of relative pairs given their identity by descent at an arbitrary chromosomal location in tight linkage with the presumed QTL. The likelihood ratio test is used to assess the linkage model compared to the simpler polygenic model with no variance due to that QTL. The findings are reported as logarithm of the odds (LOD) scores (i.e., the \log_{10} of the likelihood ratio). Inflated LOD scores are adjusted for potential phenotype distribution effects by comparing the scores against an empirical distribution generated for 10,000 simulated, unlinked markers [Blangero et al. 2000]. I took LOD = 2.5 as suggestive evidence of linkage based on linkage analysis of a simulated phenotype. The simulated phenotype was constructed by summing the allele dosage of seven adjacent SNPs on chromosome 3. The resulting QTL had a peak LOD score of 129.2; the peak LOD score outside this region was 1.67.

1.5.4.4 Genomewide association analyses – Specific Aim 3 *Overall questions: Do specific SNPs (or genes) influence two measures of BMD: lumbar spine and femoral neck BMD in populations with European and African ancestry?*

The promise of GWA studies was first proposed by Risch and Merikangas in 1996. A GWAS is a study that tests for association at hundreds of thousands to millions of variant sites across the genome without an *a priori* hypothesis about which genes or other genetic elements may be associated with the trait of interest. The causal sequence variation is not assumed to be in the marker set, but the method requires a set of markers sufficiently dense to capture associations with functional sites not directly tested, via linkage disequilibrium. Unlike linkage analysis, GWAS generally makes use of data from unrelated individuals, thus it is usually easier to collect large samples for association analysis compared to the large pedigrees required for linkage analysis. Furthermore, compared to GWLS, GWAS can detect small effect sizes and can highlight much smaller regions. However, they are susceptible to false positives due to population stratification and false negatives due to allelic heterogeneity. They also require dense coverage. For this reason, and also to compare results from studies assayed using different genotyping platforms, additional SNPs are often imputed [Scheet and Stephens 2006; Burdick et al. 2006; Li et al. 2010b] using reference haplotypes derived from the International HapMap Project [Altshuler et al. 2005; Frazer et al. 2007] or the 1000 Genomes Project [Abecasis et al. 2010].

Because increased SNP density is required to cover the genome, the number of SNPs necessarily increases, and so does the number of statistical tests, with a concomitant increase in the number of false positive results. The number of traits examined can further inflate this false positive rate. For example, I tested ~2.6 million SNPs against two individual traits for a total of ~5 million tests. This should theoretically produce 250,000 statistically significant false positive signals at $\alpha = 0.05$, the traditional threshold for unlikeliness. Methods such as the Bonferroni ($\alpha_p = \alpha_e/n$) or Šidák [$\alpha_p = 1 - (1 - \alpha_e)^{1/n}$] correction can be employed, but are thought to be too conservative given that each SNP test is not completely independent of its neighbors. Such corrections also reduce the power of the study, making true positives more difficult to detect. Permutation tests can simulate the null distribution and so provide empirical likelihoods [Churchill and Doerge 1994], but are computationally expensive. Another problem with genomewide SNP screens is not theoretical, but empirical. The most significantly associated SNPs just seem to have a small effect size. For example, the two strongest associations reported by Xiong et al. [2009] in a genomewide association study of hip and spine BMD account for just 1% of the phenotypic variance. To compensate for this, extremely large samples are required to detect these small effects, and thus, results of my analyses were also contributed to a large consortium, comprising a total of 34,191 individuals with femoral neck and lumbar spine data (the Genetic Factors for Osteoporosis, or GEFOS, Consortium). These consortium results have not yet been published, Therefore, I present results from the HealthABC study, both as an test of previously known candidate genes, and as GWA results, but fully recognize that my sample size is inadequate to detect small effect sizes. In general, GWLS and GWAS methods can be considered as complementary, rather than competitive, as each is capable of detecting a different suite of associated variants and loci.

I performed single SNP–single trait GWA analysis on lumbar spine and femoral neck BMD from a cohort of unrelated individuals with European ancestry using linear regression of quantitative traits on genotyped markers to pinpoint associations between them. I used an additive model, $y = \mu + \beta x + \varepsilon$, wherein y is the quantitative trait of interest, x is the genotype scored as the number of effect alleles, μ is the expected value of the phenotype, ε is the error and β is the additive effect of an allele on the phenotype. For the analysis of the X chromosome in male subjects, the effect allele was coded as 2 if present. All analyses were performed using the statistical software ProbABEL [Aulchenko et al. 2010], which is designed to process imputed genotype probabilities and allele

dosages that are not confined to integer values. Data were available on ~2.6 million assayed and imputed genotypes for individuals of European descent and ~3 million for individuals of African descent.

1.5.4.5 Genomewide association analyses – Specific Aim 4 *Overall questions: Can the identified genes be replicated in another population of similar ancestry? Can they be replicated in a population of different ancestry? Are they similar in men and women? Do any of these loci overlap the linkage signals obtained from the family study?*

Replication is a mainstay of scientific investigation, and is particularly important in my analyses because of the number of tests involved. Replication of results in a comparable population is necessary to begin the process of weeding out those spurious results. The results of genomewide association analyses must be followed up with examination of the positive results in comparable populations. There are two appropriate approaches to replication: exact replication and fine mapping [Clarke et al. 2007]. Exact replication involves examining the selfsame SNP and phenotype in a sample drawn from a similar population. However, such precise replication is often not accomplished, and replication is reported when a neighboring SNP and a related phenotype are found to be associated. Such studies do not mean to intentionally obfuscate the field, but are often the result of limits of available data sets that may not include the identical SNP and phenotype originally reported. The second approach is fine mapping: the examination of other local variation in addition to the initially identified SNP. Such additional examined variation is considered justified because the SNPs chosen for genomewide studies are usually selected for genome coverage. Therefore there may be other variants nearby that could have greater correlation with the phenotype or indeed even be a functional causal influence on the phenotype. In general the exact replication study is more balanced in power, efficiency and cost. Fine mapping may be indicated when the initial finding is weak and the surrounding region has high linkage disequilibrium. However, the identification of an association with a SNP other than the original can be difficult to interpret [Clarke et al. 2007]. Since sequence data from the 1000 Genomes Project became available [Abecasis et al. 2010], some of these concerns have been mitigated. Many researchers impute additional SNPs in the region where the significant GWA result is observed [Scheet and Stephens 2006; Burdick et al. 2006; Li et al. 2010b] and combine results across multiple studies. Analyses of these additional data may facilitate identi-

fication of potentially functional SNPs that influence the trait. However, statistical identification of a potential functional SNP would need to be replicated in another population, and the mechanism would need to be determined using molecular or cell biology methods.

In addition to assessing possible replication of results between the GWLS performed in the TFS and the GWAS of the African Americans and European Americans in HealthABC, I also compared my results with external data resources such as the HuGE Navigator and NHGRI catalog of published genomewide association studies.

1.6 SPECIFIC AIMS

- 1 Examine the phenotypic variation and covariation in bone, muscle and fat traits. **(Chapter 2)**
 - (a) Select bone, muscle and fat phenotypes in the Tobago Bone Health Study and the Tobago Family Health Study based on completeness of data, literature studies and correlation with other traits.
 - (b) Construct composite phenotypes by hierarchical cluster analysis and principal component analysis using data on the Tobago Bone Health Study. Use these techniques to assess the relationships between the various traits. Do the traits fall into a few large groups or many small ones? Do the clusters make sense biologically? Are the relationships revealed by the cluster analysis consistent with those revealed by the principal components? Do the composite traits make sense biologically?
- 2 Determine the effects of covariates and genetic factors on the individual and composite traits using data from the Tobago Family Health Study. **(Chapters 2 and 3)**
 - (a) Determine the heritability of composite traits versus individual traits.
 - (b) Locate QTLs for the individual and composite phenotypes to genetic regions using linkage analysis methods on data from the Tobago Family Health Study. Is there any overlap of QTLs between the composite traits and the individual traits that make them up, or among any of the traits?
 - (c) Determine the genetic correlation among the individual traits.

3 Identify loci (SNPs) associated with variation in two bone traits (lumbar spine and femoral neck BMD) in European Americans using data from the Dynamics of Health, Aging and Body Composition Study by performing (1) agnostic GWA and (2) replication of previously identified loci.

(Chapter 4)

- (a) Test for associations with 2.5 million genotypes (both assayed and imputed) for the autosomes and X chromosome in European Americans.
- (b) Fine map suggestive and significant loci (SNPs) using data imputed from the 1000 Genomes Project.
- (c) Test whether suggestive or significant SNPs affect an important clinical measure of osteoporosis: fracture risk.
- (d) Test whether 20 SNPs (or loci) identified in a previous consortium also influence femoral neck or lumbar spine BMD or fracture risk in HealthABC participants.

4 Determine whether loci influencing lumbar spine and femoral neck BMD in African Americans identified by association analyses are (1) the same as those in European Americans and (2) overlap with QTL regions for bone traits identified in the Tobago Family Health Study. **(Chapter 5)**

- (a) Test for associations with 3-million SNP genotypes (both assayed and imputed) for the autosomes in African Americans and determine whether there is any overlap with the European American results or the linkage results from the Tobago Family Study.
- (b) Test whether 20 SNPs (or loci) identified in a previous consortium study also influence femoral neck or lumbar spine BMD in HealthABC participants.

2.0 PHENOTYPE CHARACTERIZATION IN AFRO-CARIBBEAN MEN

2.1 INTRODUCTION

Common geriatric disorders of body composition such as osteoporosis, sarcopenia and age-related fat redistribution afflict millions of people worldwide. Understanding their etiology and interrelatedness could aid in developing interventions that could delay their onset or mitigate their impact. However, such disorders have complex origins and interact in complicated ways that hinder the ability to capture them with a simple, easily interpretable outcome measure.

Osteoporosis, for instance is often characterized by bone mineral density (BMD). This single trait provides a slice of information, but does not adequately capture the macro- and microarchitecture of the bones nor the variation in BMD at different sites in the skeleton. Characterizing the interrelatedness of a variety of body composition traits and the development of composite endophenotypes could improve our ability to determine risk factors or biomarkers, including genetic markers.

The aim in this chapter is to examine the phenotypic relationships between twenty-two bone-, muscle- and fat-related traits and to construct composite endophenotypes from them in the Tobago Bone Health Study (TBHS) and Tobago Family Health Study (TFS). Additionally, the heritabilities of the individual and composite traits will be determined for the TFS participants.

2.2 METHODS

2.2.1 Study Populations

Populations from two studies were examined in this chapter: the Tobago Bone Health Study (TBHS) and the Tobago Family Health Study (TFS).

TBHS is a follow-up study of the Tobago Prostate Cancer Survey, a collection of approximately 3,170 men over the age of 40 who participated in a population-based prostate cancer screening study on the island of Tobago, Trinidad and Tobago [Bunker et al. 2002]. Approximate 60% of study-eligible men representative of the island's parishes participated in the Cancer Survey between 1998 and 2003. For TBHS, body composition was assessed at a follow-up examination (2004–2007) using peripheral quantitative computed tomography (pQCT) and dual-energy x-ray absorptiometry (DXA). TBHS included 2,031 of the men from the Cancer Survey as well as 451 new participants. In general, this population has low (~6%) non-African admixture [Miljkovic-Gacic et al. 2005]. For the current study, I examined 1,937 unrelated men of African descent—individuals who reported four grandparents of African ancestry.

TFS is a study of genetic and environmental factors influencing a variety of phenotypes, including body composition, lipid profiles, etc., also conducted on Tobago. Probands for TFS were chosen from the Tobago Prostate Cancer Survey [Bunker et al. 2002]. Families of probands with the largest self-reported sibships were recruited first and all family members were recruited without regard to any disease or trait. Data are available on a total of 470 individuals comprising 284 women and 186 men in seven large multigenerational families of African descent of sizes: 153, 97, 96, 49, 28, 26 and 21 (mean family size = 67.14). Genotypes from a 6,000-SNP linkage panel, described below, were used to verify reported familial relationships, and after cleaning a total of 4,206 relative pairs were available for analysis, including 365 parent–offspring, 473 full siblings, 104 grandparent–grandchild, 1,099 avuncular, 89 half-siblings and 1,364 cousins and 712 more distant relationships.

Both studies were approved by the Institutional Review Boards of the University of Pittsburgh and the Tobago Division of Health and Social Sciences and all participants gave written, informed consent.

2.2.2 Phenotypes

Twenty-two bone-, muscle- and fat-related phenotypes were analyzed. As previously described (Section 1.5.2.1) the traits were measured by whole body dual-energy x-ray absorptiometry (DXA) using a QDR 4500W densitometer (Hologic) or peripheral quantitative computed tomography (pQCT) using an XCT 2000 densitometer (Stratec Medizintechnik). Briefly, the muscle- and fat-related traits were measured by DXA and comprised means of the right and left measures of both arm and leg lean mass and fat mass. Two bone-related traits were also obtained using DXA: tibia length and radius length. DXA scans were analyzed using the software QDR 8.26a. Radius length was measured from the olecranon to the styloid process of the ulna. Tibia length was measured from the medial malleolus to the medial condyle of the tibia. The other sixteen bone-related traits were measured by pQCT. Scans were taken at the various sites to assess the different bones types present at each location—primarily trabecular bone at the epiphyseal site and primarily cortical bone at the diaphyseal site. Single axial tomographic slices of the distal epiphyseal (4% of length) and diaphyseal (33% or 66% of length) radius and tibia were scanned according to standardized measurement and analysis procedures. Image processing was performed using Stratec software version 5.5E. The sixteen pQCT bone-related traits included in the current analyses are: total bone area and trabecular BMD at 4% of the radius and of the tibia; cortical area, cortical BMD, cortical thickness, periosteal circumference and endosteal circumference at 33% of the radius and of the tibia; and total BMD and cortical BMD at 66% of the tibia. All of these traits were available in both the TFS population and the TBHS population, and measured in the same manner. I did not include traits, such as body mass index or standing height, that were highly collinear with the chosen traits.

2.2.3 Statistical Analyses

Initial statistical analyses were performed in R 2.11.1 [R Development Core Team 2008]. All measures underwent a series of quality control procedures. I first assessed whether measurements varied across time. Measurements that exhibited correlation with the clinic date were adjusted using locally weighted polynomial regression (LOESS) with the best fit determined by minimizing Akaike's information criterion. Traits adjusted for clinic date in TBHS are tibia length, tibial total area, tibial cortical area, tibial cortical thickness, tibial total density and 66%-tibial cortical density; and in TFS, tibia

length, tibia total density and 66%-tibial cortical density. Trait distributions were subsequently inspected for non-normality, and the relative value of potential transformations were assessed using Shapiro–Wilk tests. Transformations that substantially reduced non-normality were applied. The same transformation per trait was applied in both the TBHS and TFS data sets. Arm fat mass and radial and tibial periosteal circumference were transformed by natural logarithms, whereas leg fat mass and radial and tibial endosteal circumference were transformed by square roots. No other traits were modified. Observations that were greater than four standard deviations (SD) from the mean were classified as outliers and were removed. In the TBHS cohort, an average of three observations (range: 0–13) were removed from each trait. The traits from which more than four data were removed were tibia length ($n = 9$), radial cortical density ($n = 9$), tibial cortical density ($n = 13$), radial cortical thickness ($n = 5$) and 66%-tibial cortical density ($n = 8$). In the TFS cohort, no more than two outlying observations were removed from any trait.

Relationships among traits were explored using hierarchical clustering and principal component analysis methods. Hierarchical clustering was accomplished using the pairwise phenotypic Pearson correlation as the distance metric. The resulting dendrograms were plotted adjacent to heatmaps of the correlations, with the traits ordered according the clustering analysis. Based on previous reports [Sheu et al. 2009], I performed a secondary analysis of the TBHS participants stratified by older and younger than age 60. This cutoff was selected to create two groups of approximately equivalent size.

Next, I developed composite phenotypes using linear combinations of the bone, fat, and lean traits. Principal component analysis of the twenty-two traits in TBHS was performed, and the first n eigenvectors (principal component loadings) that accounted for at least 80% of the total variance that were obtained from TBHS were used to calculate principal components (PCs) for the TFS population. Heritability of these PCs as well as the individual endophenotypes was then estimated using methods described below.

2.2.4 Genetic Analysis

The residual heritabilities of the traits and the principal components were estimated in TFS using SOLAR (Sequential Oligogenic Linkage Analysis Routines) 4.2.0 [Almasy and Blangero 1998b;

Amos 1994]. Covariates were assessed as described in Section 1.5.2.2. Age, age squared, sex and menopause status were screened for significance and included in the model if significant at $\alpha = 0.1$.

2.3 RESULTS

2.3.1 Subject Characteristics

The general characteristics and endophenotypes of the subjects in TBHS and TFS are presented in Tables 2.1 and 2.2. In general, the TBHS participants are older than the TFS members, which reflects each study's design. Body mass index (BMI) is higher among the TBHS men (27.5 kg/m^2) and the TFS men (26.7 kg/m^2), and the women higher still (29.3 kg/m^2). The men in both TBHS and TFS smoked at about the same rate ($\sim 11\%$), but very few women ($\sim 1\%$) smoked. About 30% of the TFS men drank > 1 drink/week, whereas the TBHS men drank less (18.3%). Very few of the women drank more than one drink a week (2.5%). Supplemental calcium and vitamin D use was greatest in the TBHS men, with $\sim 20\%$ and $\sim 30\%$ taking the respective supplements. The TFS Women took vitamin D at about the same rate ($\sim 18\%$), but fewer took supplemental calcium ($\sim 25\%$). The TFS men took the supplements at rates of $\sim 9\%$ and $\sim 8\%$ respectively. Prevalence of hypertension and diabetes was similar in both TFS men and TFS women: hypertension, 30.4% vs 27.4%; diabetes, 13.1% vs 17.6%, respectively. The TFS women had greater rates of cardiovascular disease (CVD) and arthritis compared to the TFS men: CVD, 6.0% vs 3.8%; arthritis, 12.1% vs 7.0%. About 32% of women were post-menopausal.

For nearly all endophenotypes, the TFS and TBHS men have similar values. The TFS men generally have greater radial trabecular BMD values compared to the TBHS men (240.9 mg/cm^3 vs 207.1 mg/cm^3). For fourteen of the twenty-two traits, women had smaller values than both the TFS and TBHS men. However, the TFS women had much greater arm and leg fat mass. Tibia and radial trabecular BMD and tibial total BMD values in the women were larger than the TBHS men but smaller than the TFS men. Women had higher values for cortical BMD at 33% radius and 33% and 66% tibia than both the TBHS men and the TFS men.

Table 2.1: Tobago Characteristics

Characteristic	TFS (<i>n</i> = 470)					
	TBHS (<i>n</i> = 1,937)		Men (<i>n</i> = 186)		Women (<i>n</i> = 284)	
	mean/ <i>n</i>	SD/%	mean/ <i>n</i>	SD/%	mean/ <i>n</i>	SD/%
Age (yr)	58.9	10.4	42.7	17.0	42.7	16.7
Anthropometric						
BMI (kg/m ²)	27.5	4.9	26.7	4.9	29.3	7.0
Waist circumference (cm)	93.1	11.7	90.4	12.2	89.9	16.8
Height (cm)	175.0	6.9	177.3	7.1	166.0	8.9
Weight (kg)	84.4	16.4	84.0	17.2	81.1	19.4
Lifestyle						
Current smoking	203	10.5%	21	11.4%	2	0.7%
Alcohol consumption (> 1 drink/week)	354	18.3%	55	29.6%	7	2.5%
Walking (min/week)	59.7	65.0	53.5	73.0	44.2	109.5
Television viewing time (h/week)	2.4	1.2	16.6	8.5	15.5	7.7
Current milk consumption (times/week)	—	—	3.9	2.8	4.7	2.9
Current caffeine consumption (mg/day)	—	—	90.2	162.3	79.5	83.2
Current suppl. vitamin D use	372	19.2%	18	9.4%	52	18.4%
Current suppl. calcium use	575	29.7%	16	8.3%	70	24.8%
Medical conditions						
Hypertension	—	—	57	30.4%	78	27.4%
Diabetes	318	16.4%	24	13.1%	50	17.6%
Cardiovascular disease	—	—	7	3.8%	17	6.0%
Arthritis	—	—	13	7.0%	34	12.1%
Reproductive						
Current oral contraceptive use	—	—	—	—	94	33.0%
Parity	—	—	—	—	219	77.1%
Postmenopausal	—	—	—	—	91	31.9%

Table 2.2: Tobago Phenotypes

Characteristic	Abbrev.	TBS (<i>n</i> = 1937)		TFS (<i>n</i> = 470)			
		mean	SD	Men (<i>n</i> = 186)		Women (<i>n</i> = 284)	
				mean	SD	mean	SD
Arm							
Radius length (mm)	radLength	308.4	17.3	305.7	17.2	281.3	18.8
Lean mass (g)	armLean	4377.4	775.2	4420.6	767.3	3026.6	714.4
Fat mass (g)	armFat	1091.9	690.3	912.9	668.3	2474.7	1689.0
at 4% radius							
Total area (mm ²)	r4TotArea	345.9	57.9	354.5	61.6	255.1	45.5
Trabecular BMD (mg/cm ³)	r4TrabDen	207.1	49.7	240.9	38.5	209.0	40.4
at 33% radius							
Cortical area (mm ²)	r33CrtArea	116.8	14.5	117.1	13.2	83.4	10.9
Cortical BMD (mg/cm ³)	r33CrtDen	1212.1	25.1	1212.7	22.1	1221.9	26.3
Cortical thickness (mm)	r33CrtThk	3.6	0.4	3.7	0.4	3.2	0.5
Periosteal circumference (mm)	r33PeriC	43.6	3.2	43.4	3.2	36.4	2.9
Endosteal circumference (mm)	r33EndoC	20.8	3.9	20.1	4.0	16.3	4.2
Leg							
Tibia length (mm)	tibLength	416.7	27.6	398.9	28.3	374.8	30.1
Lean mass (g)	legLean	10976.6	1676.5	11391.0	1689.6	8640.6	1627.0
Fat mass (g)	legFat	2897.9	1190.6	2816.3	1431.0	5506.1	1923.6
at 4% tibia							
Total area (mm ²)	t4TotArea	1190.0	148.1	1251.8	153.3	996.3	134.8
Trabecular BMD (mg/cm ³)	t4TrabDen	227.5	41.5	259.9	35.7	241.9	34.2
at 33% tibia							
Cortical area (mm ²)	t33CrtArea	354.3	43.4	346.9	49.5	266.3	40.2
Cortical BMD (mg/cm ³)	t33CrtDen	1177.0	24.9	1181.6	24.2	1186.2	29.9
Cortical thickness (mm)	t33CrtThk	5.7	0.7	5.6	0.7	4.8	0.7
Periosteal circumference (mm)	t33PeriC	80.5	5.4	79.5	6.1	71.3	5.4
Endosteal circumference (mm)	t33EndoC	44.8	7.1	44.3	7.0	41.4	6.8
at 66% tibia							
Total BMD (mg/cm ³)	t66TotDen	652.6	80.1	696.3	78.5	689.0	90.6
Cortical BMD (mg/cm ³)	t66CrtDen	1122.7	27.8	1138.2	24.7	1143.5	33.5

2.3.2 Hierarchical Clustering Analysis

To simultaneously assess relationships among the measures of bone, muscle and fat traits in the arm and leg (these traits were unadjusted for covariates), I performed hierarchical clustering analysis on all twenty-two traits for the TBHS men and obtained a dendrogram and heatmap (Figure 2.1).

As can be seen, two large clusters of traits were identified that can be loosely described as (1) a “geometry group,” that also includes lean mass, and (2) a “density group,” that also includes cortical thickness and endosteal circumference (Table 2.3). Measures of arm and leg fat mass are correlated with lean mass, and so are loosely contained in the “geometry group”, but uncorrelated with the bone traits. Overall, the strongest correlations are between the same trait measured in the arm and leg, for example, tibial and radial cortical thickness. The only exceptions to this arm–leg pairing are the radial endosteal circumference, tibial endosteal circumference and tibial total BMD triad and the three measures of cortical BMD (33% radius and 33% and 66% tibia). The heatmap highlights correlation substructure not visible in the somewhat one-dimensional dendrogram. There are “islands” of correlation between the major clusters, for example, cortical thickness (“density group”) is moderately correlated with cortical area and lean mass (“geometry group”). Additionally endosteal circumference (“density group”) and periosteal circumference (“geometry group”) are correlated.

Hierarchical clustering analysis of the TBHS men stratified into two age groups, those aged 60 years and older and those younger, reveals the same overall pattern (Figures 2.2 and 2.3). There are two notable differences however. Firstly, for both age groups, fat mass sorts out more noticeably into its own cluster. Secondly, among the < 60 men, the correlation between the “density” group traits is less than among the ≥ 60 men and less than in the overall analysis.

2.3.3 Principal Component Analysis

We next performed principal component analyses to develop composite traits that may represent underlying endophenotypic dimensions. The first seven PCs based on the phenotypic correlations among the twenty-two bone, muscle and fat traits account for 79.4% of the total phenotypic variance. The trait loadings (eigenvectors) and cumulative variances (eigenvalues) for the first ten PCs are given in Table 2.4. To further illustrate the contributions of each trait to the eigenvectors, a plot of

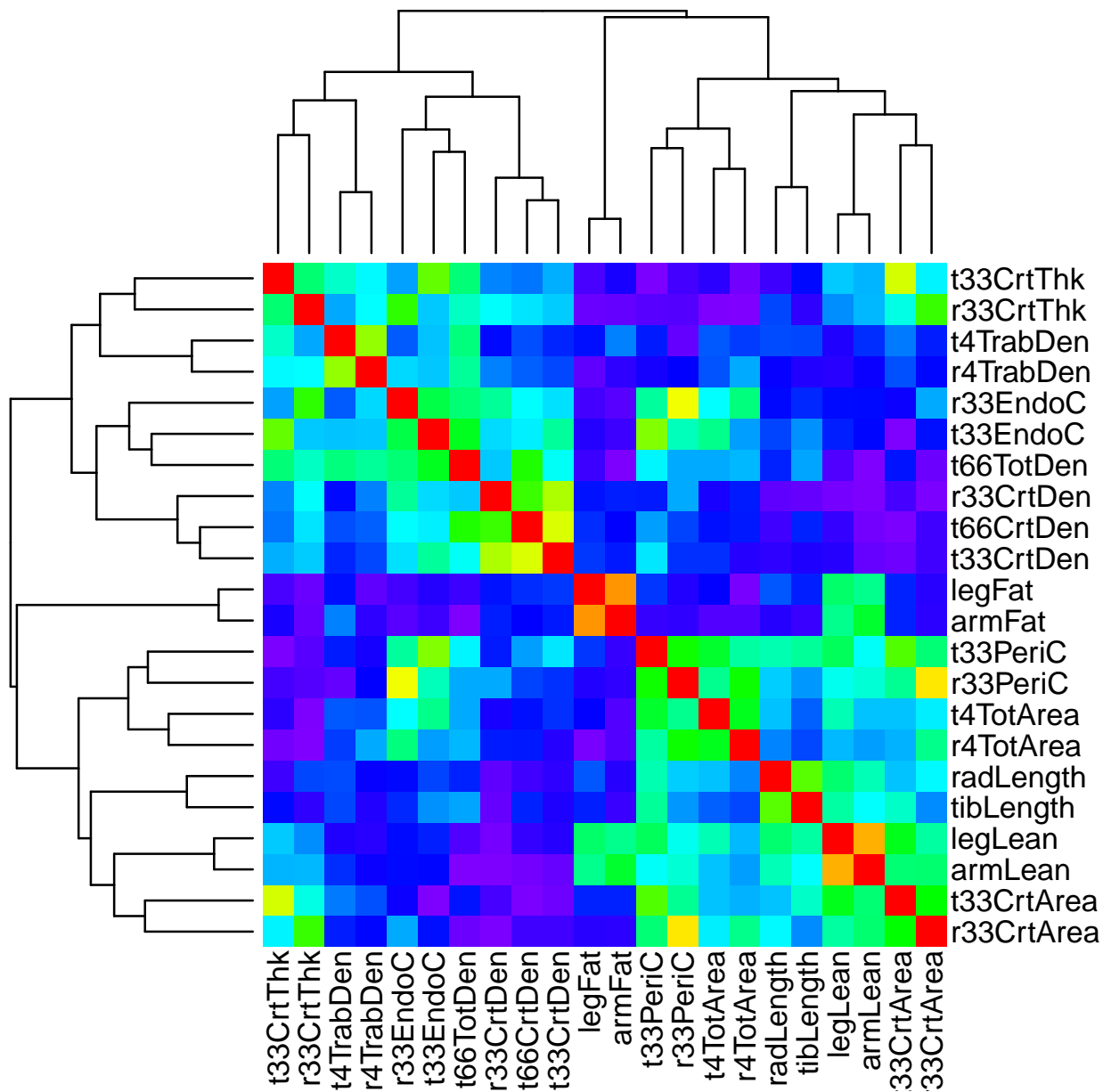


Figure 2.1: Phenotypic Correlations in TBHS participants

The colors indicate the degree of correlation with red equivalent to $r = 1$ and purple, to $r = 0$, so that the greater the correlation the “hotter” the color. Abbreviations for the traits can be found in Table 2.2.

Table 2.3: Hierarchical Clustering Groups

“Density Group”	“Geometry Group”	“Fat Mass Group”
r4TrabDen	r33PeriC	armFat
t4TrabDen	t33PeriC	legFat
r33CrtDen	r4TotArea	
t33CrtDen	t4TotArea	
t66CrtDen	radLength	
t66TotDen	tibLength	
r33CrtThk	r33CrtArea	
t33CrtThk	t33CrtArea	
r33EndoC	armLean	
t33EndoC	legLean	

the first three principal components, with the unsigned loading components of each eigenvector rescaled from 0 to 1, is presented in Figure 2.4.

The PC composite endophenotypes recapitulate many of the relationships among the traits as illustrated by the clustering analysis. For example, PC1 accounts for 26% of the total trait variance and primarily contains contributions from the “geometry” traits, but also includes endosteal circumference. PC2 accounts for 20% of the variance and has large contributions from the “density” traits, but also includes contributions from cortical area (a “geometry” trait). Both arm and leg lean mass measures contribute to both PC1 and PC2, whereas fat mass is the largest contributor to PC3; PC3 accounts for 10% of the variance. PC4–PC7 comprise a mix of traits and each accounts for $\leq 8\%$ of the variance.

2.3.4 Heritability

To determine whether the composite traits derived from phenotypic relationships may represent effects of a common set of genes, I simultaneously estimated heritability and screened for the effects of sex, age, age squared and menopause status. I also analyzed each individual bone-, muscle- and fat-related measure. The results are presented in Table 2.5 and graphically in Figure 2.5. For all traits but 66%-tibia total BMD and PC7, sex was highly significant ($p < 0.0001$). Age and age squared were borderline significant to highly significant for 24 of the 29 analyzed traits. Menopause status

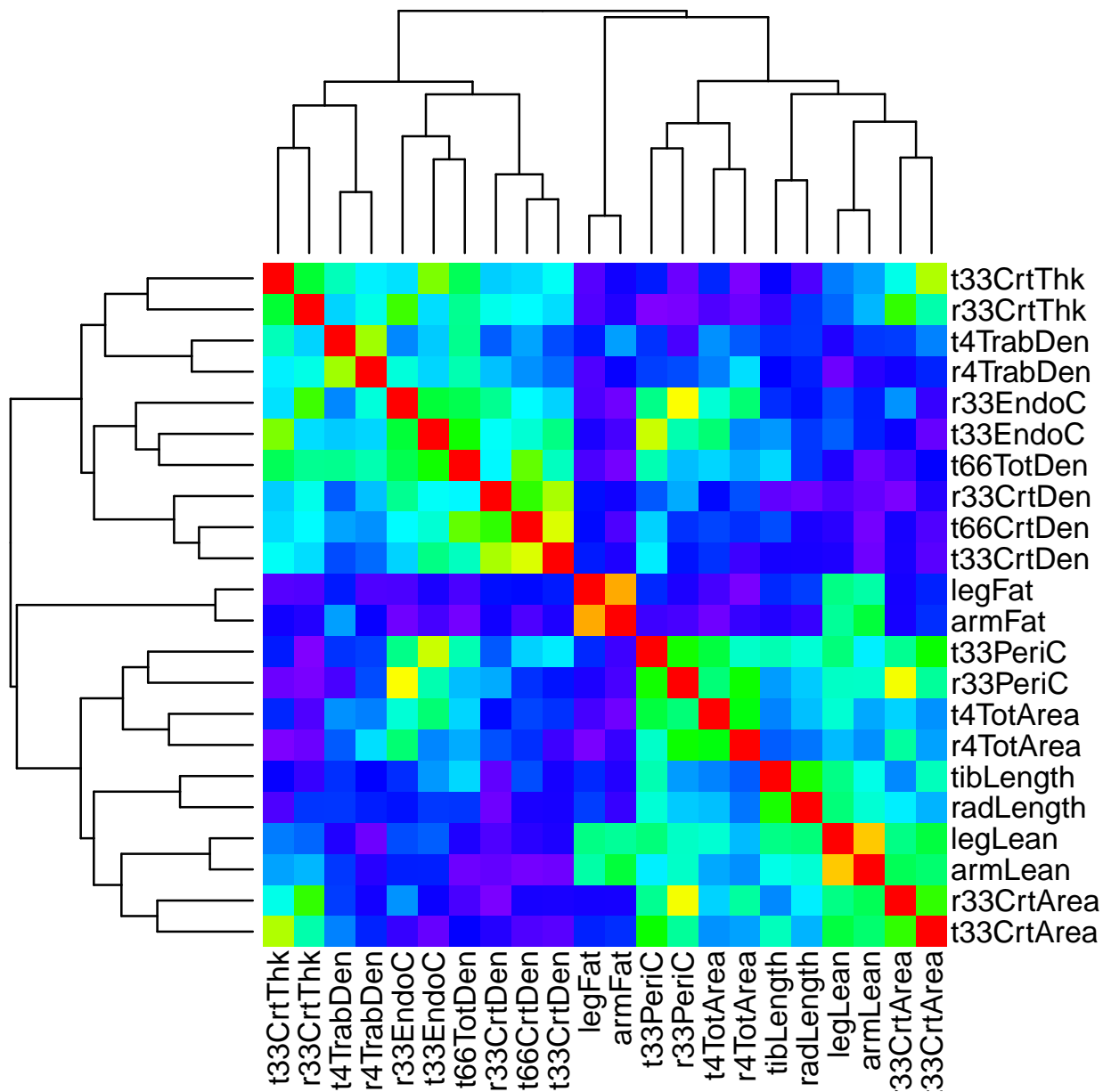


Figure 2.2: Phenotypic Correlations in TBHS participants (age ≥ 60)

The colors indicate the degree of correlation with red equivalent to $r = 1$ and purple, to $r = 0$, so that the greater the correlation the “hotter” the color. Abbreviations for the traits can be found in Table 2.2.

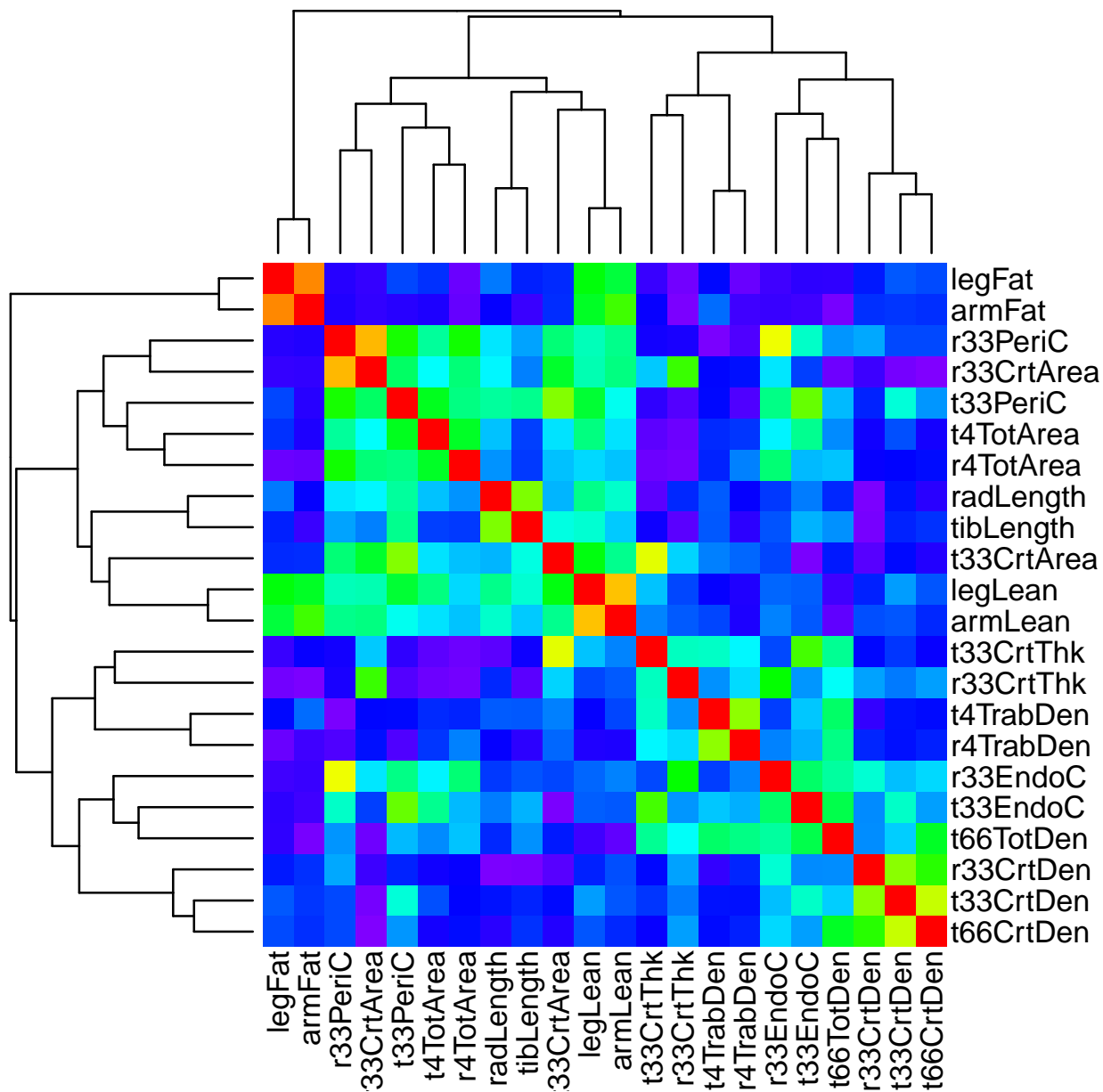


Figure 2.3: Phenotypic Correlations in TBHS participants (age < 60)

The colors indicate the degree of correlation with red equivalent to $r = 1$ and purple, to $r = 0$, so that the greater the correlation the “hotter” the color. Abbreviations for the traits can be found in Table 2.2.

Table 2.4: Tobago Men Principal Components

	PC1	PC2	PC3	PC4	PC5	PC6	PC7	PC8	PC9	PC10
Cum. Var.	0.259	0.458	0.565	0.642	0.704	0.753	0.797	0.837	0.868	0.897
t33CrtThk	0.030	0.367	-0.003	-0.195	-0.225	-0.430	-0.143	0.171	0.114	-0.063
r33CrtThk	0.026	0.352	-0.117	0.028	-0.159	0.174	0.571	-0.142	0.137	-0.091
t4TrabDen	0.096	0.249	0.207	-0.354	0.095	0.300	-0.213	-0.030	-0.198	-0.135
r4TrabDen	0.111	0.251	0.135	-0.267	-0.051	0.469	-0.207	-0.044	-0.249	-0.210
r33EndoC	-0.274	-0.175	-0.068	-0.247	0.275	-0.157	-0.390	-0.180	-0.018	0.084
t33EndoC	-0.267	-0.212	-0.033	0.077	0.098	0.502	-0.013	0.080	0.202	0.148
t66TotDen	0.207	0.276	0.017	-0.122	0.037	-0.005	0.025	0.090	-0.103	0.678
r33CrtDen	0.152	0.220	-0.241	0.334	0.165	0.144	-0.190	0.108	0.151	-0.339
t66CrtDen	0.178	0.226	-0.240	0.190	0.367	0.063	-0.118	0.004	0.063	0.396
t33CrtDen	0.181	0.219	-0.263	0.223	0.353	-0.074	-0.195	-0.084	0.080	-0.198
legFat	-0.135	0.102	0.483	0.185	0.220	-0.077	0.059	-0.018	0.257	-0.045
armFat	-0.109	0.117	0.516	0.115	0.277	-0.079	0.057	-0.055	0.233	-0.024
r33PeriC	-0.321	0.058	-0.177	-0.285	0.214	-0.055	-0.027	-0.332	0.083	0.034
t33PeriC	-0.337	0.034	-0.105	-0.006	-0.120	0.278	-0.122	0.263	0.330	0.097
r4TotArea	-0.246	0.007	-0.236	-0.094	0.221	-0.225	0.179	0.166	-0.293	-0.241
t4TotArea	-0.263	0.006	-0.139	0.052	0.165	0.075	0.169	0.523	-0.274	-0.002
radLength	-0.224	0.112	-0.070	0.345	-0.246	0.009	-0.074	-0.313	-0.287	0.218
tibLength	-0.219	0.090	-0.051	0.315	-0.373	0.008	-0.327	-0.239	-0.037	-0.070
t33CrtArea	-0.210	0.300	-0.057	-0.168	-0.235	-0.118	-0.197	0.303	0.328	0.036
r33CrtArea	-0.238	0.249	-0.206	-0.208	0.081	0.054	0.296	-0.352	0.147	-0.026
legLean	-0.263	0.236	0.162	0.185	0.016	-0.019	-0.021	0.158	-0.286	0.020
armLean	-0.237	0.244	0.195	0.144	0.127	-0.036	0.038	-0.038	-0.300	0.023

Loading components ≥ 2 and ≤ -2 are typeset in bold and loading components between -2 and 2 in gray. This threshold was chosen arbitrarily to highlight the relative contributions of each trait to the loadings. The traits from the “density” group are highlighted in light red; the traits from the “fat mass” group, in light yellow; and the traits from the “geometry” group, in light blue.

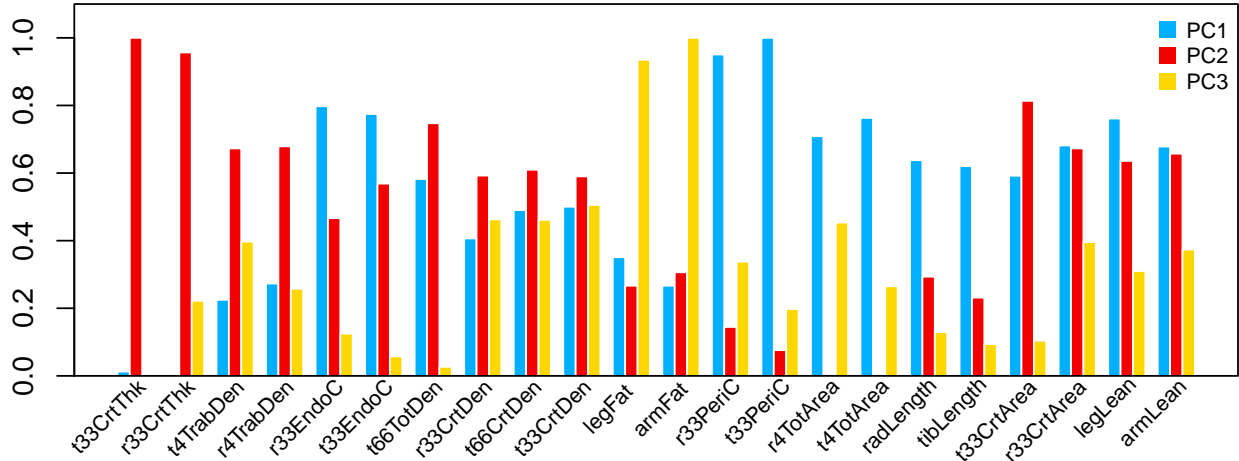


Figure 2.4: First Three Principal Components of Phenotypes in TBHS participants

The unsigned loading components of each eigenvector were rescaled from 0 to 1 (within each eigenvector) aid in visualizing the distribution of the endophenotypes among the PCs.

was a significant covariate for the three measures of cortical BMD ($p < 1.20 \times 10^{-9}$). In general, the covariates accounted for more of the variation in “geometry” traits (16%–70%) versus the “density” traits (8%–34%). Covariates accounted for ~42%–59% of the variation in the first four PCs and 1%–16% of the next three PCs. After accounting for the significant covariates, the residual heritabilities of the composite endophenotypes and the individual measures of bone, muscle, and fat range from 0.206 for radial cortical thickness to 0.763 for tibial trabecular density.

All heritability estimates are statistically significant (p value range: 0.007 to 1.02×10^{-22}). The heritabilities of the composite traits range from 0.306 for PC7 to 0.696 for PC1 (p value range: 0.001 to 9.87×10^{-14}). There are no obvious relationships between the residual heritabilities of the individual components and the composite traits, in part because heritabilities of the individual traits vary widely. The heritability of PC3 ($h_r^2 = 0.539$) falls above the two measures of fat mass, arm fat mass (0.535) and leg fat mass (0.449).

Table 2.5: Tobago Families Heritabilities

Trait	n	h_r^2	S.E.	p	Covariates p				σ_E^2
					Age	Age ²	Sex	Menopause	
t4TrabDen	419	0.763	0.092	2.42×10^{-18}	5.79×10^{-18}	1.02×10^{-3}	8.20×10^{-8}		0.161
t33PeriC	419	0.729	0.097	2.19×10^{-18}	3.01×10^{-5}	2.25×10^{-2}	1.56×10^{-47}		0.386
t4TotArea	419	0.720	0.084	1.02×10^{-22}		9.24×10^{-2}	9.22×10^{-63}		0.477
PC1	388	0.696	0.115	9.87×10^{-14}	8.38×10^{-7}		1.75×10^{-58}		0.464
r4TrabDen	439	0.691	0.096	1.62×10^{-16}	2.46×10^{-11}		2.82×10^{-18}		0.200
r33PeriC	439	0.680	0.096	4.09×10^{-18}	9.65×10^{-11}	9.08×10^{-6}	3.79×10^{-98}		0.611
t33EndoC	419	0.671	0.104	1.26×10^{-14}	1.58×10^{-4}	1.55×10^{-2}	5.33×10^{-7}		0.098
r4TotArea	436	0.648	0.090	4.65×10^{-17}	4.34×10^{-7}	4.66×10^{-2}	4.51×10^{-73}		0.500
armLean	443	0.611	0.101	1.80×10^{-11}	5.85×10^{-2}	4.26×10^{-13}	1.72×10^{-73}		0.501
r33CrtArea	439	0.605	0.097	1.17×10^{-14}	1.60×10^{-4}	1.07×10^{-14}	2.51×10^{-122}		0.702
t33CrtDen	416	0.553	0.096	6.31×10^{-12}		3.47×10^{-14}	9.25×10^{-8}	9.69×10^{-12}	0.291
PC3	388	0.539	0.122	9.00×10^{-7}	7.51×10^{-2}	2.84×10^{-3}	2.06×10^{-59}		0.490
armFat	443	0.535	0.105	3.09×10^{-10}	1.28×10^{-12}	2.74×10^{-6}	9.14×10^{-44}		0.388
t66TotDen	422	0.530	0.106	5.84×10^{-9}	2.30×10^{-7}	8.87×10^{-4}			0.079
PC4	388	0.524	0.100	3.30×10^{-9}	1.55×10^{-2}	1.46×10^{-8}	2.26×10^{-47}		0.423
legLean	443	0.493	0.110	3.92×10^{-8}		6.91×10^{-8}	3.34×10^{-57}		0.439
legFat	443	0.449	0.103	3.77×10^{-8}	3.07×10^{-5}	8.03×10^{-5}	2.23×10^{-54}		0.425
t66CrtDen	420	0.446	0.110	2.20×10^{-6}	8.49×10^{-2}	1.27×10^{-10}	3.48×10^{-7}	1.20×10^{-9}	0.263
PC2	388	0.439	0.117	7.00×10^{-6}	2.29×10^{-2}	5.17×10^{-18}	4.22×10^{-41}		0.443
t33CrtArea	420	0.435	0.095	2.94×10^{-8}	1.77×10^{-2}	8.18×10^{-8}	5.14×10^{-62}		0.482
PC6	388	0.414	0.122	6.00×10^{-6}	4.34×10^{-8}	1.89×10^{-2}	1.69×10^{-4}		0.110
PC5	388	0.382	0.104	7.00×10^{-7}	7.31×10^{-4}	1.51×10^{-6}	1.23×10^{-11}		0.164
radLength	439	0.382	0.099	7.43×10^{-9}			4.75×10^{-37}		0.320
t33CrtThk	420	0.330	0.107	1.33×10^{-4}		2.92×10^{-10}	3.92×10^{-32}		0.325
r33EndoC	437	0.321	0.101	5.80×10^{-6}	1.41×10^{-8}		1.01×10^{-22}		0.237
r33CrtDen	434	0.316	0.094	1.81×10^{-5}	1.39×10^{-3}	2.63×10^{-16}	3.63×10^{-13}	7.00×10^{-14}	0.278
PC7	388	0.306	0.117	1.47×10^{-3}	2.95×10^{-2}				0.007
tibLength	420	0.288	0.102	1.63×10^{-4}	1.22×10^{-3}		5.56×10^{-16}		0.161
r33CrtThk	439	0.206	0.107	7.06×10^{-3}	9.50×10^{-3}	2.03×10^{-8}	1.18×10^{-32}		0.341

The traits from the “density” group are highlighted in light red; the traits from the “fat mass” group, in light yellow; and the traits from the “geometry” group, in light blue. PCs 1, 2 and 3 are highlighted with the color of the groups that contribute most to their eigenvectors. The PCs are in boldface text. σ_E^2 is the variance attributable to the modeled covariates.

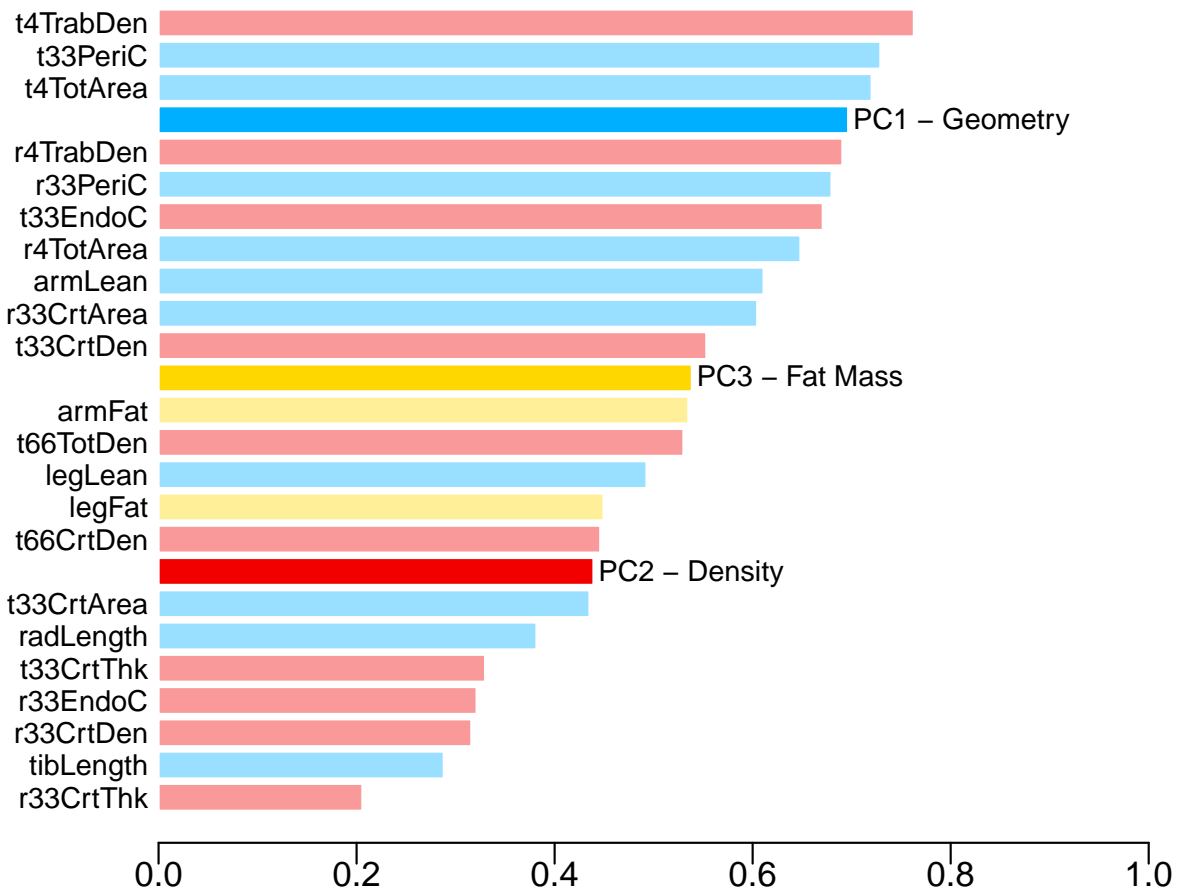


Figure 2.5: Tobago Families Residual Heritabilities

PC4-7 not shown in this figure for clarity.

2.4 DISCUSSION

With an aim to examine the relationships among endophenotypes of body composition in a population of African descent, I explored the relationships of twenty-two bone-, muscle and fat-related measures of the arm and leg in 1,937 Afro-Caribbean men from Tobago. Hierarchical clustering revealed that the traits sorted into three general groups: (1) a “density group” consisting of measures of cortical and trabecular BMD as well as cortical thickness and endosteal circumference, (2) a “geometry group” consisting of measures of bone length, periosteal circumference, bone area and lean mass, and (3) a “fat mass” group consisting arm and leg fat mass. It was also observed that the gross pattern of clustering remains the same over time, as analyses of men stratified into an older and younger cohort produced the same patterns. Although there was evidence that the internal correlation of the “density group” increases with age.

To develop composite endophenotypes that might reflect underlying trends among the body composition traits, principal components were developed in TBHS and were found to be generally analogous to the results of the hierarchical clustering. The loadings from the first seven PCs were applied to the same set of phenotypes of the TFS participants to generate a set of PCs for genetic analysis.

To assess the genetic contribution to the twenty-two individual and seven composite endophenotypes, residual heritabilities were calculated for all traits. The heritabilities ranged from modest (0.206) to high (0.763), and all were statistically significant. There was no apparent pattern or clustering of the traits from different groups, nor of the PCs, although the higher ordinal PCs tended to have greater heritability. That is in general, the greater the proportion of total sample variance attributable to a PC, the greater the proportion of genetic variance for that PC. The most dominant PC consists of mainly “geometry” traits with additional contributions from the two measures of endosteal circumference. This PC also had high heritability ($h^2 = 0.696$) indicating that traits such as bone length and bone area are influenced more by genetic contributions than PC2, which consists mainly of “density” traits. PC2 has a moderate heritability (0.439) and may be more highly affected by environmental inputs.

The creation of heritable principal components for measures of body composition points toward pleiotropic relations among each PCs’ components. These PCs could be extended to gene mapping,

to identify loci that affect multiple measures. The characterization of such genes could enhance our understanding of the genetic architecture of body composition.

3.0 GENOMEWIDE LINKAGE STUDY IN AFRO-CARIBBEANS

3.1 INTRODUCTION

Osteoporosis, sarcopenia and changes in body fat distribution are complex, age-related conditions that result from the effects of genes and environmental factors [Pocock et al. 1987; Seeman et al. 1996; Maes et al. 1997; Koller et al. 2000, 2001; Karasik et al. 2004; Huygens et al. 2004; Hsu et al. 2005; Wang et al. 2007b; Prior et al. 2007]. Considerable research has been done to identify genes influencing endophenotypes for osteoporosis, sarcopenia and body fat distribution separately. For example, linkage and whole genome association studies have identified genes influencing areal bone mineral density (BMD), e.g., *LRP5* (low density lipoprotein receptor-related protein 5), *ESR1* (estrogen receptor 1), *TNFRFS11B* (tumor necrosis factor receptor superfamily, member 11b; osteoprotegerin; or OPG), *TGFBR3* (transforming growth factor, β receptor III) [Richards et al. 2008; Stykarsdottir et al. 2008; Xiong et al. 2009]; lean mass, e.g., *TRHR* (thyrotropin-releasing hormone receptor) [Liu et al. 2009a]; and body mass index (BMI), e.g., *PPARG* (peroxisome proliferator-activated receptor γ), *ADIPOQ* (adiponectin), *MC4R* (melanocortin 4 receptor), *FTO* (*Fatso* homolog) [Fox et al. 2007; Thorleifsson et al. 2008; Willer et al. 2008; Timpson et al. 2008; Ling et al. 2009; Meyre et al. 2009; Heard-Costa et al. 2009]. However, variation in these known genes does not account for all of the known genetic variation in these bone-, muscle- and fat-related traits, indicating that additional genetic variants remain to be identified. In addition, few studies have been performed among individuals with non-European ancestry. Genetic studies of additional endophenotypes, such as volumetric measures of cortical and trabecular bone may reveal additional loci that influence susceptibility to osteoporosis, sarcopenia and body fat redistribution. Furthermore, our current knowledge of embryonic and fetal development, as well as results from epidemiological studies, indicate that a common set of genetic and environmental factors may influence all three traits [Glauber et al. 1995;

Churchill 1996; Frost 2003; Shore et al. 2006; Sun et al. 2006; Lee et al. 2007; Wang et al. 2007d; Videman et al. 2007; Karasik and Kiel 2008; Devaney et al. 2009; Schindeler et al. 2009; Karasik et al. 2009]. Thus, genetic analyses of several traits simultaneously, in populations with differing ancestry, may reveal additional loci.

Using multivariate methods, I have identified clusters of endophenotypes for bone, muscle and fat traits and developed measures of composite phenotypes (Chapter 2). Individually, similar endophenotypes have been reported to be heritable among individuals with European [Hsu et al. 2005; Karasik et al. 2009] and African ancestry [Hsu et al. 2005; Wang et al. 2007b], however, few studies have been done to identify quantitative trait loci (QTLs) that influence these traits among individuals of European ancestry [Thomas and Burguera 2002; Liu et al. 2004; Chinappen-Horsley et al. 2008; Karasik et al. 2009] or of African ancestry [Koller et al. 1998]. In this chapter, to identify QTLs that influence the endophenotypes or composite traits, I performed variance components linkage analyses and compared the results of these analyses to determine if QTLs influence more than one trait. Then, I estimated the genetic correlation among traits for which evidence of pleiotropic QTLs is observed.

3.2 METHODS

3.2.1 Study Population

In this chapter I used the participants in the Tobago Family Health Study (TFS) described in Chapter 2. Briefly, the TFS population comprises 470 women and men (ages ≥ 18 years) in seven multigenerational families of African descent (mean family size = 67; total number of relationships: 4,206). Pedigrees can be found in Appendix B.

This study was approved by the Institutional Review Boards of the University of Pittsburgh and the Tobago Division of Health and Social Sciences and all participants gave written, informed consent.

3.2.2 Phenotypes

The twenty-two bone-, muscle- and fat-related endophenotypes and seven composite endophenotypes analyzed in Chapter 2 were carried forward for analysis in this chapter. The muscle-related traits were arm and leg lean mass measured by dual-energy x-ray absorptiometry (DXA). The fat-related traits were arm and leg fat mass, also measured by DXA. Bone geometry traits were tibia and radius length, measured by DXA, and total bone area at 4% of the radius and of the tibia and cortical area, cortical thickness, periosteal circumference and endosteal circumference at 33% of the radius and of the tibia, measured by peripheral quantitative computed tomography (pQCT). BMD traits were trabecular BMD at 4% of the radius and of the tibia, cortical BMD at 33% of the radius and of the tibia and total BMD and cortical BMD at 66% of the tibia and were also determined by pQCT.

Composite endophenotypes were generated by principal component (PC) analysis as described in Chapter 2. Briefly, because the individuals in TFS are not independent, the eigenvectors were calculated using the same twenty-two bone-, muscle- and fat-related phenotypes in 1,937 unrelated men of African ancestry from the Tobago Bone Health Study (TBHS), a study of body composition also preformed as a follow up of the Tobago Prostate Cancer Survey. The eigenvectors were then applied to the phenotypes in TFS to produce principal components. The first seven PCs, which account for > 80% of the overall variance, represent combinations of three general groups groups of traits, defined as “geometry,” “density” and “fat-related.” The traits that compose each group can be found in Table 2.3.

3.2.3 Markers

The 470 individuals from TFS were genotyped on an Infinium HumanLinkage-12 BeadChip Assay (Illumina), a single-nucleotide polymorphism (SNP) linkage panel that covers 93.2% of the genome. After excluding SNPs with a call rate < 90%, a Hardy–Weinberg equilibrium p value < 0.001, a minor allele frequency (MAF) < 0.05 and that were incompatible with multipoint identify-by-descent (MIBD) estimation using LOKI [Heath 1997] (that is, less than 1 cM apart), a total of 1,516 autosomal SNPs remained. The final SNP set had a median MAF = 0.325 with median spacing of 1.92 cM.

3.2.4 Statistical Analyses

Initial statistical analyses were performed in R 2.11.1 [R Development Core Team 2008]. All 22 bone-, muscle- and fat-related measures underwent a series of quality control procedures described in Chapter 2 including transformations to normality and outlier removal. Seven composite endophenotypes were generated as described above and in Chapter 2. The effects of covariates and estimation of heritability of the twenty-two traits and seven endophenotypes were also previously described (Chapter 2). For the univariate and bivariate analyses described below, I analyzed the residuals of the twenty-two individual and seven composite traits derived from the heritability analyses.

3.2.5 Genetic Analysis

Univariate linkage analysis, bivariate linkage analysis and bivariate correlation decomposition were accomplished using SOLAR (Sequential Oligogenic Linkage Analysis Routines) 4.2.0 [Almasy and Blangero 1998b; Amos 1994]. Adjustment for covariates was performed as described in Section 1.5.2.2. Univariate multipoint variance-components linkage analysis was performed for each trait and PC using LOKI-calculated MIBDs for the autosomes only. A likelihood ratio test for linkage was conducted by comparing the likelihoods of the models with and without the QTL, given the data. Logarithm of the odds (LOD) scores were calculated by taking the \log_{10} of the test statistic. A LOD score greater than 2.5 was taken as suggestive evidence of linkage, based upon background noise in a simulated linkage analysis of a trait constructed as the sum of several SNPs' allele dosages (Section 1.5.4.3). The 2 LOD confidence interval of each QTL was taken as the width from the maximum LOD out to the maximum $- 2$ on each side. To adjust for potential inflation due to residual phenotypic sibling correlation or deviations from normality, a simulation of the null distribution for each trait that showed evidence of a QTL was generated to calculate an empirical LOD adjustment constant [Allison et al. 1999; Blangero et al. 2000, 2001].

Bivariate linkage analysis, which tests for simultaneous linkage of two traits to a genetic region, was performed for those pairs of traits for which there was evidence of linkage at the same locations.

The correlation (ρ_P) between each pair of traits was also decomposed into two components: genetic (ρ_G) and environmental (ρ_E). Models with the estimated genetic correlation were tested

against models with $\rho_G = 0$ and $\rho_G = 1$ to assess whether genetic elements underlying each pair of traits are independent or completely the same, respectively.

3.3 RESULTS

3.3.1 Subject Characteristics

Characteristics of the subjects in TFS are presented in Tables 2.1 and 2.2 and are described in Section 2.3.1.

3.3.2 Univariate Linkage Analysis

Univariate linkage analysis was performed on twenty-two traits and seven composite endophenotypes. Eight endophenotypes mapped to one location each on the genome with LOD scores greater than 2.5, and one endophenotype mapped to two locations (Table 3.1). Two endophenotypes mapped to locations with LOD scores greater than 3.3. If $\text{LOD} = 3.3$ is taken as equivalent to $p = 0.05$ for a genomewide scan [Lander and Schork 1994], then testing for 29 traits would be expected to produce 1.45 false positives. With two seen here, there appears to be an excess. None of the traits required significant adjustment for inflation (range 0.96–1.16); only radial cortical BMD required downward adjustment ($k = 0.96$). I detected significant evidence for a QTL on chromosome10q26.3–qter that influenced both PC1 and tibial periosteal circumference (LOD scores of 3.45 and 3.12 respectively (Figure 3.2). Another significant QTL influencing both arm fat mass and PC3 mapped to chromosome 21pter–q21.1 with LOD scores of 3.66 and 2.82 (Figure 3.6). Leg fat mass, arm lean muscle mass and leg lean muscle mass also had non-significant linkage peaks at this location with LOD scores of 1.81, 2.09 and 1.86 (Figure 3.6). I also identified several regions with suggestive evidence for QTLs. A 38.2 Mb region from 1p31.1 to 1p34.1 showed linkage to PC4 with a peak LOD of 2.76 (Figure 3.1). A region on 10q21.1–q23.1 showed linkage to radial cortical density (peak $\text{LOD} = 2.52$; Figure 3.2). Two traits also showed linkage to chromosome 12, tibia cortical thickness and radial cortical density, with LODs of 2.67 and 2.97 (unadjusted) respectively; however, they did not map to overlapping regions of the chromosome (12q12–q21.31 and 12q24.23–qter; Figure 3.3). A 20.5 Mb

region from 17pter–p11.2 was linked to radial total area (LOD = 2.62; Figure 3.4). Finally, a 10.4 Mb region from 20p12.3–p12.1 was linked to radial periosteal circumference (LOD = 2.72; Figure 3.5). Genomewide plots of all 29 traits can be found in Figures C1–C29 in Appendix C.

Table 3.1: Univariate LOD Scores

Trait	<i>n</i>	Covariates	h_r^2	Chr	Peak			Position		
					cM	LOD	h_{QTL}^2	Cytogenetic	Genetic (cM)	Physical (Mb)
PC4	388	A, A ² , S	0.524	1	97	2.76	0.445	1p34.1–p31.1	81–118	46.4–84.6
r33CrtDen	428	A, A ² , S, M	0.316	10	87	2.52	0.361	10q21.1–q23.1	76–114	59.9–84.6
PC1	388	A, S	0.696	10	182	3.45	0.485	10q26.3–qter	176–190	131.4–135.4
t33PeriC	419	A, A ² , S	0.729	10	190	3.12	0.368	10q26.3–qter	173–190	130.7–135.4
t33CrtThk	420	A ² , S	0.330	12	88	2.67	0.330	12q12–q21.31	59–100	44.0–84.0
r33CrtDen	428	A, A ² , S, M	0.316	12	175	2.97	0.313	12q24.23–qter	145–191	117.3–132.3
r4TotArea	436	A, A ² , S	0.648	17	33	2.62	0.334	17pter–p11.2	0–51	0.0–20.5
r33PeriC	439	A, A ² , S	0.680	20	29	2.72	0.414	20p12.3–p12.1	14–40	5.2–15.6
armFat	443	A, A ² , S	0.535	21	7	3.66	0.315	21pter–q21.1	0–14	0.0–19.3
PC3	388	A, A ² , S	0.539	21	12	2.82	0.372	21pter–q21.1	0–18	0.0–21.2

A = age; A² = age squared; S = sex; M = menopause. h_r^2 is the residual heritability of the trait. h_{QTL}^2 is the estimated residual heritability due to a QTL at this locus.

3.3.3 Bivariate Genetic Correlation and Linkage Analyses

To further investigate the whether the univariate linkage signals for a QTL on chromosome 21 for arm and leg lean and fat mass were due to coincident linkage or possible pleiotropic effects of a QTL, I estimated bivariate genetic correlations for the fat and lean mass traits (Table 3.2) and performed bivariate linkage analyses for four pairs of traits: arm fat mass/leg fat mass, arm lean mass/leg lean mass, arm fat mass/arm lean mass and leg fat mass/leg lean mass (Figure 3.7 and Table 3.3). To further investigate whether the univariate linkage signals for a QTL on chromosome 10 indicated a QTL with pleiotropic effects, I also estimated the genetic correlations of the major components of PC1 (Table 3.4).

The heritabilities of arm and leg lean and fat mass are moderate (ranging from 0.42 to 0.58, $p < 3.77 \times 10^{-8}$ for all) and the genetic correlations between arm and leg fat and arm and leg lean mass were high, 0.78 ($p_{\rho_G=1} = 1.00 \times 10^{-7}$) and 0.84 ($p_{\rho_G=1} < 6.00 \times 10^{-7}$), respectively. The genetic

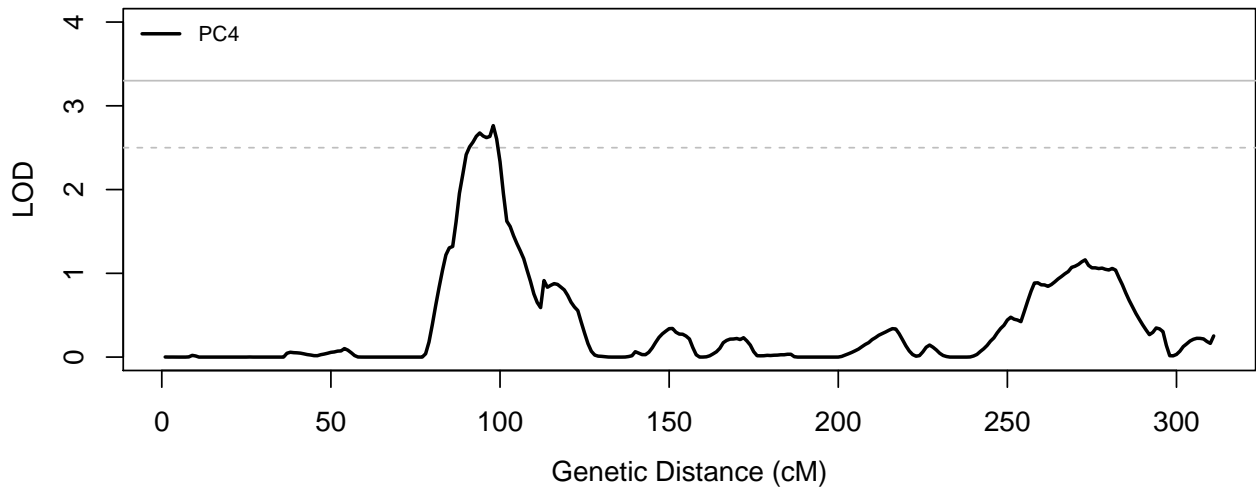


Figure 3.1: Chromosome 1 Univariate QTL

The solid gray line is at LOD = 3.3, statistical significance in this study. The dashed gray line is at LOD = 2.5, suggestive significance in this study.

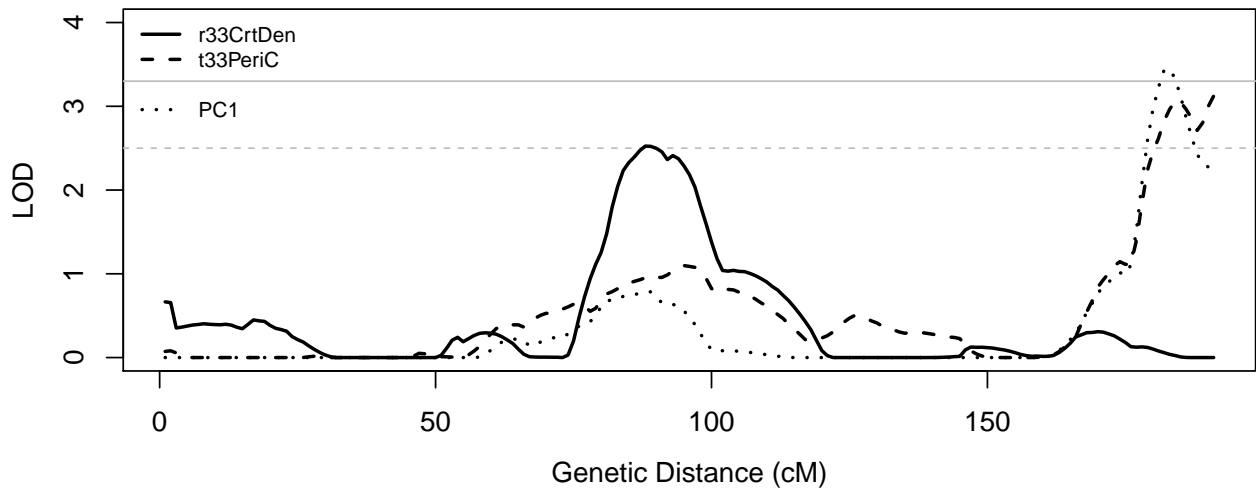


Figure 3.2: Chromosome 10 Univariate QTLs

The solid gray line is at LOD = 3.3, statistical significance in this study. The dashed gray line is at LOD = 2.5, suggestive significance in this study.

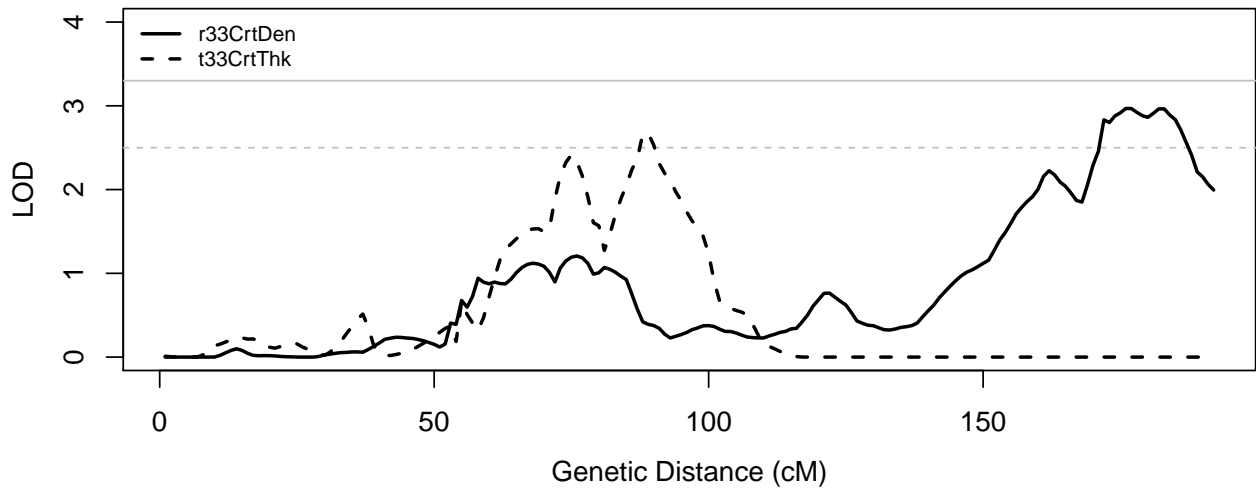


Figure 3.3: Chromosome 12 Univariate QTLs

The solid gray line is at LOD = 3.3, statistical significance in this study. The dashed gray line is at LOD = 2.5, suggestive significance in this study.

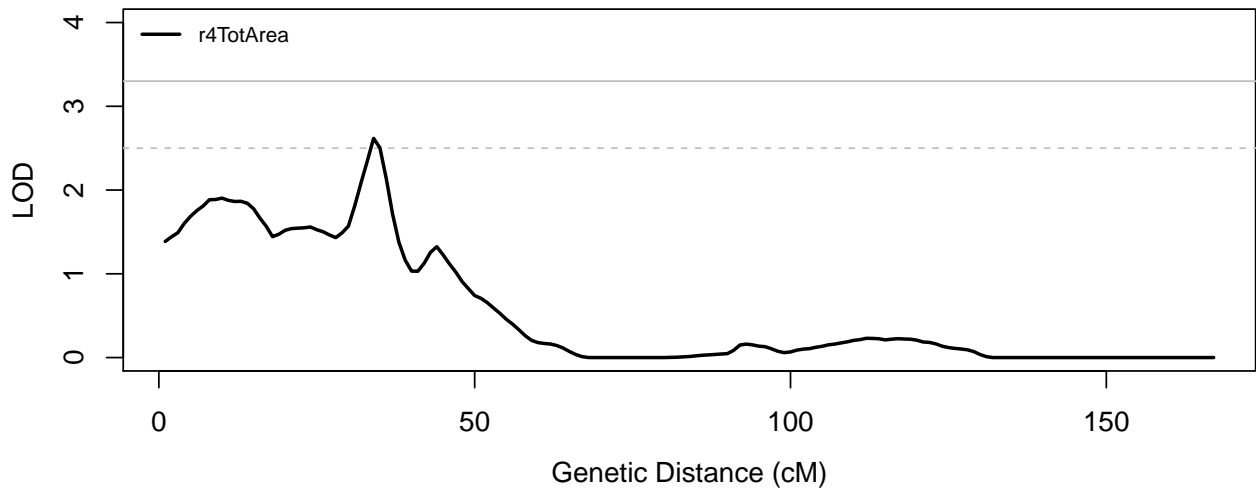


Figure 3.4: Chromosome 17 Univariate QTL

The solid gray line is at LOD = 3.3, statistical significance in this study. The dashed gray line is at LOD = 2.5, suggestive significance in this study.

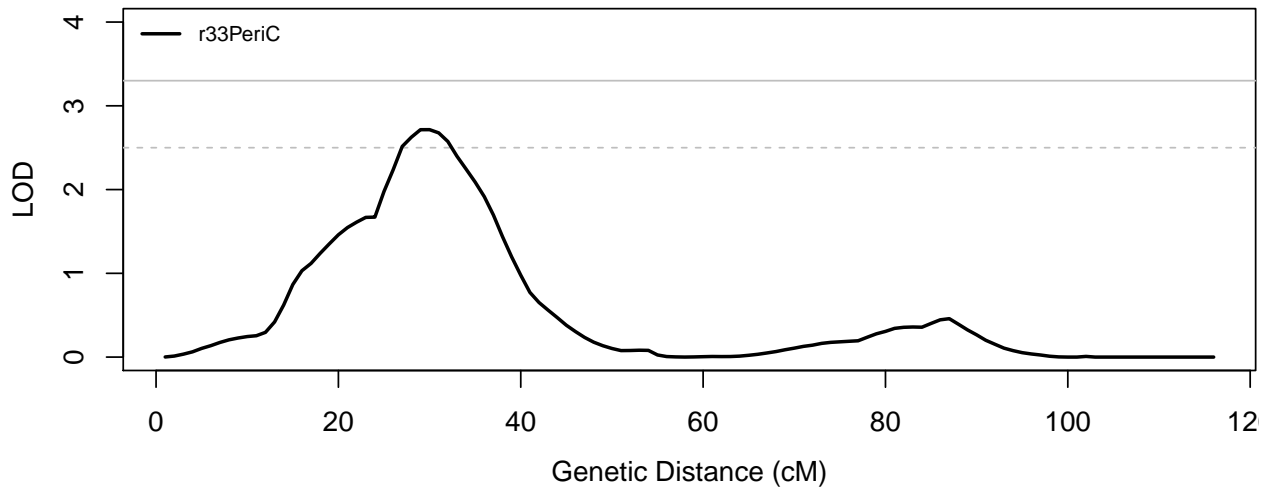


Figure 3.5: Chromosome 20 Univariate QTL

The solid gray line is at LOD = 3.3, statistical significance in this study. The dashed gray line is at LOD = 2.5, suggestive significance in this study.

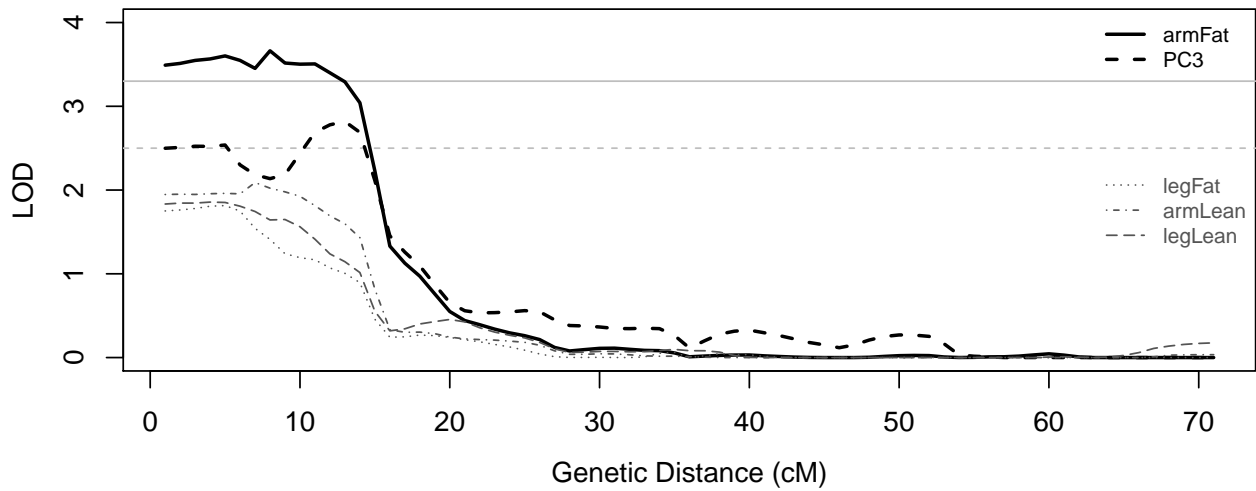


Figure 3.6: Chromosome 21 Univariate QTLs

The solid gray line is at LOD = 3.3, statistical significance in this study. The dashed gray line is at LOD = 2.5, suggestive significance in this study.

correlation for arm fat and arm lean mass was also high, 0.703, while leg fat and leg lean mass were moderate, 0.53. All four pairs of traits examined in the bivariate linkage analysis exhibited significant or potential bivariate linkage on chromosome 21 at the same location as univariate analyses of each trait separately, as well as PC3, in which both fat mass traits are a major contributor (Figure 3.7). The LOD_{2df} scores were 2.94, 3.30, 1.72 and 1.72 for arm fat/leg fat mass, arm lean/arm fat mass, arm lean/leg lean mass and leg lean/leg fat mass respectively. Thus, this QTL is likely to have pleiotropic effects on the fat and lean mass related traits.

There is also potential evidence of a pleiotropic locus on chromosome 10q26.3–qter where putative QTLs for both the composite trait PC1 and the individual trait tibial periosteal circumference overlap (Figure 3.2). The individual traits that make up PC1, including tibial periosteal circumference, all exhibit moderate to high genetic correlation (Table 3.4), ranging from 0.358 to 0.888.

Table 3.2: Genetic Correlations — Lean Muscle and Fat Mass

	legFat	armFat	legLean	armLean
legFat	0.449	0.776	0.526	0.601
armFat		0.535	0.426	0.703
legLean			0.493	0.839
armLean				0.611

The genetic correlations are located in the top triangle of the matrix. Heritabilities for each trait are set in boldface text down the diagonal. If $\rho_G = 0$ was not rejected the estimate of ρ_G is not shown, and if $\rho_G = 1$ was not rejected, the estimate is in gray.

3.4 DISCUSSION

As epidemiological evidence accumulates and developmental processes are better understood, the interrelationships between variation in bone, muscle and fat tissues, including variation that extends to conditions such as osteoporosis, sarcopenia and age-related changes in fat distribution, have become more apparent. In the past two decades, several genes have been identified that influence endophenotypes for these conditions. Nonetheless, these genes do not account for all of the known heritability of these endophenotypes, and thus more genes need to be located and under-

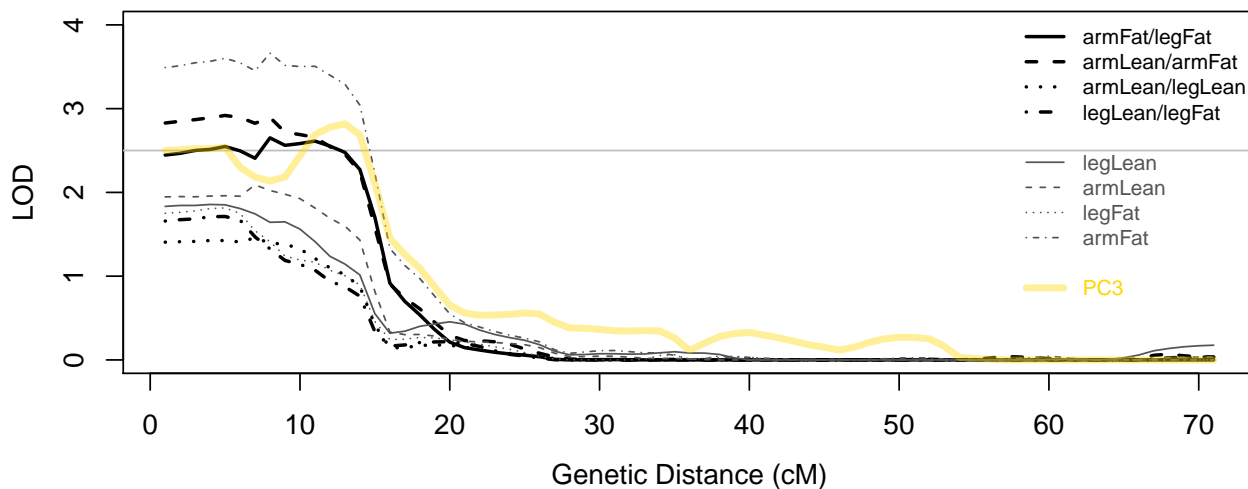


Figure 3.7: Chromosome 21 Bivariate QTLs

The solid gray line is at LOD = 2.5, suggestive significance in this study. The bivariate LOD_{2df} scores are not strictly comparable to the univariate LOD scores because each is tested with a different number of degrees of freedom. They are displayed together here to illustrate their positional overlap.

Table 3.3: Bivariate LOD Scores on 21pter–q21.1

Trait 1		Trait 2			Peak	
Trait	$h_{r_1}^2$	$h_{QTL_1}^2$	Trait	$h_{r_2}^2$	$h_{QTL_2}^2$	LOD _{2df}
armFat	0.535	0.316	legFat	0.449	0.199	2.65
armLean	0.611	0.215	armFat	0.535	0.309	2.92
armLean	0.0611	0.268	legLean	0.493	0.243	1.46
legFat	0.449	0.203	legLean	0.493	0.205	1.71

$h_{r_1}^2$ and $h_{r_2}^2$ are the residual heritabilities of the first and second trait respectively. $h_{QTL_1}^2$ and $h_{QTL_2}^2$ are the estimated residual heritabilities due to a QTL at this locus for the first and second trait respectively.

Table 3.4: Genetic Correlations — PC1

	r33	t33	t33	r33	t4Tot	r4Tot	rad	tib	t33Crt	r33Crt	leg	arm
	EndoC	EndoC	PeriC	PeriC	Area	Area	Length	Length	Area	Area	Lean	Lean
r33EndoC	0.321	0.877	0.864	0.880	0.573	0.591			0.587	0.718	0.537	
t33EndoC		0.671	0.888	0.753	0.580	0.602	0.467	0.562	0.434	0.557	0.594	0.310
t33PeriC			0.729	0.842	0.578	0.595	0.600	0.586	0.804	0.651	0.721	0.490
r33PeriC				0.680	0.592	0.633	0.602	0.461	0.654	0.951	0.658	0.502
t4TotArea					0.720	0.697	0.407	0.619	0.302	0.469	0.536	0.383
r4TotArea						0.648	0.358		0.447	0.587	0.400	0.277
radLength							0.382	0.683	0.490	0.573	0.900	0.437
tibLength								0.288	0.443	0.446	0.647	0.430
t33CrtArea									0.435	0.618	0.691	0.508
r33CrtArea										0.605	0.668	0.617
legLean											0.493	0.839
armLean												0.611

The genetic correlations are located in the top triangle of the matrix. Heritabilities for each trait are set in boldface text down the diagonal. If $\rho_G = 0$ was not rejected the estimate of ρ_G is not shown, and if $\rho_G = 1$ was not rejected, the estimate is in gray.

stood. Linkage analysis methods have been used successfully to identify genes that influence many traits, including traits related to the endophenotypes examined here. Conducting linkage analysis on multiple related traits as well as on composites of those traits could aid in identifying genes with pleiotropic effects.

Nine traits and/or composite endophenotypes exhibited suggestive evidence for QTLs at eight autosomal locations: PC4 at 1p34.1–p31.1, radial cortical density on 10q21.1–q23.1, PC1 and tibial periosteal circumference on 10q26.3–qter, radial cortical density at 12q12–q21.31, tibial cortical thickness at 12q24.23–qter, radial total area at 17pter–p11.2, radial periosteal circumference at 20p12.3–p12.1, and PC3 and arm fat mass at 21pter–q21.1. Thus, except for two pairs of traits, I observed no overlap of QTLs. This result is somewhat surprising given the known developmental and phenotypic correlations among these traits. However, quantitative trait linkage analyses will only detect QTLs that have a relatively large effect on the traits of interest. Additionally, the sample size is small and although extended multigenerational pedigrees enhance the ability to trace transmission of characters and alleles between relatives, I might not have the power to detect more subtle effects that might be characteristic of pleiotropy.

Two of the prospective QTLs in particular have good evidence to support them: 10q26.3–qter and 21pter–q21.1.

3.4.1 10q26.3–qter

Principal component 1 has significant contributions from “geometry” traits—periosteal circumference, total bone area, bone length, cortical bone area and lean mass—as well as some contributions from “density” traits—endosteal circumference and 66% tibial total density. Both PC1 and tibial periosteal circumference show evidence of a QTL located in a ~4.7 Mb region of chromosome 10q26.3–qter. The two linkage peaks virtually overlap; although PC1 peaks at 10qter whereas tibial periosteal circumference peaks just proximal to the end of the chromosome. This region of the chromosome includes 47 genes. There is a potential candidate gene about 1 Mb distal to the peak LOD score at ~134.0 Mb: *ADAM8* (a disintegrin-like and metalloprotease domain-containing protein 8), which has been shown to be involved in osteoclastogenesis [Choi et al. 2001; Peeters et al. 2003; Roodman 2006; Rao et al. 2006; Granholm et al. 2007] and to potentially play a role in bone response to inflammatory conditions [Ainola et al. 2009; Ishizuka et al. 2010].

3.4.2 21pter–q21.1

The fat- and muscle-related traits, bivariate pairs thereof and PC3 all exhibit evidence of linkage with various levels of significance to 21pter–q21.1, a 21.2 Mb region encompassing the proximal half of chromosome 21 including the centromere. However, the first SNP available for chromosome 21 is at 15 Mb (4 cM) on 21q11.2. Considering the more limited region from 21q11.2 to q21.1, there are 21 genes in the region. One potential candidate gene, *PDE3A* (phosphodiesterase 3A, cGMP-inhibited), is expressed in adipose tissues [Löbber et al. 1996] and has altered expression correlated with weight loss following Roux-en-Y gastric bypass surgery [Kim et al. 2008].

3.4.3 Other Suggestive Quantitative Trait Loci

LEPR (leptin receptor) on 1p31.3, under the PC4 linkage peak on 1p34.1–p31.1, has been examined for associations with body composition traits, primarily adiposity, with mixed results [for review

see Paracchini et al. 2005]. Mutation in the homologous rat gene is responsible for the extreme obesity phenotype of the Zucker *fatty* rat [Phillips et al. 1996; Takaya et al. 1996], which also serves as an animal model for ossification of posterior longitudinal ligament (OPLL) [Okano et al. 1997]. A small study of Japanese OPLL patients ($n = 172$) and controls ($n = 93$) showed a modest association between *LEPR* variants and degree of OPLL [Tahara et al. 2005]. The broad linkage region (40 Mb) for radial cortical thickness on 12q12–q21.31 includes slightly less than half of the q arm of 12. *VDR* (vitamin D receptor), located on 12q13.11, is associated with vitamin D–dependent rickets type 2A [Hughes et al. 1988; Kristjansson et al. 1993] and has been suggested to play a role in height [Xiong et al. 2005]. However, evidence is not strong for the role of common variation in *VDR* to modify BMD or fracture risk [Uitterlinden et al. 2006]. Missense polymorphisms in *P2RX7* (purinergic receptor P2X, ligand-gated ion channel, 7), which is located on 12q24 under a linkage signal for radial cortical BMD, have been associated with vertebral fractures [Ohlendorff et al. 2007], and *P2X7* knockout mice exhibit reduced bone mineral content and increased trabecular bone resorption [Ke et al. 2003]. A QTL for osteoporosis and hip and spine BMD has previously been reported on 20p12.3 and *BMP2* has been proposed to be the candidate gene for this linkage result [Styrkarsdottir et al. 2003].

3.4.4 General Conclusion

Strong evidence for two potential QTLs have been observed in this study of a set of twenty-two individual and seven composite endophenotypes: one QTL located on 10q26.3–qter for PC1 and tibia periosteal circumference and another QTL on 21pter–q21.1 for PC3 and arm fat mass. Fine-mapping of these putative QTLs in a similar population using association analysis with genotyped and imputed SNPs covering the regions under the linkage signals will be necessary to identify causal variants.

Measures of body composition, particularly bone-related traits, have not been thoroughly studied in populations of African ancestry. Further studies in African-ancestry populations such as the population of Tobago could increase our understanding of that particular population as well as providing a comparison for populations with European, Asian or Native American ancestry.

4.0 GENOMEWIDE ASSOCIATION STUDY IN EUROPEAN AMERICANS

4.1 INTRODUCTION

The promise of genomewide association studies (GWAS) was first proposed by Risch and Merikangas in 1996. In the 15 years since that initial proposal, 918 GWAS of complex traits and disorders (as of June 16, 2011, according to the National Human Genome Research Institute (NHGRI), www.genome.gov/gwastudies) have been performed, and many loci have been identified. The effect sizes of these loci have often proven to be small, and therefore GWA studies can require very large sample sizes to have adequate statistical power to detect such effects. Such large samples have required the collaboration of multiple studies into meta-analysis consortia.

Thirteen GWA studies of areal bone mineral density (BMD) of the hip or spine have been published to date [Kiel et al. 2007; Richards et al. 2008; Stykarsdottir et al. 2008; Xiong et al. 2009; Timpson et al. 2009; Stykarsdottir et al. 2009; Paternoster et al. 2010; Koller et al. 2010; Guo et al. 2010b; Gupta et al. 2011; Duncan et al. 2011], as well as five studies of osteoporosis [Liu et al. 2009b; Guo et al. 2010a; Hsu et al. 2010; Karasik et al. 2010; Tung et al. 2011]. These studies ranged in size from large single populations (1,141 participants) [Kiel et al. 2007] to large consortia of multiple single studies. One of the largest consortia for studies of osteoporosis and bone-related traits is the Genetic Factors for Osteoporosis (GEFOS) Consortium, a collaboration of researchers from Australia, Canada, China, Greece, Iceland, the Netherlands, Sweden, the United Kingdom and the United States who are interested in identifying the common risk gene variants for osteoporosis. In 2009 the GEFOS Consortium analyzed data on areal BMD of the spine and femoral neck in 19,195 Northern Europeans and identified single-nucleotide polymorphisms (SNPs) in 20 loci associated with these two traits (Rivadeneira et al.). The consortium is currently completing a larger GWAS of lumbar spine and femoral neck bone mineral density in 34,191 individuals from multiple studies

with replication of significant and suggestive loci in an additional 50,933 subjects (bone mineral density) and 31,016 fracture cases and 102,444 controls [Estrada et al. 2010a,b, 2011].

In this chapter, I present the results of my contributions to the Consortium's efforts—GWA studies of areal BMD of the femoral neck and lumbar spine in European American participants in the Dynamics of Health, Aging, and Body Composition (HealthABC) study, which were part of the current GEFOS discovery cohort. I also present results of GWA studies of fracture risk in these subjects, which were part of the GEFOS fracture follow-up case and control cohorts. Finally, I report on the results of replication and fine mapping of twenty previously identified loci [Rivadeneira et al. 2009] in HealthABC using SNPs imputed from 1000 Genomes Project data [Abecasis et al. 2010].

4.2 METHODS

4.2.1 Study Population

The Dynamics of Health, Aging and Body Composition Study (HealthABC) is a multicenter longitudinal study of changes in body composition among older men and women ascertained to be disability-free at baseline. The study population comprises 3,075 men and women, ages 70–79 years. Approximately a third of the men ($n = 488$) and half of the women ($n = 651$) are African American; the remainder, European American ($n = 1,663$; Table 4.1). Subjects were recruited in Pittsburgh, Pennsylvania, and Memphis, Tennessee. Individuals in HealthABC were designated as European Americans or African Americans based on eigenanalyses of their genotypes, including ancestry informative markers. These analyses were performed by my colleagues at Wake Forest University. The current GWA analyses were done using data on European Americans (784 women and 879 men).

The institutional review boards at both clinical centers approved the study, and all participants provided written informed consent.

4.2.2 Bone Mineral Density

Areal bone mineral density (BMD) was measured using dual-energy x-ray absorptiometry (DXA) scans of the whole body and proximal femur as described in Section 1.5.2.1. Femoral neck BMD

(FNBMD) was available for 868 European American men and 775 European American women. Lumbar spine BMD (LSBMD) was available for 870 European American men and 778 European American women.

4.2.3 Fractures

Fracture incidents for HealthABC participants were recorded after the individuals were enrolled in the study. Fracture sites (e.g., pelvis or femur), fracture types (fragility, traumatic, pathologic, stress, other and unknown) and age at fracture for each incident were recorded. For the current analyses, two classes of fractures were defined: “all types” and “non-vertebral.” “All types of fracture” cases included individuals who had any fractures during the study excluding fractures that resulted from excessive trauma and fractures of the fingers, toes and skull. No medical records nor radiographic evidence were required for this category. Non-vertebral fracture cases included subjects who had any fractures during the study except those as a result of excessive trauma and those of the fingers, toes, skull and vertebrae. Radiographic evidence was required for this category.

4.2.4 Genotyping and Imputation

Genotyping of the HealthABC participants was performed by the Center for Inherited Disease Research (CIDR) using the Illumina Human1M-Duo BeadChip system. The following quality control measures were implemented: All data on individual samples were removed from the data if the genotyping for the sample failed overall ($< 97\%$ SNPs genotyped), if the chromosome sex did not match the reported sex or if first-degree relatedness was detected using the single-nucleotide polymorphism (SNP) data. All data on specific SNPs were removed from the data file if the SNP had a minor allele frequency (MAF) $\leq 1\%$, was called with $\leq 97\%$ success, or had a Hardy–Weinberg equilibrium (HWE) test p value $\leq 10^{-6}$. A total of 1,151,215 autosomal SNPs were successfully genotyped in 1,663 European American individuals and were carried forward to imputation.

Imputation was performed using MACH 1.0.16 [Li et al. 2010b] and the HapMap II phased haplotypes [Frazer et al. 2007] as the reference. Genotypes were available for 914,263 SNPs based on the HapMap Centre d’Étude du Polymorphisme Humain (CEPH) reference panel (rel. 22, b36).

A total of 2,543,887 genotyped and imputed autosomal SNPs were ultimately available for analysis as part of the “HapMap SNP” set.

A total of 40,591 chromosome X SNPs were successfully genotyped in all European Americans subjects. An additional 37,607 SNPs were imputed using a method similar to that used for the autosomes for a total of 78,198 chromosome X SNPs. The chromosome X SNPs were included in the “HapMap SNP set” for a total of 2,622,085 SNPs.

Follow-up studies and fine mapping were done using data from a second set of 6,858,264 genotyped and imputed autosomal SNPs that were available as part of the “1000 Genomes SNP set.” Approximately 1.2 million SNPs (autosome and X-chromosome) were successfully genotyped and available on 1,663 European American subjects. The additional ~5.6 million SNPs were imputed using the 1000 Genomes [Abecasis et al. 2010] reference haplotypes (June 2010 release).

The HapMap imputation and initial quality control was performed by Yongmei Liu and Kurt Lohman of Wake Forest University. The 1000 Genomes imputation was performed by Michael Nalls of the National Institutes of Health.

4.2.5 Statistical Analysis

4.2.5.1 Association analysis methods Three analyses were performed for each trait: men only, women only, and both sexes together (pooled-gender).

For FNBMD and LSBMD, residuals of each untransformed trait were generated in men and women separately. To maintain consistency across all studies participating in GEFOS, the following covariates were incorporated into the linear regression model for BMD: age, age squared, weight, clinical site and ancestry principal components (PCs). For the pooled-gender analyses, the residuals from the men and the women were combined.

For the fractures, logistic regression was performed with age, age squared, weight, standing height, clinical site and ancestry PCs as covariates. For the pooled-gender analyses, sex was also included as a covariate. These analyses were performed using R 2.11.1 [R Development Core Team 2008].

Regression analyses were performed using additive allele-dosage models in ProbABEL 0.1-3 [Aulchenko et al. 2010]. ProbABEL allows for the use of imputation-generated genotypic probabil-

ities in regression analysis without constraining the AA/AB/BB genotypes to 1/0/0, 0/1/0 or 0/0/1. Sandwich standard errors (SE) were calculated to control for inflation caused by small population size and low allele frequencies. The association results were filtered for imputation quality ($r^2 > 0.3$) [Li et al. 2010b] and minor allele frequency ($> 5\%$) to remove low quality and rare SNPs that could produce spurious results. The genomic control correction factor λ [Devlin and Roeder 1999; Bacanu et al. 2002] was calculated for each of the four traits in each of the three analysis groups (men, women and pooled-gender) from the p values with the lowest decile removed using the GenABEL [Aulchenko et al. 2010] package in R. Odds ratios (OR) for fracture risk were calculated as e^β . The upper and lower 95% confidence intervals were calculated as $e^{\beta \pm z_{97.5\%} SE}$.

The thresholds for significance and suggestiveness of associated loci, $p < 5 \times 10^{-8}$ and $p < 5 \times 10^{-6}$ respectively, will be used here [Frazer et al. 2007; Pe'er et al. 2008]. These are the same thresholds used in the GEFOS consortium analyses. Similarly, “associated” loci were defined as regions 1 Mb up- and downstream of SNPs with the most significant p values (“peak SNPs”).

4.2.5.2 Statistical power Power of the GWA analyses for the HealthABC cohort was estimated using QUANTO 1.2.4 [Gauderman and Morrison 2006]. For the quantitative BMD traits, power was modeled to detect a SNP that accounted for 0.5% of residual variance of a trait. This parameter was chosen based upon the results of Rivadeneira et al. [2009]. For the discrete fracture traits, power was modeled to detect an odds ratio of 1.5 with a population prevalence of 15%. These parameter choices are based upon the typical odds ratios reported for GWAS (www.genome.gov/gwastudies); the population prevalence is based upon the non-vertebral fracture incidence observed in HealthABC.

4.2.5.3 Replication and fine mapping In addition to the GWAS described above, the 20 previously identified loci [Rivadeneira et al. 2009] were examined for associations with FNBMD and LS-BMD in the HealthABC cohort. The most significant SNP at each locus, as reported by Rivadeneira et al., was taken as the midpoint of a 2 Mb region. The 1000 Genomes SNPs within each region were tested for association, in the pooled-gender residual sets only, using ProbABEL as above. The $-\log_{10}$ -transformed p values for each SNP vs physical position for the interesting loci presented

below were annotated with recombination rates and gene positions using LocusZoom 1.1 [Pruim et al. 2010].

4.3 RESULTS

4.3.1 Subject Characteristics

Characteristics of the European American subjects in the HealthABC study are presented in Table 4.1, and differences between women and men were assessed using t tests, Wilcoxon rank sum tests or χ^2 tests as appropriate. Women and men in the study had similar ages (73.6 years vs 73.9 years respectively), rates of smoking (7.7% vs 5.2% respectively), activity levels, (85.8 vs 82.7 kcal/kg/wk respectively) as well as rates of hypertension (45.4% vs 42.1%, respectively) and cardiovascular disease (7.6% vs 7.2% respectively). Compared to women, men were significantly ($p < 10^{-8}$ for all) taller, heavier and had larger waist circumferences and body mass indices (BMIs). The men also drank more than women (45.1% vs 29.1%) and had nearly twice the prevalence of diabetes (14.0% vs 7.6%). Arthritis was almost twice as common in women as men (15.1% vs 8.7%). The differences in height, weight, waist circumference, BMI, alcohol consumption, diabetes prevalence and arthritis prevalence were statistically significant (all $p < 0.001$).

Both measures of areal BMD were greater in men (FNBMD and LSBMD each $p < 2.2 \times 10^{-16}$). Fracture incidence was greater in women (all fractures $p = 1.56 \times 10^{-11}$; non-vertebral fractures $p = 6.10 \times 10^{-10}$).

4.3.2 Genomewide Association Analysis of Bone Mineral Density

Genomewide association analysis was performed in 868 men and 775 women with measured FNBMD and in 870 men and 778 women with measured LSBMD using 2,622,085 genotyped and HapMap-imputed SNPs. Between 410,334 and 412,055 SNPs were removed to due poor imputation quality or small minor allele frequencies, leaving between 2,210,030 and 2,211,751 SNPs available for analysis. (Different numbers of SNPs were available for each analysis due to MAF differences among the groups.) After performing quality control, I calculated the genomic control inflation fac-

Table 4.1: HealthABC Population Characteristics

Characteristic	Men (<i>n</i> = 879)		Women (<i>n</i> = 784)		<i>p</i>
	mean/ <i>n</i>	SD/%	mean/ <i>n</i>	SD/%	
Age (yr)	73.9	2.9	73.6	2.8	0.056
Anthropometric					
BMI (kg/m ²)	27.1	3.7	26.1	4.5	4.60 × 10 ⁻⁸
Waist circumference (cm)	101.9	11.7	96.1	12.4	< 2.20 × 10 ⁻¹⁶
Height (cm)	173.6	6.4	159.4	5.8	< 2.20 × 10 ⁻¹⁶
Weight (kg)	81.6	12.4	66.4	12.1	< 2.20 × 10 ⁻¹⁶
Lifestyle					
Current smoking	46	5.2%	60	7.7%	0.056
Alcohol (> 1 drink/week)	396	45.1%	228	29.1%	2.97 × 10 ⁻¹¹
Activity (kcal/kg/week)	82.7	64.9	85.8	63.5	0.112
Medical conditions					
Hypertension	370	42.1%	356	45.4%	0.194
Diabetes	123	14.0%	60	7.6%	3.92 × 10 ⁻⁵
Cardiovascular disease	63	7.2%	60	7.6%	0.838
Arthritis	76	8.7%	118	15.1%	7.41 × 10 ⁻⁵
BMD					
Femoral neck (g/cm ³)	766.0	126.4	650.1	108.7	< 2.20 × 10 ⁻¹⁶
Lumbar spine (g/cm ³)	1079.7	206.0	913.5	174.3	< 2.20 × 10 ⁻¹⁶
Fracture Incidence					
All types of fractures	109	12.4%	199	25.4%	1.56 × 10 ⁻¹¹
Non-vertebral fractures	88	10.0%	165	21.1%	6.10 × 10 ⁻¹⁰

SD = standard deviations

tor λ for each analytical group and trait; these values ranged from 1.01 to 1.02, which is within the acceptable range for GWAS studies (Table 4.2). The quantile–quantile (QQ) plots of the FNBMD and LSBMD pooled-gender analysis are presented in Figures 4.1 and 4.2. The striking deviation from the expected slope in the QQ plot of p values for the FNBMD analysis (Figure 4.1) is eliminated when the 72 SNPs on chromosome 3p24.1 with p values $\leq 5 \times 10^{-6}$ are removed; this locus is discussed further below. Finally, I calculated the power to detect SNPs that account for 0.5% of the residual phenotypic variance in the HealthABC cohort at two significance levels, $p \leq 5 \times 10^{-6}$ (for suggestive association) and $p \leq 5 \times 10^{-8}$ (for significant association). As expected because of its sample size, the HealthABC cohorts had low power to detect associations (Table 4.2).

Table 4.2: European American BMD Analyses

Trait	Sex	n		Power*		λ
		Samples	SNPs	$p = 5 \times 10^{-8}$	$p = 5 \times 10^{-6}$	
FNBMD	Men	868	2,211,751	0.0004	0.0066	1.02
	Women	775	2,210,047	0.0003	0.0047	1.01
	Pooled	1,643	2,211,517	0.0049	0.0450	1.02
LSBMD	Men	870	2,211,717	0.0004	0.0066	1.02
	Women	778	2,210,030	0.0003	0.0048	1.01
	Pooled	1,648	2,211,496	0.0050	0.0455	1.01

*Additive model, $R^2 = 0.005$

The results of the GWA analyses of FNBMD and LSBMD overall, and in men and women separately are presented as Manhattan plots in Figures 4.3, 4.4 and in Figures E1–E4 in Appendix E. Of the 13,266,558 tests performed for the two BMD phenotypes examined in three groups (men, women and pooled-gender), 192 tests of 189 SNPs in 28 loci reached the suggestive threshold of 5×10^{-6} . None reached the genomewide significance threshold of 5×10^{-8} . Across both phenotypes and all groups, the most significant 26 autosomal and 2 X-chromosomal SNPs per locus are listed in Table 4.3. Two regions, 13q33.3 and 16q21 (Figure G19 and Figures G23 and G24 respectively), showed suggestive association with both LSBMD and FNBMD. In fact, for the 13q33.3 region, the same SNP, *rs17382033*, had the minimal p value for both traits [FNBMD ($p = 1.33 \times 10^{-7}$) and LSBMD ($p = 2.23 \times 10^{-6}$)]. This SNP is within 80 kb of *TNFSF13B*, a member of the tumor necrosis factor superfamily. In contrast, the suggestive association in the 16q21 region may be attributable to two different loci 4.5 Mb apart. The SNP associated with LSBMD in men is closest to *NDRG4*

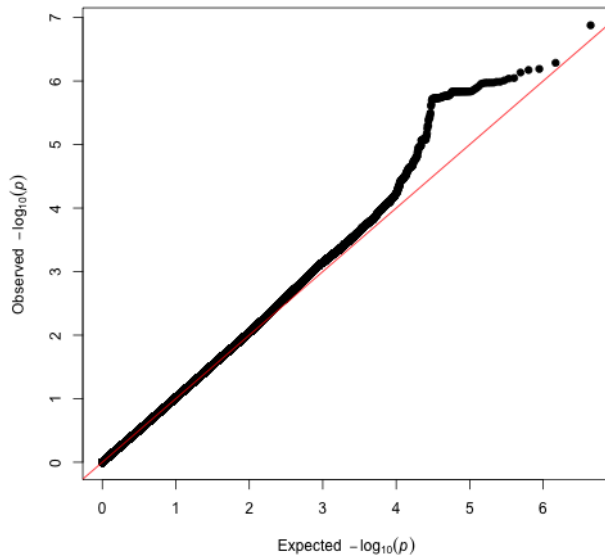


Figure 4.1: QQ Plot FNBMD Pooled*

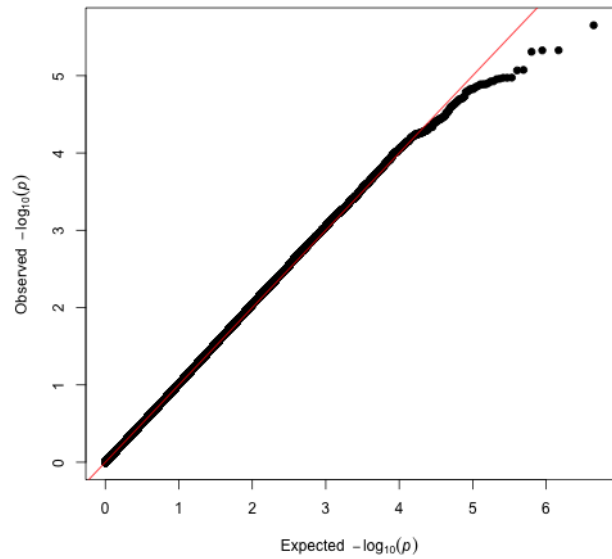


Figure 4.2: QQ Plot LSBMD Pooled

* “Pooled” here refers to the pooled-gender analyses.

(*N-myc* downstream regulated gene family member 4), whereas the SNP associated with FNBMD overall is closest to *CDH8* (cadherin 8, type 2). A complete list of the 188 results with p values less than 5×10^{-6} can be found Tables F1–F6 in Appendix F.

Plots of the $-\log_{10}$ -transformed p values against the physical positions within each of the 28 loci are presented in Figures G1–G28 in Appendix G. A complete list of the 192 tests with p values less than 5×10^{-6} can be found in Tables F1–F6 in Appendix F.

None of the 26 autosomal loci seen here overlap with the 20 loci reported by Rivadeneira et al. [2009]. This is not surprising given my power to detect the effect sizes reported in the GEFOS study ($-0.120 < \beta < 0.107$); there was just 13% power to detect the largest effect size ($\beta = -0.120$ for *rs9533090* [Rivadeneira et al. 2009]) associated with a SNP with a MAF of 50% at $p = 5 \times 10^{-6}$ with the pooled-gender sample. Additionally, differences in genetic background and environmental factors could account for differences in associations between reported SNPs and the examined traits.

One way to assess whether the same or different genes in an associated region influence one or more traits (for example, the 16q21 region) is to plot all SNP associations across a region. Such plots may also facilitate fine mapping, and perhaps identification, of possible functional SNPs. To gain

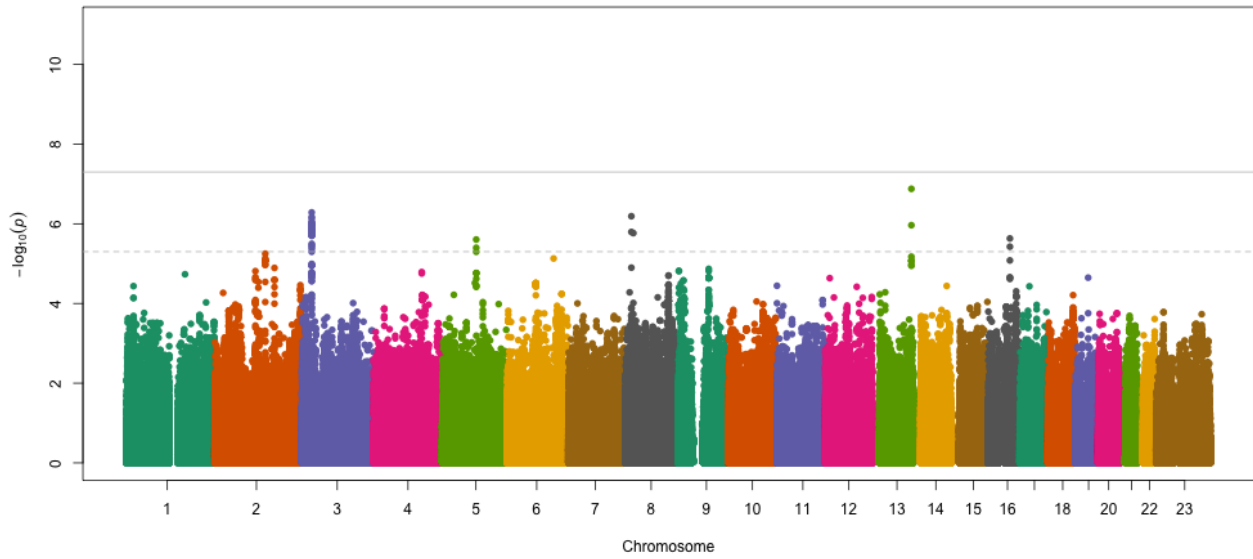


Figure 4.3: Manhattan Plot FNBMD Pooled

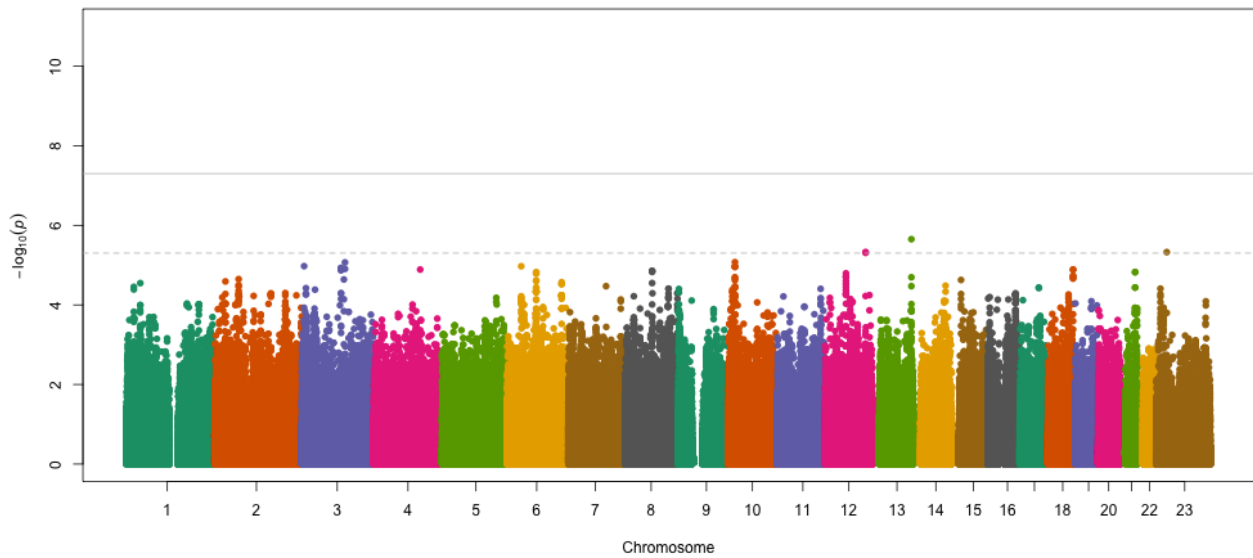


Figure 4.4: Manhattan Plot LSBMD Pooled

Table 4.3: BMD Loci – European Americans

Locus	SNP	Position	Nearest Gene	Distance (kb)	Alleles	MAF	Type	β	SE	p	Trait
1q23.1	rs2054993	156772592	OR6Y1	10.9	G/T	0.44	I	-0.239	0.050	1.92×10^{-6}	FNM
2q36.3	rs13010707	227250306	IRS1	54.0	C/T	0.13	I	-0.356	0.075	2.09×10^{-6}	LSM
2q37.3	rs6718108	240102747	HDAC4	115.2	A/G	0.33	G	0.252	0.055	4.98×10^{-6}	LSW
3p24.1	rs11717372	27202560	NEK10	29.5	G/A	0.26	I	0.202	0.040	5.17×10^{-7}	FNP
3p14.1	rs9813487	69115174	C3orf64	0.0	T/C	0.20	I	0.290	0.062	3.08×10^{-6}	LSM
4p16.1	rs10804984	6700002	MRFAP1	4.7	C/A	0.32	I	0.278	0.057	1.12×10^{-6}	LSW
5q14.3	rs2973839	91112451	LOC100129716	360.2	A/G	0.11	I	0.354	0.077	3.63×10^{-6}	FNM
5q15	rs3909479	94813710	FAM81B	1.8	C/T	0.10	G	-0.272	0.058	2.48×10^{-6}	FNP
5q32	rs318373	143300064	HMHB1	119.6	T/C	0.47	G	-0.248	0.053	3.09×10^{-6}	LSW
6p25.1	rs736004	5067728	LYRM4	0.0	C/T	0.10	G	-0.422	0.088	1.56×10^{-6}	FNW
7q21.11	rs1397005	80718618	SEMA3C	332.0	A/G	0.28	G	0.271	0.059	4.26×10^{-6}	LSW
7q34	rs10954649	138789091	KLRG2	0.0	C/T	0.35	G	-0.247	0.052	1.87×10^{-6}	FNM
8p22	rs13252590	16566118	FGF20	328.6	A/T	0.47	I	0.174	0.035	6.45×10^{-7}	FNP
8p21.3	rs12114940	22104735	BMP1	0.0	T/G	0.45	G	0.173	0.036	1.71×10^{-6}	FNP
8q22.1	rs278530	94279598	LOC642924	148.3	C/T	0.31	G	-0.257	0.056	4.52×10^{-6}	LSW
12q24.13	rs12309051	112610534	RBM19	128.4	C/T	0.33	G	-0.171	0.037	4.69×10^{-6}	LSP
12q24.31	rs12578256	123368433	FAM101A	1.9	T/A	0.18	I	-0.296	0.063	2.33×10^{-6}	LSM
13q33.1	rs640960	100560051	NALCN	0.0	C/T	0.27	G	0.295	0.058	4.26×10^{-7}	LSW
13q33.3	rs17382033	107839404	TNFSF13B	80.6	C/A	0.09	G	0.329	0.062	1.33×10^{-7}	FNP
14q23.1	rs1113590	61073336	PRKCH	0.0	A/C	0.09	I	0.478	0.091	1.40×10^{-7}	LSW
15q14	rs16962904	34443595	C15orf41	215.5	A/G	0.33	I	-0.284	0.057	7.48×10^{-7}	FNW
15q25.3	rs957029	85753369	NCRNA00052	167.8	G/C	0.23	I	0.296	0.059	4.91×10^{-7}	FNM
16q21	rs11076239	57038674	NDRG4	16.4	G/A	0.32	I	0.247	0.054	4.39×10^{-6}	LSM
16q21	rs2962454	61494729	CDH8	866.5	G/A	0.24	G	0.191	0.040	2.33×10^{-6}	FNP
19q12	rs2190800	33143105	LOC148189	166.4	T/G	0.42	G	0.229	0.049	3.21×10^{-6}	FNM
19q13.11	rs8109254	37388860	ZNF507	139.5	A/C	0.05	I	0.514	0.111	3.66×10^{-6}	FNM
Xp21.1	rs331360	32169468	DMD	86.0	G/A	0.23	G	-0.176	0.038	3.40×10^{-6}	LSM
Xq28	rs11795763	149755133	CD99L2	0.0	T/C	0.16	I	-0.338	0.069	8.67×10^{-7}	FNW

Alleles are given in the form: major allele/minor allele. The minor allele is modeled as the effect allele. FNP = femoral neck BMD pooled. FNM = femoral neck BMD in men. FNW = femoral neck BMD in women. LSP = lumbar spine BMD pooled. LSM = lumbar spine BMD in men. LSW = lumbar spine BMD in women. SNP types: G = genotyped; I = imputed.

insights into the genetic architecture of the suggestive regions of association, including information on recombination and linkage disequilibrium, as well as associations with additional imputed SNPs, I plotted the $-\log_{10}$ -transformed p values for each SNP in each region against the physical positions within each of the 28 loci (Figures G1–G28 in Appendix G). Although none of these regions obtained genomewide significance, I present results from the 3p24.1 region to illustrate this process. The most significant SNP in the 3p24.1 locus is *rs11717372* (Figure 4.5). This locus was also examined in the 1000 Genomes SNP set, and the results are presented in (Figure 4.6). Seventy-one additional HapMap SNPs in this region have p values less than 5×10^{-6} , and all are in linkage disequilibrium with *rs11717372* ($r^2 > 0.834$, $D' > 0.947$). The nearest gene to *rs11717372* is *NEK10* (never in mitosis a (NIMA)-related kinase 10), 29.5 kb distal to the SNP. The remaining correlated SNPs stretch from this most significant SNP to approximately the midpoint of the gene. The addition of the 1000 Genomes SNPs does not narrow the associated region.

4.3.3 Genomewide Association Analysis of Fracture Risk

Among the 1,661 individuals for whom data were available, 308 individuals had fractures and 253 had non-vertebral fractures. Starting with a total of 2,608,508 genotyped and HapMap-imputed SNPs available on these individuals, 368,264 SNPs were removed due to low imputation quality or rarity, leaving 2,240,244 SNPs available for continued analysis. Genomic control inflation factors were acceptable, λ ranged from 1.00 to 1.02 (Table 4.4), and inspection of the quantile–quantile plots of the FNBMD and LSBMD pooled analysis revealed no concerns (Figures 4.7 and 4.8). As with the analyses of the areal BMD traits, I had limited power to detect significant associations in the HealthABC cohort.

The results of the GWA analyses of the all fractures and non-vertebral fractures pooled-gender analyses are presented in Figures 4.9 and 4.10. Plots of the analyses in men and women can be found in Figures E5–E8 in Appendix E. Of the 13,441,464 statistical tests executed for the two definitions of fractures examined in three sets (men, women and pooled-gender), 51 tests of 49 SNPs in 20 loci reached the suggestive threshold of 5×10^{-6} . Of those, 9 tests in 9 SNPs at 1 locus reached the genomewide significance threshold of 5×10^{-8} . All nine of these SNPs are located on 9q31.3, are in high LD ($r^2 = 1$) and have low MAFs of 0.062–0.064. The low MAF, and so small numbers in the

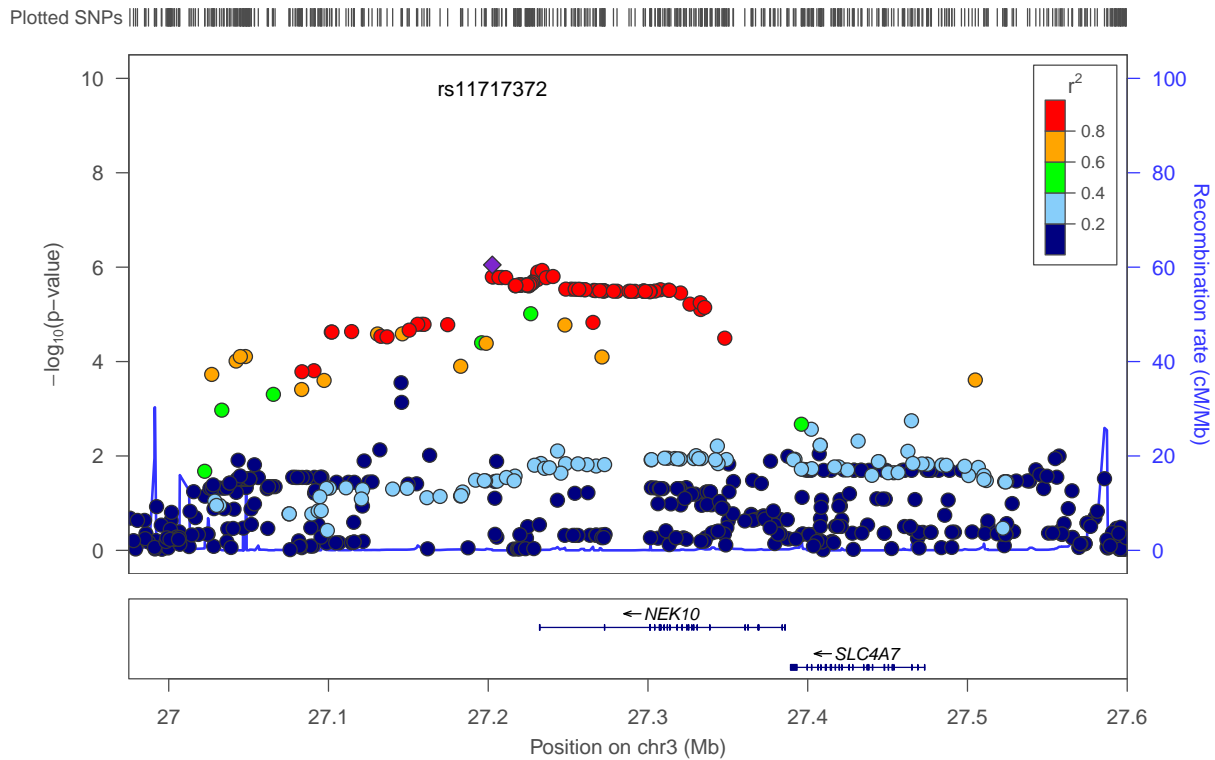


Figure 4.5: Association between FNBMD and HapMap SNPs around *rs11717372* (3p24.1)

This figure displays the SNPs between putative recombination hotspots at 27.0 Mb and 27.8 Mb. The SNP with the lowest p value in the analysis at this locus is denoted by a purple diamond. The other SNPs are color-coded according to correlation (HapMap Phase II CEU) with the most significant SNP, from red indicating $0.8 < r^2 < 1.0$ to dark blue indicating $0.0 < r^2 < 0.2$. Known genes, with their exon, introns and orientation notes are plotted below the SNPs. HapMap recombination rates (cM/Mb) are plotted as a blue line behind the SNPs. SNP coverage is noted by tick marks above the plot.

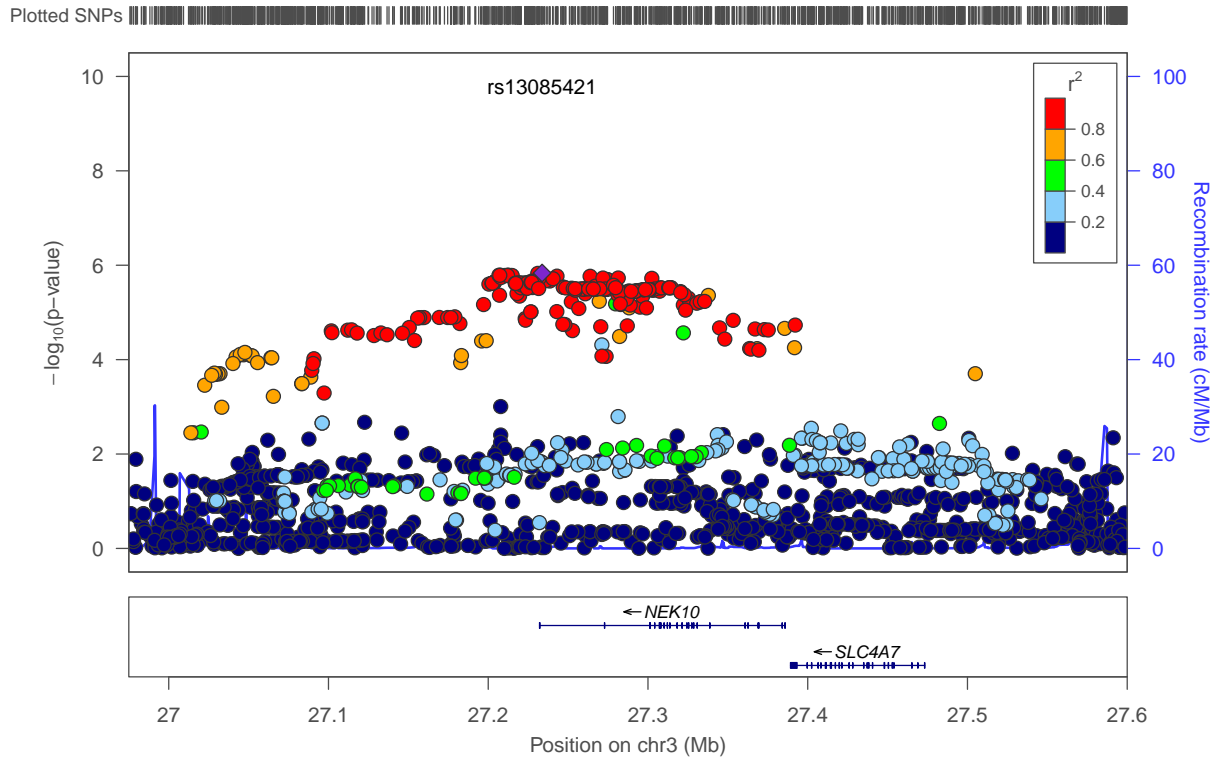


Figure 4.6: Association between FNBMD and 1000 Genomes SNPs around *rs11717372* (3p24.1)

This figure displays the SNPs between the same putative recombination hotspots at 27.0 Mb and 27.8 Mb as Figure 4.5. The SNP with the lowest p value in the analysis at this locus is denoted by a purple diamond. The other SNPs are color-coded according to correlation (1000 Genomes June 2010 CEU) with the most significant SNP, from red indicating $0.8 < r^2 < 1.0$ to dark blue indicating $0.0 < r^2 < 0.2$. Known genes, with their exon, introns and orientation notes are plotted below the SNPs. HapMap recombination rates (cM/Mb) are plotted as a blue line behind the SNPs. SNP coverage is noted by tick marks above the plot.

Table 4.4: European American Fracture Analyses

Trait	Sex	<i>n</i>			Power at odds-ratio = 1.5						λ
					$p = 5 \times 10^{-8}$			$p = 5 \times 10^{-6}$			
		Cases	Controls	SNPs	0.05*	0.25*	0.50*	0.05*	0.25*	0.50*	
All Types	Men	109	769	2,240,896	0.0000	0.0017	0.0037	0.0006	0.0201	0.0367	1.00
	Women	199	584	2,240,896	0.0001	0.0098	0.0231	0.0017	0.0741	0.1340	1.00
	Pooled	308	1,353	2,240,896	0.0005	0.0829	0.1697	0.0075	0.3087	0.4726	0.99
Non-Vertebral	Men	88	790	2,240,896	0.0000	0.0008	0.0017	0.0004	0.0115	0.0208	1.00
	Women	165	618	2,240,896	0.0000	0.0058	0.0135	0.0012	0.0506	0.0924	1.01
	Pooled	253	1,408	2,240,896	0.0003	0.0457	0.0979	0.0048	0.2115	0.3419	1.00

* Minor allele frequency

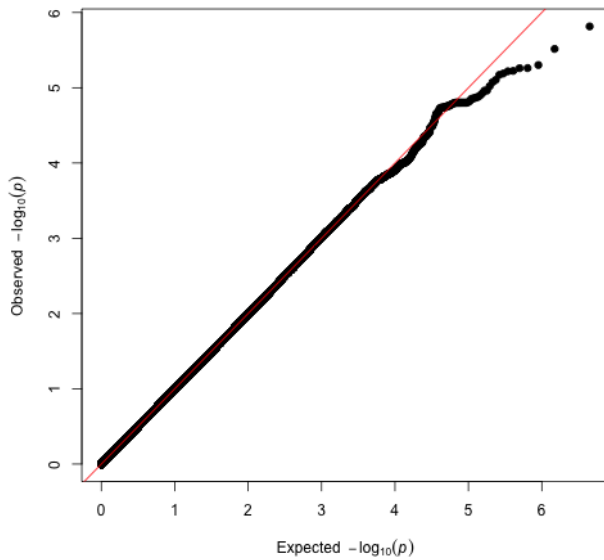


Figure 4.7: QQ Plot All Fractures Pooled*

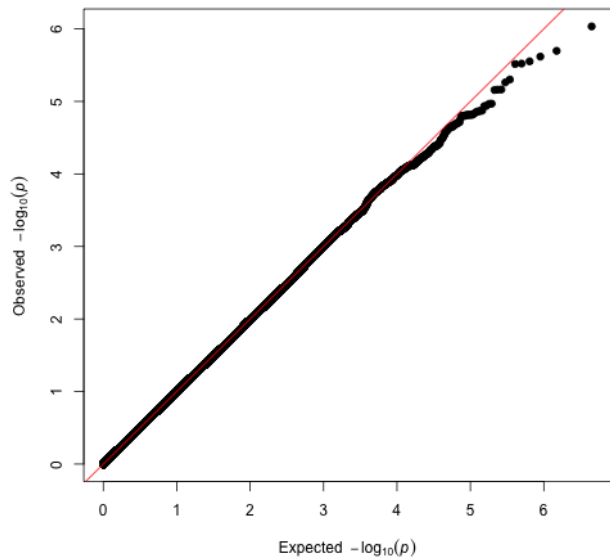


Figure 4.8: QQ Plot Non-Vert. Fractures Pooled

* "Pooled" here refers to the pooled-gender analyses.

minor-allele homozygote class, suggests that this result may be spurious [Lam et al. 2007; Tabangin et al. 2009]. At MAF = 0.06, just one of the fracture cases would be predicted to be homozygous. The 20 most significant SNPs per locus and phenotype/group are given in Table 4.5 and a complete list of the 51 tests with p values less than 5×10^{-6} can be found in Appendix F Tables F7–F12. Also, for each of the 20 suggestive regions, plots of the $-\log_{10}$ -transformed p values against the physical positions for all SNPs within each of the 20 regions were made (Figures H1–H20 in Appendix H.) None of these plots are notable, especially because none of the 28 potential candidate loci for BMD (Table 4.3) are significantly associated with either fracture trait (data not shown). Thus, none of the 28 potential candidate loci show clinical significance in this analysis.

4.3.4 Replication of GEFOS Results

In the current analytical setting, I would not expect to publish results from a GWAS of the HealthABC cohort because of its small sample size. However, this cohort could be used for replication and possibly fine mapping of consortium results. To this end, a total of 96,842 1000 Genomes SNPs in 20 previously identified candidate loci [Rivadeneira et al. 2009] were tested for association with FNBMD and LSBMD. After employing the same exclusion criteria described in the previous two sections to remove poorly imputed and rare variants, 74,246 SNPs—an average of 3,712 per locus—remained for analysis. Results of the replication analysis of the most significant SNP at each of the 20 loci observed by Rivadeneira et al. are given in Table 4.6.

Plots of the results of the replication analysis for all 20 loci are presented in Figures I1–I20 in appendix I. The best examples of replication are for *CTNNB1* (β -catenin), *ESR1* and *TNFRSF11B* (Figures 4.11, 4.12 and 4.13, respectively; see also Figures I4, I7 and I10). For Figures 4.11–4.13 the purple diamond indicates the replicated SNP rather than the most significant SNP on the plot.

The SNP with the greatest significance reported by Rivadeneira et al. near *CTNNB1* is *rs87938* for FNBMD, for which I observe a p value of 3.01×10^{-4} for LSBMD and 0.022 for FNBMD in the HealthABC participants. Nearby SNPs show greater significance in HealthABC, with *rs62259232*, 30.5 kb proximal to *rs87938*, giving a p value of 3.12×10^{-5} for LSBMD. Rivadeneira et al. reported associations of both FNBMD and LSBMD with SNPs near *ESR1*. The peak SNP observed in that study (*rs2504063*) is not significant in HealthABC ($p = 0.296$ for LSBMD; $p = 0.133$ for FNBMD).

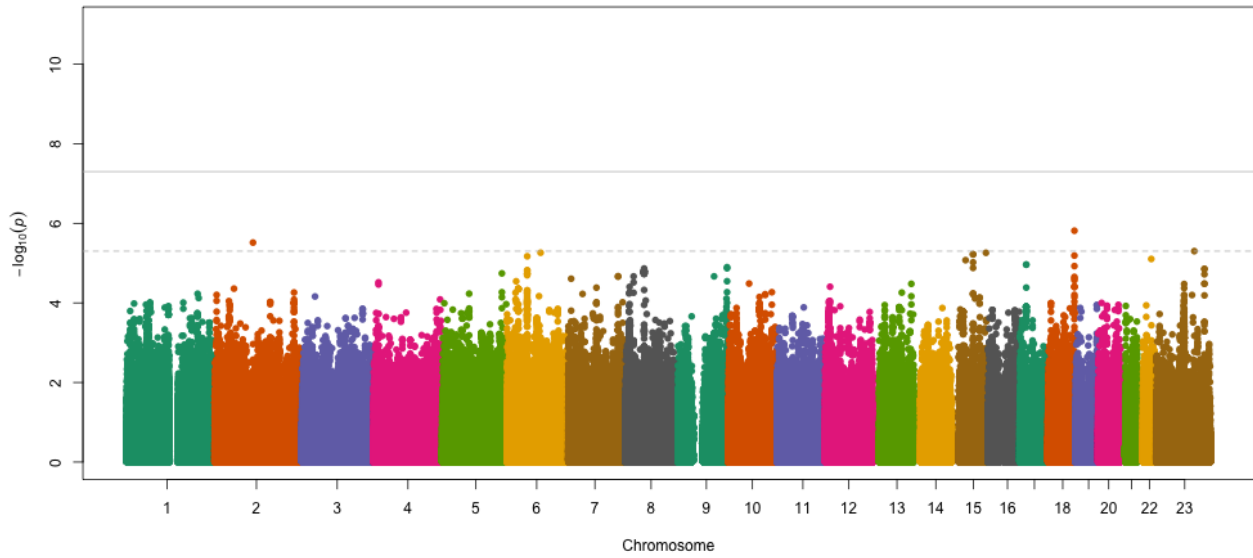


Figure 4.9: Manhattan Plot All Fractures Pooled

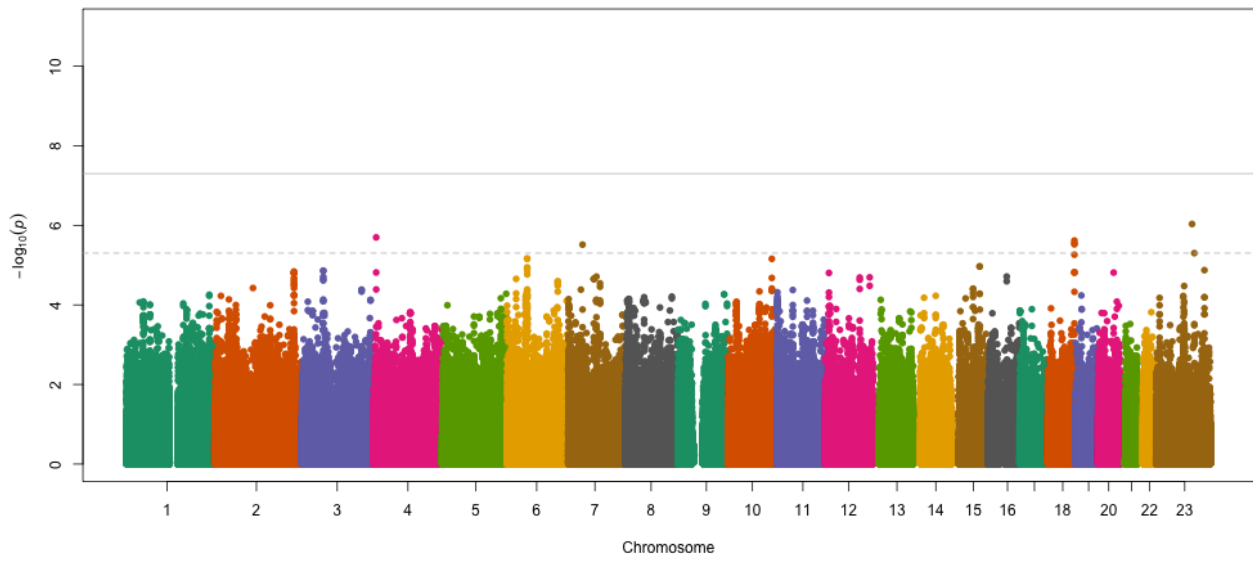


Figure 4.10: Manhattan Plot Non-Vertebral Fractures Pooled

Table 4.5: Fracture Loci – European Americans

Locus	SNP	Position	Nearest Distance		Alleles	MAF	Type	OR	95%CI	<i>p</i>	Trait
			Gene	(kb)							
2p24.1	<i>rs7567544</i>	20256283	<i>SDC1</i>	7.8	G/C	0.45	I	0.52	(0.40, 0.68)	3.10×10^{-6}	AFW
2q12.2	<i>rs7575679</i>	106373899	<i>PLGLA</i>	0.0	G/A	0.13	I	2.51	(1.71, 3.70)	3.05×10^{-6}	AFP
3p14.3	<i>rs9654002</i>	54461737	<i>ESRG</i>	179.5	A/C	0.37	I	2.54	(1.70, 3.79)	4.82×10^{-6}	NVM
3q24	<i>rs6809471</i>	146615470	<i>PLOD2</i>	654.4	G/A	0.32	G	0.41	(0.29, 0.58)	3.11×10^{-7}	AFM
4p16.1	<i>rs6849590</i>	7483478	<i>PSAPL1</i>	0.0	G/A	0.26	G	0.55	(0.44, 0.71)	2.01×10^{-6}	NVP
4q34.2	<i>rs17688188</i>	177708053	<i>VEGFC</i>	133.6	G/A	0.26	I	1.82	(1.41, 2.35)	4.33×10^{-6}	AFW
6p21.31	<i>rs9368834</i>	34968742	<i>ANKS1A</i>	0.0	T/G	0.11	G	2.74	(1.81, 4.14)	1.67×10^{-6}	NVM
7p14.1	<i>rs2329399</i>	39508393	<i>POU6F2</i>	37.5	A/C	0.42	G	0.60	(0.49, 0.74)	3.05×10^{-6}	NVP
7q36.3	<i>rs288746</i>	155299433	<i>SHH</i>	1.7	A/G	0.12	G	2.51	(1.70, 3.69)	3.26×10^{-6}	NVM
8p23.1	<i>rs4840583</i>	11673355	<i>NEIL2</i>	0.0	C/T	0.46	G	1.80	(1.42, 2.29)	1.52×10^{-6}	AFW
8p21.2	<i>rs10096579</i>	24165000	<i>ADAM28</i>	42.5	G/T	0.15	G	2.15	(1.56, 2.97)	2.99×10^{-6}	NVW
9q31.3	<i>rs10979528</i>	110621948	<i>ACTL7B</i>	34.7	T/G	0.06	I	0.35	(0.26, 0.48)	1.61×10^{-11}	NVM
10p14	<i>rs2296734</i>	7851413	<i>KIN</i>	0.0	G/C	0.43	I	0.45	(0.33, 0.61)	4.64×10^{-7}	AFM
12p13.2	<i>rs2607894</i>	10635183	<i>KLRAP1</i>	0.0	G/T	0.38	G	0.43	(0.31, 0.61)	1.14×10^{-6}	NVM
14q13.1	<i>rs17100963</i>	32932268	<i>NPAS3</i>	0.0	G/A	0.08	G	2.98	(1.96, 4.51)	2.71×10^{-7}	AFM
15q25.3	<i>rs7164422</i>	84331644	<i>AGBL1</i>	154.6	A/G	0.06	G	3.14	(2.00, 4.93)	6.28×10^{-7}	AFM
18q23	<i>rs12955627</i>	73834676	<i>GALR1</i>	723.6	T/C	0.20	I	1.77	(1.40, 2.24)	1.53×10^{-6}	AFP
Xp22.2	<i>rs4073740</i>	12206155	<i>FRMPD4</i>	0.0	G/A	0.24	G	1.75	(1.39, 2.20)	1.57×10^{-6}	NVM
Xq22.2	<i>rs2983097</i>	102552937	<i>NGFRAP1</i>	33.3	A/G	0.06	G	2.04	(1.54, 2.72)	9.25×10^{-7}	NVP
Xq22.3	<i>rs4893537</i>	108857735	<i>ACSL4</i>	0.0	T/C	0.06	G	1.82	(1.41, 2.36)	4.99×10^{-6}	NVP

Alleles are given in the form: major allele/minor allele. The minor allele is modeled as the effect allele. AFP = all fractures pooled. AFM = all fractures in men. AFW = all fractures in women. NVP = non-vertebral fractures pooled. NVM = non-vertebral fractures in men. NVW = non-vertebral fractures in women. SNP types: G = genotyped; I = imputed.

Table 4.6: Replication Analysis of GEFOS BMD SNPs in HealthABC

Locus	SNP	Nearest Gene	Distance (kb)	GEFOS		HealthABC FNBMD			HealthABC LSBMD		
				Trait	β	β	SE	p	β	SE	p
1p36.12	<i>rs7524102</i>	<i>ZBTB40</i>	79.9	LSBMD	0.094	0.042	0.044	3.41×10^{-1}	0.060	0.055	2.77×10^{-1}
1p31.3	<i>rs1430742</i>	<i>GPR177</i>	14.1	LSBMD	0.105	0.005	0.041	9.12×10^{-1}	0.065	0.061	2.83×10^{-1}
2p16.2	<i>rs11898505</i>	<i>SPTBN1</i>	0.0	LSBMD	0.067	0.048	0.038	2.01×10^{-1}	-0.003	0.050	9.51×10^{-1}
3p22.1	<i>rs87938</i>	<i>CTNNB1</i>	103.3	FNBMD	-0.070	-0.077	0.034	2.16×10^{-2}	-0.140	0.039	3.01×10^{-4}
4q22.1	<i>rs1471403</i>	<i>MEPE</i>	7.3	LSBMD	0.068	0.038	0.037	3.01×10^{-1}	-0.014	0.048	7.68×10^{-1}
5q14.3	<i>rs1366594</i>	<i>MEF2C</i>	176.1	FNBMD	-0.085	-0.074	0.033	2.57×10^{-2}	-0.013	0.043	7.53×10^{-1}
6q25.1	<i>rs2504063</i>	<i>ESR1</i>	36.1	LSBMD	-0.078	-0.054	0.036	1.33×10^{-1}	-0.044	0.042	2.96×10^{-1}
7p14.1	<i>rs1524058</i>	<i>STARD3NL</i>	81.7	LSBMD	-0.070	-0.067	0.035	5.86×10^{-2}	-0.133	0.047	4.67×10^{-3}
7q21.3	<i>rs7781370</i>	<i>FLJ42280</i>	0.7	FNBMD	-0.083	-0.066	0.036	6.63×10^{-2}	-0.037	0.046	4.25×10^{-1}
8q24.12	<i>rs2062377</i>	<i>TNFRSF11B</i>	43.0	LSBMD	0.094	0.134	0.034	8.72×10^{-5}	0.114	0.047	1.51×10^{-2}
11p15.2	<i>rs7117858</i>	<i>SOX6</i>	293.5	FNBMD	0.088	0.080	0.043	5.91×10^{-2}	0.048	0.056	3.96×10^{-1}
11p13	<i>rs16921914</i>	<i>DCDC5</i>	73.4	LSBMD	0.077	0.008	0.039	8.36×10^{-1}	0.056	0.047	2.36×10^{-1}
11p11.2	<i>rs7932354</i>	<i>ARHGAP1</i>	0.1	FNBMD	0.073	0.031	0.041	4.47×10^{-1}	-0.017	0.053	7.50×10^{-1}
11q13.2	<i>rs599083</i>	<i>LRP5</i>	0.0	LSBMD	-0.067	-0.074	0.037	4.63×10^{-2}	-0.091	0.046	4.88×10^{-2}
12q13.13	<i>rs2016266</i>	<i>SP7</i>	0.0	LSBMD	0.070	0.011	0.038	7.71×10^{-1}	0.075	0.045	9.48×10^{-2}
13q14.11	<i>rs9533090</i>	<i>AKAP11</i>	54.0	LSBMD	-0.120	0.009	0.035	8.00×10^{-1}	-0.003	0.049	9.49×10^{-1}
16q24.1	<i>rs10048146</i>	<i>FOXL1</i>	95.4	LSBMD	-0.093	-0.041	0.044	3.54×10^{-1}	-0.034	0.059	5.68×10^{-1}
17q21.31	<i>rs228769</i>	<i>HDAC5</i>	0.0	FNBMD	0.081	0.110	0.043	1.09×10^{-2}	0.108	0.053	4.12×10^{-2}
17q21.31	<i>rs9303521</i>	<i>CRHR1</i>	56.4	LSBMD	-0.068	0.043	0.036	2.31×10^{-1}	0.003	0.044	9.39×10^{-1}
18q21.33	<i>rs884205</i>	<i>TNFRSF11A</i>	1.4	LSBMD	-0.078	-0.029	0.040	4.72×10^{-1}	-0.012	0.053	8.27×10^{-1}

The trait and β for each SNP as reported by GEFOS [Rivadeneira et al. 2009] are given for comparison. The same effect alleles that were used in the GEFOS models were also used here.

However, a cluster of SNPs 190 kb centromeric to this reported SNP have much lower p values; the minimum p value is 1.54×10^{-5} for FNBMD. SNPs near *TNFRSF11B* were also associated with both FNBMD and LSBMD in the report by GEFOS. The most significant SNP *rs2062377* also showed good evidence of association in the HealthABC participants, but just for FNBMD ($p = 8.72 \times 10^{-5}$) and not LSBMD ($p = 0.015$). *rs6469792*, 1 kb distal to *rs2062377* was more significant in HealthABC at $p = 1.45 \times 10^{-5}$ for FNBMD.

4.4 DISCUSSION

4.4.1 Association with Bone Mineral Density

In agnostic tests of association between two measures of bone mineral density and genomewide markers in the HealthABC cohort, 27 loci were identified as suggestive based upon a p value threshold of 5×10^{-6} . However, no SNPs reached genomewide significance (5×10^{-8}) and none of these 27 loci overlap with previously identified loci for either BMD or osteoporosis [e.g., Rivadeneira et al. 2009]. Given the low power of this study to detect previously reported effect sizes, this result is not entirely surprising. The effect sizes reported by Rivadeneira et al. [2009] range from -0.120 to 0.107 ($< 0.7\%$ of the residual variance). This study had 13% power to detect the extremes of that range at $p = 5 \times 10^{-6}$. A sample of 4,045 would be necessary to detect this effect size with 80% power (MAF = 0.5, $\beta = -0.120$). Differences in the genetic background and in environmental factors could also result in the lack of association between reported SNPs and traits. Nonetheless, a few of the results are potentially interesting.

The most promising locus of suggestive significance is on 3p24.1 ($p = 5.17 \times 10^{-7}$ for FNBMD (Figure 4.6). A previously identified candidate region lies on 3p22.1, with *CTNNB1* as the highlighted gene in that region [Rivadeneira et al. 2009]. This locus, however, lies 13.9 Mb distal to region with the lowest p value in the HealthABC cohort, and it is unlikely that the HealthABC suggestive SNPs, which lie between recombination hotspots at 27.0 Mb ($r = 30.3$ cM/Mb) and 27.8 Mb ($r = 54.7$ cM/Mb), are showing association with causal variants in the region around *CTNNB1*. The association signals in the HealthABC cohort are closer to the *NEK10* locus. *NEK10* encodes NIMA

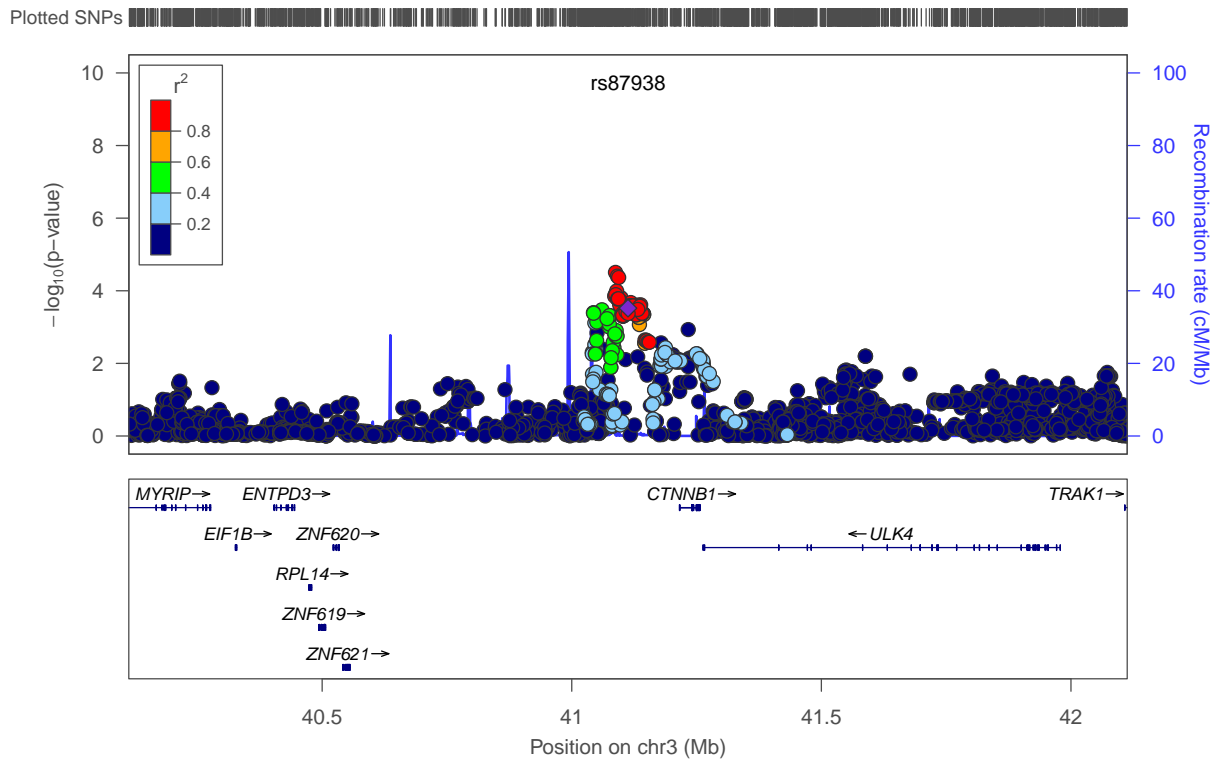


Figure 4.11: Association between LSBMD and 1000 Genomes SNPs around *CTNNB1* (3p22.1)

This figure displays the SNPs within a 2 Mb window centered on *rs87938*, which is denoted by a purple diamond. The other SNPs are color-coded according to correlation (1000 Genomes June 2010 CEU) with the most significant SNP, from red indicating $0.8 < r^2 < 1.0$ to dark blue indicating $0.0 < r^2 < 0.2$. Known genes, with their exon, introns and orientation notes are plotted below the SNPs. HapMap recombination rates (cM/Mb) are plotted as a blue line behind the SNPs. SNP coverage is noted by tick marks above the plot.

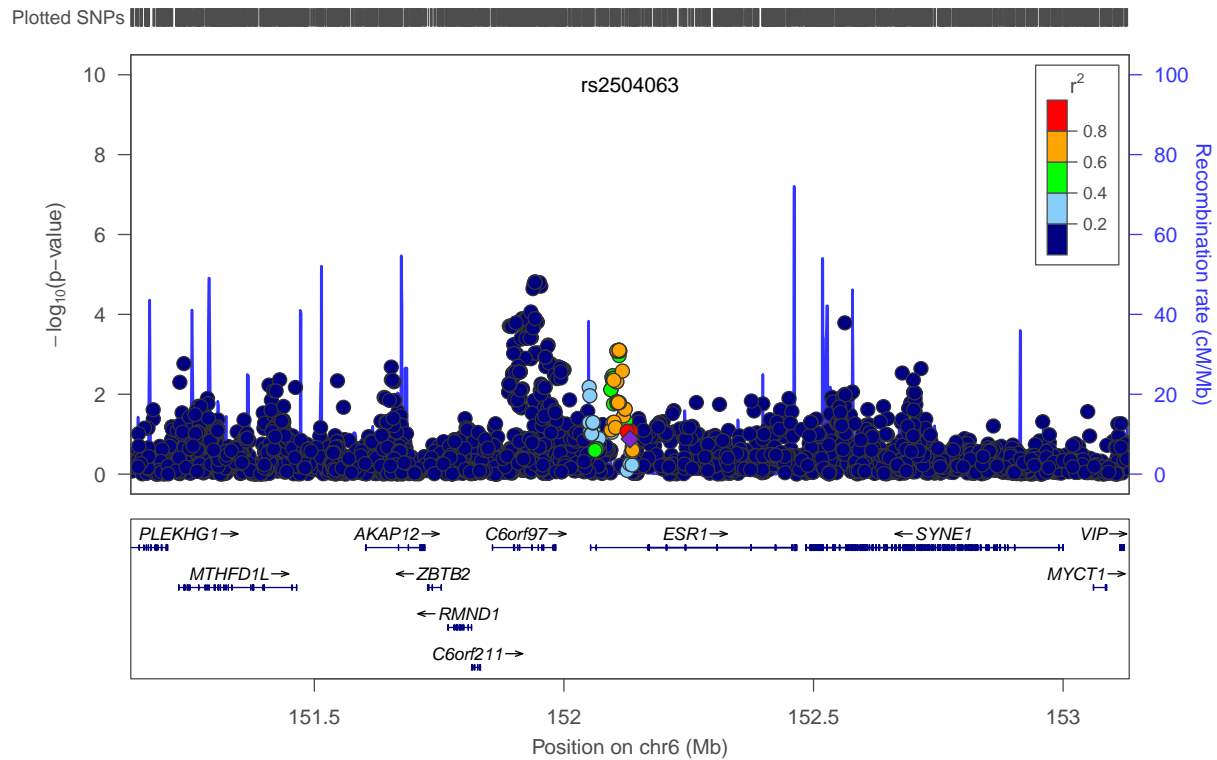


Figure 4.12: Association between FNBMD and 1000 Genomes SNPs around *ESR1* (6q25.1)

This figure displays the SNPs within a 2 Mb window centered on *rs2504063*, which is denoted by a purple diamond. The other SNPs are color-coded according to correlation (1000 Genomes June 2010 CEU) with the most significant SNP, from red indicating $0.8 < r^2 < 1.0$ to dark blue indicating $0.0 < r^2 < 0.2$. Known genes, with their exon, introns and orientation notes are plotted below the SNPs. HapMap recombination rates (cM/Mb) are plotted as a blue line behind the SNPs. SNP coverage is noted by tick marks above the plot.

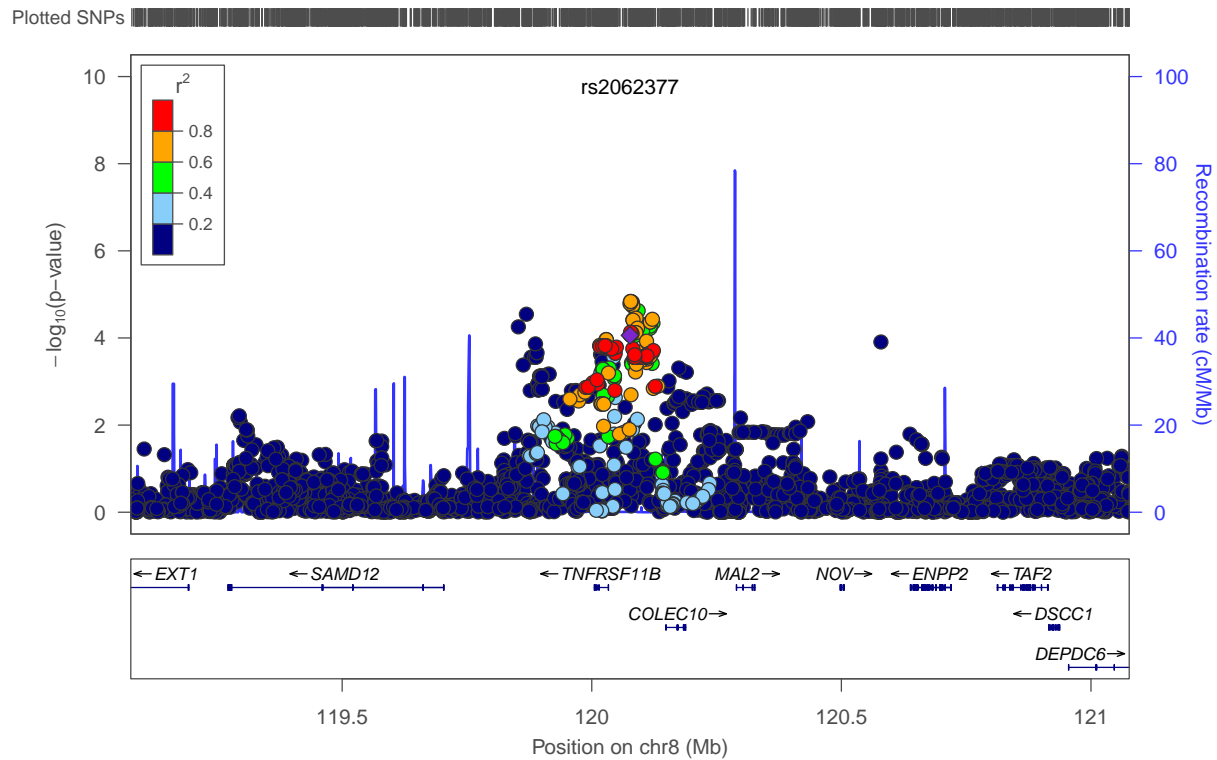


Figure 4.13: Association between FNBMD and 1000 Genomes SNPs around *TNFRSF11B* (8q24.12)

This figure displays the SNPs within a 2 Mb window centered on *rs2062377*, which is denoted by a purple diamond. The other SNPs are color-coded according to correlation (1000 Genomes June 2010 CEU) with the most significant SNP, from red indicating $0.8 < r^2 < 1.0$ to dark blue indicating $0.0 < r^2 < 0.2$. Known genes, with their exon, introns and orientation notes are plotted below the SNPs. HapMap recombination rates (cM/Mb) are plotted as a blue line behind the SNPs. SNP coverage is noted by tick marks above the plot.

(never in mitosis a)-related kinase 10 (Nek10). Nek10 is a mediator of G₂/M cell cycle arrest after ultraviolet irradiation [Moniz and Stambolic 2010] and variants in this locus have been associated with breast cancer risk [Ahmed et al. 2009].

A more promising candidate gene, located just 3.3 kb distal to *NEK10*, is *SLC4A7*, which encodes solute carrier family 4, sodium bicarbonate cotransporter, member 7, also known as sodium bicarbonate cotransporter 3 (NBC3) [Pushkin et al. 1999] or electroneutral sodium bicarbonate cotransporter (NBCn1) [Aalkjær and Hughes 1991; Choi et al. 2000]. Two SNPs with *p* values of 1.85×10^{-5} and 5.58×10^{-5} in the 1000 Genomes imputed data are located within the 3'-untranslated region (UTR) of *SLC4A7* (*rs41295960* and *rs41276515*, *SLC4A7:c.*1076A>G* and *SLC4A7:c.*1525A>G* respectively). No other SNPs with *p* values less than 10^{-4} are located within the annotated transcription region, but one SNP, *rs9871261* (*p* = 1.98×10^{-4}), lies 31.6 kb upstream of the *SLC4A7* transcription start site. NBCn1 is expressed in osteoclasts [Bouyer et al. 2006], the cells that resorb bone during bone remodeling. Indeed, it has been localized to the ruffled border of the cell that faces the resorptive cavity and has been shown to be necessary for hydroxyapatite degradation [Riihonen et al. 2010]. This protein has also been reported to reside in the membranes of matrix vesicles budding from osteoblast-like cells [Thouverey et al. 2011], although Riihonen et al. did not see evidence of its presence in osteoblasts.

Slc4a7 has also been knocked-out in mice, and these animals exhibited blindness and auditory impairment similar to Usher syndrome [Bok et al. 2003]. No skeletal abnormalities were noted, but they probably were not assessed for, given the presence of the other severe impairments. If silencing of *Slc4a7* results in deficient osteoclast activity, the resulting skeletal phenotype would presumably be osteopetrosis, similar to that seen in *op/op* mice [Marks and Lane 1976]. *op/op* mice have a mutation in *Csfl* [Yoshida et al. 1990], the gene encoding colony stimulating factor-1 (CSF-1), which together with receptor activator of nuclear factor κ B ligand (RANKL) is necessary for osteoclastogenesis.

Although there are no reports of association of variants in the *SLC4A7* locus with BMD, the recent evidence of its function in osteoclasts and osteoblasts combined with the association observed in the HealthABC European Americans makes this an excellent candidate gene for additional work. Because none of the functional variation in *SLC4A7* shows evidence of association with variation in BMD, it is likely that the association is not due to variation in the protein's function as a consequence

of changes to its amino acid sequence, but rather due to variation in regulation of its expression. Also, if this locus truly does influence variation in areal BMD, the effect size observed—1.6% of the residual variance—is probably overestimated due to the winner’s curse, and this could be one reason for why it hasn’t been observed in other GWAS.

Prior to publishing this result, a necessary first step is replication in another, similar population, such as the Study of Osteoporotic Fractures (SOF) in women or the Osteoporotic Fractures in Men (MrOS) Study, to reduce the likelihood of type I error. Although testing for replication in a similar population increases the probability of detecting true signals, replication in a population with a different linkage disequilibrium pattern could aid in narrowing the region of association, if the signal is present. Functional studies could also be useful in determining the impact of these variants on *NBCn1* expression, bone resorptive activity, osteoclast survival and osteoclast intracellular pH.

In summary, although *SLC4A7* is a highly plausible biological candidate gene, it remains possible that *NEK10* is the true source of the signal in this region and that we are simply ignorant of its role in affecting bone mineral density.

Two additional promising candidate genes include *BMP1* (bone morphogenetic protein 1) on 8p21.3 and *PRKCH* (protein kinase C η ; PKC η) on 14q23.1. *BMP1* has long been known to be involved in ossification [Wozney et al. 1988; Hopkins et al. 2007] and has recently been shown to heighten bone repair in rats and rabbits and increase formation of mineralized bone *in vitro* [Grgurevic et al. 2011]. Much less is known about the involvement of PKC η in bone metabolism. However, increased expression was correlated with increased osteocalcin and bone sialoprotein expression and alkaline phosphatase activity in differentiating osteoblastic cells Lampasso et al. [2006], and *PRKCH* was recently proposed as a candidate gene in a report of a GWAS data-mining study of multiple bone strength traits [Gupta et al. 2011].

In considering associated markers, it is nature to initially focus on the nearest genes. However, it is necessary to remember that putative regulatory variants (expression quantitative trait loci or eQTLs) might not affect a nearby gene (*cis*-eQTLs), but could affect genes at a distant site in the genome (*trans*-eQTLs) [Nicolae et al. 2010; Cox et al. 2010; Below et al. 2011].

4.4.2 Association with Fracture Incidence

Genomewide tests for association with two definitions of fracture incidence, identified 17 potential loci with p values $< 5 \times 10^{-6}$. However, none of the 17 loci associated with either fracture trait in the HealthABC cohort overlap with the 20 candidate loci revealed by the GEFOS Consortium [Rivadeneira et al. 2009] (see also Table 4.6). Interestingly, nine SNPs—all in high LD ($r^2 = 1$) in one locus had p values $< 5 \times 10^{-8}$. Further inspection revealed that all of these SNPs had minor allele frequencies less than 0.064. These SNPs are located on 9q31.3. None of the other SNPs in the region showed any evidence of association (Figure H12). Therefore, this observation is probably a false positive due to small sample size and low allele frequency. We had 47% power to detect an odds ratio of 1.5 with an allele frequency of 0.5 in the pooled-gender “all types of fracture” analysis. Given that many GWAS have reported odds ratios less than this, the Health ABC cohort is severely underpowered as a stand-alone study, but has contributed to a large consortium meta-analysis.

Nevertheless, a few of the suggestive loci for fracture risk in the HealthABC cohort have some skeletal involvement. SNP *rs6809471* on 3q24 (Figure H4) is 650 kb away from *PLOD2*, a gene that encodes procollagen-lysine, 2-oxoglutarate 5-dioxygenase 2. Homozygous mutations in *PLOD2* have been shown to cause Bruck syndrome [van der Slot et al. 2003; Ha-Vinh et al. 2004], a disorder that includes osteogenesis imperfecta [McPherson and Clemens 1997]. *rs17688188* on 4q34.2 (Figure H6) near *VEGFC* showed association at $p = 4.33 \times 10^{-6}$. It was the only SNP in this region with $p < 5 \times 10^{-6}$. *VEGFC* has been observed to increase in expression and to increase bone resorption in RANKL-stimulated mouse cells [Zhang et al. 2008].

rs288746 on 7q36.3 (Figure H9) is 1.7 kb upstream of *SHH* (sonic hedgehog). Sonic hedgehog is an important cytokine in organ morphogenesis, and disruption of *Shh* in mice results in, among other things, absence of the vertebral column and ventral portion of the ribs [Chiang et al. 1996]. The association observed here, however, is with non-vertebral fractures. Finally, two SNPs, *rs12964230* and *rs12955627* (Figure H17), are associated with non-vertebral fractures ($p = 2.41 \times 10^{-6}$) and all types of fractures ($p = 1.53 \times 10^{-6}$) respectively, and are located 661.9 kb and 723.6 kb downstream respectively of *GALR1* (galanin receptor-1). Galanin, a neuropeptide, is upregulated in fractured bones of rats, and both galanin- and GALR1-like immunoreactivity was present in the fracture cal-

lus [McDonald et al. 2003]. McDonald et al. [2007] also showed that galanin can promote bone formation after fracture.

Although the statistical power in this study is poor, follow up studies of these regions could yield important insights into fracture risk.

4.4.3 Replication of Prior GEFOS Results

I examined twenty previously identified candidate loci for LSBMD and FNBMD from Rivadeneira et al. [2009]. Although many of the loci cited therein, such as *LRP5*, *ESR1* and *TNFSF11* have long been associated with skeletal tissue and bone mineral density and so hardly require validation from this study, it is interesting to see how these loci replicate in my sample of 1,663 men and women. None of the loci showed association with either LSBMD or FNBMD in the HapMap SNP set at $p < 5 \times 10^{-6}$. Targeted examination with the 1000 Genomes SNP set showed evidence of association with two of the genes, *CTNNB1*, *ESR1* *TNFRSF11B*, all of which are well known to be associated with bone formation.

4.4.3.1 *CTNNB1* (β -catenin) A total of 2,908 SNPs were examined at this locus (Figure 4.11), and three SNPs (*rs62259232*, *rs391459* and *rs419918*) located 124.4 kb upstream of *CTNNB1* have p values $\leq 10^{-4}$. Although none of the variants had p values less than the Bonferroni-corrected $p = 1.72 \times 10^{-5}$, because of the LD among the SNPs, this correction is likely overly conservative. *CTNNB1* is the gene for β -catenin, a member of the canonical Wnt signaling pathway. β -catenin is essential (1) for differentiation of progenitor cells into osteoblasts during embryogenesis [Day et al. 2005; Hill et al. 2005] and (2) in bone remodeling because it negatively regulates osteoprotegerin expression in osteoblasts [Glass et al. 2005]. Despite its plausibility as a candidate gene, Rivadeneira et al. [2009] were the first to observe an association between variants near this gene and variation in bone mineral density. Candidate gene studies of bone mineral density in postmenopausal Korean women [Lee et al. 2010] and spinal fractures in Slovenians [Mencej-Bedrač et al. 2009] failed to observe an association.

4.4.3.2 *ESR1* (estrogen receptor 1) A total of 4,275 SNPs were examined at this locus (Figure 4.11). Nine SNPs had p values $\leq 10^{-4}$ across a 20 kb region located 217 kb–100 kb (depending on the transcript) upstream of *ESR1*. Examining Figures 4.12 and I7 reveals two potential signals at this locus on either side of a 40 cM/Mb recombination peak. Rivadeneira et al. [2009] observed this as well, with genomewide significant signals at both locations. Stykarsdottir et al. [2008] reported associations between both FNBM and LSBMD and several uncorrelated SNPs and suggest that at least three association signals reside in this region. The SNPs seen in this study lie in the 5'-flanking region of *ESR1*, which has multiple promoters and transcript variants [Koř et al. 2001], and could therefore influence expression [Stykarsdottir et al. 2008]. Sequence variations in *ESR1* has been reported to be associated with BMD and/or fracture risk in many studies [e.g., Ioannidis et al. 2002; Lei et al. 2010] including recent GWA studies of FN and LSBMD [Stykarsdottir et al. 2008, 2009]. Estrogen has long been known play a role in bone metabolism [Turner et al. 1994; Prince 1994].

4.4.3.3 *TNFRSF11B* (tumor necrosis factor receptor superfamily, member 11b; osteoprotegerin)

At the *TNFRSF11B* locus that encodes osteoprotegerin (OPG), 3,856 SNPs were examined (Figure 4.13) of which 61 SNPs had p values $< 10^{-4}$. Again, none of the SNPs had a p value less than the Bonferroni-corrected p -value of 1.30×10^{-5} . The most significant SNP (*rs6469792*) has a p value of 1.45×10^{-5} , but, as stated above, this p value is too conservative. OPG acts as a decoy receptor for RANKL [Sheikh and Fornace 2000; Shin et al. 2008], preventing RANKL from binding to RANK and inhibiting osteoclastogenesis [Simonet et al. 1997]. Associations between variants in the *TNFRSF11B* region, in addition to being reported by Rivadeneira et al. [2009], have also been observed for bone mineral density by Stykarsdottir et al. [2008], Richards et al. [2008] and Hsu et al. [2010].

4.4.4 General Conclusions

Of the 20 previously identified candidate genes that influence areal BMD of the lumbar spine and femoral neck in European Americans, three of them, *CTNNA1*, *ESR1* and *TNFRSF11B* were tentatively replicated in my analysis of the HealthABC cohort using the 1000 Genomes SNP set. These results are not unexpected because of the lack of power due to sample size given the estimated effect sizes. Additionally differences between HealthABC and the samples in the meta-analysis due

to different study ascertainment schemes as well as differences in environmental factors between the United States and Europe could lead to failures to replicate many of the prior studies results. Nevertheless, due to the nature of the HealthABC sample, which is a uniform older healthy population, I might have an enhanced ability to observe associations as compared to a larger meta-analysis composed of studies which have different objectives and ascertainment biases.

Despite the limitations of performing a GWAS in the relatively small HealthABC cohort, I identified several potentially interesting candidate genes, especially *SLC4A7*, *BMP1* and *PRKCH* for BMD and *PLOD2*, *VEGFC*, *SHH* and *GALR1* for fracture risk. Additional association studies are necessary to validate these findings in other populations. If these genes are replicated, functional studies could be performed to determine the biological nature of the impact of variants observed in the genes on bone mineral density and fracture risk.

5.0 GENOMEWIDE ASSOCIATION STUDY IN AFRICAN AMERICANS

5.1 INTRODUCTION

Thirteen genomewide association studies (GWAS) of bone mineral density (BMD) and four of osteoporosis have been conducted to date, but only two included individuals of African ancestry and in both studies, data on African ancestry individuals were used as a replication [Xiong et al. 2009; Koller et al. 2010]. Koller et al. and Ichikawa et al. [2010] examined femoral neck and lumbar spine bone mineral density in 512 pre-menopausal African American women as a replication of single nucleotide polymorphisms (SNPs) identified as part of genomewide scan in European American women from Indiana, and also as a replication of genes identified from the large Genetic Factors for Osteoporosis (GEFOS) Consortium study [Rivadeneira et al. 2009]. They reported replication of SNPs in *ESR1* (estrogen receptor 1), *SP7* (Sp7 transcription factor; osterix), and a chromosome 4 intergenic region. Xiong et al. [2009] examined lumbar spine BMD (LSBMD) and femoral neck BMD (FNBMD) in 908 Tobagonian men of West African ancestry—subjects drawn at random from the Tobago Bone Health Study (TBHS) that I examined in Chapter 2. Again, data on the African ancestry individuals were used to replicate results from a GWAS performed in European ancestry U.S. subjects. The investigators report that polymorphisms in two genes, *ADAMTS18* (a disintegrin-like and metallopeptidase domain-containing protein 8) and *TGFBR3* (transforming growth factor, β receptor III), were replicated across multiple ethnic group. Two additional GWAS, one for bone mineral density [Kung et al. 2011] and one for osteoporosis [Guo et al. 2010a] have been conducted using subjects of non-European descent—in these cases, Chinese from Hong Kong (Kung et al.) and Xī'ān and Chángshā (Guo et al.). Therefore, no GWAS have been performed using data from individuals with African ancestry in the “discovery” cohort. Measures of several bone related traits vary among ethnic groups. For example, areal femoral neck BMD is higher among men and women with

African ancestry versus those with European ancestry [Wang et al. 2007b]. Furthermore, areal and volumetric BMD as highly heritable in all ethnic groups. Therefore GWA studies in non-European populations are necessary to gain a complete account of human variation influencing BMD and susceptibility to osteoporosis.

In the current report, I present results from the first genomewide association study in which African Americans are the discovery cohort, although I recognize that the sample size is small for a GWAS. These results will be compared with the results of the GWAS conducted in the Dynamics of Health, Aging and Body Composition (HealthABC) Study European Americans that was explored in Chapter 4, the results of the GEFOS study of areal BMD [Rivadeneira et al. 2009], as well as the results of the phenotype and linkage analyses in Afro-Caribbeans in Chapters 2 and 3. These comparisons could provide insights regarding similar and disparate effects of common variants among the different population groups. Finally, I use the data on African Americans to assess whether results from the GWAS of European ancestry individuals are replicated among the African American.

5.2 METHODS

5.2.1 Study Population

The HealthABC Study is a longitudinal study of African and European Americans (see also Chapters 1 and 4). In the current study, phenotype and genotype data on 1,139 African Americans were analyzed (651 women and 488 men). The institutional review boards at both the University of Pittsburgh and the University of Tennessee approved the study, and all participants gave written, informed consent.

5.2.2 Phenotype Definitions

As described in Section 1.5.2.1, areal BMD was measured using dual-energy x-ray absorptiometry (DXA) at the proximal femur and the whole body. Measures of FNBMMD were available in 480 African American men and 647 African American women, and measures of LSBMD were available in 483 African American men and 647 African American women.

5.2.3 Genotyping and Imputation

Genotyping was performed by the Center for Inherited Disease Research (CIDR) using the Illumina Human1M-Duo BeadChip system. Quality control protocols were identical to those described in Chapter 4; samples were excluded for low call rate ($< 97\%$ SNPs genotyped), mismatch between reported and chromosomal sex, and first degree relatedness. 1,151,215 SNPs were successfully genotyped in 1,139 African American individuals. SNPs with an MAF $> 1\%$, a call rate $> 97\%$ and a HWE test p value $> 10^{-6}$ were used for imputation. A total of 3,021,329 SNPs were ultimately available for analysis in the African Americans. Imputation was performed by Yongmei Liu and Kurt Lohman at Wake Forest University using MACH 1.0.16 [Li et al. 2010b] and the HapMap II phased haplotypes [Frazer et al. 2007] as the reference.

5.2.4 Statistical Analyses

5.2.4.1 Association analysis methods The statistical methods used in the analysis of data from the African American cohort from HealthABC are identical to those described in Section 4.2.5. Briefly, prior to performing association analyses, residuals of each untransformed BMD trait were calculated separately in men and women, and these residuals were combined for the pooled-gender analyses. To be consistent with results obtained on European American in HealthABC (see Chapter 4) and other reported studies, the following covariates were included in the model: age, age squared, weight, clinical center and ancestry principal components (PCs). Linear regression of the residuals was performed using data from the HapMap SNP set separately in men and in women as well as in the both sets of residuals pooled together. Regression was performed using ProABEL using the option to calculate robust (sandwich) standard errors. To remove poorly inferred genotypes and rare variants, GWA results were filtered for imputation quality ($r^2 > 0.3$) and minor allele frequency (MAF $> 5\%$). Genomic control inflation factors were calculated for each of the analysis groups. Unless stated otherwise, all analyses were performed using the statistical computing routines, R 2.11.1 [R Development Core Team 2008]. The p value thresholds for significant and suggestive results were 5×10^{-8} and 5×10^{-6} , respectively, identical to those used in Chapter 4. Likewise, “associated loci” were defined as the regions 1 Mb up- and downstream of SNPs with the most significant p values (“peak SNPs”).

5.2.4.2 Power to detect genomewide association in the HealthABC African American cohort

Power was calculated using QUANTO 1.2.4 [Gauderman and Morrison 2006]. For BMD, power was estimated for an additive genetic model of the SNP genotypes, in which the SNP genotypes accounted for 0.5% of the residual variation of the trait at the two GWA levels of significance.

5.2.4.3 Replication and fine mapping

In addition to the GWA analyses of FNBMD and LSBMD, I also tested whether any of the 26 autosomal loci identified in the GWAS of the European American cohort of HealthABC (Chapter 4) or whether any of the 20 loci identified by the GEFOS Consortium [Rivadeneira et al. 2009] were associated with FNBMD or LSBMD in African Americans. The most significant SNP at each locus was taken as the midpoint of a 2 Mb region.

5.3 RESULTS

5.3.1 Subject Characteristics

Characteristics of the African American subjects in the HealthABC study are presented in Table 5.1 and differences between men and women were assessed using t tests (for normal quantitative data), Wilcoxon rank sum tests (for non-normal quantitative data) and χ^2 statistics (for frequency data). Women and men in the study had similar ages (73.4 vs 73.5 years, respectively), activity levels (76.0 kcal/kg/week vs 79.8 kcal/kg/week, respectively), as well as rates of diabetes and cardiovascular disease (21.1% vs 22.6% and 8.9% vs 8.3%, respectively). As expected, men were significantly taller and heavier (173 cm vs 160 cm), but women had higher BMIs (29.6 kg/m² vs 27.2 kg/m²), all p values < 0.001. More men than women consumed alcohol (26.9% vs 10%) and smoked (21.4% vs 12.8%), both p values < 0.001. More than 50% of all individuals had been diagnosed with hypertension, but the frequency was significantly higher in women than men (63.7% vs 57.0%, respectively). The frequency of arthritis in women was more than twice that in men (12% vs 52%). As expected, both measures of LSBMD and FNBMD were greater in men than in women (both $p < 2.2 \times 10^{-16}$).

Table 5.1: HealthABC Population Characteristics

Characteristic	Men ($n = 488$)		Women ($n = 651$)		p
	mean/ n	SD/%	mean/ n	SD/%	
Age (yr)	73.5	2.8	73.4	3.0	0.341
Anthropometric					
BMI (kg/m^2)	27.2	4.4	29.6	5.8	1.99×10^{-13}
Waist circumference (cm)	99.4	12.5	101.0	14.7	0.144
Height (cm)	173.0	7.0	159.6	6.5	$< 2.20 \times 10^{-16}$
Weight (kg)	81.5	14.6	75.4	15.5	$< 2.20 \times 10^{-16}$
Lifestyle					
Current smoking	104	21.4%	83	12.8%	1.62×10^{-4}
Alcohol (> 1 drink/week)	131	26.9%	65	10.0%	1.81×10^{-13}
Activity (kcal/kg/week)	79.8	78.8	81.7	76.0	0.064
Medical conditions					
Hypertension	278	57.0%	415	63.7%	4.64×10^{-4}
Diabetes	110	22.6%	137	21.1%	0.581
Cardiovascular disease	41	8.3%	58	8.9%	0.824
Arthritis	25	5.2%	78	12.0%	1.36×10^{-4}
BMD					
Femoral neck (g/cm^3)	849.2	141.7	751.1	131.2	$< 2.20 \times 10^{-16}$
Lumbar spine (g/cm^3)	1152.2	234.3	993.7	193.2	$< 2.20 \times 10^{-16}$

5.3.2 Genomewide Association Analysis of Bone Mineral Density

Genomewide association analysis was performed in 1,130 African ancestry men and women with BMD data using 3,021,329 genotyped and HapMap-imputed SNPs. Between 561,887 and 568,273 SNPs were excluded to due poor imputation quality ($r^2 < 0.3$) or small minor allele frequencies (MAF < 0.05), leaving between 2,453,056 and 2,459,442 SNPs available for association analyses. (Different numbers of SNPs were available for each analysis due to MAF differences among the groups.) The genomic control inflation factor λ ranged from 1.01 to 1.03 (Table 5.2) and quantile-quantile plots of the FNBMD and LSBMD pooled analysis are presented in Figures 5.1 and 5.2. These results indicate that p values from GWAS analyses on the pooled-gender data are not likely to be inflated. On the other hand, p values from GWA analyses performed in African American men and women separately appear to be inflated (see Figures D9 and D12 in Appendix D). Because results of the GWA analyses performed in men and women separately are likely to be biased, I discuss the results of the pooled-gender data only.

Table 5.2: African American BMD Analyses

Trait	Sex	n		Power*		λ
		Samples	SNPs	$p = 5 \times 10^{-8}$	$p = 5 \times 10^{-6}$	
FNBMD	Men	480	2,454,508	0.0000	0.0013	1.03
	Women	647	2,459,452	0.0001	0.0029	1.01
	Pooled	1,127	2,458,958	0.0011	0.0143	1.01
LSBMD	Men	483	2,453,586	0.0000	0.0013	1.01
	Women	647	2,453,068	0.0001	0.0029	1.02
	Pooled	1,130	2,459,339	0.0011	0.0145	1.01

*Additive model, $R^2 = 0.005$

Results of the GWA analyses of FNBMD and LSBMD in men and women combined (pooled-gender) are presented as Manhattan plots in Figures 5.3 and 5.4. Of the 14,738,911 statistical tests performed in the analyses of FNBMD and LSBMD in the pooled-gender sample, 44 SNPs in 24 loci (or regions) reached the genomewide suggestive threshold of 5×10^{-6} although none reached the GWAS significance threshold 5×10^{-8} (Table 5.3). For most of the loci, it is a single SNP that crosses the suggestive threshold, even near genes known to be part of bone-related pathways like *PTH* (parathyroid hormone). On the other hand, one of the loci with multiple (although highly

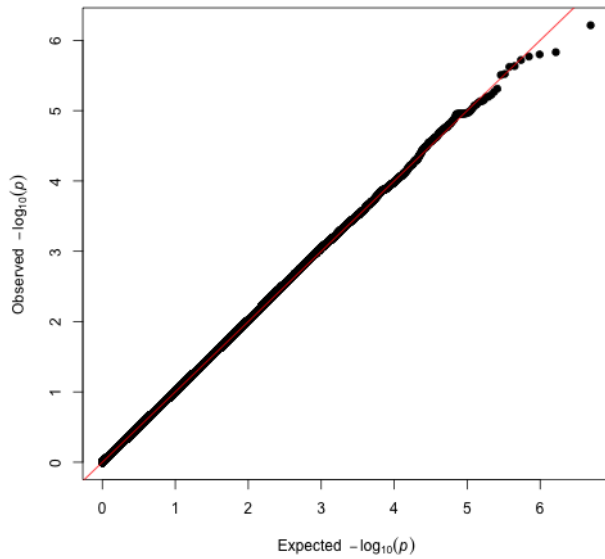


Figure 5.1: QQ Plot FNBMD Pooled*

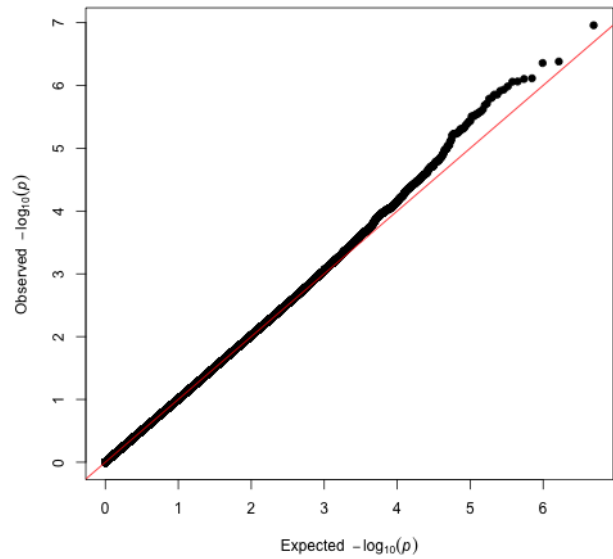


Figure 5.2: QQ Plot LSBMD Pooled

* “Pooled” here refers to the pooled-gender analyses.

correlated) SNPs showing suggestive evidence of association, lies in a large intergenic region with the nearest gene (*LRR4C*, leucine rich repeat containing 4C) 1.5 Mb away (Figure 5.5).

5.3.3 Replication of Results from European American GWAS

One of the potentially most interesting results from the GWAS performed in European Americans in HealthABC (Chapter 4), was the the association of FNBMD with SNPs near *SLC4A7*. Analysis of SNPs within the *SLC4A7* region and FNBMD and LSBMD in African Americans in HealthABC was performed to potentially replicate this result. No polymorphisms in or near *SLC4A7*, had p value less than 10^{-6} for either trait in the pooled-gender group (data not shown). However, a modest association between these SNPs and FNBMD in men occurs between 27 Mb and 27.6 Mb on chromosome 3 (figure 5.6). The peak SNP (*rs9867945*; *NEK10*:363–5169C>T; *SLC4A7*:c.*49333C>T) is associated at $p = 1.07 \times 10^{-5}$.

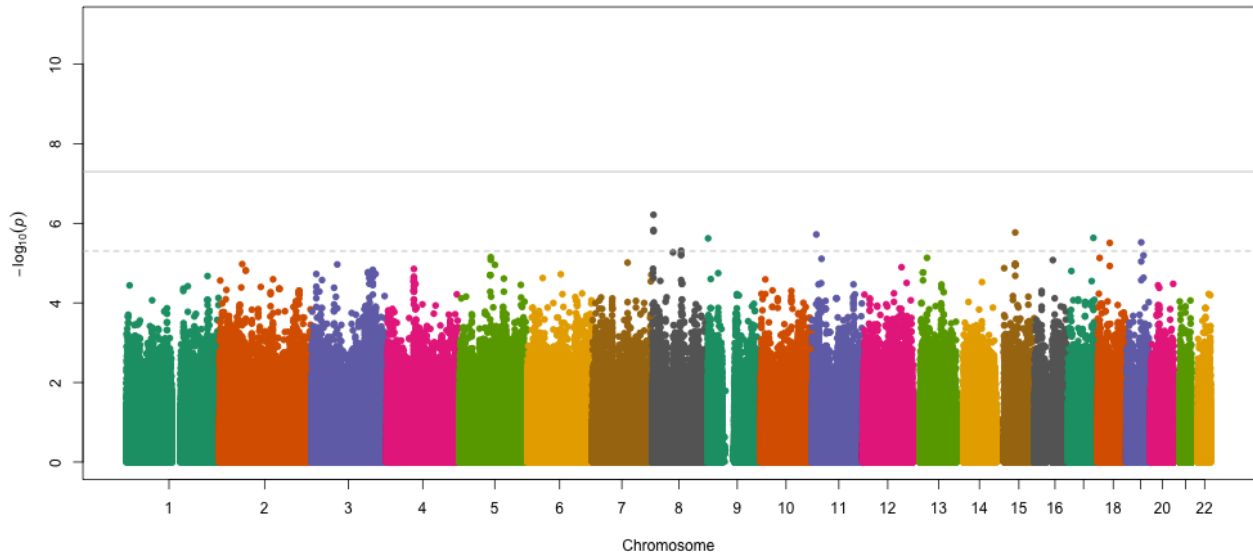


Figure 5.3: Manhattan Plot FNBMD Pooled-Gender – African Americans

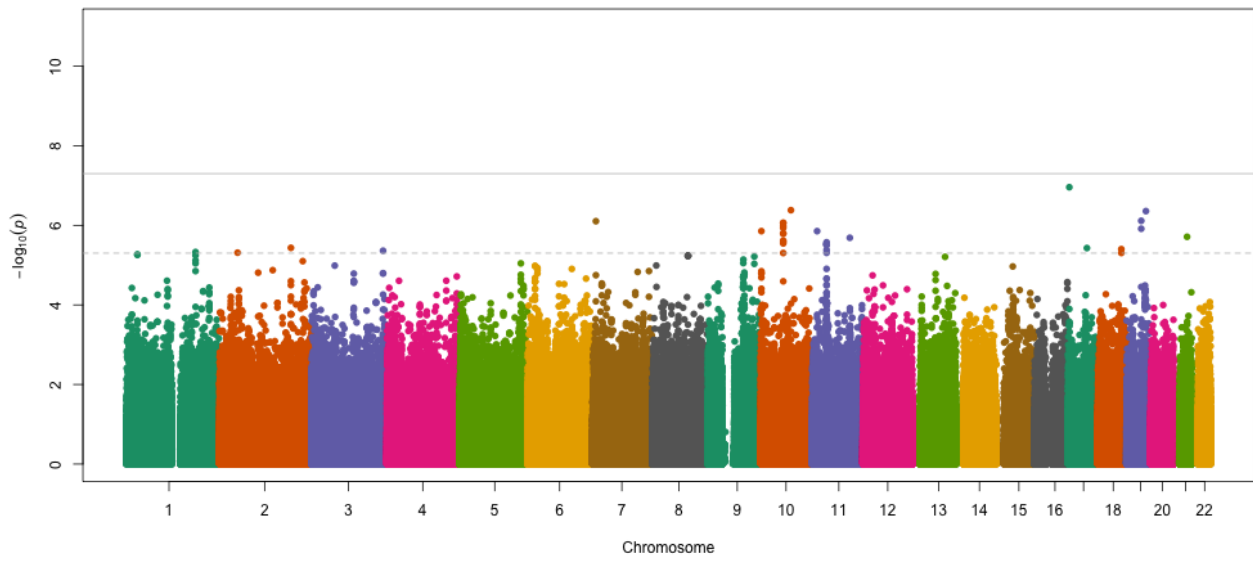


Figure 5.4: Manhattan Plot LSBMD Pooled-Gender – African Americans

Table 5.3: BMD Loci – African Americans

Locus	SNP	Position	Nearest Gene	Distance (kb)	Alleles	MAF	Type	β	SE	p	Trait
1q25.3	<i>rs2281415</i>	183659468	<i>IVNS1ABP</i>	106.4	C/T	0.26	G	0.234	0.051	4.69×10^{-6}	LSP
2p21	<i>rs13408008</i>	47519201	<i>MSH2</i>	0.0	T/G	0.08	I	-0.341	0.075	4.86×10^{-6}	LSP
2q32.1	<i>rs6712733</i>	188501483	<i>GULP1</i>	364.2	T/G	0.25	G	0.236	0.051	3.68×10^{-6}	LSP
3q27.3	<i>rs10937334</i>	189237130	<i>LOC339929</i>	114.6	C/T	0.14	I	-0.267	0.058	4.34×10^{-6}	LSP
7p21.3	<i>rs7794562</i>	9671676	<i>PER4</i>	29.7	T/C	0.17	I	-0.277	0.056	7.86×10^{-7}	LSP
8p23.2	<i>rs10216608</i>	3032465	<i>CSMD1</i>	0.0	A/T	0.09	I	-0.368	0.074	6.10×10^{-7}	FNP
8q21.11	<i>rs16939006</i>	76043194	<i>CRISPLD1</i>	16.1	T/C	0.46	G	0.190	0.042	4.87×10^{-6}	FNP
9p24.3	<i>rs2279986</i>	1032284	<i>DMRT2</i>	8.1	G/T	0.40	G	-0.210	0.045	2.38×10^{-6}	FNP
10p15.3	<i>rs2813457</i>	1562799	<i>NCRNA00168</i>	0.0	C/T	0.07	I	-0.345	0.072	1.40×10^{-6}	LSP
10q21.1	<i>rs12241361</i>	59279878	<i>IPMK</i>	341.4	C/T	0.19	I	0.282	0.057	8.64×10^{-7}	LSP
10q22.3	<i>rs16935728</i>	79663373	<i>RPS24</i>	176.8	G/T	0.11	I	-0.345	0.068	4.16×10^{-7}	LSP
11p15.3	<i>rs12417203</i>	11429804	<i>CSNK2A1P</i>	98.3	T/G	0.23	G	-0.226	0.047	1.90×10^{-6}	FNP
11p15.2	<i>rs11605876</i>	13516168	<i>PTH</i>	42.0	G/C	0.20	I	-0.256	0.053	1.40×10^{-6}	LSP
11p12	<i>rs10501203</i>	38592016	<i>LRRC4C</i>	1500.3	A/T	0.20	I	0.261	0.056	2.66×10^{-6}	LSP
11q22.1	<i>rs10894988</i>	99969329	<i>ARHGAP42</i>	94.3	G/A	0.18	I	-0.264	0.056	2.05×10^{-6}	LSP
15q21.2	<i>rs2305709</i>	49762877	<i>SCG3</i>	0.0	C/A	0.05	I	0.465	0.097	1.70×10^{-6}	FNP
17p13.2	<i>rs758641</i>	3793551	<i>ATP2A3</i>	0.0	A/G	0.39	G	-0.239	0.045	1.10×10^{-7}	LSP
17q22	<i>rs17745091</i>	50293796	<i>TOM1L1</i>	39.3	T/C	0.21	I	-0.238	0.051	3.72×10^{-6}	LSP
17q24.3	<i>rs9898716</i>	67428011	<i>SOX9</i>	200.7	A/C	0.14	I	-0.290	0.061	2.32×10^{-6}	FNP
18q12.2	<i>rs16967627</i>	32092618	<i>MOCOS</i>	0.0	C/T	0.06	I	-0.380	0.082	3.11×10^{-6}	FNP
18q22.1	<i>rs12607377</i>	62565126	<i>CDH19</i>	142.9	T/C	0.08	I	-0.298	0.065	3.97×10^{-6}	LSP
19q13.11	<i>rs10412883</i>	39096596	<i>KCTD15</i>	98.1	G/A	0.09	I	-0.378	0.076	7.68×10^{-7}	LSP
19q13.32	<i>rs10404733</i>	51450642	<i>IGFL1</i>	24.3	A/C	0.21	I	-0.308	0.061	4.39×10^{-7}	LSP
21q22.11	<i>rs2834247</i>	33978599	<i>ITSN1</i>	0.0	G/A	0.11	I	-0.326	0.068	1.94×10^{-6}	LSP

Alleles are given in the form: major allele/minor allele. The minor allele is modeled as the effect allele. FNP = femoral neck BMD pooled-gender. FNM = femoral neck BMD in men. FNW = femoral neck BMD in women. LSP = lumbar spine BMD pooled-gender. LSM = lumbar spine BMD in men. LSW = lumbar spine BMD in women. SNP types: G = genotyped; I = imputed.

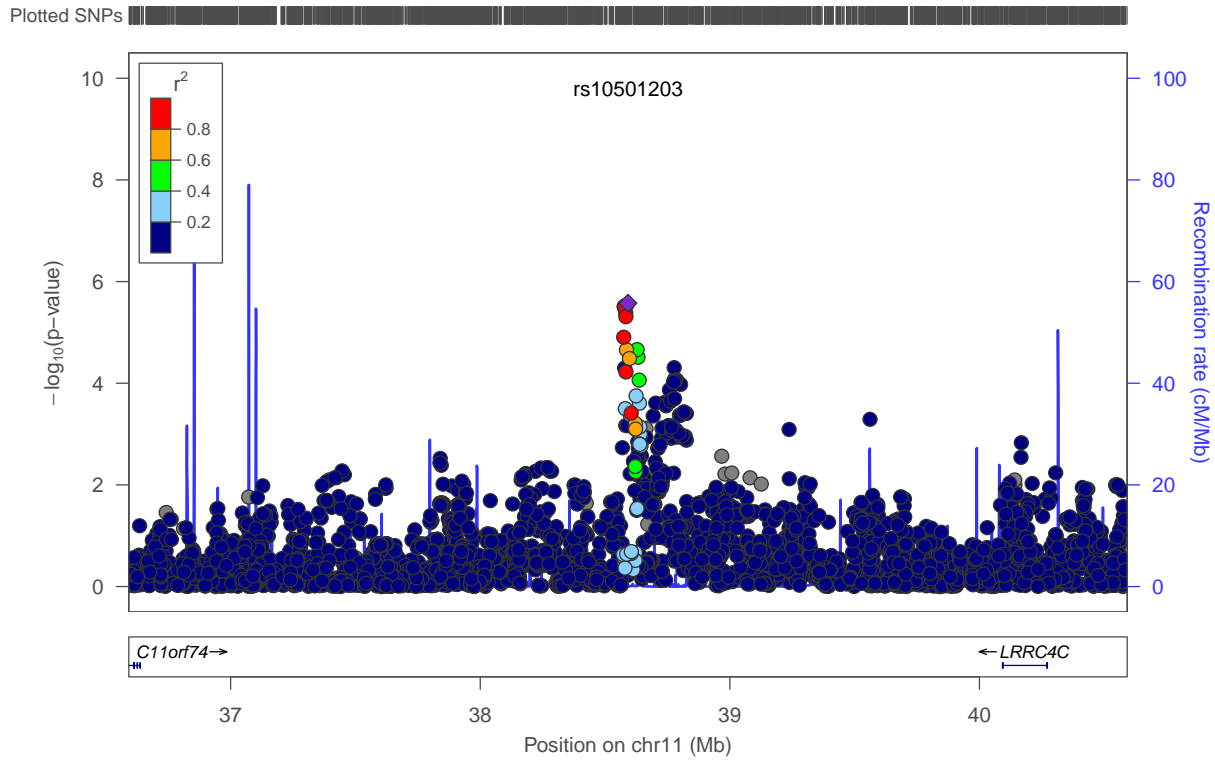


Figure 5.5: Association between LSBMD and HapMap SNPs around *rs10501203* (11p12)

This figure displays the SNPs within a 4 Mb window centered on *rs10501203*, which is denoted by a purple diamond. This is a broader region than in most of the other plots, to illustrate the apparently intergenic nature of this signal. The other SNPs are color-coded according to correlation (HapMap Phase II YRI) with the most significant SNP, from red indicating $0.8 < r^2 < 1.0$ to dark blue indicating $0.0 < r^2 < 0.2$. Known genes, with their exon, introns and orientation notes are plotted below the SNPs. HapMap recombination rates (cM/Mb) are plotted as a blue line behind the SNPs. SNP coverage is noted by tick marks above the plot.

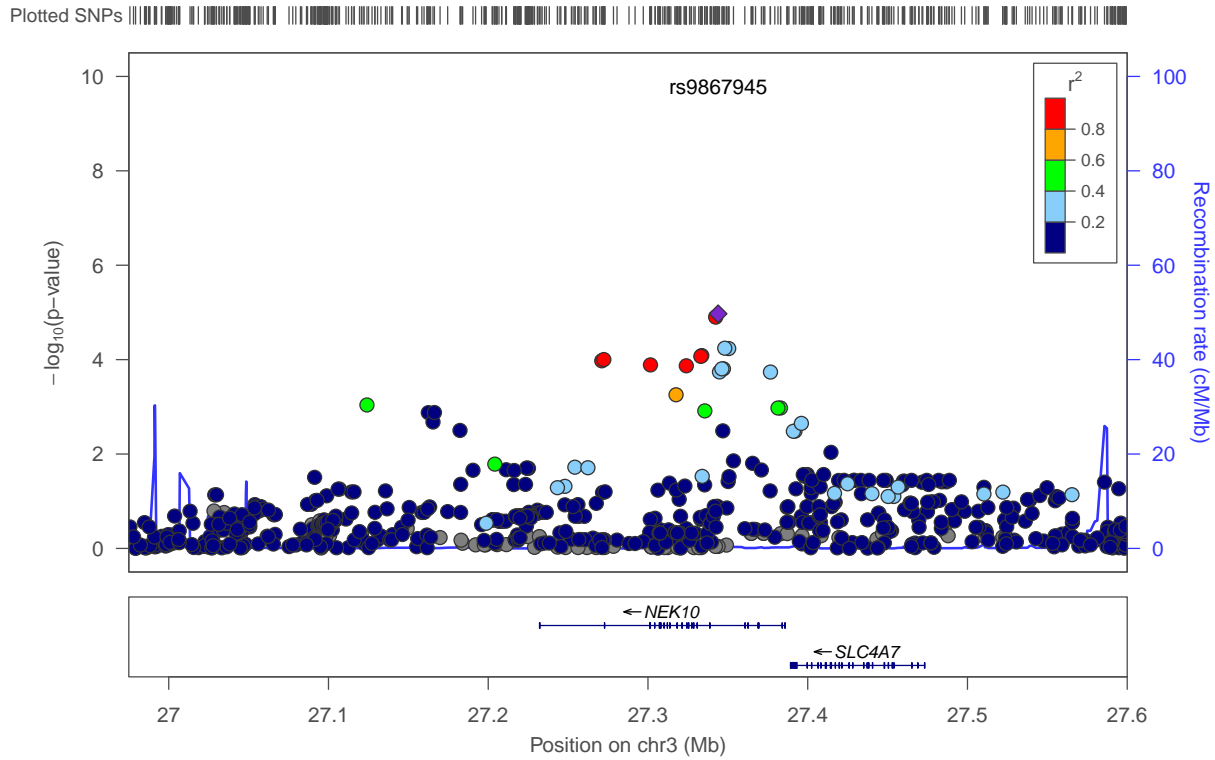


Figure 5.6: Association between FNBMD and HapMap SNPs around *rs11717372* (3p24.1)

This figure displays the SNPs between the same putative recombination hotspots at 27.0 Mb and 27.8 Mb as Figures 4.5 and 4.6. The SNP with the lowest p value in the analysis at this locus is denoted by a purple diamond. The other SNPs are color-coded according to correlation (HapMap Phase II YRI) with the most significant SNP, from red indicating $0.8 < r^2 < 1.0$ to dark blue indicating $0.0 < r^2 < 0.2$. Known genes, with their exon, introns and orientation notes are plotted below the SNPs. HapMap recombination rates (cM/Mb) are plotted as a blue line behind the SNPs. SNP coverage is noted by tick marks above the plot.

Also, none of the 26 potential autosomal loci identified in the European American analyses nor the 20 loci identified by Rivadeneira et al. [2009] showed good evidence of replication in the African American analyses (data not shown).

5.3.4 Identification of Potential Candidate Genes under Linkage Peaks

One method by which to potentially identify QTLs from a linkage analysis is to perform association analyses of SNPs under the QTL linkage peak. As described in Chapter 3, the strongest linkage signal for QTL for bone-related traits in the Tobago Family Health Study was located on chromosome 10q26.3–qter. This QTL influenced periosteal circumference of the tibia (maximum LOD = 3.12), as well as the composite trait, PC1 (maximum LOD = 3.45). Figure 5.7 displays the association results for LSBMD from the pooled-gender sample within the QTL region of interest. As can be seen, no associations stand out distinctively from the background noise. There is a potential candidate gene about 1 Mb telomeric to the peak LOD score, *ADAM8*, which has been shown to play a role in osteoclastogenesis. This gene was discussed in Section 3.4.1.

5.4 DISCUSSION

5.4.1 Association with Bone Mineral Density

Based upon genomewide scans of femoral neck and lumbar spine BMD in African Americans from the HealthABC study, 24 potential candidate loci (or regions) have been identified with p values $< 5 \times 10^{-6}$, although none achieved genomewide significance. Nevertheless, two of the 24 loci are potentially associated with bone metabolism. On 11p15.2, a single variant, *rs11605876* shows evidence of association with LSBMD in the pooled-gender sample ($p = 1.40 \times 10^{-6}$). This SNP is 42 kb upstream of *PTH* (parathyroid hormone), a key regulator of calcium homeostasis that acts through indirect stimulation of osteoclast differentiation [Poole and Reeve 2005]. Variation in and around *PTH* has been the subject of multiple studies of various aspects of bone morphology. It has been associated with BMD [Zhang et al. 2005; Laaksonen et al. 2009; Guo et al. 2010b], hip geometry [Tenne et al. 2010] and fracture risk [Tenne et al. 2008] in some but not all studies [Lei et al. 2005; Zmuda

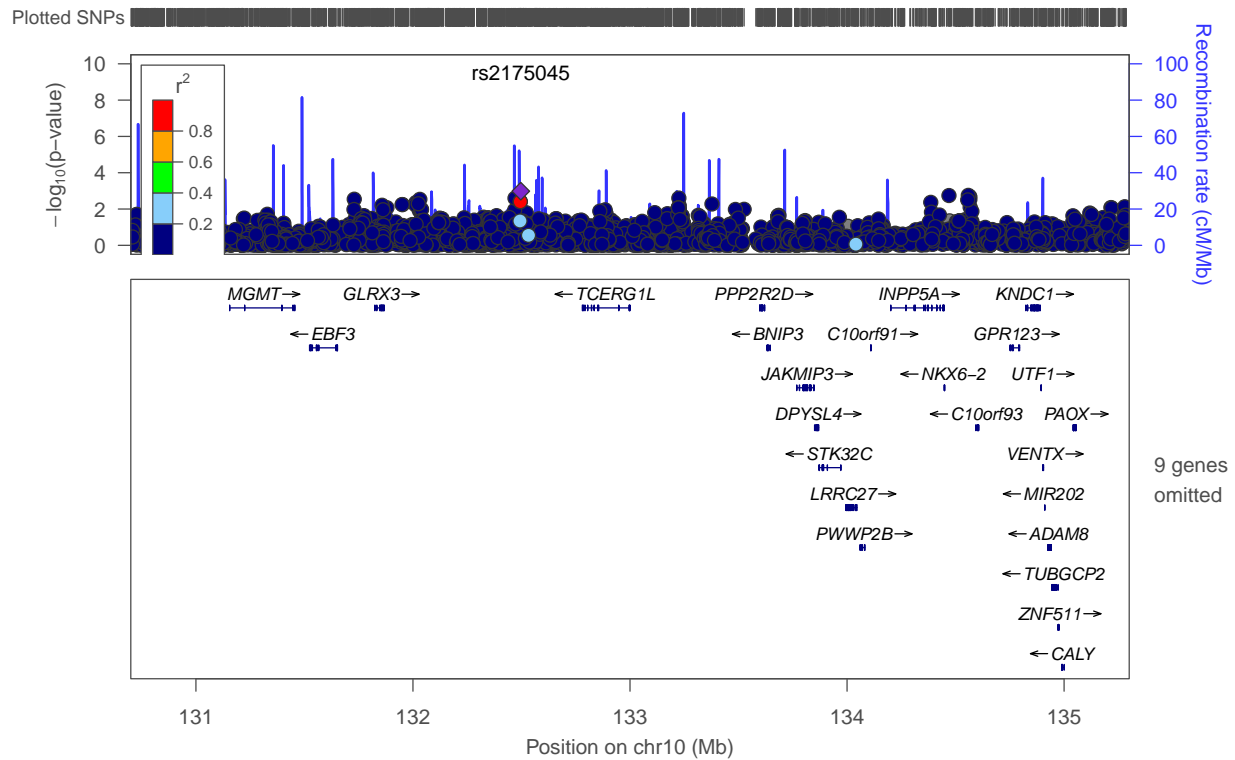


Figure 5.7: Association between LSBMD and HapMap SNPs on 10q26.3–qter

This figure displays the SNPs within a 4 Mb region located under the 10q26.3–qter linkage signal for PC1 and tibial periosteal circumference (Figure 3.2). The most significant SNP is denoted by a purple diamond. The other SNPs are color-coded according to correlation (HapMap Phase II YRI) with the most significant SNP, from red indicating $0.8 < r^2 < 1.0$ to dark blue indicating $0.0 < r^2 < 0.2$. Known genes, with their exon, introns and orientation notes are plotted below the SNPs. HapMap recombination rates (cM/Mb) are plotted as a blue line behind the SNPs. SNP coverage is noted by tick marks above the plot.

et al. 2010; Giroux et al. 2010]. *rs9898716* is located on 17q24.3 near *SOX9* (*SRY* (sex determining region Y)-box 9) and showed suggestive association with femoral neck BMD in the pooled-gender sample (2.32×10^{-6}). *Sox9* is an essential factor in chondrocyte differentiation [Lefebvre et al. 1997].

None of the 24 potential candidate genes identified in African Americans overlaps with previously identified candidate genes from either the GWAS of European Americans in HealthABC (Chapter 4) or from the GEFOS consortium [Rivadeneira et al. 2009]. There are several reasons for this lack of concordance. First, the current study is underpowered, with just 1.5% power to detect a SNP that accounts for 0.5% of the residual variance in FNBMD or LSBMD. Second, for many of the 24 loci, only a single SNP in the region achieves suggestive (5×10^{-6}) significance, so several of these results are likely to be spurious. Third, almost all of the previous GWAS have been performed using data on individuals with European ancestry, and we know there are significant mean differences in genetic architecture of BMD across ancestral groups [Dvornyk et al. 2003; Wang et al. 2007b; Shaffer et al. 2007]. Thus, some of the associations may reflect true differences between individuals with European and African ancestry.

5.4.2 Replication of Potential Candidate Loci from Association Analyses of BMD in European Americans

5.4.2.1 *SLC4A7* (solute carrier family 4, sodium bicarbonate cotransporter, member 7) In the HealthABC European Americans, the *SLC4A7* locus was associated with FNBMD in the pooled-gender sample. However, in the African Americans, this peak is seen only in men and for lumber spine BMD, rather than femoral neck BMD, thus I was not able to definitively replicate the association with *SLC4A7*. Several reasons for this lack of replication include: the original association is spurious, the genetic architecture of BMD differs between European Americans and African Americans, and areal BMD is a crude measure with lots of “noise.” Followup replication in a population with European ancestry will be required. Nonetheless, the association results in the African Americans suggest that natural common variation at this locus might be associated with variation in BMD.

5.4.2.2 Identification of QTLs from Linkage Analyses in Afro-Caribbeans This cohort of African Americans may also serve as a cohort for the linkage regions identified in Chapter 3. The strongest

QTL signal for bone-related traits obtained from analyses of the Tobago Family Study (Chapter 3), was located on chromosome 10q26.3. One gene of interest under this locus and not far (1 Mb) from the location of the peak LOD score is *ADAM8* (a disinegrin-like and metallopeptidase domain-containing protein 8), the gene for an enzyme that has been shown to affect the differentiation of precursor cells into osteoclasts (Section 3.4.1).

Because the linkage signals are so broad, ~4 Mb for the QTL on chromosome 10, and because I was not examining the same traits used in the linkage study, it is unlikely that the genes seen here are the causal genes for the traits examined in the Tobago Family Study. However, I performed this analysis to illustrate how a combination of linkage analyses and association analyses can be used to identify genes influencing body composition traits.

5.4.3 General Conclusions

A search for regions associated with femoral neck and lumbar spine bone mineral density in 1,139 healthy African American men and women revealed 24 loci with peak SNPs with suggestive p values $< 5 \times 10^{-6}$. Due to the small sample size, the modest anticipated effect sizes of true variants and the number of tests performed, this study has insufficient power to provide definitive associated loci. However, several of the loci contain plausible candidate genes that are worthy of follow up and it represent the first discovery GWAS of areal BMD of the lumbar spine and femoral neck in a population with African ancestry.

Comparisons of the results of association studies of African Americans to the studies of European Americans and Afro-Caribbeans may facilitate our understanding of the genetic architecture of bone related traits. However, such studies are hampered by differences in population size and the lack of similar phenotypes. Although I detected some interesting leads, additional studies will be necessary to truly validate any associations.

6.0 CONCLUSIONS

The prevalence of osteoporosis, sarcopenia and changes in body fat distribution—three common, complex, age-related disorders—is an important public health issue [Looker et al. 1997; Iannuzzi-Sucich et al. 2002; Visser et al. 2002; Johnell and Kanis 2006; Burge et al. 2007; Chien et al. 2008]. Identification of genes that influence these traits, or endophenotypes for these traits, could facilitate development of interventions to mitigate the effects of these disorders. In addition, endophenotypes (e.g., bone, muscle, and fat tissue) are known to covary [Reid et al. 1992; Glauber et al. 1995; Visser et al. 1998a,b; Karasik and Kiel 2008; Beck et al. 2009], and this covariation may be due to developmental, homeostatic, mechanical or geriatric processes [Glauber et al. 1995; Visser et al. 2002; Frost 2003; Shore et al. 2006; Lee et al. 2007; Karasik and Kiel 2008; Devaney et al. 2009; Schindeler et al. 2009]. Population variation in these processes may partly be due to genetic variation that influences multiple endophenotypes, that is, pleiotropy. Little is known about possible pleiotropic effects on endophenotypes for osteoporosis, sarcopenia and body fat distribution, especially in populations with non-European ancestry. Characterization of these effects for use in multivariate genetic analyses, and/or development of composite endophenotypes, should increase power to identify specific pleiotropic genes. Identification of such genes could eventually lead to insights regarding the genetic architecture of these traits.

In my dissertation project, I explored pleiotropic relationships among bone, muscle, and fat endophenotypes to answer three general questions: (1) “What are the phenotypic relationships among specific bone, muscle and fat endophenotypes?” (2) “Is there evidence of pleiotropic effects on these endophenotypes?” and (3) “Do specific genes influence two bone endophenotypes and are these identical in different ethnic groups?”

6.1 SUMMARY OF MAJOR RESULTS

General Question 1: What are the phenotypic relationships among measures of bone mineral density and geometry, lean mass and fat mass at multiple skeletal sites?

To assess the phenotypic relationships among twenty-two endophenotypes for bone, muscle and fat traits, I performed hierarchical clustering and principal components analysis using data from the Tobago Bone Health Study (TBHS), a study of 1,937 Afro-Caribbean men from the island of Tobago. The hierarchical clustering analyses revealed that these endophenotypes fall into three groups (Figure 2.1): (1) a “density group” that comprises bone mineral density, cortical bone thickness and endosteal circumference; (2) a “geometry group” that comprises the remaining measures of bone geometry and measures of lean muscle mass; and (3) a “fat mass group” that comprises the measures of fat mass. These general patterns were similar in both younger and older men.

Principal component (PC) analysis of the Tobagonian men largely recapitulated the results of the hierarchical clustering analysis (Table 2.4 and Figure 2.4): “geometry” traits contributed the most to PC1, “density” traits contributed most to PC2 and “fat mass” traits contributed the most to PC3. These PC loadings were used to generate composite phenotypes from data on 470 members of the Tobago Family Health Study (TFS).

General Question 2: Are the bone, muscle and fat endophenotypes (both individual and composite) heritable among individuals with African ancestry and is there evidence for pleiotropy?

All individual and composite endophenotypes were heritable in the TFS; residual heritabilities ranged from 0.206 to 0.763 (all $p < 6.10 \times 10^{-3}$; Table 2.5). Furthermore, there was significant evidence for pleiotropy. For example, quantitative trait linkage analyses revealed significant evidence that a QTL on chromosome 10q26.3–qter influences PC1 (comprised of multiple endophenotypes) and tibial periosteal circumference (maximum LOD = 3.45 and 3.12 respectively). Consistent with the linkage results, genetic correlations among the traits of the “geometry” group (which comprise much of the variation in PC1) are moderate to high (ρ_G range: 0.411–0.851). These results indicate that this region on chromosome 10q might harbor pleiotropic genes with variants that affect multiple bone geometry and muscle traits.

Another QTL, on chromosome 21, significantly influences variation in PC3 and arm fat mass (maximum LOD = 3.66 and 2.82 respectively), indicating pleiotropic effects on multiple “fat mass”

endophenotypes. In addition, linkage peaks for leg fat mass and arm and leg lean mass also occurred at the same region of chromosome 21pter–q21.1, although this evidence for linkage was not strong. Followup bivariate linkage analyses of the measures of fat mass and muscle mass also points to a common locus on chromosome 21. Bivariate linkage analysis of arm lean mass and fat mass revealed a bivariate linkage peak on 21 with a suggestive maximum LOD_{2df} score = 2.92; analysis of arm and leg fat mass on chromosome 21 also showed a maximum LOD_{2df} = 2.65. These linkage results are consistent with the high genetic correlation among these traits (ρ_G range: 0.426–0.839), indicating that a QTL on chromosome 21 may have pleiotropic effects on fat and muscle mass.

General Question 3: Do specific SNPs (or genes) influence two measures of BMD: lumbar spine and femoral neck BMD in populations with European and African ancestry?

Genomewide association studies (GWAS) were conducted in two populations of healthy older Americans: 1,663 men and women of European descent and 1,139 men and women of African descent. Femoral neck and lumbar spine bone mineral density were examined in the European and African Americans; total fractures and non-vertebral fractures were examined in the European Americans only. Over 2.6 million single-nucleotide polymorphisms (SNPs) and over 3 million SNPs were available for the European and African Americans respectively. An additional 4.6 million SNPs were available for the European Americans from the 1000 Genomes Project and were used for targeted follow-up of the most promising results from the European Americans as well as of loci identified in a previous GWAS.

One locus was identified with statistical significance ($p < 5 \times 10^{-8}$), although likely a spurious results due to minor allele frequency, and an additional 71 were observed at suggestive levels ($p < 5 \times 10^{-6}$) (Table 4.3, 4.5 and 5.3). One of the most promising loci on 3p24.1 (Figures 4.5, 4.6 and 5.6) is associated with femoral neck BMD and includes an excellent candidate gene, *SLC4A7*, encoding a sodium bicarbonate cotransporter expressed in the bone-interfacing surface of osteoclasts [Riihonen et al. 2010]. Other genes identified as positional and biological candidates were *BMP1*, *PRKCH*, *PLOD2*, *VEGFC*, *SHH*, *GALR1*, *PTH*, *SOX9* and *ADAM8*.

CTNNA1, *ESR1* and *TNFRSF11B*, genes known previously to be associated with bone mineral density [Rivadeneira et al. 2009], were also validated in this study (Figures 4.11, 4.12 and 4.13 respectively).

6.2 STRENGTHS AND LIMITATIONS

This study had multiple strengths including measures of bone derived from pQCT, which has higher resolution than phenotypes derived from DXA. pQCT allows the measurement of volumetric BMD, as opposed to areal BMD from DXA, thus removing the effect of bone size on the estimate of BMD. pQCT also facilitates the examination of myriad bone components, such as discriminating between BMD of trabecular and cortical bone, which might have both common and unique genetic and environmental factors influencing them. Unfortunately, the pQCT measures were only available on the Tobago populations, and not the HealthABC population, thus limiting comparisons between the two groups.

Another strength of the study is large population of unrelated individuals that enabled development of composite endophenotypes and large, multigenerational families that increased the power of heritability and linkage analyses to detect QTLs within families. The use of principal components facilitates the targeting of the underlying phenotypic dimensions of multiple semi-correlated traits. The advantage of the large pedigrees is mitigated somewhat by the total sample size. Only QTLs with large effect would be detected. Additionally, of the 6,000 SNPs genotyped for the linkage panel, 75% had to be discarded to calculate multipoint identity-by-descent estimates in the large complicated Tobago pedigrees. Such information could be useful if harnessed, especially given the reduced information that (biallelic) SNPs themselves provide to trace transmission within families.

This study also included the first GWAS of BMD with African Americans as a discovery cohort, whereas two prior studies that included subjects of African descent [Xiong et al. 2009; Koller et al. 2010] examined them as follow-up replication cohorts. Conducting a genomewide scan in a non-European population allows for the examination of variants not assessed in populations of European descent. Discoveries of genes with unique effects in populations of African descent may aid in correcting health disparities between populations with differing susceptibilities to disorders such as osteoporosis or obesity. Another strength of the GWA analyses in this study is that genotypes from dense SNP panels were available in European and African American men and women, and were supplemented with imputed SNPs from the International HapMap Consortium and the 1000 Genomes Project. These dense arrays provide ample coverage for the detection of association signals. Dense coverage in both population groups enables us to conduct direct comparisons of signals

identified in each. However, the power of this study to detect association is severely hampered by the sizes of the samples.

6.3 FUTURE DIRECTIONS

There are several avenues of follow-up available for this study.

6.3.1 Validation

Foremost, the raw data for all SNPs exhibiting evidence of association in this study must be examined. Misclassification of individuals into genotype clusters can result in false positive results and must be ruled out as a source of error.

Replication is a hallmark of the scientific process, and studies that aim to reproduce the associations seen here are essential. For instance, one next step would be to replicate the *SLC4A7* result in another population. Genomewide SNP data are available for the Study of Osteoporotic Fractures in Women (SOF) or the Study of Osteoporotic Fractures in Men (MrOS), and replication of the genomewide association results in these populations is an obvious possibility.

6.3.2 Fine Mapping

My linkage analyses have revealed two potential QTLs. Narrowing the regions of interest would be a helpful first step. We used just 25% of the SNPs in our linkage panel to calculate multipoint identity-by-descent (MIBD) estimates, and the remaining 75% can still be used. Multiallelic haplotypes could be constructed from the full 6,000-SNP linkage panel using Mendel [Lange et al. 2001] to assign unambiguous haplotypes within the 1 cM intervals that LOKI cannot use. Such haplotypes would allow us to overcome LOKI's 1 cM limitation on MIBD estimation as well as serving as stand-ins for more informative multiallelic microsatellites. Such haplotypes could provide better tracing of transmission between relatives. This might increase the power to detect linkage signals as well as potentially narrowing the linkage peaks so far observed. The collection of additional families could also increase the power of the linkage analyses.

Nevertheless, a narrower QTL region might still encompass a dozen genes, so association studies of SNPs with dense coverage of the regions of interest or targeted resequencing and SNP discovery in those regions could further pinpoint the causal elements. An obvious follow-up population for the two QTLs observed here is the Tobago Bone Health Study (TBHS).

Fine mapping is also necessary as a follow-up of the GWAS results, as the most significant SNPs themselves are not likely to be causal, but are likely to be in linkage disequilibrium with causal variants.

6.3.3 Functional Assessment

Given our understanding of the function of *SLC4A7*, hypotheses about how both deleterious and beneficial regulatory variants and deleterious functional variants would affect NBCn1's function and the subsequent consequence for phenotypes could direct selection of traits to explore for association with variants in this region.

If the *SLC4A7* locus is replicated, then further studies of *SLC4A7* in mice and in cultured osteoclasts could extend our knowledge of the implications of variation in that region on bone-related phenotypes. Basic expression studies might reveal whether variation between 27.0 Mb and 27.8 Mb on chromosome 3 affects the expression of *NEK10*, *SLC4A7* or both. *SLC4A7* is expressed in the thick ascending limb and collecting duct cells of the kidney [Boron and Boulpaep 1983; Choi et al. 2000; Vorum et al. 2000], so expression assays in COS-1 cells, which are derived from the kidney cells of the African green monkey [Jensen et al. 1964; Gluzman 1981], might facilitate such assays. In addition, functional studies of osteoclasts induced from CD¹⁴⁺ cells isolated from peripheral blood of subjects with and without *rs11717372* or another correlated SNP could also reveal whether NBCn1 mRNA levels [Livak and Schmittgen 2001], cytoplasmic and membrane-bound protein levels [Vorum et al. 2000] or bone resorption activity [Riihonen et al. 2010] are affected by that variation. Finally, *Slc4a7*^{-/-} mice exist [Bok et al. 2003] so it might be possible to knock in human versions of *SLC4A7* with and without identified variants to see if phenotypic differences in bone mineral density or response of osteoclasts to chronic metabolic acidosis [Kwon et al. 2002; Riihonen et al. 2010] arise.

6.3.4 Data Mining

Tremendous resources have been spent to genotype the HealthABC participants at millions of SNPs. Additional information, beyond simply collecting the most obvious association results, can be gleaned from such a rich data set. In addition to attempts to validate the standout loci from a GWAS, it is imperative that we employ methods that can help us sort the many true positives from among the false positives lying at and just below the suggestive loci threshold. Pathway-based methods [Wang et al. 2007a; Holmans et al. 2009; Torkamani and Schork 2009; Li et al. 2010a; Gupta et al. 2011] can be used to see if particular metabolic pathways or networks are overrepresented among the suggestive signals. Allelic heterogeneity is a significant problem for GWAS, as different individuals with the same phenotype state can result from different alleles in the same gene. Association studies are limited in their ability to detect such associations. Algorithms that cluster together alleles into genes or gene families [Morgenthaler and Thilly 2007; Li and Leal 2008; Madsen and Browning 2009; Hoffmann et al. 2010] might allow us to associate phenotypes with larger genetic elements and overcome the limitations of weak power imposed by the small minor allele frequencies of rare SNPs.

6.4 PUBLIC HEALTH SIGNIFICANCE

Age-related changes in body composition are a significant public health issue. Osteoporosis affects up to 18% of women and up to 6% of men over the age 50, with a concomitant increase in fracture risk [Looker et al. 1997]. Accompanying changes in muscle quality and mass and in fat distribution and mass modulate the risk of fractures as well as influencing other aspects of quality of life [Johnell and Kanis 2006; Burge et al. 2007]. An increased understanding of the relationships between bone, muscle and fat tissue and the genetic architecture that underlies them could lead to interventions to delay or mitigate the detrimental effects of aging on these components of body composition.

The effect sizes and risk ratios of genetic variants associated with changes in quantitative traits such as bone mineral density or fat mass or with susceptibility to conditions like osteoporosis, sarcopenia and obesity have proven to be diminutive in many cases at least in the predominantly European populations most commonly examined. Although the predictive power of such variants for

the general population is ambiguous now, the cumulative impact of discovered variants could prove informative for a small segment of the population that carry a high burden of deleterious alleles.

While the hypothesis that common variants account for a large amount of a trait's heritability has not generally been borne out, rare variants that have significant impacts on the quality of life for families that carry them are known and efforts to discover and describe them should continue. Furthermore, while the predictive value of naturally occurring variation is uncertain, such variation does illuminate genes, gene products, regulatory elements, metabolic pathways and regulatory networks that are important to development, maintenance, disease and senescence of components of body composition. These genes and so forth then serve as potential targets for interventions to delay onset or mitigate the impact of conditions like osteoporosis. For instance, therapies which reduce NBCn1 activity in osteoclasts might aid in restoring the bone remodeling imbalance that underlies this condition.

Comparisons between populations with different susceptibilities to disease can lead to greater insights into the underlying causes. The prevalence of osteoporosis is 18% in European American women and is 6% in African American women. While a portion of the difference in risk is likely due to environmental differences, a component may be genetic. Further exploration in understudied groups, such as populations of African ancestry, could produce discoveries that benefit both groups.

APPENDIX A

ABBREVIATIONS

Table A1: Abbreviations

<i>ADAM8</i>	a disintegrin-like and metallopeptidase (ADAM) domain-containing protein 8
<i>ADAMTS18</i>	ADAM with thrombospondin type 1 motif, 18
<i>ADIPOQ</i>	adiponectin
<i>ACVR1</i>	activin A receptor, type I
BMD	bone mineral density
BMI	bone mass index
<i>BMP1</i>	bone morphogenetic protein 1
<i>BMP2</i>	bone morphogenetic protein 2
<i>CDH8</i>	cadherin 8, type 2
CEPH	Centre d'Étude du Polymorphisme Humain
CEU	Utah residents with Northern and Western European ancestry from the CEPH collection
cGMP	cyclic guanosine monophosphate
chr	chromosome
CIDR	Center for Inherited Disease Research
cM	centimorgan
CT	computed tomography
<i>CTNNB1</i>	catenin (cadherin-associated protein), β 1, 88 kDa
CVD	cardiovascular disease
DXA	dual-energy x-ray absorptiometry
<i>ESR1</i>	estrogen receptor 1
FNBMd	femoral neck bone mineral density
FRAX	Fracture Risk Assessment Tool
<i>FTO</i>	<i>Fatso</i> homolog (fat mass and obesity-associated)
<i>GALR1</i>	galanin receptor 1
GEFOS	Genetic Factors for Osteoporosis
GWA	genomewide association
GWAS	genomewide association study

Continued on next page

Table A1 — continued from previous page

GWLS	genomewide linkage study
HealthABC	Dynamics of Health, Aging and Body Composition Study
HuGE	human genome epidemiology
HWE	Hardy–Weinberg equilibrium
<i>IRS</i>	insulin receptor substrate 1
kb	kilobase
kDa	kilodalton
LD	linkage disequilibrium
<i>LEPR</i>	leptin receptor
LOD	logarithm of odds
LOD _{2df}	logarithm of odds (two-degrees-of-freedom test)
LOESS	locally weighted scatterplot smoothing
<i>LRP5</i>	low density lipoprotein receptor–related protein 5
<i>LRRC4C</i>	leucine rich repeat containing 4C
LSBMD	lumbar spine bone mineral density
MAF	minor allele frequency
Mb	megabase
<i>MC4R</i>	melanocortin 4 receptor
MIBD	multipoint identity-by-descent
mRNA	messenger RNA
MrOS	Study of Osteoporotic Fractures in Men
MyoD	myogenic differentiation 1
NCB3	sodium bicarbonate cotransporter 3
NCBI	National Center for Biotechnology Information
NCBn1	electroneutral sodium bicarbonate cotransporter 1
<i>NDRG4</i>	<i>N-myc</i> downstream regulated gene family member 4
<i>NEK10</i>	never in mitosis gene a (NIMA)–related kinase 10
NHGRI	National Human Genome Research Institute
OPG	osteoprotegerin
OPLL	ossification of posterior longitudinal ligament
OR	odds ratio
OSX	osterix
<i>P2RX7</i>	purinergic receptor P2X, ligand-gated ion channel, 7
PC	principle component
<i>PDE3A</i>	phosphodiesterase 3A, cGMP-inhibited
PKC η	protein kinase C, η
<i>PLOD2</i>	procollagen-lysine, 2-oxoglutarate 5-dioxygenase 2
<i>PPARG</i>	peroxisome proliferator–activated receptor γ
PPAR γ	peroxisome proliferator–activated receptor γ
pQCT	peripheral quantitative computed tomography
<i>PRKCH</i>	protein kinase C, η
<i>PTH</i>	parathyroid hormone
QQ	quantile–quantile
QTL	quantitative trait locus
QUS	quantitative ultrasound
RANK	receptor activator of nuclear factor κ B

Continued on next page

Table A1 — continued from previous page

RANKL	receptor activator of nuclear factor κ B ligand
RNA	ribonucleic acid
Runx2	Runt-related transcription factor 2
SD	standard deviation
SE	standard error
<i>SHH</i>	sonic hedgehog
<i>SLC4A7</i>	solute carrier family 4, sodium bicarbonate cotransporter, member 7
SNP	single-nucleotide polymorphism
SOF	Study of Osteoporotic Fractures
SOLAR	Sequential Oligogenic Linkage Analysis Routines
SOX9	<i>SRY</i> (sex determining region Y)-box 9
<i>SP7</i>	Sp7 transcription factor (osterix)
TBHS	Tobago Bone Health Study
TFS	Tobago Family Health Study
<i>TGFBR3</i>	transforming growth factor, β receptor III
<i>TNFRSF11A</i>	tumor necrosis factor receptor superfamily, member 11a, NF- κ B activator (RANK)
<i>TNFRSF11B</i>	tumor necrosis factor receptor superfamily, member 11b (osteoprotegerin)
<i>TNFSF11</i>	tumor necrosis factor (ligand) superfamily, member 11 (RANKL)
<i>TRHR</i>	thyrotropin-releasing hormone receptor
UTR	untranslated region
<i>VDR</i>	vitamin D (1,25-dihydroxyvitamin D ₃) receptor
<i>VEGFC</i>	vascular endothelial growth factor C
WHO	World Health Organization
YRI	Yorùbá in Ìbàdàn, Nigeria
<i>ZBTB40</i>	zinc finger and bric à brac–tramtrack–broad-complex (BTB) domain containing 40

APPENDIX B

TOBAGO FAMILY HEALTH STUDY PEDIGREES

The pedigrees in this appendix were drawn using Cranefoot 3.2 [Mäkinen et al. 2005]. Symbols colored in black represent phenotyped individuals.

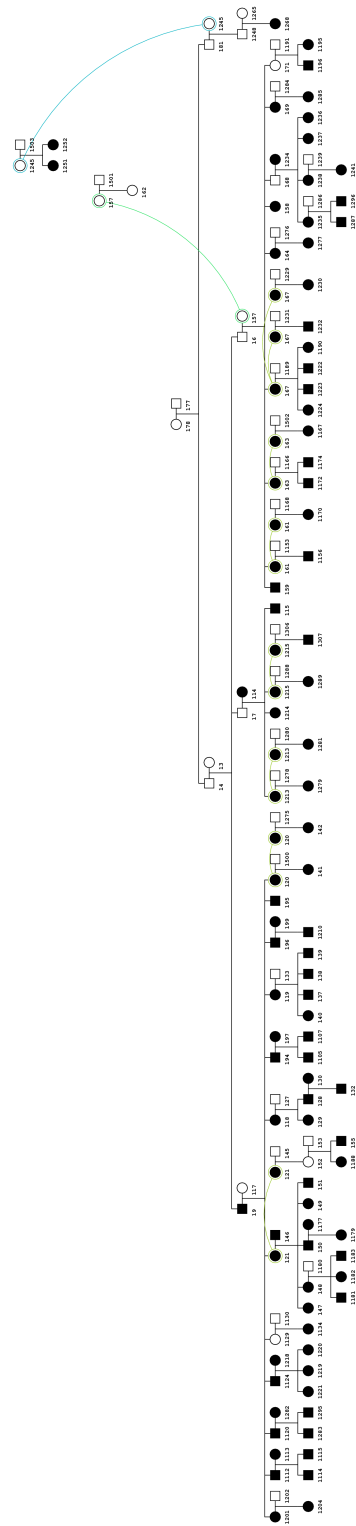


Figure B1: Pedigree 1

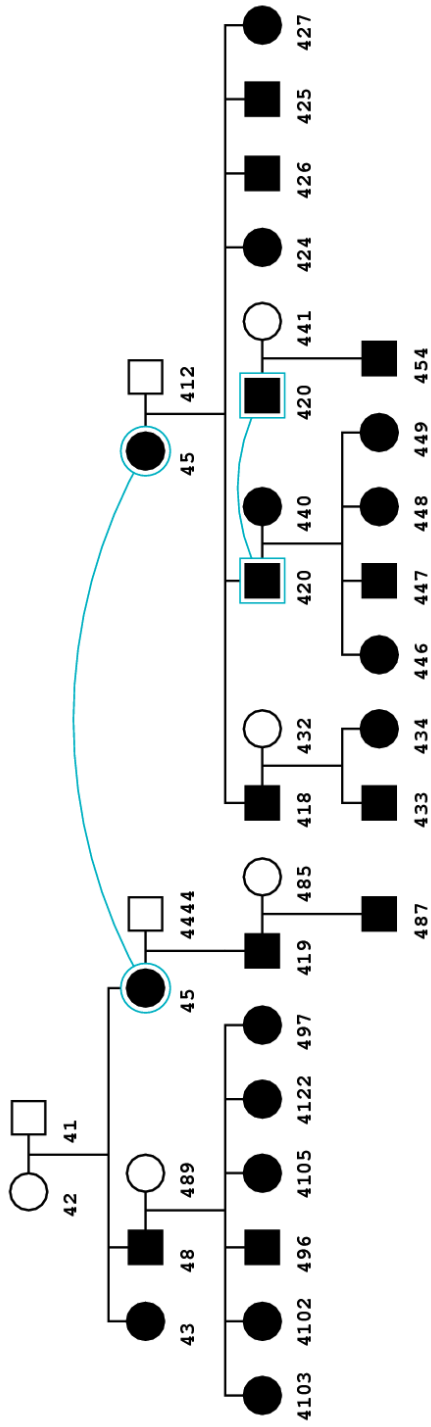


Figure B4: Pedigree 4

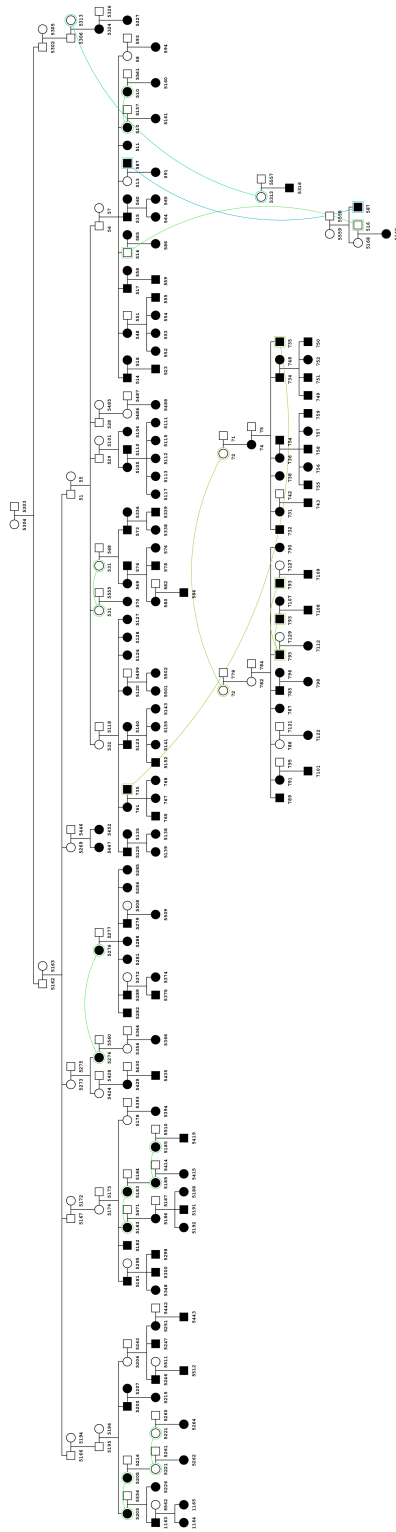


Figure B5: Pedigrees 5 and 7

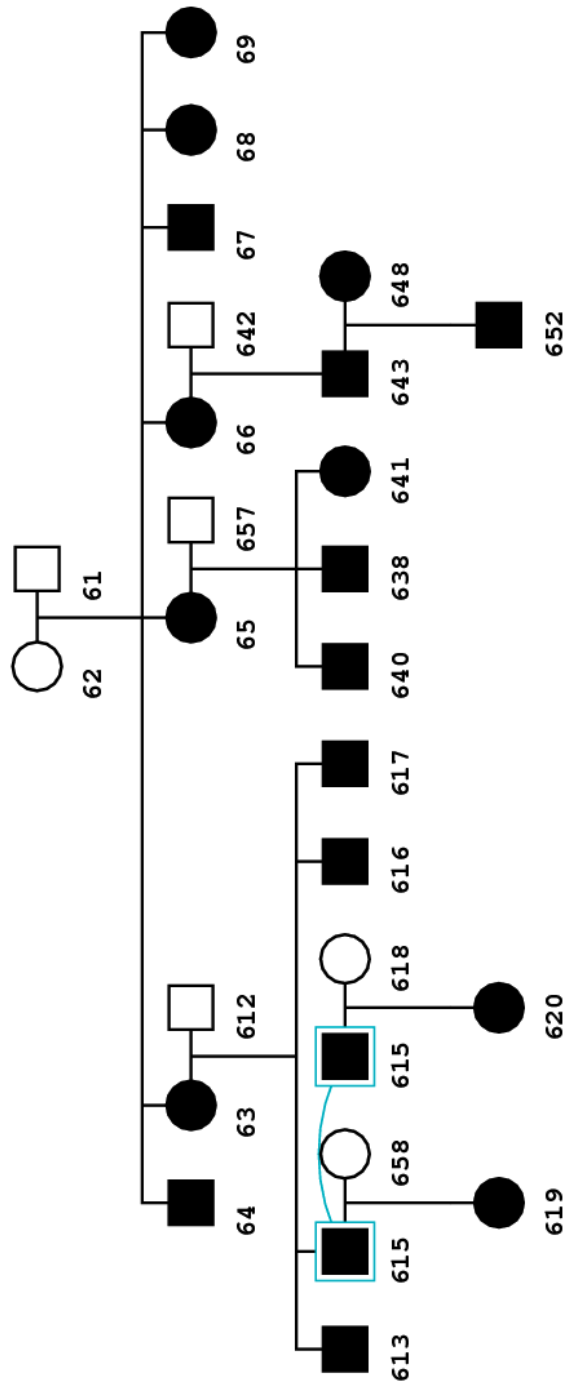


Figure B6: Pedigree 6

APPENDIX C

LINKAGE PLOTS

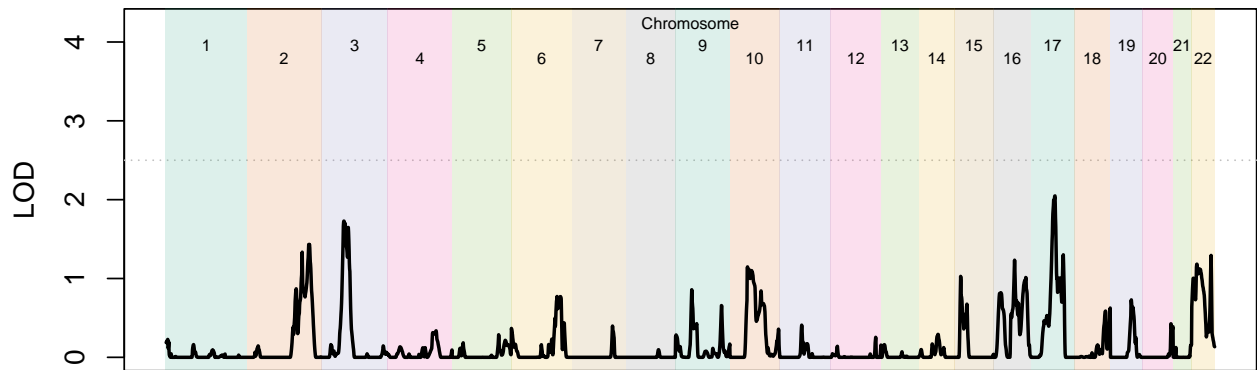


Figure C1: Radius Length

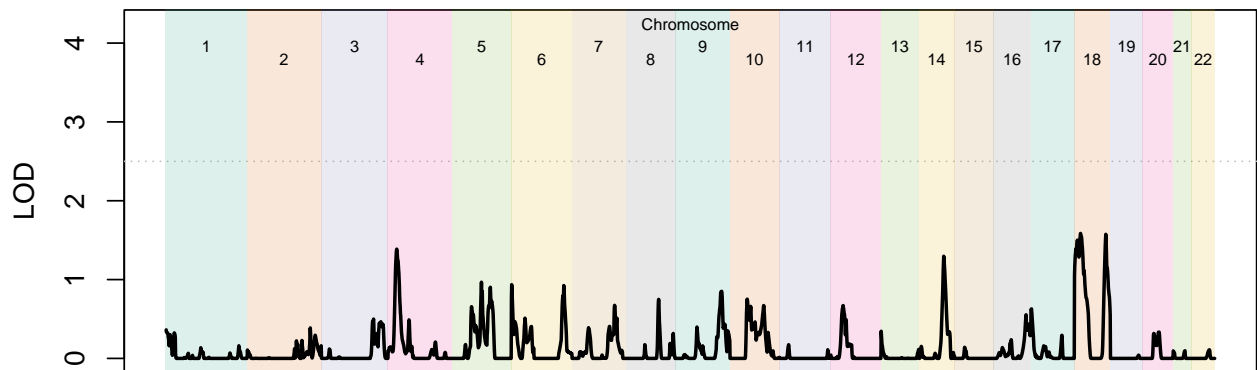


Figure C2: Tibia Length

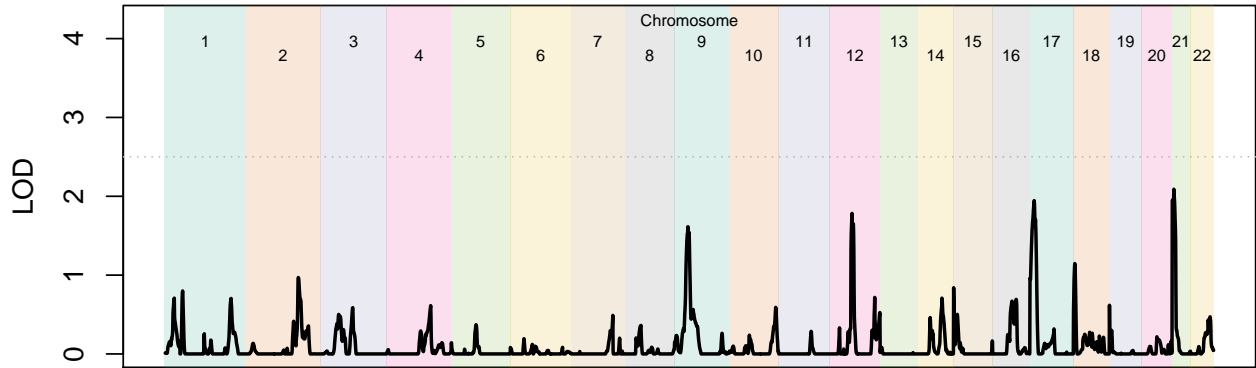


Figure C3: Arm Lean Muscle Mass

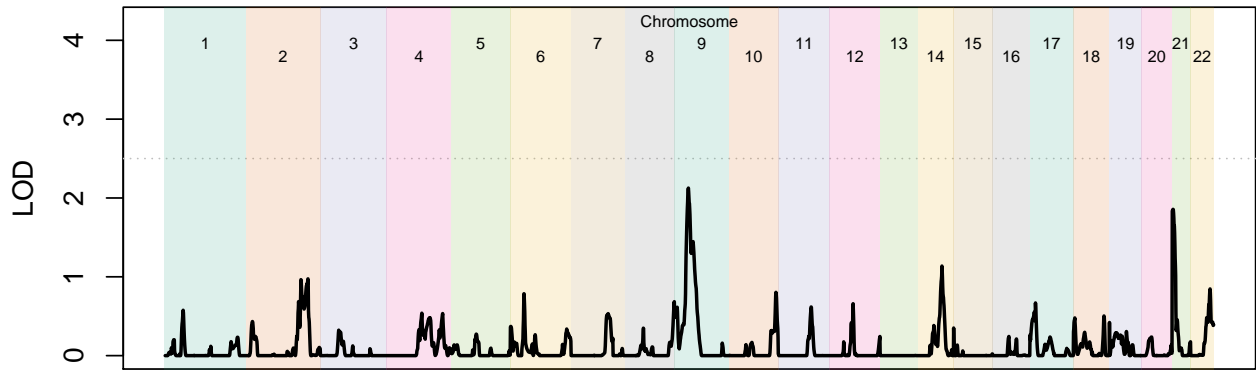


Figure C4: Leg Lean Muscle Mass

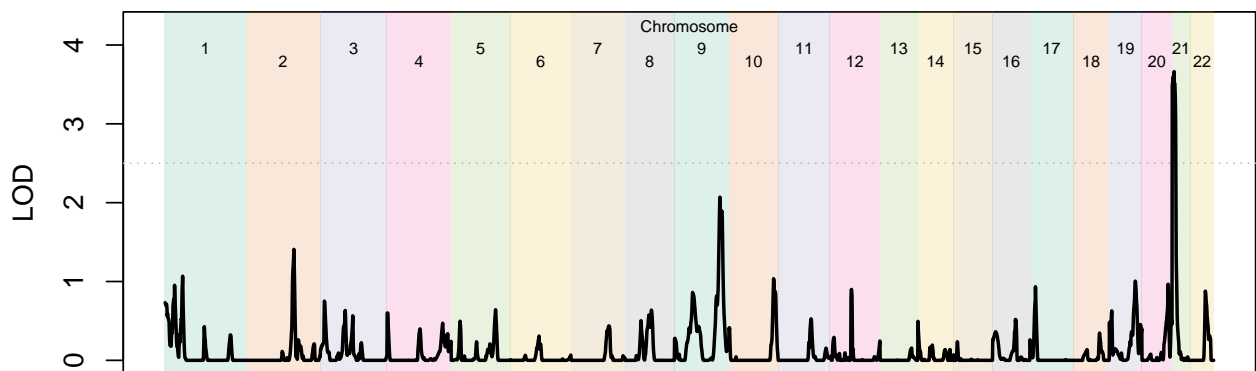


Figure C5: Arm Fat Mass

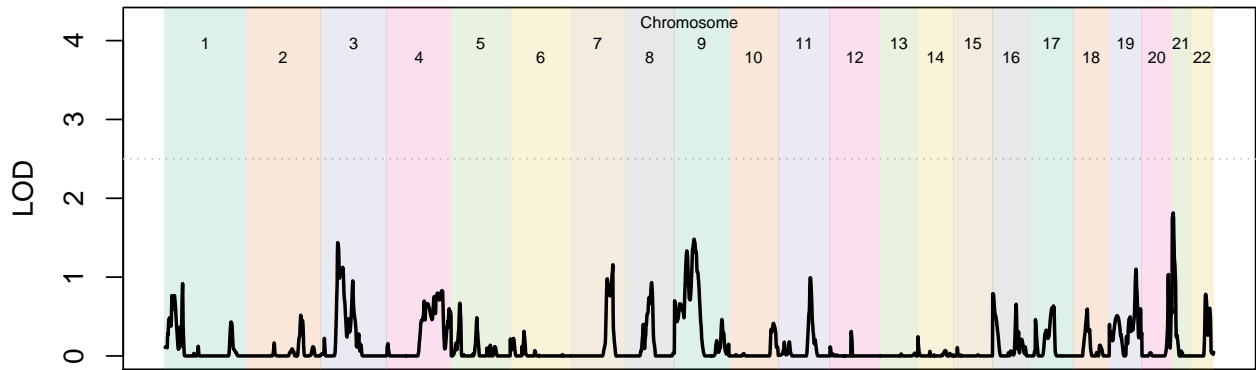


Figure C6: Leg Fat Mass

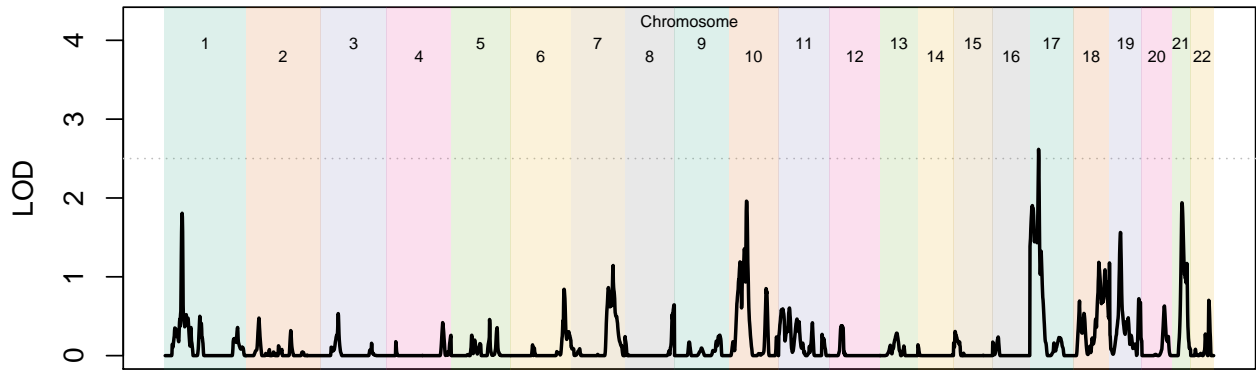


Figure C7: 4% Radius Total Area

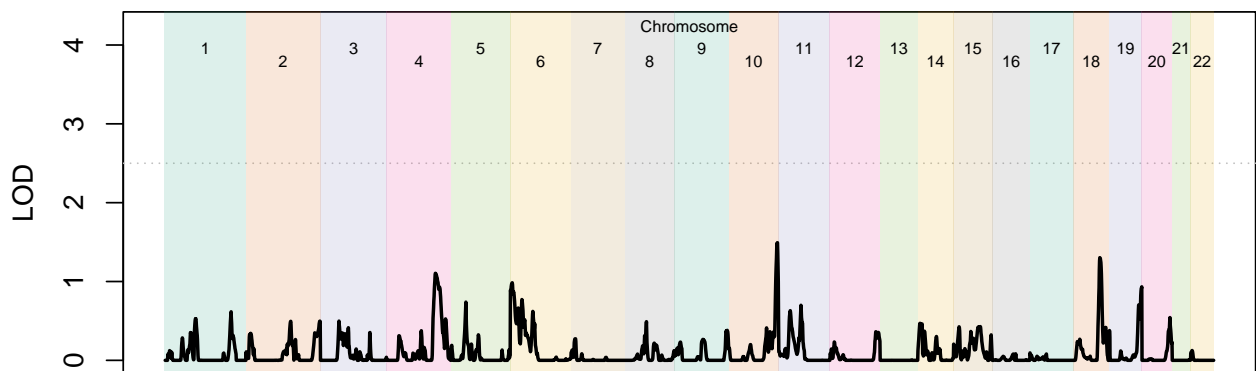


Figure C8: 4% Tibia Total Area

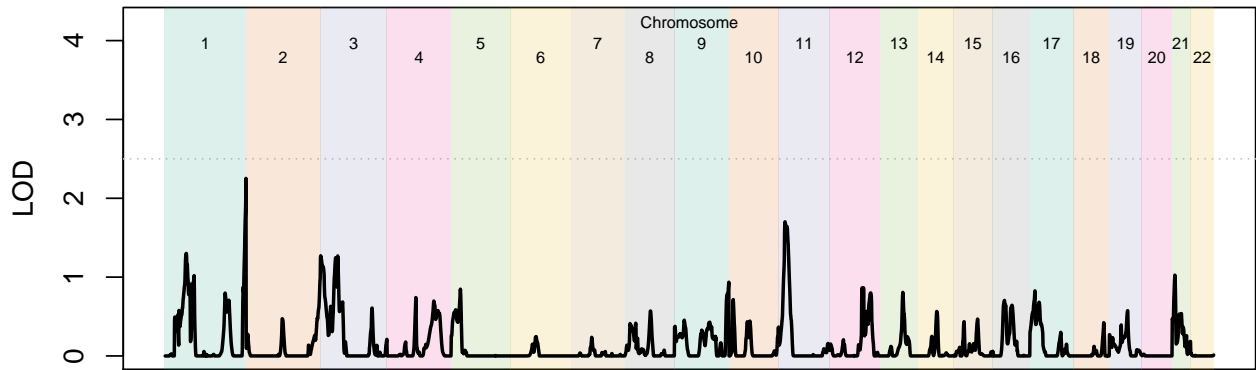


Figure C9: 4% Radius Trabecular Bone Mineral Density

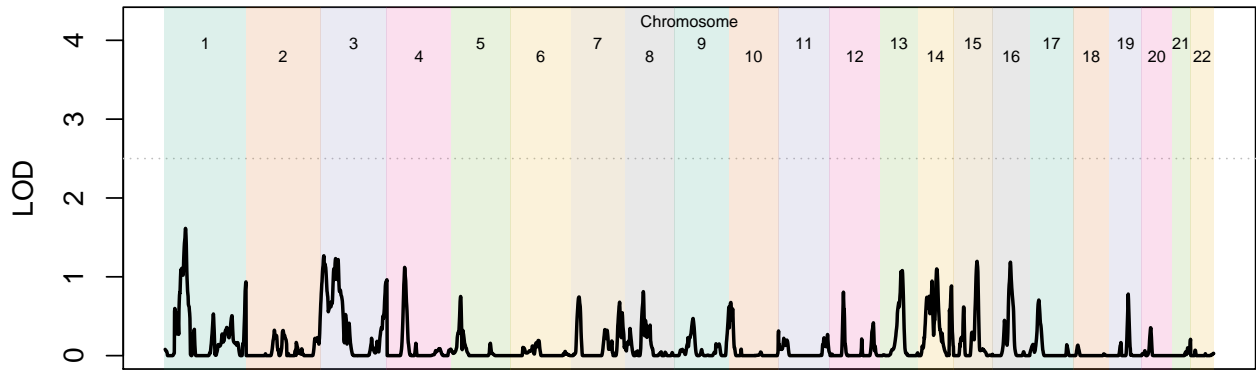


Figure C10: 4% Tibia Trabecular Bone Mineral Density

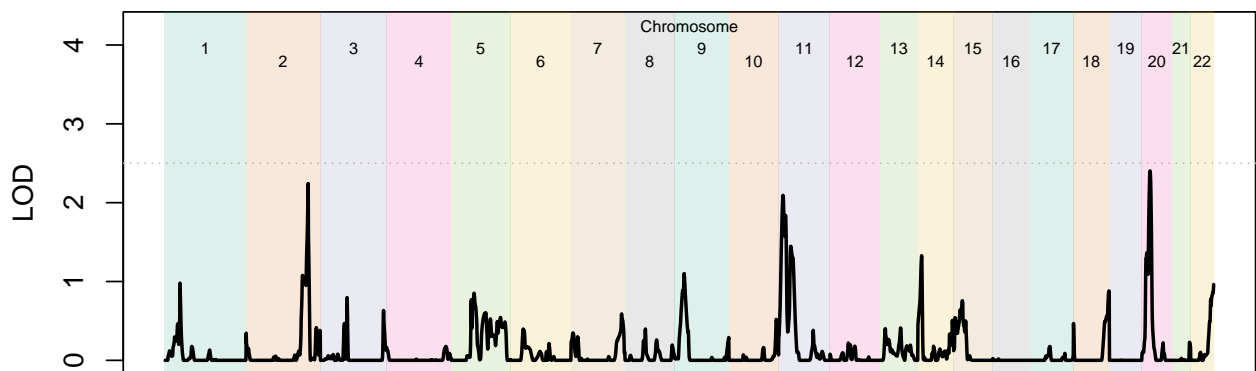


Figure C11: 33% Radius Cortical Area

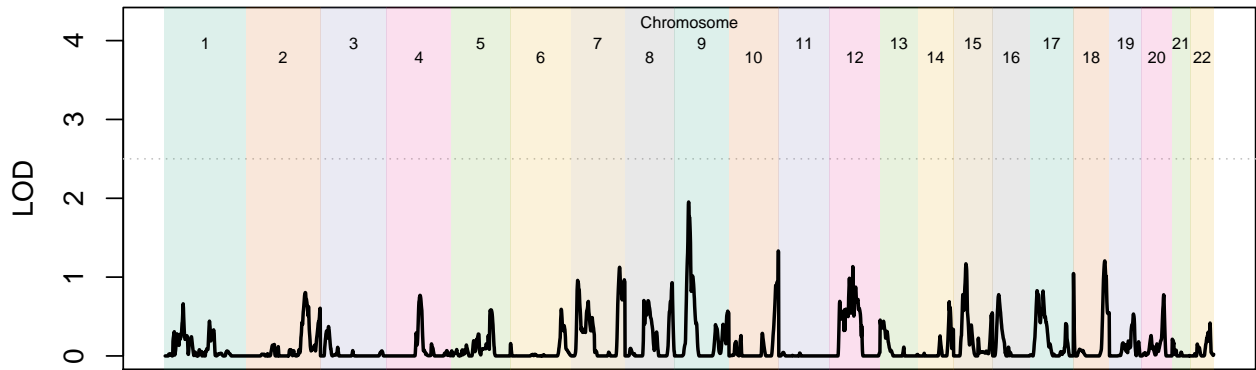


Figure C12: 33% Tibia Cortical Area

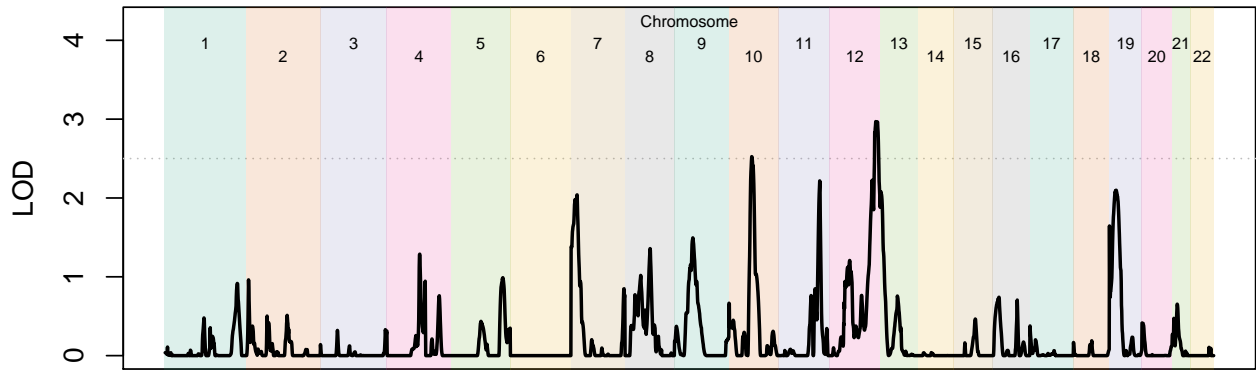


Figure C13: 33% Radius Cortical Bone Mineral Density

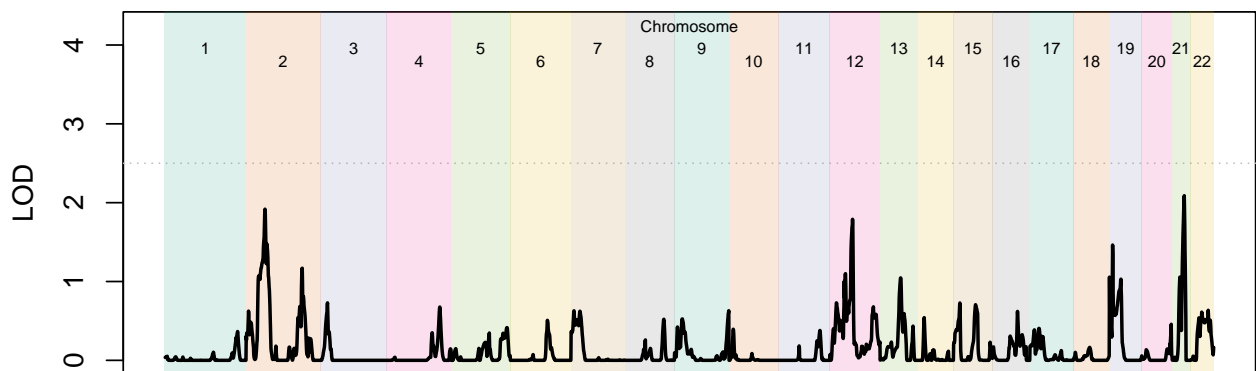


Figure C14: 33% Tibia Cortical Bone Mineral Density

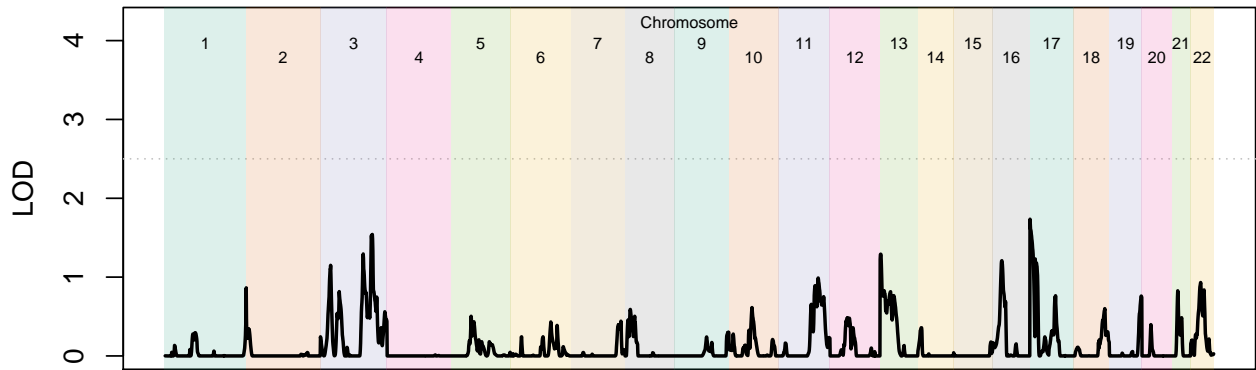


Figure C15: 33% Radius Cortical Thickness

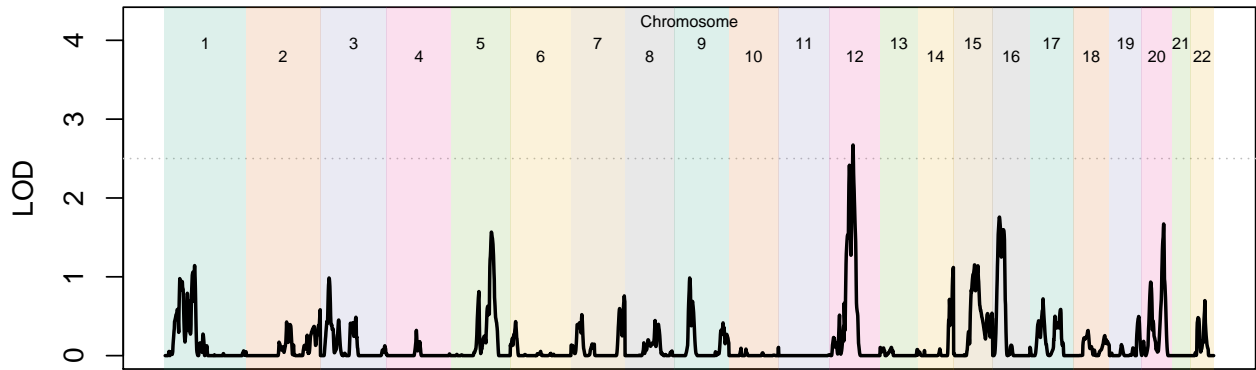


Figure C16: 33% Tabia Cortical Thickness

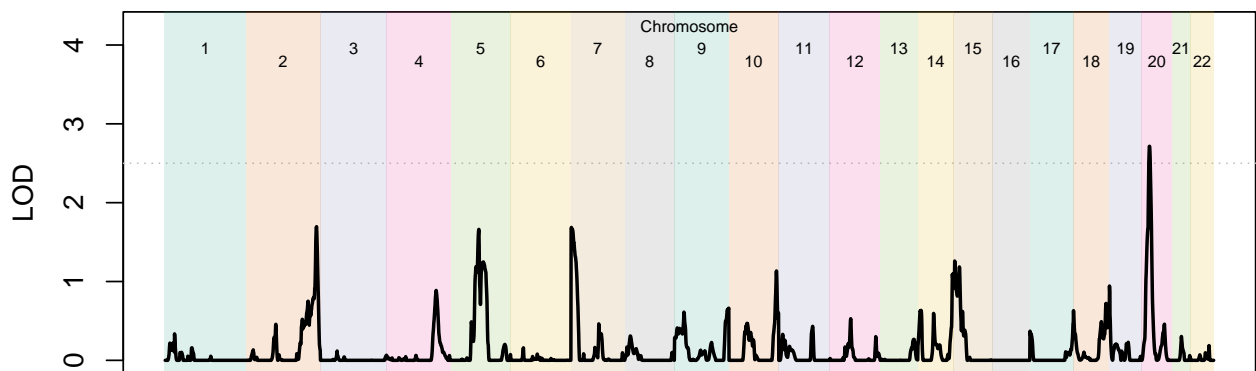


Figure C17: 33% Radius Periosteal Circumference

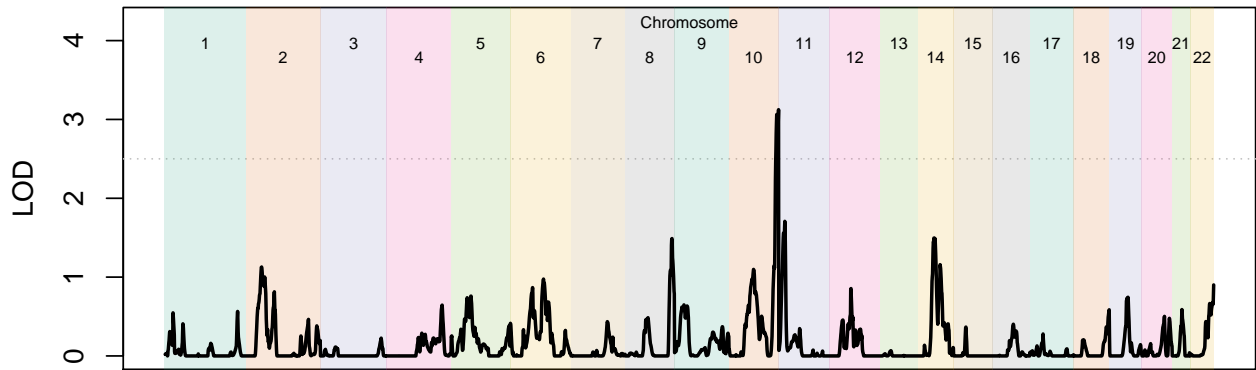


Figure C18: 33% Tibia Periosteal Circumference

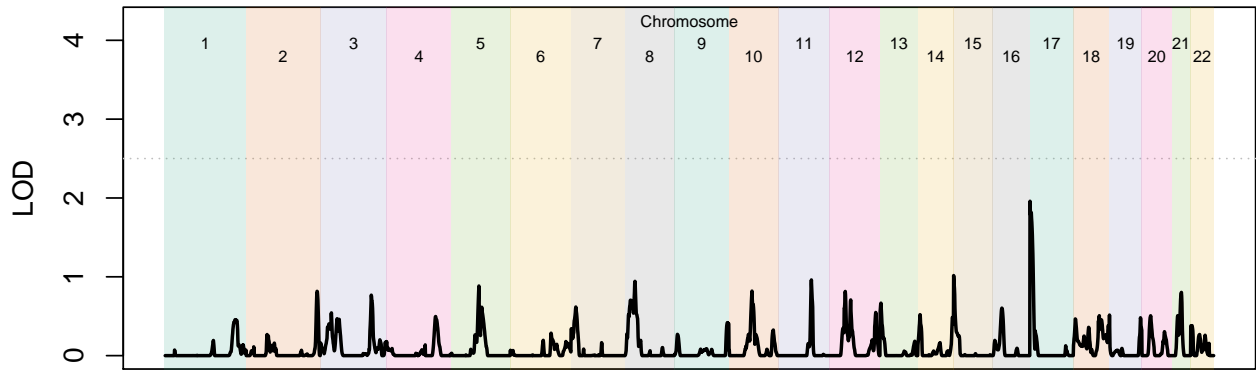


Figure C19: 33% Radius Endosteal Circumference

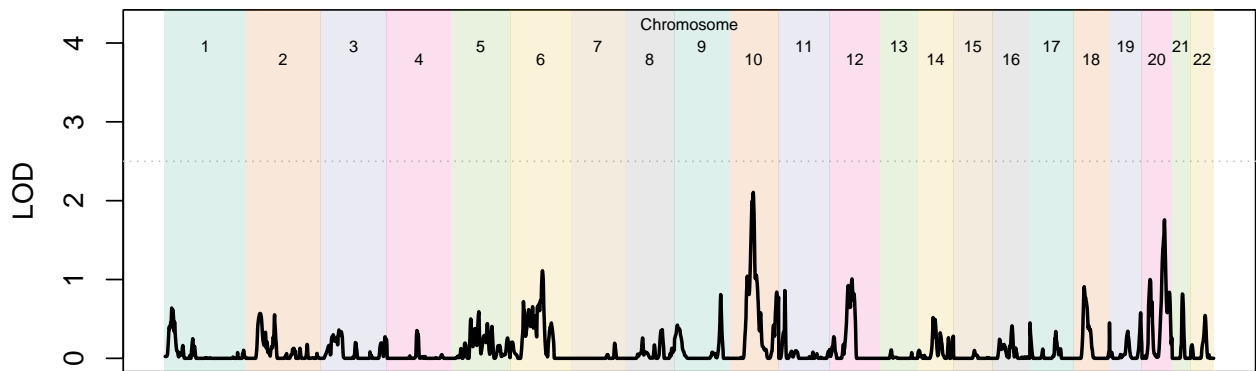


Figure C20: 33% Tibia Endosteal Circumference

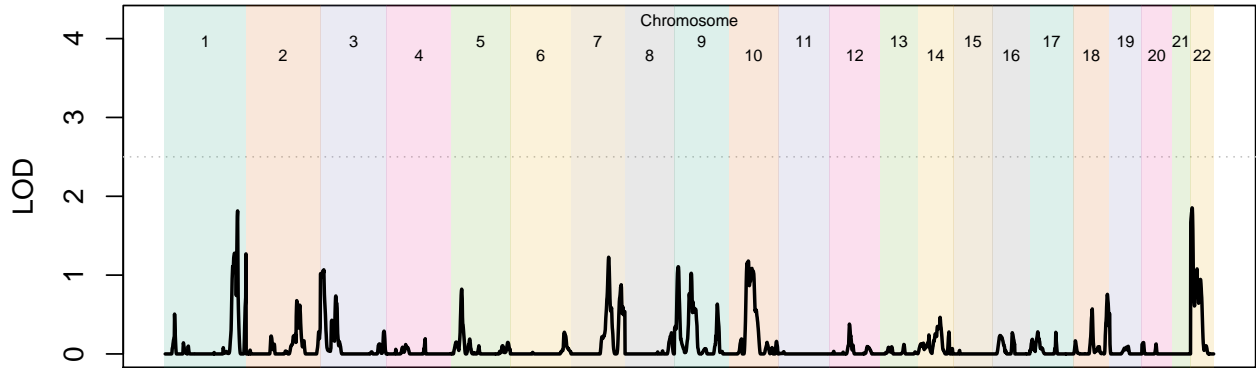


Figure C21: 66% Total Bone Mineral Density

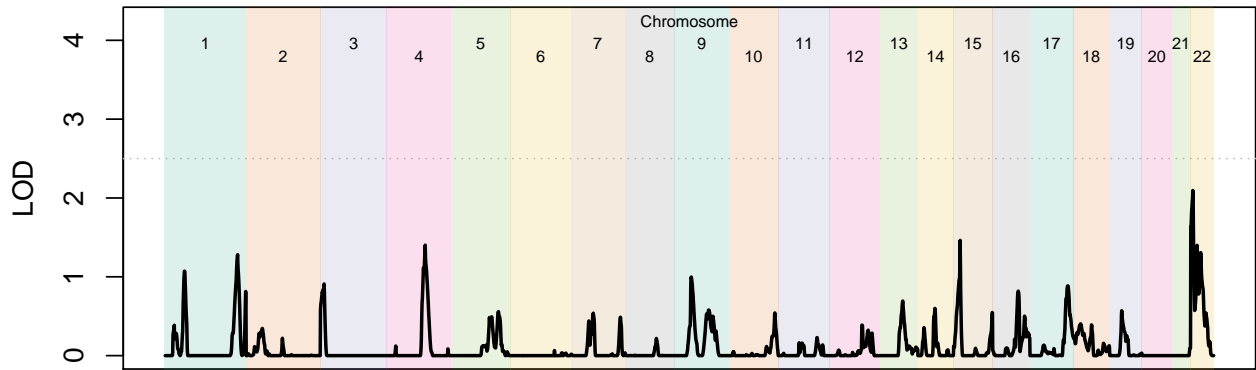


Figure C22: 66% Tibia Cortical Bone Mineral Density

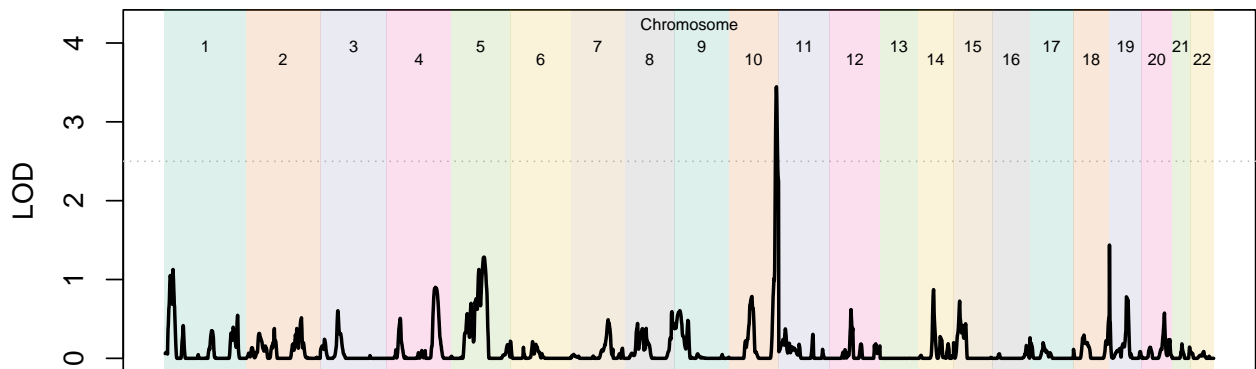


Figure C23: Principal Component 1

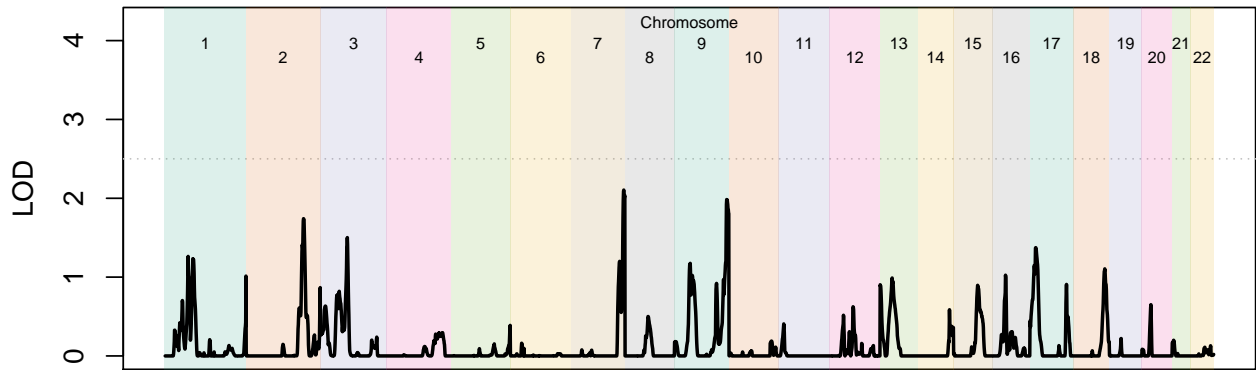


Figure C24: Principal Component 2

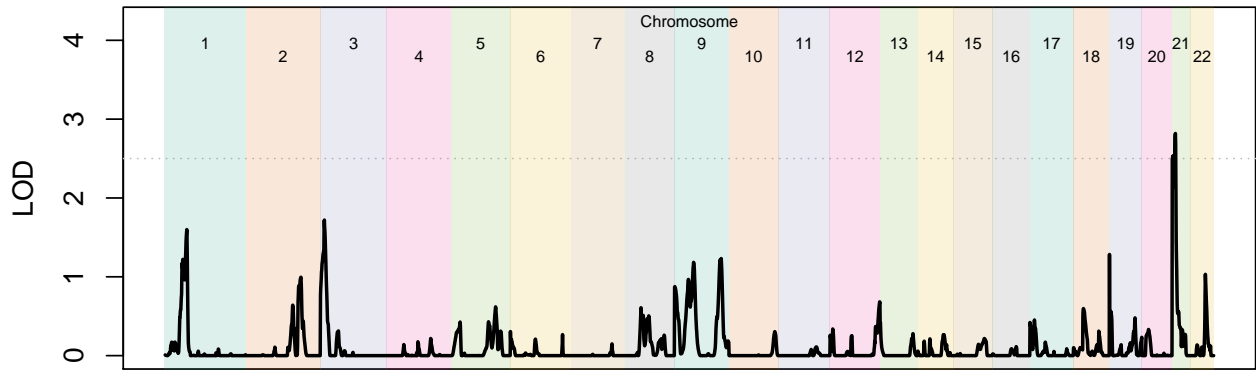


Figure C25: Principal Component 3

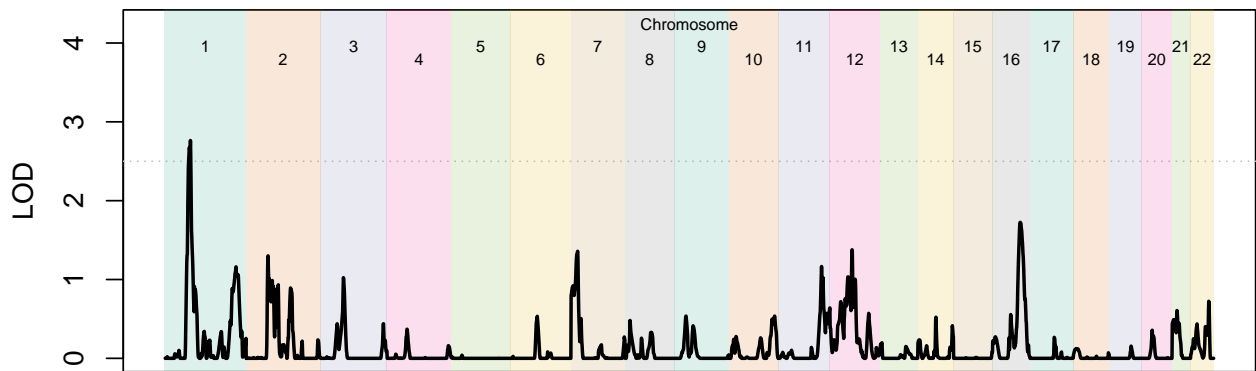


Figure C26: Principal Component 4

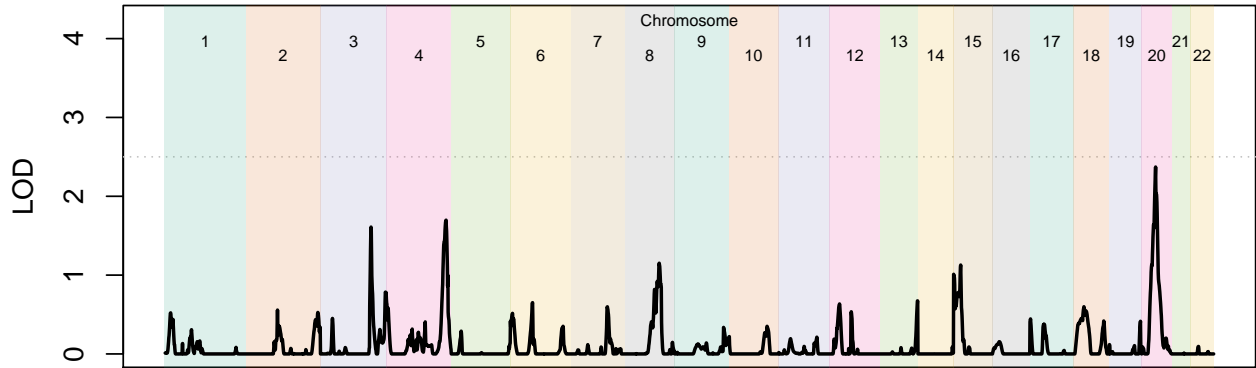


Figure C27: Principal Component 5

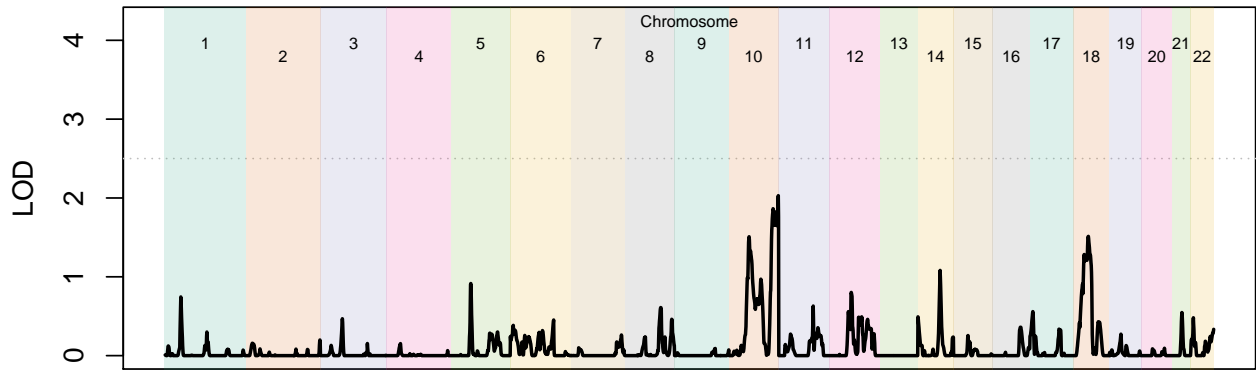


Figure C28: Principal Component 6

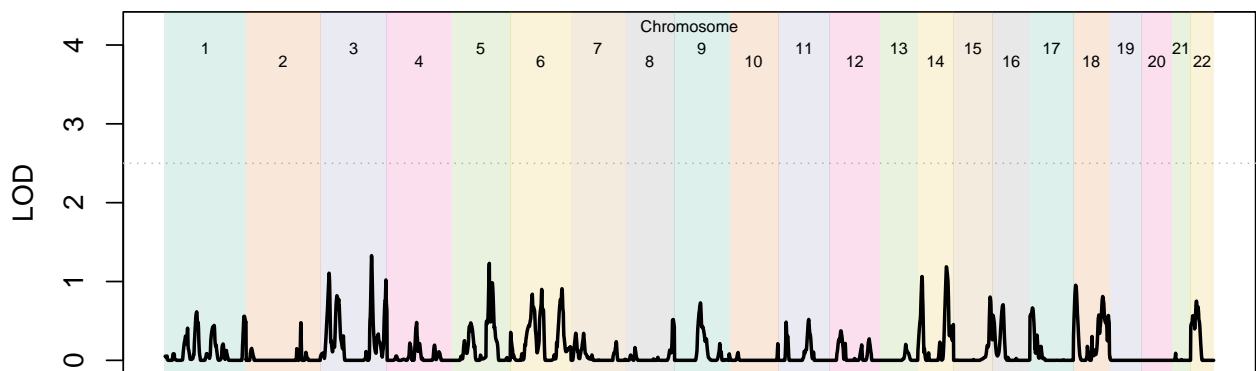


Figure C29: Principal Component 7

APPENDIX D

QUANTILE-QUANTILE PLOTS

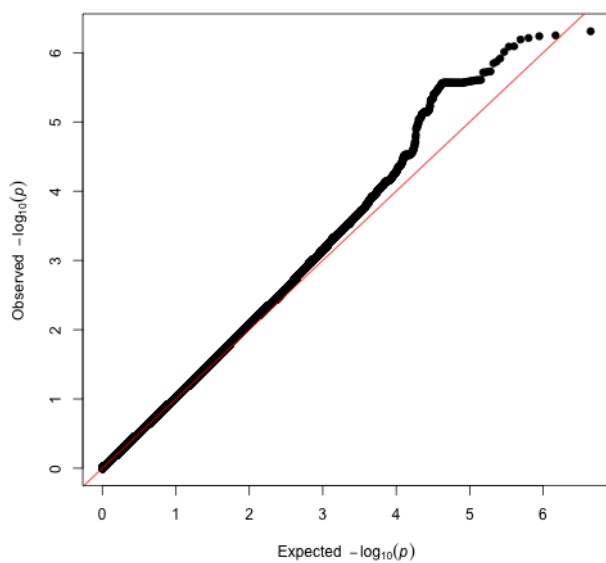


Figure D1: QQ Plot FNBMD Eur. Am. Men

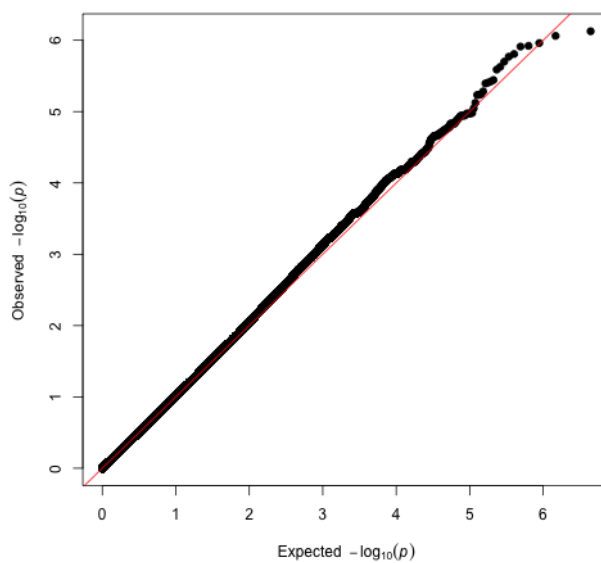


Figure D2: QQ Plot FNBMD Eur. Am. Women

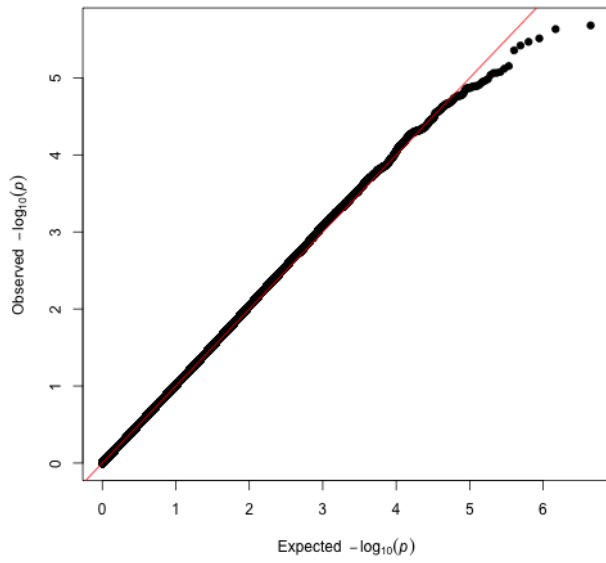


Figure D3: QQ Plot LSBMD Eur. Am. Men

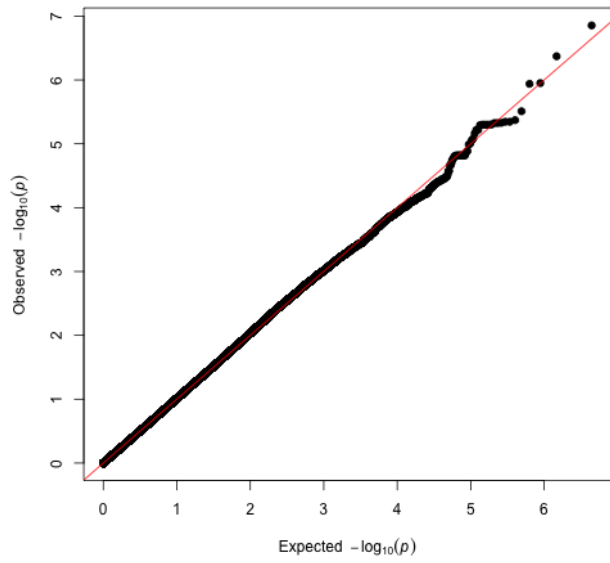


Figure D4: QQ Plot LSBMD Eur. Am. Women

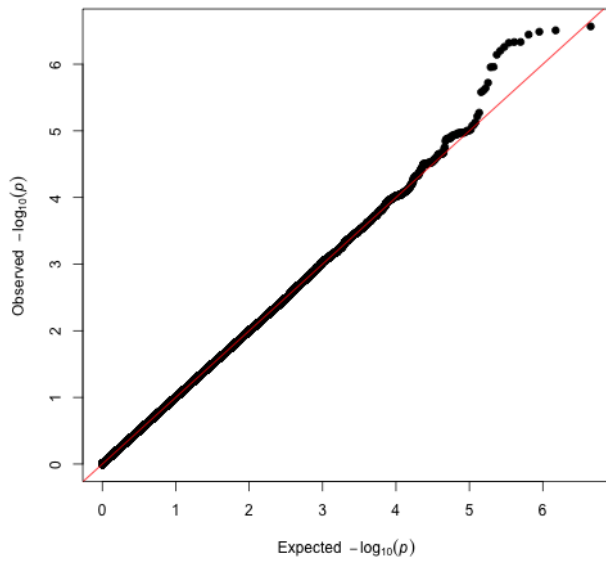


Figure D5: QQ Plot All Fx Eur. Am. Men

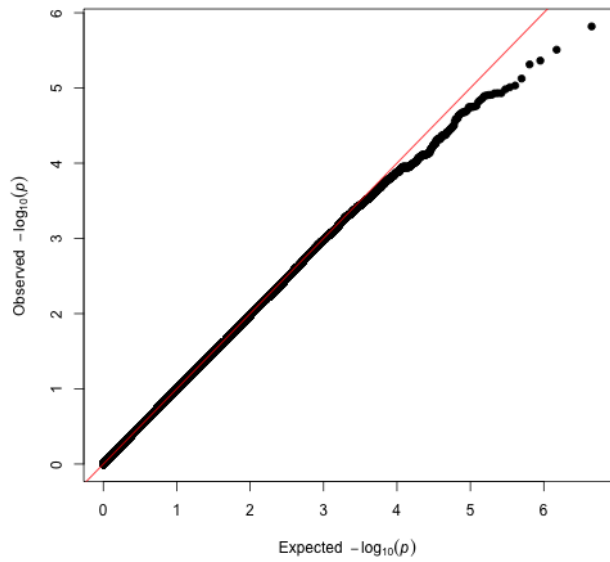


Figure D6: QQ Plot All Fx Eur. Am. Women

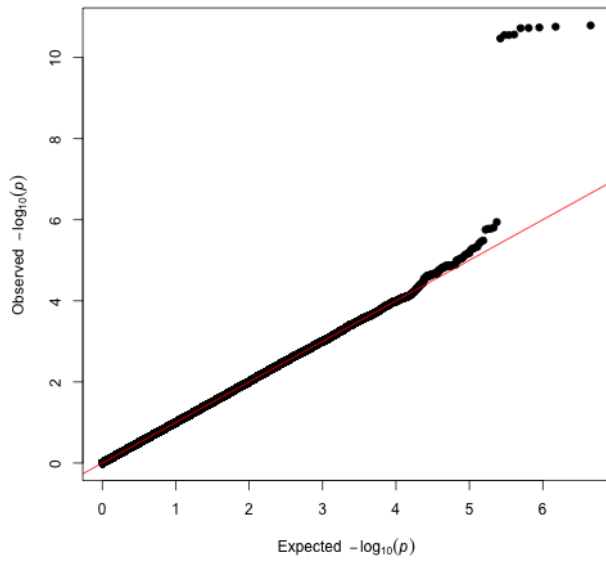


Figure D7: QQ Plot N.-V. Fx Eur. Am. Men

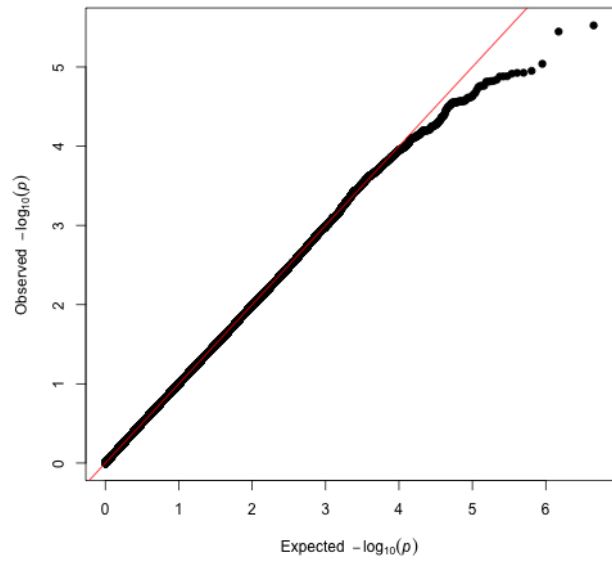


Figure D8: QQ Plot N.-V. Fx Eur. Am. Women

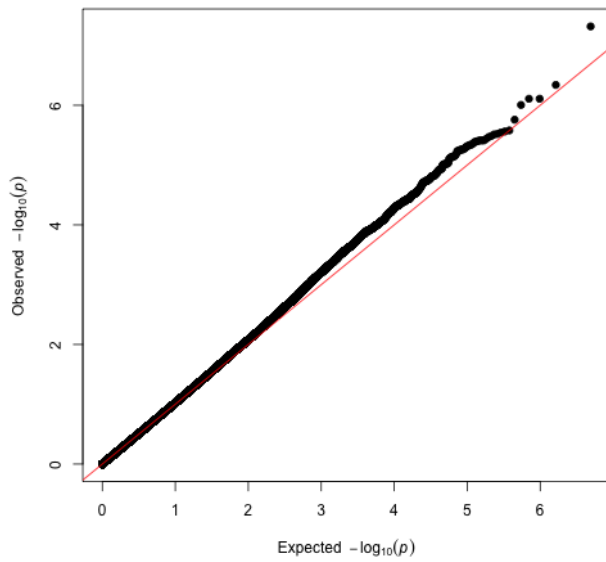


Figure D9: QQ Plot FNBMD Afr. Am. Men

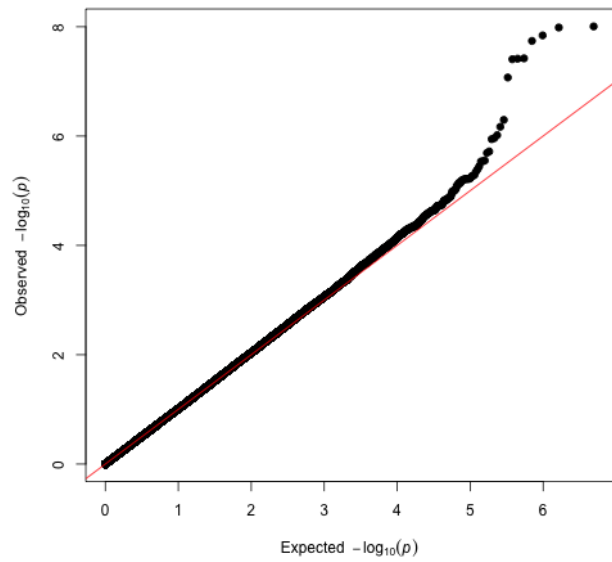


Figure D10: QQ Plot FNBMD Afr. Am. Women

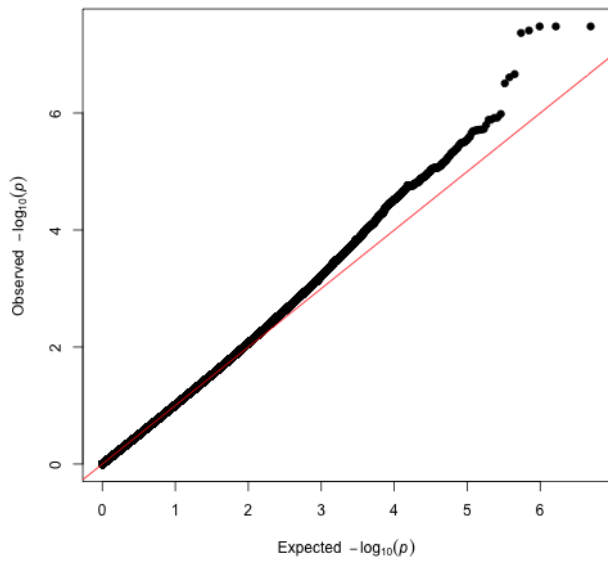


Figure D11: QQ Plot LSBMD Afr. Am. Men

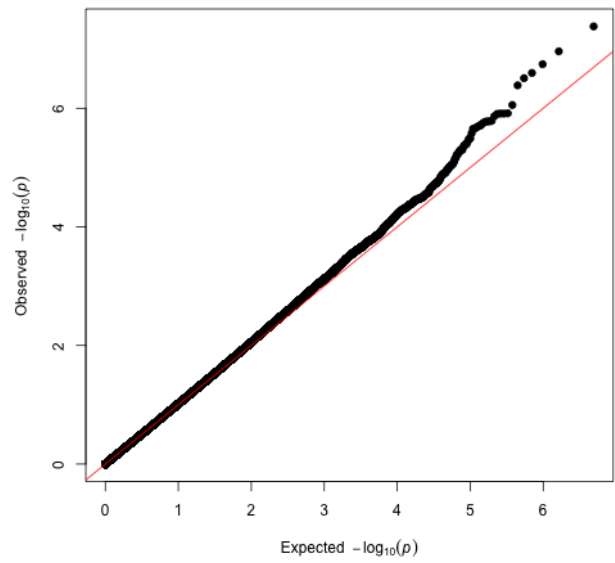


Figure D12: QQ Plot LSBMD Afr. Am. Women

APPENDIX E

MANHATTAN PLOTS

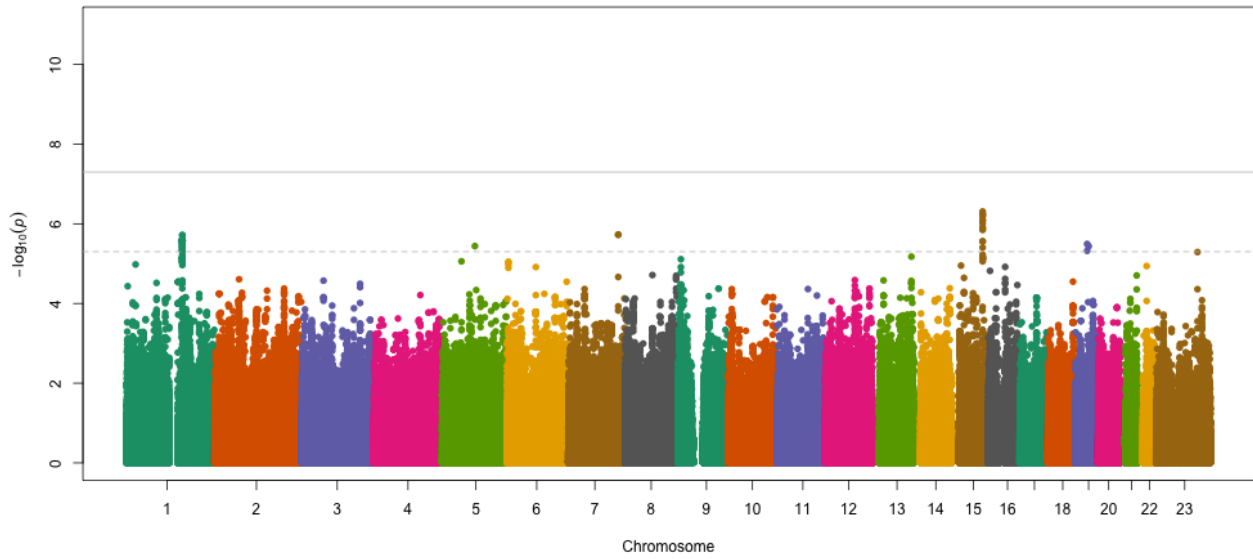


Figure E1: Manhattan Plot for FNBMD in European American Men

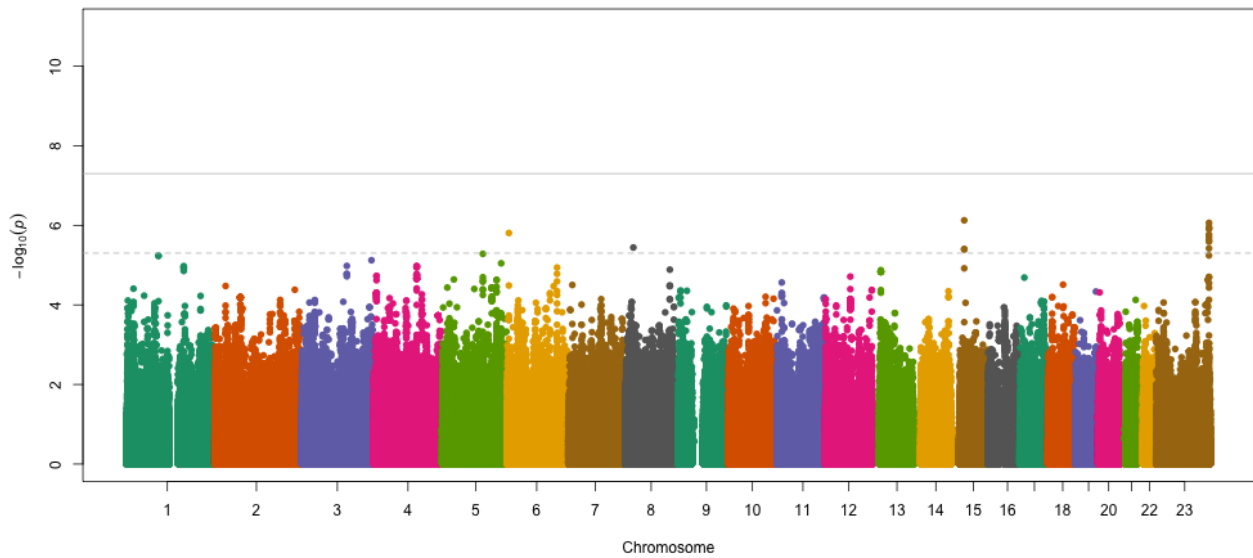


Figure E2: Manhattan Plot for FNBMD in European American Women

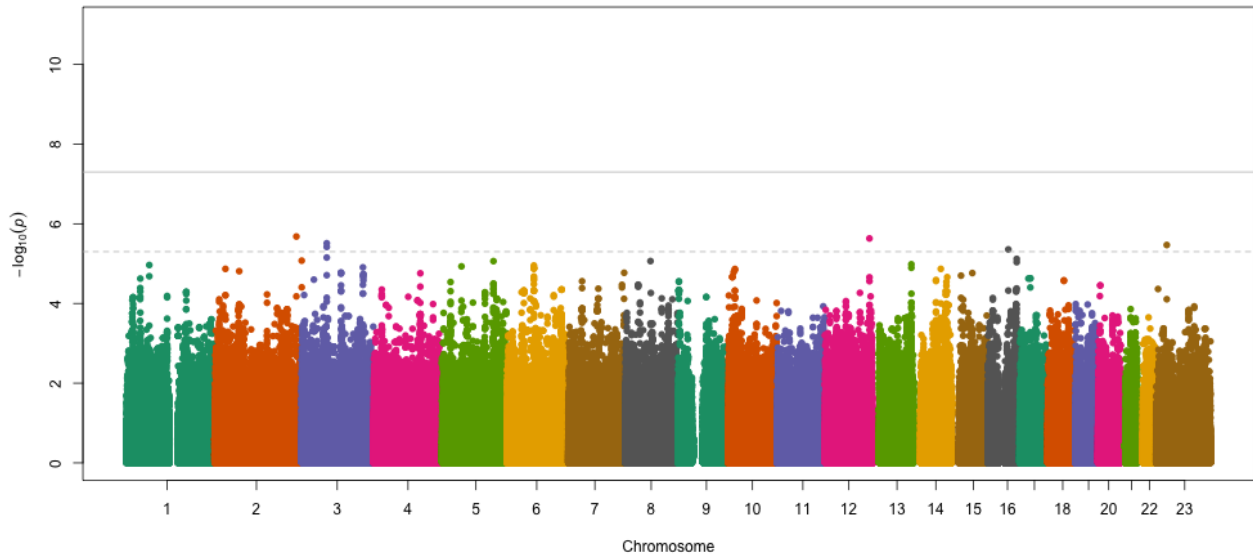


Figure E3: Manhattan Plot for LSBMD in European American Men

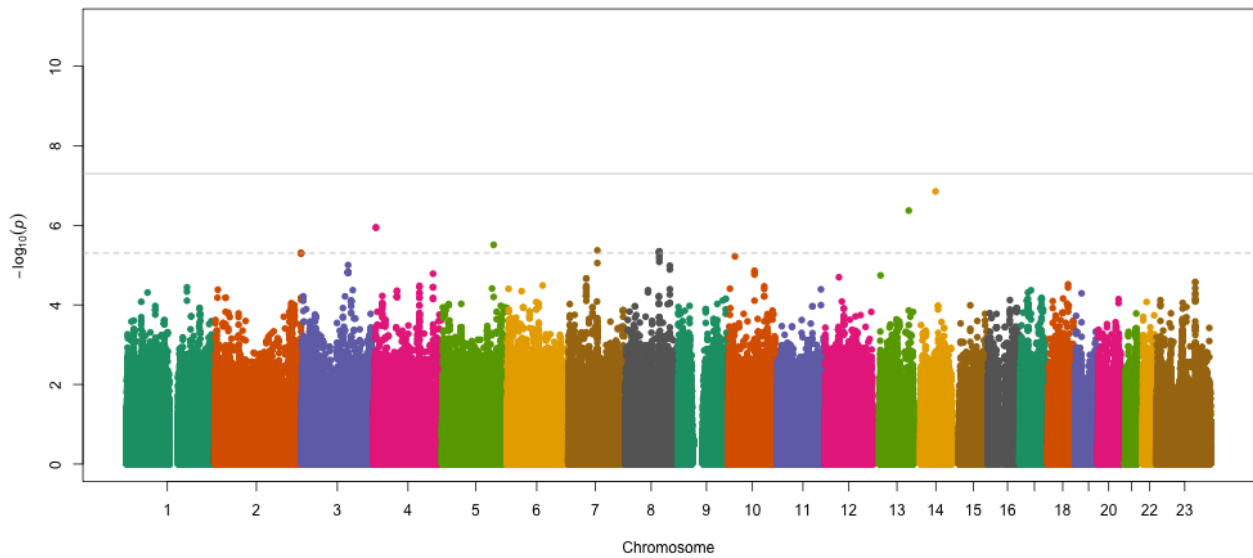


Figure E4: Manhattan Plot for LSBMD in European American Women

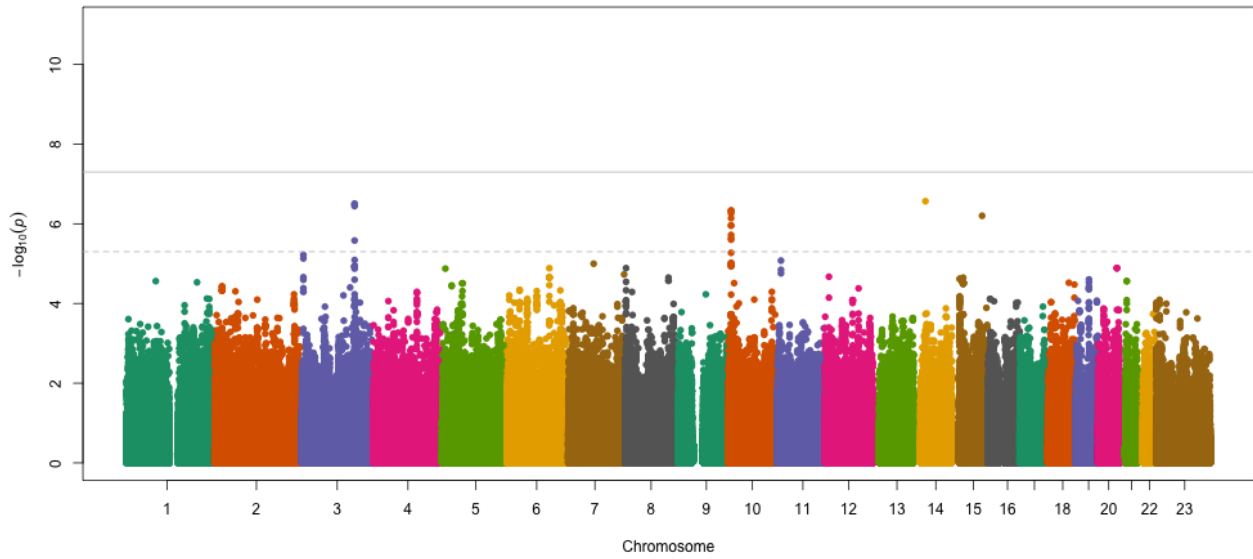


Figure E5: Manhattan Plot for All Fractures in European American Men

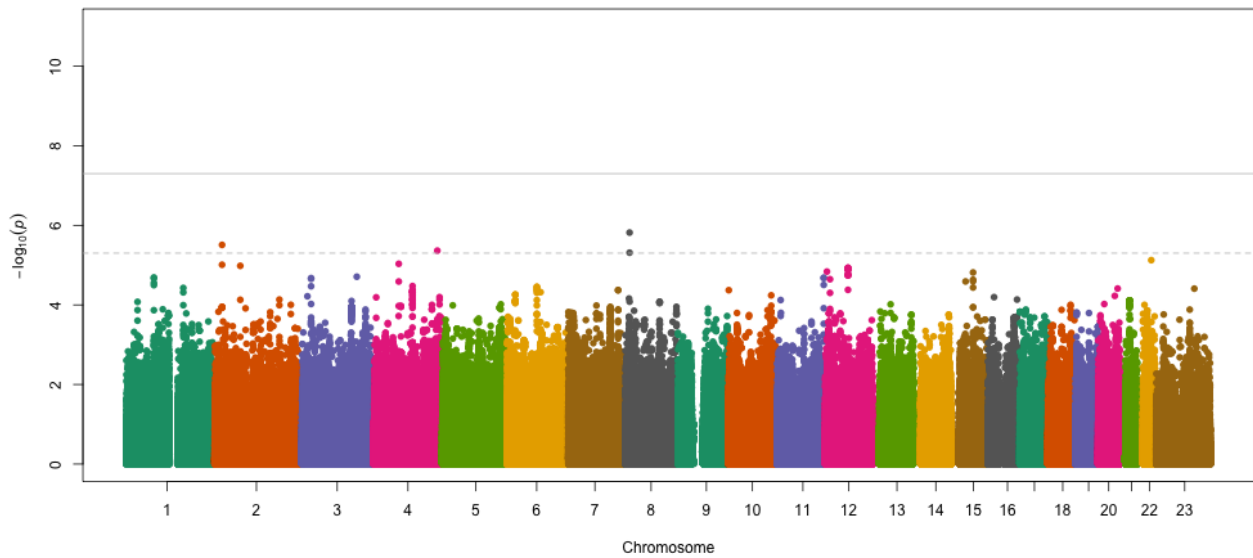


Figure E6: Manhattan Plot for All Fractures in European American Women

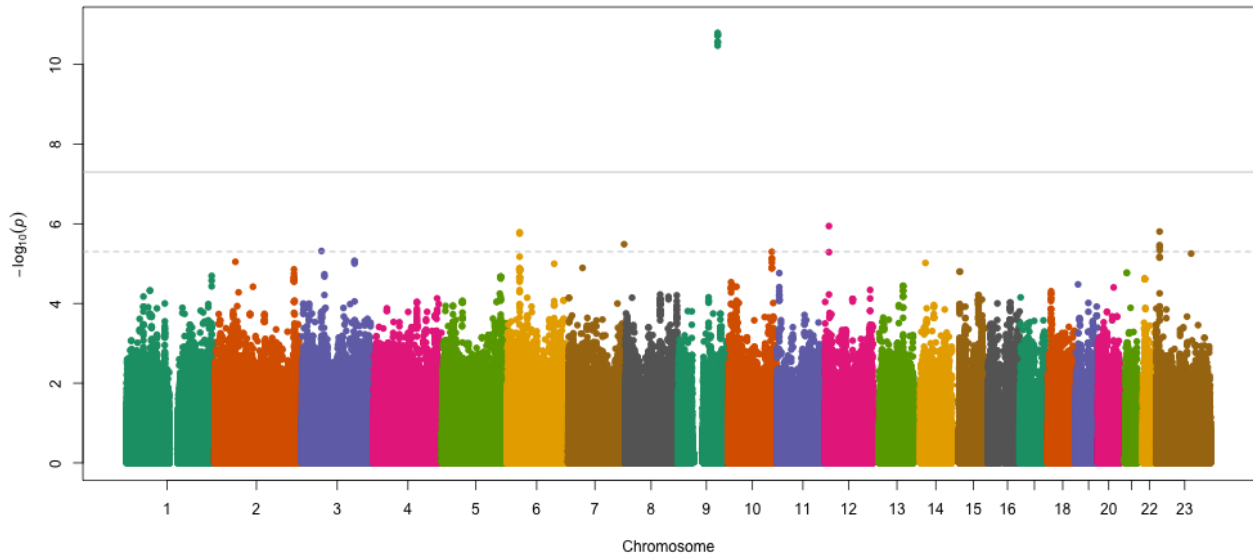


Figure E7: Manhattan Plot for Non-Vertebral Fractures in European American Men

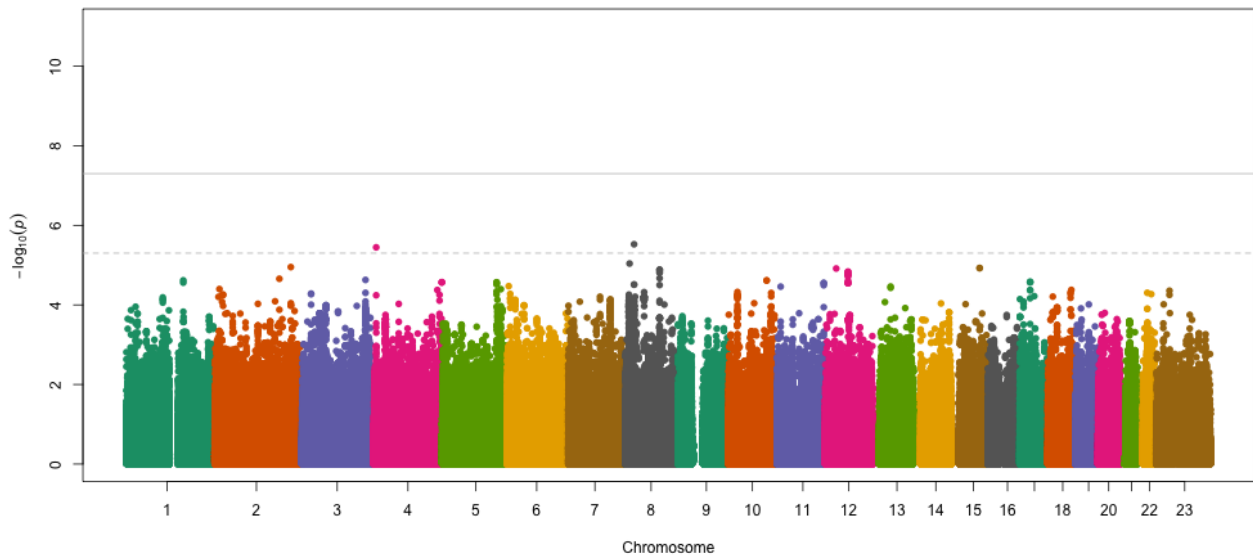


Figure E8: Manhattan Plot for Non-Vertebral Fractures in European American Women

APPENDIX F

SNPS WITH SUGGESTIVE P VALUES

Table F1: FNBMD Pooled Hits – European Americans

Locus	SNP	Position	Nearest Gene	Distance (kb)	Alleles	MAF	Type	β	s.e.	p
3p24.1	<i>rs11717372</i>	27202560	<i>NEK10</i>	29.5	G/A	0.26	I	0.202	0.040	5.17×10^{-7}
	<i>rs11717314</i>	27202583	<i>NEK10</i>	29.5	C/T	0.27	I	0.195	0.040	1.03×10^{-6}
	<i>rs10510596</i>	27203014	<i>NEK10</i>	29.1	G/A	0.27	I	0.195	0.040	1.03×10^{-6}
	<i>rs11928525</i>	27206723	<i>NEK10</i>	25.4	T/C	0.27	I	0.195	0.040	1.06×10^{-6}
	<i>rs11926580</i>	27208380	<i>NEK10</i>	23.7	G/T	0.27	I	0.195	0.040	1.06×10^{-6}
	<i>rs11926556</i>	27208502	<i>NEK10</i>	23.6	C/A	0.27	G	0.195	0.040	1.06×10^{-6}
	<i>rs11928916</i>	27210944	<i>NEK10</i>	21.2	C/A	0.27	I	0.195	0.040	1.06×10^{-6}
	<i>rs724243</i>	27216940	<i>NEK10</i>	15.2	C/A	0.27	I	0.191	0.040	1.46×10^{-6}
	<i>rs724244</i>	27217157	<i>NEK10</i>	14.9	C/T	0.27	G	0.191	0.040	1.46×10^{-6}
	<i>rs724245</i>	27217244	<i>NEK10</i>	14.9	G/T	0.27	I	0.191	0.040	1.46×10^{-6}
	<i>rs17680166</i>	27218049	<i>NEK10</i>	14.1	G/C	0.27	I	0.191	0.040	1.47×10^{-6}
	<i>rs11923983</i>	27218483	<i>NEK10</i>	13.6	A/C	0.27	I	0.191	0.040	1.47×10^{-6}
	<i>rs11712907</i>	27219569	<i>NEK10</i>	12.5	T/C	0.27	I	0.191	0.040	1.47×10^{-6}
	<i>rs11708854</i>	27219577	<i>NEK10</i>	12.5	G/A	0.27	I	0.191	0.040	1.47×10^{-6}
	<i>rs11708844</i>	27219713	<i>NEK10</i>	12.4	C/T	0.27	I	0.190	0.040	1.47×10^{-6}
	<i>rs6792693</i>	27220229	<i>NEK10</i>	11.9	A/G	0.27	G	0.190	0.040	1.47×10^{-6}
	<i>rs11129268</i>	27220397	<i>NEK10</i>	11.7	G/A	0.27	I	0.190	0.040	1.47×10^{-6}
	<i>rs11709858</i>	27220422	<i>NEK10</i>	11.7	C/T	0.27	I	0.190	0.040	1.47×10^{-6}
	<i>rs4973755</i>	27223167	<i>NEK10</i>	8.9	G/A	0.27	I	0.190	0.040	1.47×10^{-6}
	<i>rs6793827</i>	27224116	<i>NEK10</i>	8.0	C/T	0.27	I	0.190	0.040	1.47×10^{-6}
	<i>rs6806213</i>	27224288	<i>NEK10</i>	7.8	A/G	0.27	I	0.190	0.040	1.47×10^{-6}
	<i>rs6806325</i>	27224359	<i>NEK10</i>	7.7	A/G	0.27	I	0.190	0.040	1.47×10^{-6}
	<i>rs13063897</i>	27225007	<i>NEK10</i>	7.1	C/G	0.27	I	0.190	0.040	1.47×10^{-6}
	<i>rs13079813</i>	27225396	<i>NEK10</i>	6.7	G/A	0.28	I	0.191	0.040	1.55×10^{-6}
	<i>rs11713802</i>	27225862	<i>NEK10</i>	6.2	T/C	0.27	I	0.190	0.040	1.47×10^{-6}
	<i>rs4973860</i>	27225895	<i>NEK10</i>	6.2	A/G	0.27	G	0.190	0.040	1.47×10^{-6}

Continued on next page

Table F1 — continued from previous page

Locus	SNP	Position	Nearest Distance		Alleles	MAF	Type	β	s.e.	p
			Gene	(kb)						
<i>rs4973861</i>		27226054	<i>NEK10</i>	6.0	G/T	0.27	I	0.191	0.040	1.44×10^{-6}
<i>rs2120893</i>		27227022	<i>NEK10</i>	5.1	G/A	0.27	I	0.191	0.040	1.38×10^{-6}
<i>rs11920408</i>		27227707	<i>NEK10</i>	4.4	C/T	0.27	I	0.191	0.040	1.32×10^{-6}
<i>rs11928065</i>		27227773	<i>NEK10</i>	4.3	A/G	0.27	I	0.192	0.040	1.27×10^{-6}
<i>rs11129269</i>		27228718	<i>NEK10</i>	3.4	A/G	0.27	I	0.192	0.040	1.20×10^{-6}
<i>rs11715168</i>		27230796	<i>NEK10</i>	1.3	G/T	0.27	I	0.193	0.040	1.11×10^{-6}
<i>rs11715136</i>		27230868	<i>NEK10</i>	1.2	C/T	0.27	I	0.195	0.040	8.98×10^{-7}
<i>rs11720211</i>		27231039	<i>NEK10</i>	1.1	T/A	0.27	I	0.196	0.040	7.35×10^{-7}
<i>rs13085421</i>		27233737	<i>NEK10</i>	0.0	A/G	0.28	G	0.197	0.040	6.70×10^{-7}
<i>rs1596701</i>		27236343	<i>NEK10</i>	0.0	T/C	0.28	I	0.194	0.040	9.79×10^{-7}
<i>rs6796032</i>		27240555	<i>NEK10</i>	0.0	C/A	0.28	I	0.195	0.040	9.14×10^{-7}
<i>rs2218472</i>		27248568	<i>NEK10</i>	0.0	T/C	0.27	I	0.190	0.040	1.68×10^{-6}
<i>rs2197435</i>		27252047	<i>NEK10</i>	0.0	C/G	0.27	I	0.190	0.040	1.68×10^{-6}
<i>rs4586769</i>		27254427	<i>NEK10</i>	0.0	G/A	0.27	I	0.190	0.040	1.69×10^{-6}
<i>rs7626869</i>		27256693	<i>NEK10</i>	0.0	T/A	0.27	I	0.190	0.040	1.70×10^{-6}
<i>rs1158719</i>		27256773	<i>NEK10</i>	0.0	C/A	0.27	G	0.190	0.040	1.70×10^{-6}
<i>rs11129271</i>		27258121	<i>NEK10</i>	0.0	A/T	0.27	I	0.190	0.040	1.71×10^{-6}
<i>rs11925748</i>		27260236	<i>NEK10</i>	0.0	A/T	0.27	I	0.190	0.040	1.72×10^{-6}
<i>rs1373769</i>		27260670	<i>NEK10</i>	0.0	C/T	0.27	I	0.190	0.040	1.73×10^{-6}
<i>rs10865813</i>		27266147	<i>NEK10</i>	0.0	C/T	0.27	I	0.190	0.040	1.80×10^{-6}
<i>rs11129274</i>		27267085	<i>NEK10</i>	0.0	T/C	0.27	I	0.190	0.040	1.81×10^{-6}
<i>rs2120887</i>		27269837	<i>NEK10</i>	0.0	A/G	0.27	G	0.190	0.040	1.82×10^{-6}
<i>rs1550769</i>		27271800	<i>NEK10</i>	0.0	C/G	0.27	I	0.190	0.040	1.83×10^{-6}
<i>rs1550768</i>		27271826	<i>NEK10</i>	0.0	A/T	0.27	I	0.190	0.040	1.84×10^{-6}
<i>rs12488147</i>		27272623	<i>NEK10</i>	0.0	A/T	0.27	I	0.190	0.040	1.84×10^{-6}
<i>rs12494667</i>		27272688	<i>NEK10</i>	0.0	C/A	0.27	G	0.190	0.040	1.84×10^{-6}
<i>rs6804742</i>		27278400	<i>NEK10</i>	0.0	C/T	0.27	I	0.189	0.040	1.87×10^{-6}
<i>rs11129278</i>		27280618	<i>NEK10</i>	0.0	G/C	0.27	I	0.189	0.040	1.87×10^{-6}
<i>rs12486588</i>		27288126	<i>NEK10</i>	0.0	G/T	0.27	G	0.189	0.040	1.88×10^{-6}
<i>rs7635995</i>		27289490	<i>NEK10</i>	0.0	T/G	0.27	I	0.189	0.040	1.88×10^{-6}
<i>rs4973868</i>		27291923	<i>NEK10</i>	0.0	C/A	0.27	G	0.189	0.040	1.88×10^{-6}
<i>rs1542152</i>		27297069	<i>NEK10</i>	0.0	A/T	0.27	I	0.190	0.040	1.87×10^{-6}
<i>rs11919927</i>		27297211	<i>NEK10</i>	0.0	G/A	0.27	I	0.190	0.040	1.86×10^{-6}
<i>rs11129279</i>		27297347	<i>NEK10</i>	0.0	A/C	0.27	I	0.190	0.040	1.87×10^{-6}
<i>rs6788621</i>		27298386	<i>NEK10</i>	0.0	C/T	0.27	I	0.189	0.040	1.89×10^{-6}
<i>rs11129280</i>		27301101	<i>NEK10</i>	0.0	G/T	0.27	G	0.189	0.040	1.92×10^{-6}
<i>rs10510594</i>		27301455	<i>NEK10</i>	0.0	A/G	0.27	G	0.189	0.040	1.91×10^{-6}
<i>rs10510593</i>		27304421	<i>NEK10</i>	0.0	A/C	0.27	I	0.189	0.040	1.86×10^{-6}
<i>rs10510592</i>		27307824	<i>NEK10</i>	0.0	A/G	0.27	G	0.190	0.040	1.74×10^{-6}
<i>rs4973869</i>		27312933	<i>NEK10</i>	0.0	G/A	0.27	I	0.190	0.040	1.77×10^{-6}
<i>rs4973870</i>		27313428	<i>NEK10</i>	0.0	C/A	0.27	I	0.190	0.040	1.78×10^{-6}
<i>rs1445115</i>		27320385	<i>NEK10</i>	0.0	G/A	0.27	I	0.189	0.040	2.01×10^{-6}
<i>rs1445112</i>		27326290	<i>NEK10</i>	0.0	A/G	0.27	G	0.184	0.040	3.42×10^{-6}
<i>rs17239342</i>		27332725	<i>NEK10</i>	0.0	G/C	0.27	I	0.185	0.040	3.18×10^{-6}

Continued on next page

Table F1 — continued from previous page

Locus	SNP	Position	Nearest Distance		Alleles	MAF	Type	β	s.e.	p
			Gene	(kb)						
5q15	<i>rs12152280</i>	27333016	<i>NEK10</i>	0.0	A/T	0.25	I	0.188	0.041	4.21×10^{-6}
	<i>rs6795834</i>	27335467	<i>NEK10</i>	0.0	C/T	0.25	I	0.189	0.041	3.76×10^{-6}
	<i>rs3909479</i>	94813710	<i>FAM81B</i>	1.8	C/T	0.10	G	-0.272	0.058	2.48×10^{-6}
	<i>rs7705631</i>	94799340	<i>FAM81B</i>	0.0	A/C	0.10	I	-0.267	0.058	4.00×10^{-6}
8p22	<i>rs13252590</i>	16566118	<i>FGF20</i>	328.6	A/T	0.47	I	0.174	0.035	6.45×10^{-7}
	<i>rs1433289</i>	16565923	<i>FGF20</i>	328.8	G/A	0.40	G	0.172	0.036	1.60×10^{-6}
8p21.3	<i>rs12114940</i>	22104735	<i>BMP1</i>	0.0	T/G	0.45	G	0.173	0.036	1.71×10^{-6}
13q33.3	<i>rs17382033</i>	107839404	<i>TNFSF13B</i>	80.6	C/A	0.09	G	0.329	0.062	1.33×10^{-7}
	<i>rs2391637</i>	107843488	<i>TNFSF13B</i>	84.7	A/G	0.09	I	0.306	0.063	1.08×10^{-6}
16q21	<i>rs2962454</i>	61494729	<i>CDH8</i>	866.5	G/A	0.24	G	0.191	0.040	2.33×10^{-6}
	<i>rs2914486</i>	61494154	<i>CDH8</i>	865.9	T/C	0.25	G	0.183	0.040	3.76×10^{-6}

Table F2: FNBMD Men Hits – European Americans

Locus	SNP	Position	Nearest Distance		Alleles	MAF	Type	β	s.e.	p
			Gene	(kb)						
1q23.1	<i>rs2054993</i>	156772592	<i>OR6Y1</i>	10.9	G/T	0.44	I	-0.239	0.050	1.92×10^{-6}
	<i>rs9651046</i>	156700714	<i>OR10K1</i>	1.3	T/G	0.40	I	-0.228	0.050	4.77×10^{-6}
	<i>rs1573519</i>	156701902	<i>OR10K1</i>	0.1	A/G	0.40	G	-0.228	0.050	4.66×10^{-6}
	<i>rs12404821</i>	156706203	<i>OR10K1</i>	3.3	C/T	0.40	G	-0.228	0.050	4.66×10^{-6}
	<i>rs10908650</i>	156709125	<i>OR10K1</i>	6.2	A/G	0.40	I	-0.229	0.050	4.51×10^{-6}
	<i>rs11264997</i>	156752106	<i>OR6Y1</i>	31.4	A/G	0.44	G	-0.233	0.050	3.09×10^{-6}
	<i>rs7555174</i>	156754050	<i>OR6Y1</i>	29.5	G/A	0.44	I	-0.233	0.050	2.97×10^{-6}
	<i>rs7549581</i>	156756328	<i>OR6Y1</i>	27.2	C/T	0.43	I	-0.234	0.050	3.39×10^{-6}
	<i>rs7512592</i>	156756569	<i>OR6Y1</i>	27.0	A/G	0.43	G	-0.229	0.050	3.98×10^{-6}
	<i>rs10797020</i>	156756948	<i>OR6Y1</i>	26.6	G/A	0.43	G	-0.229	0.050	3.98×10^{-6}
	<i>rs11265003</i>	156757255	<i>OR6Y1</i>	26.3	T/C	0.43	I	-0.229	0.050	3.83×10^{-6}
	<i>rs950260</i>	156758144	<i>OR6Y1</i>	25.4	A/G	0.44	I	-0.230	0.050	3.57×10^{-6}
	<i>rs2317969</i>	156758377	<i>OR6Y1</i>	25.2	G/A	0.44	I	-0.231	0.050	3.35×10^{-6}
	<i>rs7518808</i>	156758444	<i>OR6Y1</i>	25.1	A/G	0.44	I	-0.232	0.050	3.25×10^{-6}
	<i>rs2157687</i>	156759624	<i>OR6Y1</i>	23.9	T/C	0.44	I	-0.232	0.050	3.04×10^{-6}
	<i>rs1032352</i>	156759778	<i>OR6Y1</i>	23.8	T/C	0.44	I	-0.233	0.050	2.78×10^{-6}
	<i>rs7548349</i>	156760350	<i>OR6Y1</i>	23.2	T/C	0.43	G	-0.234	0.050	2.72×10^{-6}
	<i>rs7514968</i>	156760476	<i>OR6Y1</i>	23.1	T/A	0.43	I	-0.234	0.050	2.72×10^{-6}
	<i>rs7525362</i>	156760514	<i>OR6Y1</i>	23.0	C/G	0.43	I	-0.234	0.050	2.72×10^{-6}
	<i>rs12145401</i>	156761317	<i>OR6Y1</i>	22.2	G/A	0.43	I	-0.234	0.050	2.72×10^{-6}
<i>rs6663277</i>	156761625	<i>OR6Y1</i>	21.9	T/A	0.43	I	-0.238	0.050	1.93×10^{-6}	
<i>rs6699473</i>	156761833	<i>OR6Y1</i>	21.7	T/C	0.43	G	-0.234	0.050	2.72×10^{-6}	
<i>rs6674656</i>	156762055	<i>OR6Y1</i>	21.5	A/G	0.43	G	-0.234	0.050	2.72×10^{-6}	
<i>rs10797023</i>	156763703	<i>OR6Y1</i>	19.8	C/T	0.43	I	-0.234	0.050	2.72×10^{-6}	
<i>rs6672789</i>	156763763	<i>OR6Y1</i>	19.8	C/T	0.43	I	-0.234	0.050	2.72×10^{-6}	

Continued on next page

Table F2 — continued from previous page

Locus	SNP	Position	Nearest	Distance	Alleles	MAF	Type	β	s.e.	p
			Gene	(kb)						
	<i>rs10797024</i>	156763787	<i>OR6Y1</i>	19.8	A/G	0.43	I	-0.234	0.050	2.72×10^{-6}
	<i>rs6657638</i>	156763808	<i>OR6Y1</i>	19.7	G/C	0.43	I	-0.234	0.050	2.72×10^{-6}
	<i>rs6670343</i>	156763882	<i>OR6Y1</i>	19.7	T/A	0.43	I	-0.234	0.050	2.72×10^{-6}
	<i>rs1578761</i>	156764196	<i>OR6Y1</i>	19.3	A/G	0.43	G	-0.234	0.050	2.72×10^{-6}
	<i>rs12120526</i>	156765028	<i>OR6Y1</i>	18.5	C/T	0.39	I	-0.236	0.051	3.81×10^{-6}
	<i>rs11265006</i>	156765109	<i>OR6Y1</i>	18.4	G/C	0.43	I	-0.234	0.050	2.72×10^{-6}
	<i>rs11265007</i>	156765146	<i>OR6Y1</i>	18.4	G/A	0.44	I	-0.234	0.050	2.72×10^{-6}
	<i>rs11265009</i>	156765396	<i>OR6Y1</i>	18.1	T/C	0.44	I	-0.234	0.050	2.72×10^{-6}
	<i>rs11265010</i>	156765477	<i>OR6Y1</i>	18.1	A/G	0.44	I	-0.234	0.050	2.72×10^{-6}
	<i>rs12123305</i>	156765579	<i>OR6Y1</i>	18.0	A/G	0.44	I	-0.234	0.050	2.72×10^{-6}
	<i>rs12063320</i>	156766047	<i>OR6Y1</i>	17.5	T/A	0.44	I	-0.234	0.050	2.72×10^{-6}
	<i>rs12064489</i>	156766073	<i>OR6Y1</i>	17.5	C/T	0.44	I	-0.234	0.050	2.72×10^{-6}
	<i>rs10908667</i>	156766745	<i>OR6Y1</i>	16.8	A/G	0.44	I	-0.234	0.050	2.72×10^{-6}
	<i>rs12119672</i>	156766909	<i>OR6Y1</i>	16.6	A/G	0.44	I	-0.234	0.050	2.72×10^{-6}
	<i>rs10908671</i>	156768784	<i>OR6Y1</i>	14.8	A/G	0.44	I	-0.234	0.050	2.72×10^{-6}
	<i>rs12075228</i>	156768880	<i>OR6Y1</i>	14.7	T/C	0.44	I	-0.234	0.050	2.72×10^{-6}
	<i>rs11265014</i>	156769845	<i>OR6Y1</i>	13.7	C/T	0.43	I	-0.229	0.050	4.64×10^{-6}
	<i>rs11265015</i>	156769876	<i>OR6Y1</i>	13.7	A/G	0.44	I	-0.234	0.050	2.72×10^{-6}
	<i>rs11265016</i>	156770409	<i>OR6Y1</i>	13.1	T/C	0.44	I	-0.234	0.050	2.69×10^{-6}
	<i>rs10908673</i>	156770532	<i>OR6Y1</i>	13.0	G/T	0.44	I	-0.234	0.050	2.67×10^{-6}
	<i>rs10908674</i>	156770544	<i>OR6Y1</i>	13.0	T/A	0.44	I	-0.234	0.050	2.64×10^{-6}
	<i>rs10908675</i>	156770753	<i>OR6Y1</i>	12.8	C/A	0.44	I	-0.234	0.050	2.63×10^{-6}
	<i>rs7540999</i>	156771194	<i>OR6Y1</i>	12.3	A/G	0.44	I	-0.234	0.050	2.61×10^{-6}
	<i>rs4575081</i>	156771461	<i>OR6Y1</i>	12.1	A/C	0.44	I	-0.234	0.050	2.58×10^{-6}
	<i>rs4313395</i>	156771759	<i>OR6Y1</i>	11.8	T/C	0.44	I	-0.234	0.050	2.56×10^{-6}
	<i>rs10908677</i>	156772810	<i>OR6Y1</i>	10.7	G/A	0.44	I	-0.235	0.050	2.53×10^{-6}
	<i>rs2051067</i>	156774022	<i>OR6Y1</i>	9.5	T/G	0.44	I	-0.235	0.050	2.48×10^{-6}
	<i>rs923663</i>	156774356	<i>OR6Y1</i>	9.2	T/A	0.44	I	-0.235	0.050	2.49×10^{-6}
	<i>rs975118</i>	156778069	<i>OR6Y1</i>	5.5	A/G	0.44	G	-0.235	0.050	2.50×10^{-6}
	<i>rs6697656</i>	156787361	<i>OR6Y1</i>	2.8	G/A	0.44	G	-0.235	0.050	2.47×10^{-6}
5q14.3	<i>rs2973839</i>	91112451	<i>LOC100129716</i>	360.2	A/G	0.11	I	0.354	0.077	3.63×10^{-6}
7q34	<i>rs10954649</i>	138789091	<i>KLRG2</i>	0.0	C/T	0.35	G	-0.247	0.052	1.87×10^{-6}
	<i>rs11763327</i>	138789411	<i>KLRG2</i>	0.0	T/G	0.35	I	-0.247	0.052	1.88×10^{-6}
15q25.3	<i>rs957029</i>	85753369	<i>NCRNA00052</i>	167.8	G/C	0.23	I	0.296	0.059	4.91×10^{-7}
	<i>rs9284311</i>	85729504	<i>NCRNA00052</i>	191.7	A/C	0.24	G	0.288	0.058	8.08×10^{-7}
	<i>rs8039588</i>	85731872	<i>NCRNA00052</i>	189.3	A/T	0.24	I	0.288	0.058	8.19×10^{-7}
	<i>rs921475</i>	85732343	<i>NCRNA00052</i>	188.8	G/A	0.23	I	0.284	0.059	1.35×10^{-6}
	<i>rs13379751</i>	85737626	<i>NCRNA00052</i>	183.5	A/G	0.24	G	0.287	0.059	9.74×10^{-7}
	<i>rs1442307</i>	85740218	<i>NCRNA00052</i>	180.9	G/A	0.23	G	0.292	0.059	6.46×10^{-7}
	<i>rs2881893</i>	85741977	<i>NCRNA00052</i>	179.2	A/G	0.23	I	0.293	0.059	6.13×10^{-7}
	<i>rs1867034</i>	85761018	<i>NCRNA00052</i>	160.1	G/A	0.19	G	0.300	0.064	2.75×10^{-6}
	<i>rs16940295</i>	85761129	<i>NCRNA00052</i>	160.0	G/A	0.19	I	0.299	0.064	2.78×10^{-6}
	<i>rs2348378</i>	85762003	<i>NCRNA00052</i>	159.2	G/A	0.19	I	0.312	0.062	5.62×10^{-7}
	<i>rs2679078</i>	85773433	<i>NCRNA00052</i>	147.7	G/A	0.25	I	0.289	0.058	5.78×10^{-7}

Continued on next page

Table F2 — continued from previous page

Locus	SNP	Position	Nearest		Alleles	MAF	Type	β	s.e.	p
			Gene	Distance (kb)						
	<i>rs2679072</i>	85780757	<i>NCRNA00052</i>	140.4	C/T	0.24	G	0.278	0.058	1.43×10^{-6}
	<i>rs2679069</i>	85787281	<i>NCRNA00052</i>	133.9	C/T	0.24	I	0.282	0.058	1.21×10^{-6}
	<i>rs2584136</i>	85789315	<i>NCRNA00052</i>	131.8	T/C	0.23	I	0.277	0.060	3.94×10^{-6}
19q12	<i>rs2190800</i>	33143105	<i>LOC148189</i>	166.4	T/G	0.42	G	0.229	0.049	3.21×10^{-6}
	<i>rs2190799</i>	33143082	<i>LOC148189</i>	166.4	C/T	0.40	I	0.229	0.050	4.76×10^{-6}
19q13.11	<i>rs8109254</i>	37388860	<i>ZNF507</i>	139.5	A/C	0.05	I	0.514	0.111	3.66×10^{-6}

Table F3: FNBMD Women Hits – European Americans

Locus	SNP	Position	Nearest		Alleles	MAF	Type	β	s.e.	p
			Gene	Distance (kb)						
6p25.1	<i>rs736004</i>	5067728	<i>LYRM4</i>	0.0	C/T	0.10	G	-0.422	0.088	1.56×10^{-6}
8p21.3	<i>rs12114940</i>	22104735	<i>BMP1</i>	0.0	T/G	0.45	G	0.245	0.053	3.60×10^{-6}
15q14	<i>rs16962904</i>	34443595	<i>C15orf41</i>	215.5	A/G	0.33	I	-0.284	0.057	7.48×10^{-7}
	<i>rs10518873</i>	34443995	<i>C15orf41</i>	215.1	G/A	0.33	G	-0.265	0.057	3.94×10^{-6}
	<i>rs10851990</i>	34445996	<i>C15orf41</i>	213.1	C/G	0.33	I	-0.265	0.057	4.04×10^{-6}
Xq28	<i>rs11795763</i>	149755133	<i>CD99L2</i>	0.0	T/C	0.16	I	-0.338	0.069	8.67×10^{-7}
	<i>rs12012611</i>	149720754	<i>CD99L2</i>	0.0	G/A	0.16	G	-0.341	0.071	1.70×10^{-6}
	<i>rs16995749</i>	149749844	<i>CD99L2</i>	0.0	C/A	0.16	G	-0.340	0.070	1.23×10^{-6}
	<i>rs11798706</i>	149769906	<i>CD99L2</i>	0.0	T/C	0.11	G	-0.490	0.106	3.80×10^{-6}
	<i>rs12116022</i>	149770664	<i>CD99L2</i>	0.0	G/A	0.16	I	-0.339	0.069	1.09×10^{-6}
	<i>rs4489434</i>	149772149	<i>CD99L2</i>	0.0	G/T	0.16	G	-0.336	0.069	1.20×10^{-6}
	<i>rs11798121</i>	149775837	<i>CD99L2</i>	0.0	T/C	0.16	G	-0.330	0.070	2.58×10^{-6}
	<i>rs11796789</i>	149790994	<i>CD99L2</i>	0.0	T/C	0.16	G	-0.328	0.070	2.36×10^{-6}
	<i>rs34984949</i>	149804623	<i>CD99L2</i>	0.0	G/A	0.16	G	-0.331	0.070	1.99×10^{-6}

Table F4: LSBMD Pooled Hits – European Americans

Locus	SNP	Position	Nearest Distance		Alleles	MAF	Type	β	s.e.	p
			Gene	(kb)						
12q24.13	<i>rs12309051</i>	112610534	<i>RBM19</i>	128.4	C/T	0.33	G	-0.171	0.037	4.69×10^{-6}
	<i>rs6489916</i>	112611438	<i>RBM19</i>	127.5	C/T	0.33	G	-0.170	0.037	4.91×10^{-6}
13q33.3	<i>rs17382033</i>	107839404	<i>TNFSF13B</i>	80.6	C/A	0.09	G	0.295	0.062	2.23×10^{-6}
Xp21.1	<i>rs331360</i>	32169468	<i>DMD</i>	86.0	G/A	0.23	G	-0.150	0.033	4.71×10^{-6}

Table F5: LSBMD Men Hits – European Americans

Locus	SNP	Position	Nearest Distance		Alleles	MAF	Type	β	s.e.	p
			Gene	(kb)						
2q36.3	<i>rs13010707</i>	227250306	<i>IRS1</i>	54.0	C/T	0.13	I	-0.356	0.075	2.09×10^{-6}
3p14.1	<i>rs9813487</i>	69115174	<i>C3orf64</i>	0.0	T/C	0.20	I	0.290	0.062	3.08×10^{-6}
	<i>rs6549162</i>	69117389	<i>C3orf64</i>	0.0	C/G	0.19	I	0.289	0.062	3.80×10^{-6}
12q24.31	<i>rs12578256</i>	123368433	<i>FAM101A</i>	1.9	T/A	0.18	I	-0.296	0.063	2.33×10^{-6}
16q21	<i>rs11076239</i>	57038674	<i>NDRG4</i>	16.4	G/A	0.32	I	0.247	0.054	4.39×10^{-6}
Xp21.1	<i>rs331360</i>	32169468	<i>DMD</i>	86.0	G/A	0.23	G	-0.176	0.038	3.40×10^{-6}

Table F6: LSBMD Women Hits – European Americans

Locus	SNP	Position	Nearest Distance		Alleles	MAF	Type	β	s.e.	p
			Gene	(kb)						
2q37.3	<i>rs6718108</i>	240102747	<i>HDAC4</i>	115.2	A/G	0.33	G	0.252	0.055	4.98×10^{-6}
4p16.1	<i>rs10804984</i>	6700002	<i>MRFAP1</i>	4.7	C/A	0.32	I	0.278	0.057	1.12×10^{-6}
	<i>rs4689024</i>	6700520	<i>MRFAP1</i>	5.2	T/C	0.32	G	0.277	0.057	1.15×10^{-6}
5q32	<i>rs318373</i>	143300064	<i>HMHB1</i>	119.6	T/C	0.47	G	-0.248	0.053	3.09×10^{-6}
7q21.11	<i>rs1397005</i>	80718618	<i>SEMA3C</i>	332.0	A/G	0.28	G	0.271	0.059	4.26×10^{-6}
8q22.1	<i>rs278530</i>	94279598	<i>LOC642924</i>	148.3	C/T	0.31	G	-0.257	0.056	4.52×10^{-6}
	<i>rs278548</i>	94287830	<i>LOC642924</i>	140.0	T/C	0.31	I	-0.257	0.056	4.52×10^{-6}
	<i>rs278542</i>	94291954	<i>LOC642924</i>	135.9	A/T	0.31	I	-0.256	0.056	4.69×10^{-6}
	<i>rs1483455</i>	94296725	<i>LOC642924</i>	131.1	C/A	0.25	G	-0.271	0.059	4.73×10^{-6}
	<i>rs11992459</i>	94302355	<i>LOC642924</i>	125.5	G/T	0.25	G	-0.271	0.059	4.73×10^{-6}
13q33.1	<i>rs640960</i>	100560051	<i>NALCN</i>	0.0	C/T	0.27	G	0.295	0.058	4.26×10^{-7}
14q23.1	<i>rs1113590</i>	61073336	<i>PRKCH</i>	0.0	A/C	0.09	I	0.478	0.091	1.40×10^{-7}

Table F7: All Fx Pooled Hits – European Americans

Locus	SNP	Position	NearestDistance			Alleles	MAF	Type	OR	95%CI	<i>p</i>
			Gene	(kb)							
2q12.2	<i>rs7575679</i>	106373899	<i>PLGLA</i>	0.0	G/A	0.13	I	2.51	(1.71, 3.70)	3.05×10^{-6}	
18q23	<i>rs12955627</i>	73834676	<i>GALR1</i>	723.6	T/C	0.20	I	1.77	(1.40, 2.24)	1.53×10^{-6}	
Xq22.3	<i>rs4893537</i>	108857735	<i>ACSL4</i>	0.0	T/C	0.06	G	1.82	(1.41, 2.36)	4.99×10^{-6}	

Table F8: All Fx Men – European Americans

Locus	SNP	Position	NearestDistance			Alleles	MAF	Type	OR	95%CI	<i>p</i>
			Gene	(kb)							
3q24	<i>rs6809471</i>	146615470	<i>PLOD2</i>	654.4	G/A	0.32	G	0.41	(0.29, 0.58)	3.11×10^{-7}	
	<i>rs11927695</i>	146555660	<i>PLOD2</i>	714.3	T/C	0.32	I	0.40	(0.29, 0.57)	3.26×10^{-7}	
	<i>rs7430521</i>	146563551	<i>PLOD2</i>	706.4	G/T	0.32	I	0.41	(0.29, 0.58)	3.60×10^{-7}	
	<i>rs2121848</i>	146646417	<i>PLOD2</i>	623.5	C/G	0.33	I	0.44	(0.32, 0.62)	2.63×10^{-6}	
10p14	<i>rs2296734</i>	7851413	<i>KIN</i>	0.0	G/C	0.43	I	0.45	(0.33, 0.61)	4.64×10^{-7}	
	<i>rs11592018</i>	7838976	<i>KIN</i>	0.0	A/G	0.43	I	0.46	(0.34, 0.63)	7.22×10^{-7}	
	<i>rs1887329</i>	7844710	<i>KIN</i>	0.0	C/A	0.43	I	0.45	(0.33, 0.62)	5.51×10^{-7}	
	<i>rs2026612</i>	7845487	<i>KIN</i>	0.0	C/T	0.43	G	0.45	(0.33, 0.62)	4.77×10^{-7}	
	<i>rs11596873</i>	7849081	<i>KIN</i>	0.0	G/A	0.43	I	0.45	(0.33, 0.61)	4.66×10^{-7}	
	<i>rs11255351</i>	7850077	<i>KIN</i>	0.0	C/T	0.47	I	0.47	(0.35, 0.64)	1.11×10^{-6}	
	<i>rs2148722</i>	7853159	<i>KIN</i>	0.0	G/A	0.47	I	0.47	(0.35, 0.64)	1.10×10^{-6}	
	<i>rs12413131</i>	7863288	<i>KIN</i>	0.0	G/A	0.41	I	0.46	(0.34, 0.64)	1.90×10^{-6}	
	<i>rs4749247</i>	7866138	<i>KIN</i>	0.0	G/C	0.43	I	0.48	(0.35, 0.65)	2.50×10^{-6}	
	<i>rs1244462</i>	7901028	<i>TAF3</i>	0.0	A/G	0.45	G	0.48	(0.35, 0.65)	2.30×10^{-6}	
14q13.1	<i>rs17100963</i>	32932268	<i>NPAS3</i>	0.0	G/A	0.08	G	2.98	(1.96, 4.51)	2.71×10^{-7}	
15q25.3	<i>rs7164422</i>	84331644	<i>AGBL1</i>	154.6	A/G	0.06	G	3.14	(2.00, 4.93)	6.28×10^{-7}	

Table F9: All Fx Women – European Americans

Locus	SNP	Position	NearestDistance			Alleles	MAF	Type	OR	95%CI	<i>p</i>
			Gene	(kb)							
2p24.1	<i>rs7567544</i>	20256283	<i>SDC1</i>	7.8	G/C	0.45	I	0.52	(0.40, 0.68)	3.10×10^{-6}	
4q34.2	<i>rs17688188</i>	177708053	<i>VEGFC</i>	133.6	G/A	0.26	I	1.82	(1.41, 2.35)	4.33×10^{-6}	
8p23.1	<i>rs4840583</i>	11673355	<i>NEIL2</i>	0.0	C/T	0.46	G	1.80	(1.42, 2.29)	1.52×10^{-6}	
	<i>rs8191604</i>	11674293	<i>NEIL2</i>	0.0	T/G	0.26	G	1.82	(1.41, 2.36)	4.86×10^{-6}	

Table F10: NV Fx Pooled Hits – European Americans

Locus	SNP	Position	Nearest Distance		Alleles	MAF	Type	OR	95%CI	<i>p</i>
			Gene	(kb)						
4p16.1	<i>rs6849590</i>	7483478	<i>PSAPL1</i>	0.0	G/A	0.26	G	0.55	(0.44, 0.71)	2.01×10^{-6}
7p14.1	<i>rs2329399</i>	39508393	<i>POU6F2</i>	37.5	A/C	0.42	G	0.60	(0.49, 0.74)	3.05×10^{-6}
18q23	<i>rs12964032</i>	73772518	<i>GALR1</i>	661.4	A/G	0.20	I	0.52	(0.40, 0.69)	2.81×10^{-6}
	<i>rs12964230</i>	73772973	<i>GALR1</i>	661.9	C/T	0.20	G	0.52	(0.40, 0.68)	2.41×10^{-6}
	<i>rs12604089</i>	73777155	<i>GALR1</i>	666.1	T/A	0.16	I	0.47	(0.34, 0.64)	3.01×10^{-6}
Xq22.2	<i>rs2983097</i>	102552937	<i>NGFRAP1</i>	33.3	A/G	0.06	G	2.04	(1.54, 2.72)	9.25×10^{-7}
Xq22.3	<i>rs4893537</i>	108857735	<i>ACSL4</i>	0.0	T/C	0.06	G	1.82	(1.41, 2.36)	4.99×10^{-6}

Table F11: NV Fx Men Hits – European Americans

Locus	SNP	Position	Nearest Distance		Alleles	MAF	Type	OR	95%CI	<i>p</i>
			Gene	(kb)						
3p14.3	<i>rs9654002</i>	54461737	<i>ESRG</i>	179.5	A/C	0.37	I	2.54	(1.70, 3.79)	4.82×10^{-6}
6p21.31	<i>rs9368834</i>	34968742	<i>ANKS1A</i>	0.0	T/G	0.11	G	2.74	(1.81, 4.14)	1.67×10^{-6}
	<i>rs1555107</i>	34964323	<i>TAF11</i>	0.5	C/G	0.11	I	2.74	(1.81, 4.14)	1.76×10^{-6}
	<i>rs6905468</i>	34981636	<i>ANKS1A</i>	0.0	C/A	0.11	G	2.74	(1.81, 4.14)	1.67×10^{-6}
7q36.3	<i>rs288746</i>	155299433	<i>SHH</i>	1.7	A/G	0.12	G	2.51	(1.70, 3.69)	3.26×10^{-6}
9q31.3	<i>rs10979528</i>	110621948	<i>ACTL7B</i>	34.7	T/G	0.06	I	0.35	(0.26, 0.48)	1.61×10^{-11}
	<i>rs10979533</i>	110628107	<i>ACTL7B</i>	28.6	G/T	0.06	I	0.36	(0.27, 0.48)	1.73×10^{-11}
	<i>rs12380226</i>	110629373	<i>ACTL7B</i>	27.3	T/C	0.06	I	0.36	(0.27, 0.48)	1.81×10^{-11}
	<i>rs10979537</i>	110631575	<i>ACTL7B</i>	25.1	A/G	0.06	I	0.36	(0.27, 0.48)	1.86×10^{-11}
	<i>rs10979538</i>	110631689	<i>ACTL7B</i>	25.0	A/G	0.06	I	0.36	(0.27, 0.48)	1.89×10^{-11}
	<i>rs10816737</i>	110641875	<i>ACTL7B</i>	14.8	A/C	0.06	I	0.36	(0.27, 0.49)	2.79×10^{-11}
	<i>rs16913584</i>	110642927	<i>ACTL7B</i>	13.8	G/A	0.06	G	0.36	(0.27, 0.49)	2.79×10^{-11}
	<i>rs10979546</i>	110645197	<i>ACTL7B</i>	11.5	G/T	0.06	I	0.36	(0.27, 0.49)	2.70×10^{-11}
	<i>rs10448264</i>	110653174	<i>ACTL7B</i>	3.5	G/A	0.06	G	0.35	(0.26, 0.48)	3.38×10^{-11}
12p13.2	<i>rs2607894</i>	10635183	<i>KLRAP1</i>	0.0	G/T	0.38	G	0.43	(0.31, 0.61)	1.14×10^{-6}
Xp22.2	<i>rs4073740</i>	12206155	<i>FRMPD4</i>	0.0	G/A	0.24	G	1.75	(1.39, 2.20)	1.57×10^{-6}
	<i>rs4830768</i>	12197423	<i>FRMPD4</i>	0.0	A/G	0.19	G	1.81	(1.41, 2.32)	3.43×10^{-6}
	<i>rs4073741</i>	12205866	<i>FRMPD4</i>	0.0	A/G	0.24	I	1.71	(1.36, 2.15)	3.86×10^{-6}
	<i>rs4511046</i>	12206366	<i>FRMPD4</i>	0.0	C/A	0.24	G	1.71	(1.36, 2.15)	4.65×10^{-6}

Table F12: NV Fx Women Hits – European Americans

Locus	SNP	Position	Nearest Distance		Alleles	MAF	Type	OR	95%CI	<i>p</i>
			Gene	(kb)						
4p16.1	<i>rs6849590</i>	7483478	<i>PSAPL1</i>	0.0	G/A	0.26	G	0.46	(0.33, 0.64)	3.57×10^{-6}
8p21.2	<i>rs10096579</i>	24165000	<i>ADAM28</i>	42.5	G/T	0.15	G	2.15	(1.56, 2.97)	2.99×10^{-6}

Table F13: FNBMD Pooled Hits – African Americans

Locus	SNP	Position	Nearest Distance		Alleles	MAF	Type	β	s.e.	<i>p</i>
			Gene	(kb)						
8p23.2	<i>rs10216608</i>	3032465	<i>CSMD1</i>	0.0	A/T	0.09	I	-0.368	0.074	6.10×10^{-7}
	<i>rs10216959</i>	3032337	<i>CSMD1</i>	0.0	G/C	0.08	I	-0.359	0.075	1.59×10^{-6}
	<i>rs10216980</i>	3032368	<i>CSMD1</i>	0.0	C/T	0.08	I	-0.366	0.076	1.47×10^{-6}
8q21.11	<i>rs16939006</i>	76043194	<i>CRISPLD1</i>	16.1	T/C	0.46	G	0.190	0.042	4.87×10^{-6}
9p24.3	<i>rs2279986</i>	1032284	<i>DMRT2</i>	8.1	G/T	0.40	G	-0.210	0.045	2.38×10^{-6}
11p15.3	<i>rs12417203</i>	11429804	<i>CSNK2A1P</i>	98.3	T/G	0.23	G	-0.226	0.047	1.90×10^{-6}
15q21.2	<i>rs2305709</i>	49762877	<i>SCG3</i>	0.0	C/A	0.05	I	0.465	0.097	1.70×10^{-6}
17q24.3	<i>rs9898716</i>	67428011	<i>SOX9</i>	200.7	A/C	0.14	I	-0.290	0.061	2.32×10^{-6}
18q12.2	<i>rs16967627</i>	32092618	<i>MOCOS</i>	0.0	C/T	0.06	I	-0.380	0.082	3.11×10^{-6}
	<i>rs10414586</i>	39075001	<i>KCTD15</i>	76.5	C/T	0.10	I	-0.345	0.074	3.00×10^{-6}

Table F14: LSBMD Pooled Hits – African Americans

Locus	SNP	Position	Nearest Gene	Distance (kb)	Alleles	MAF	Type	β	s.e.	p
1q25.3	<i>rs2281415</i>	183659468	<i>IVNS1ABP</i>	106.4	C/T	0.26	G	0.234	0.051	4.69×10^{-6}
2p21	<i>rs13408008</i>	47519201	<i>MSH2</i>	0.0	T/G	0.08	I	-0.341	0.075	4.86×10^{-6}
2q32.1	<i>rs6712733</i>	188501483	<i>GULP1</i>	364.2	T/G	0.25	G	0.236	0.051	3.68×10^{-6}
3q27.3	<i>rs10937334</i>	189237130	<i>LOC339929</i>	114.6	C/T	0.14	I	-0.267	0.058	4.34×10^{-6}
7p21.3	<i>rs7794562</i>	9671676	<i>PER4</i>	29.7	T/C	0.17	I	-0.277	0.056	7.86×10^{-7}
10p15.3	<i>rs2813457</i>	1562799	<i>NCRNA00168</i>	0.0	C/T	0.07	I	-0.345	0.072	1.40×10^{-6}
10q21.1	<i>rs12241361</i>	59279878	<i>IPMK</i>	341.4	C/T	0.19	I	0.282	0.057	8.64×10^{-7}
	<i>rs6481362</i>	59245691	<i>IPMK</i>	375.6	G/A	0.24	I	0.257	0.056	4.96×10^{-6}
	<i>rs2393391</i>	59249686	<i>IPMK</i>	371.6	G/A	0.19	I	0.286	0.060	1.63×10^{-6}
	<i>rs6481366</i>	59256869	<i>IPMK</i>	364.4	T/A	0.19	I	0.281	0.058	1.16×10^{-6}
	<i>rs6481369</i>	59277608	<i>IPMK</i>	343.7	C/T	0.19	G	0.282	0.057	8.72×10^{-7}
	<i>rs2215686</i>	59296448	<i>IPMK</i>	324.8	A/G	0.12	I	0.338	0.069	1.03×10^{-6}
	<i>rs17704490</i>	59312506	<i>IPMK</i>	308.8	C/T	0.12	I	0.330	0.071	2.85×10^{-6}
	<i>rs17704609</i>	59314226	<i>IPMK</i>	307.1	C/T	0.12	I	0.331	0.070	2.60×10^{-6}
	<i>rs17626174</i>	59320195	<i>IPMK</i>	301.1	A/C	0.12	G	0.332	0.070	2.41×10^{-6}
	<i>rs17626272</i>	59337175	<i>IPMK</i>	284.1	A/G	0.10	I	0.363	0.076	1.58×10^{-6}
10q22.3	<i>rs16935728</i>	79663373	<i>RPS24</i>	176.8	G/T	0.11	I	-0.345	0.068	4.16×10^{-7}
11p15.2	<i>rs11605876</i>	13516168	<i>PTH</i>	42.0	G/C	0.20	I	-0.256	0.053	1.40×10^{-6}
11p12	<i>rs10501203</i>	38592016	<i>LRRC4C</i>	1500.3	A/T	0.20	I	0.261	0.056	2.66×10^{-6}
	<i>rs1038254</i>	38576316	<i>LRRC4C</i>	1516.0	T/G	0.21	I	0.242	0.052	3.10×10^{-6}
	<i>rs4755497</i>	38578985	<i>LRRC4C</i>	1513.3	A/G	0.21	G	0.242	0.052	3.07×10^{-6}
	<i>rs11034878</i>	38579595	<i>LRRC4C</i>	1512.7	A/C	0.21	I	0.242	0.052	3.05×10^{-6}
	<i>rs11034883</i>	38583007	<i>LRRC4C</i>	1509.3	T/G	0.21	I	0.248	0.054	4.16×10^{-6}
	<i>rs7123927</i>	38583500	<i>LRRC4C</i>	1508.8	C/G	0.20	I	0.249	0.055	4.91×10^{-6}
	<i>rs11034885</i>	38587219	<i>LRRC4C</i>	1505.1	A/G	0.21	I	0.245	0.052	2.86×10^{-6}
11q22.1	<i>rs10894988</i>	99969329	<i>ARHGAP42</i>	94.3	G/A	0.18	I	-0.264	0.056	2.05×10^{-6}
17p13.2	<i>rs758641</i>	3793551	<i>ATP2A3</i>	0.0	A/G	0.39	G	-0.239	0.045	1.10×10^{-7}
17q22	<i>rs17745091</i>	50293796	<i>TOM1L1</i>	39.3	T/C	0.21	I	-0.238	0.051	3.72×10^{-6}
18q22.1	<i>rs12607377</i>	62565126	<i>CDH19</i>	142.9	T/C	0.08	I	-0.298	0.065	3.97×10^{-6}
	<i>rs11151300</i>	62549968	<i>CDH19</i>	127.8	A/G	0.08	I	-0.291	0.064	4.94×10^{-6}
19q13.11	<i>rs10412883</i>	39096596	<i>KCTD15</i>	98.1	G/A	0.09	I	-0.378	0.076	7.68×10^{-7}
	<i>rs10419694</i>	39087865	<i>KCTD15</i>	89.4	A/C	0.08	I	-0.386	0.080	1.22×10^{-6}
19q13.32	<i>rs10404733</i>	51450642	<i>IGFL1</i>	24.3	A/C	0.21	I	-0.308	0.061	4.39×10^{-7}
21q22.11	<i>rs2834247</i>	33978599	<i>ITSN1</i>	0.0	G/A	0.11	I	-0.326	0.068	1.94×10^{-6}

APPENDIX G

LOCUS PLOTS OF BMD IN EUROPEAN AMERICANS

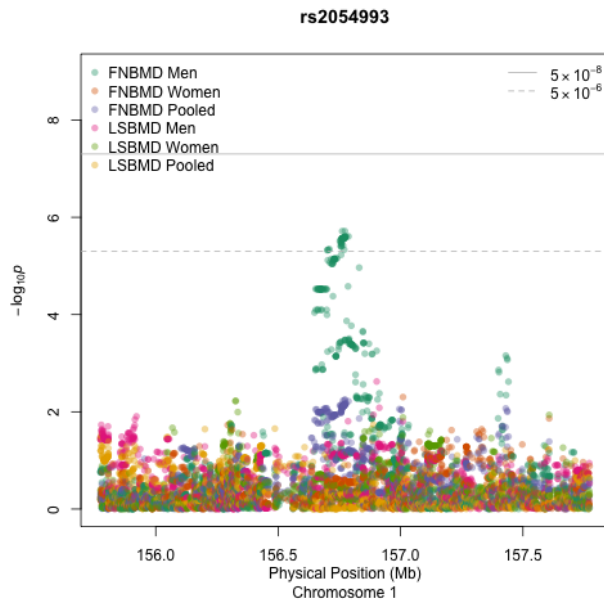


Figure G1: Eur. Am. BMD – *rs2054993*

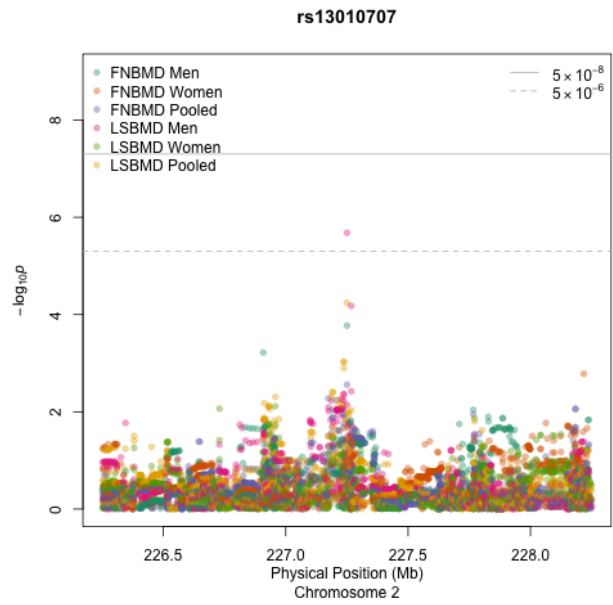


Figure G2: Eur. Am. BMD – *rs13010707*

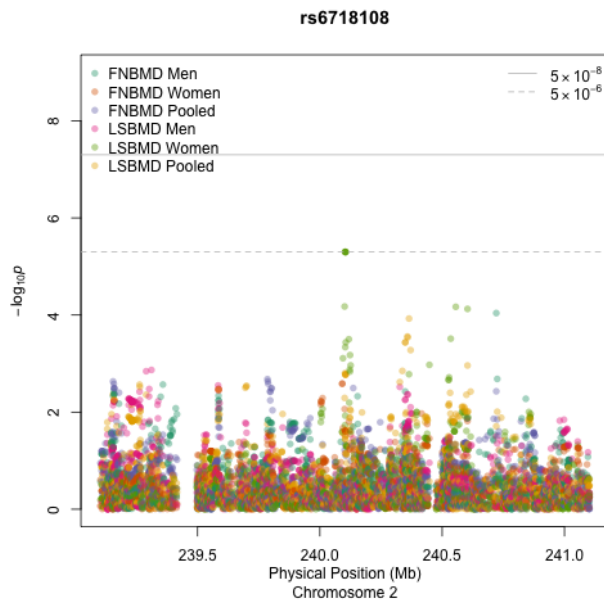


Figure G3: Eur. Am. BMD – *rs6718108*

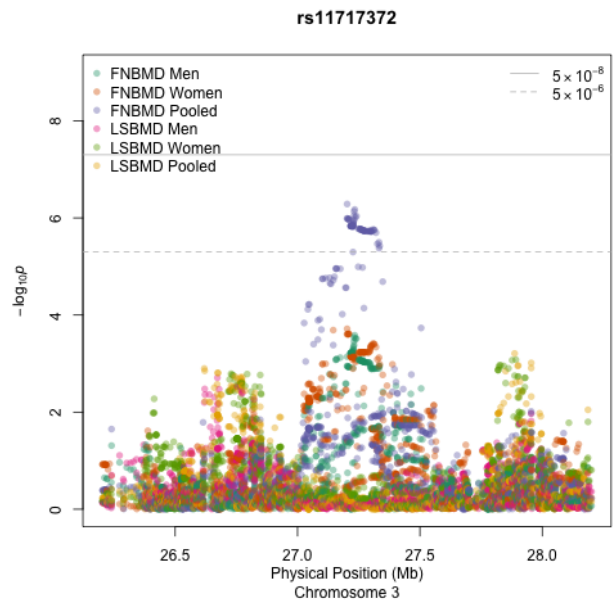


Figure G4: Eur. Am. BMD – *rs11717372*

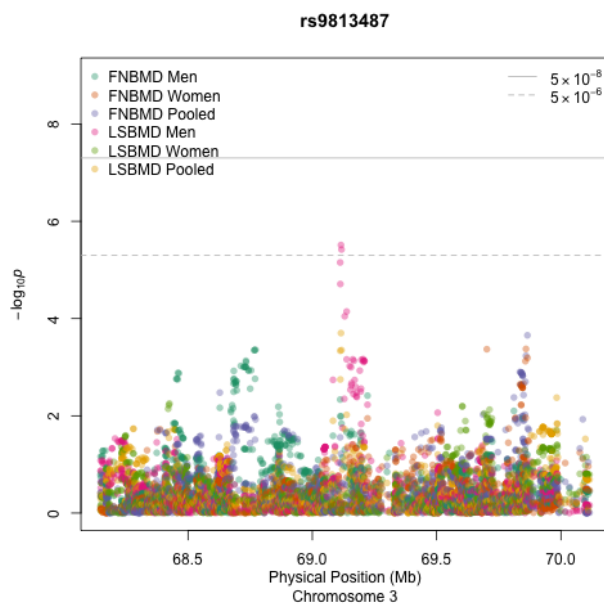


Figure G5: Eur. Am. BMD – *rs9813487*

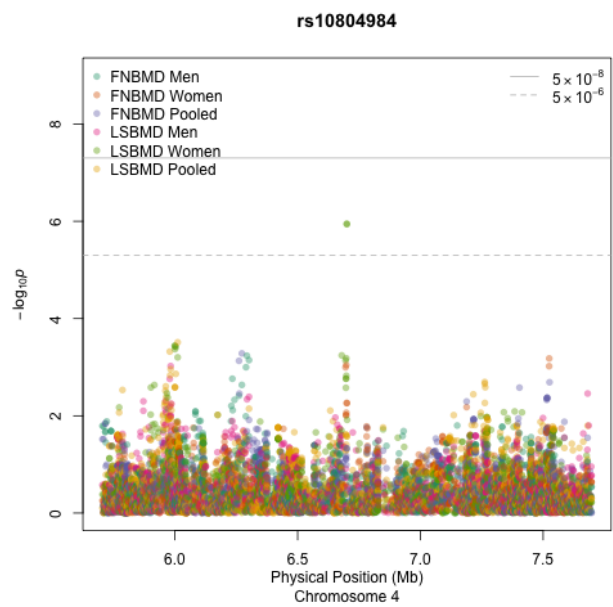


Figure G6: Eur. Am. BMD – *rs10804984*

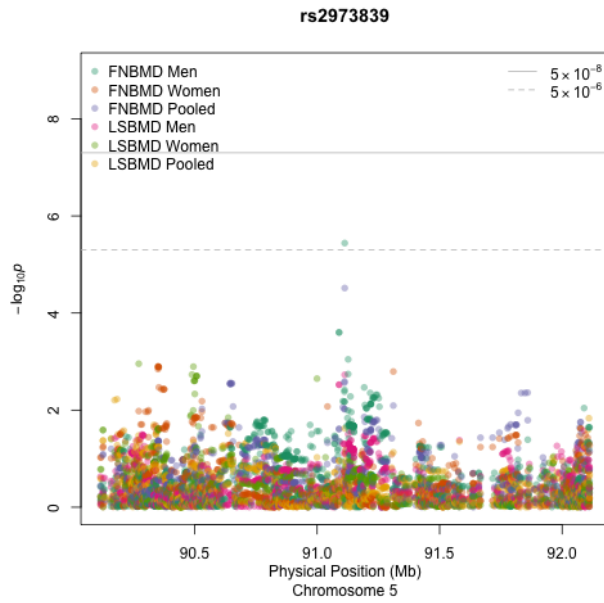


Figure G7: Eur. Am. BMD – *rs2973839*

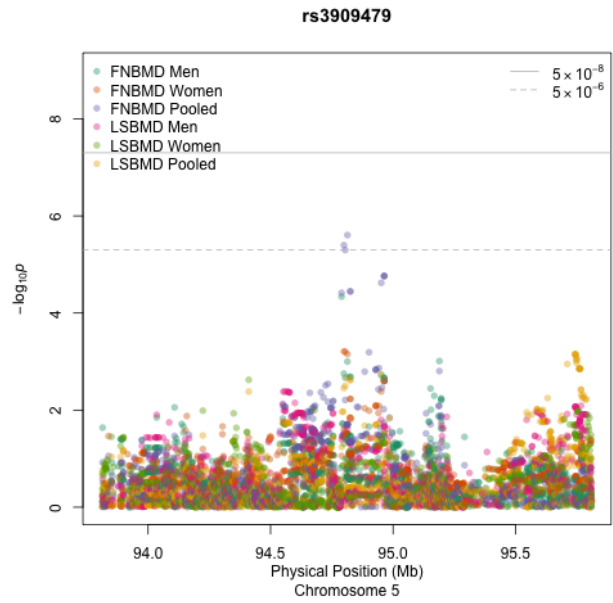


Figure G8: Eur. Am. BMD – *rs3909479*

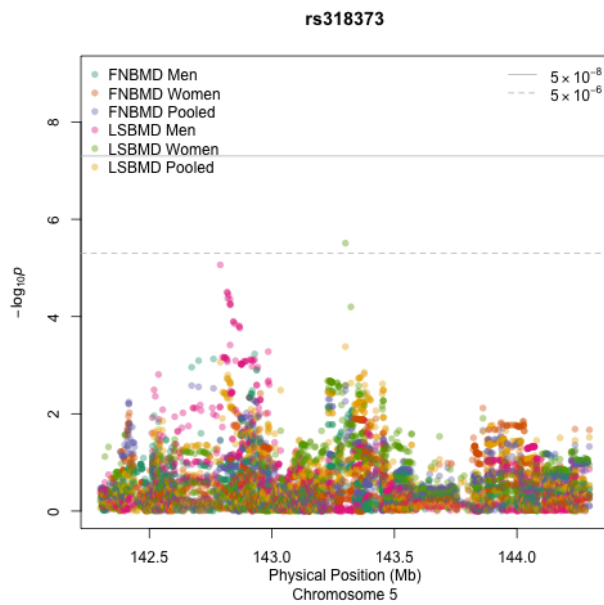


Figure G9: Eur. Am. BMD – *rs318373*

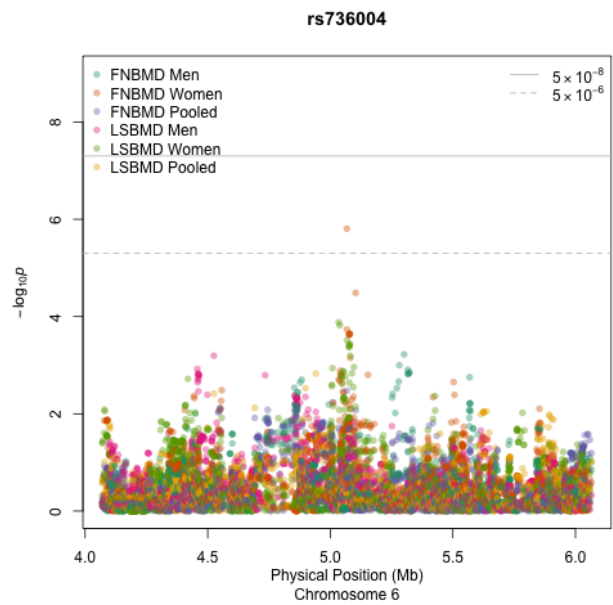


Figure G10: Eur. Am. BMD – *rs736004*

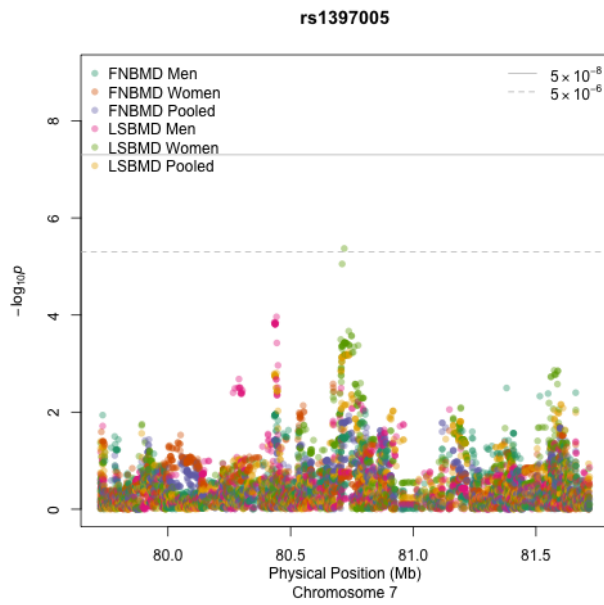


Figure G11: Eur. Am. BMD – *rs1397005*

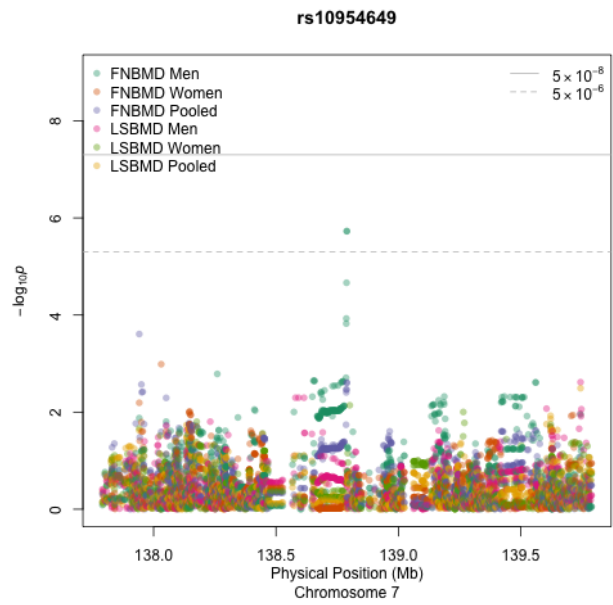


Figure G12: Eur. Am. BMD – *rs10954649*

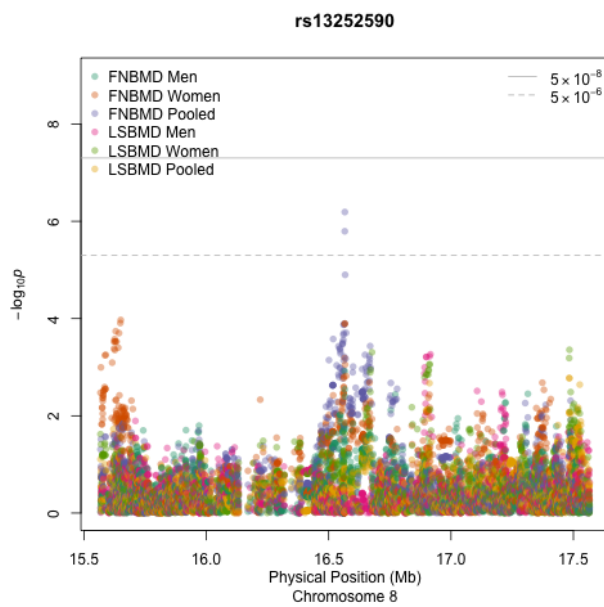


Figure G13: Eur. Am. BMD – *rs13252590*

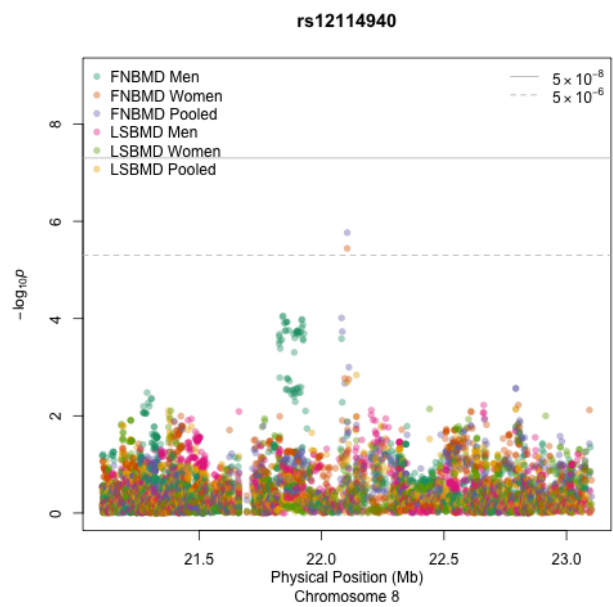


Figure G14: Eur. Am. BMD – *rs12114940*

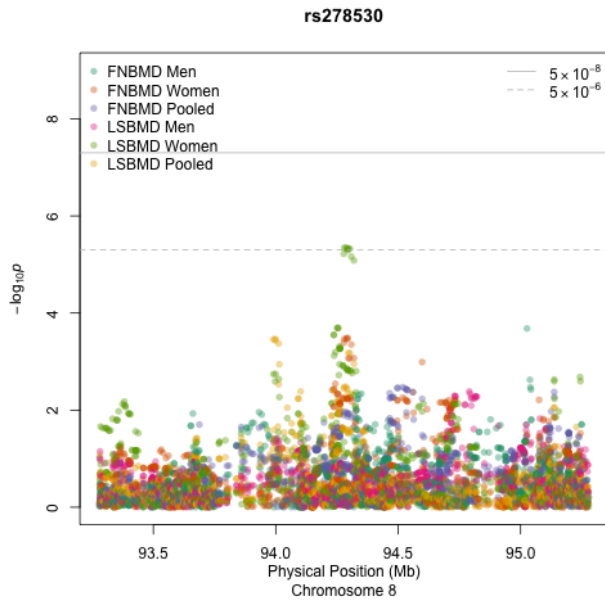


Figure G15: Eur. Am. BMD – *rs278530*

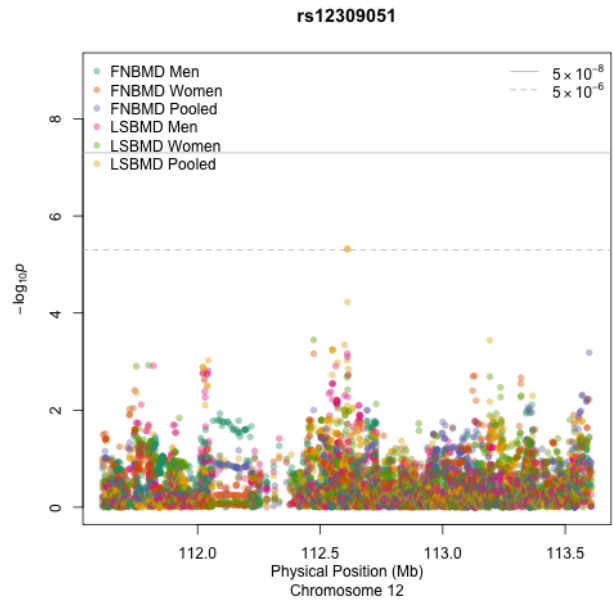


Figure G16: Eur. Am. BMD – *rs12309051*

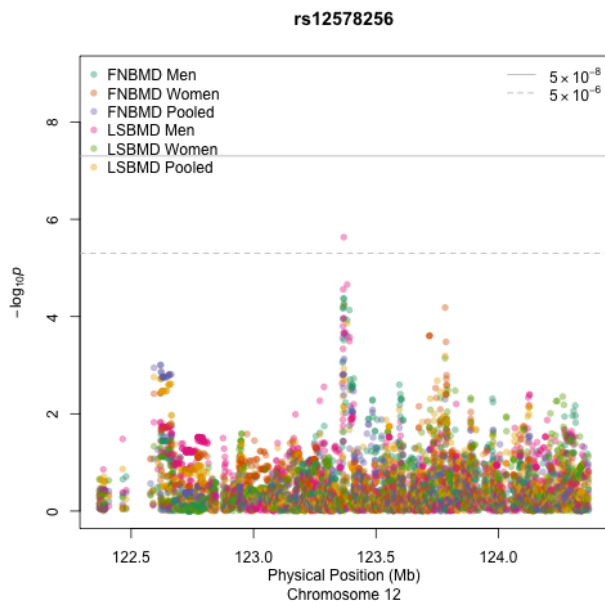


Figure G17: Eur. Am. BMD – *rs12578256*

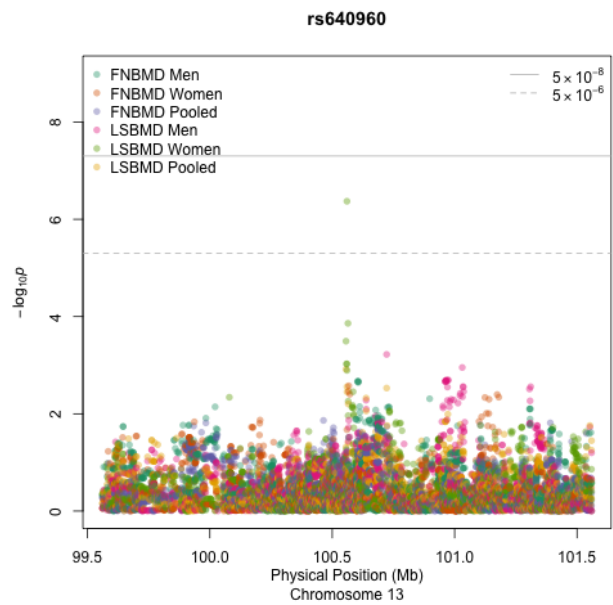


Figure G18: Eur. Am. BMD – *rs640960*

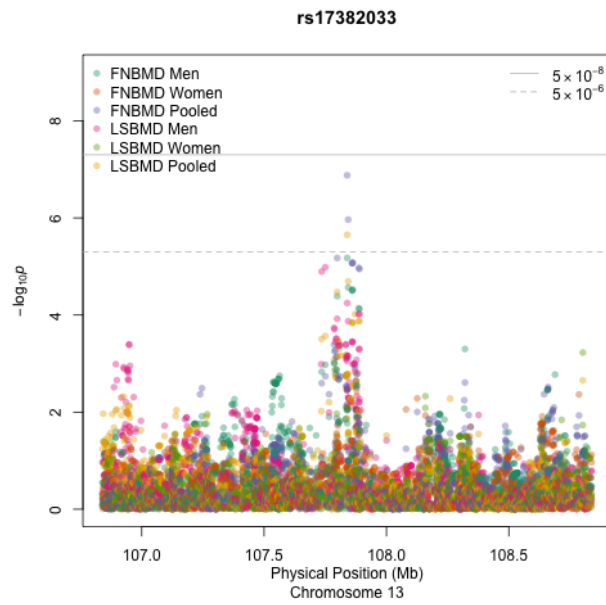


Figure G19: Eur. Am. BMD – *rs17382033*

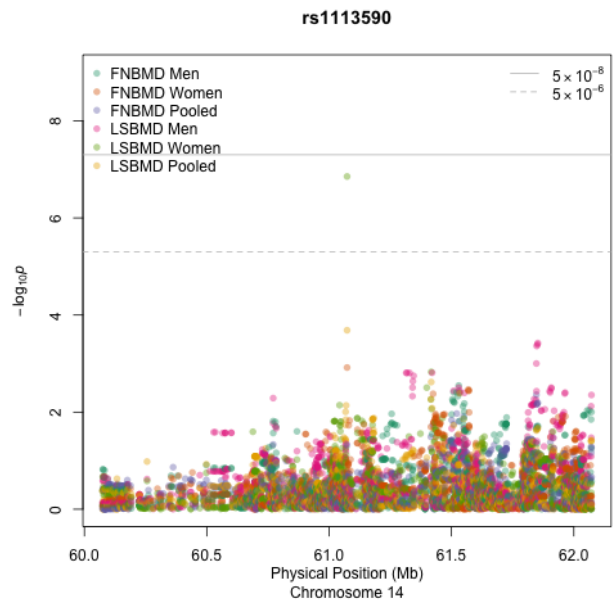


Figure G20: Eur. Am. BMD – *rs1113590*

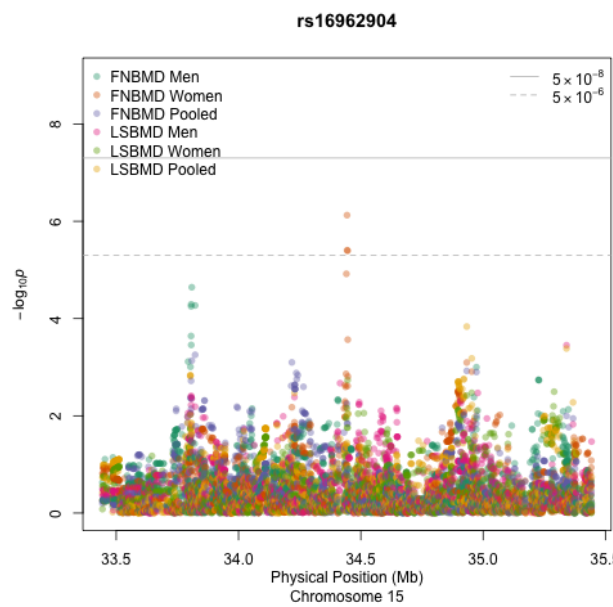


Figure G21: Eur. Am. BMD – *rs16962904*

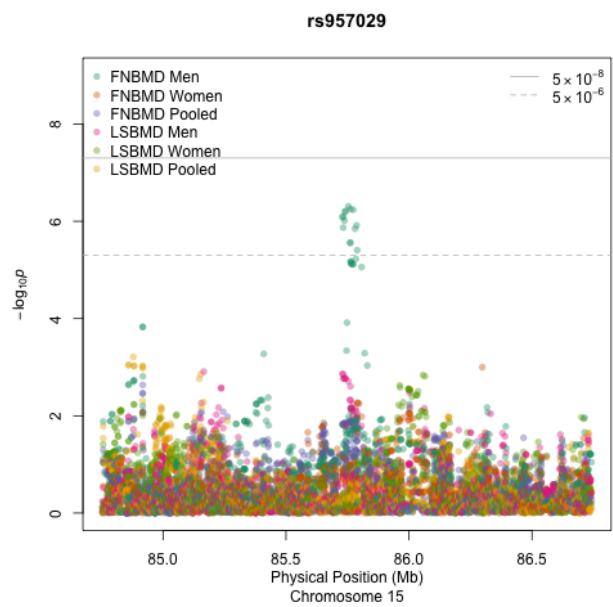


Figure G22: Eur. Am. BMD – *rs957029*

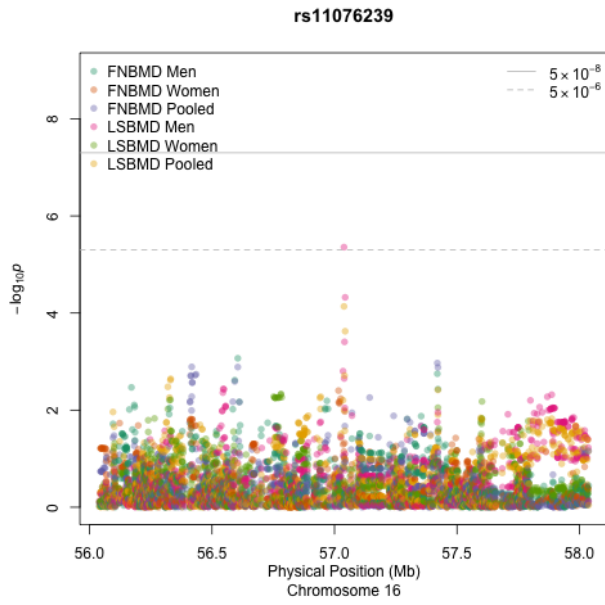


Figure G23: Eur. Am. BMD – *rs11076239*

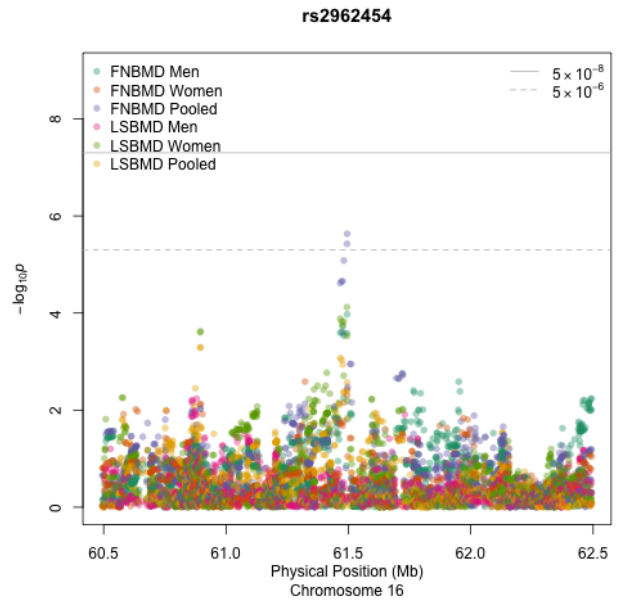


Figure G24: Eur. Am. BMD – *rs2962454*

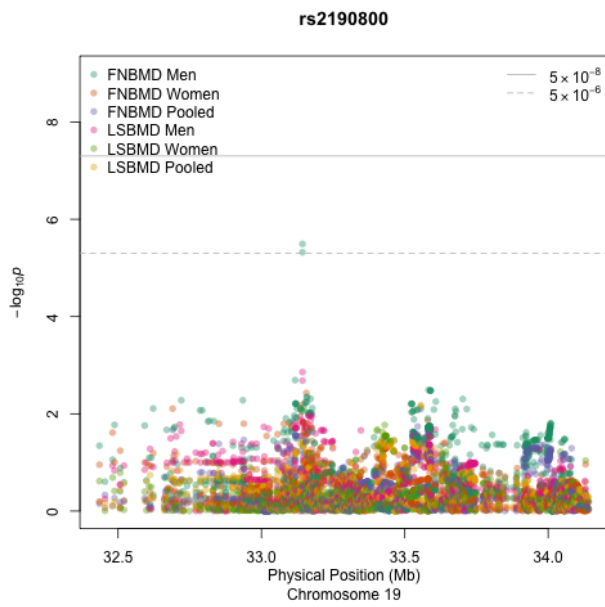


Figure G25: Eur. Am. BMD – *rs2190800*

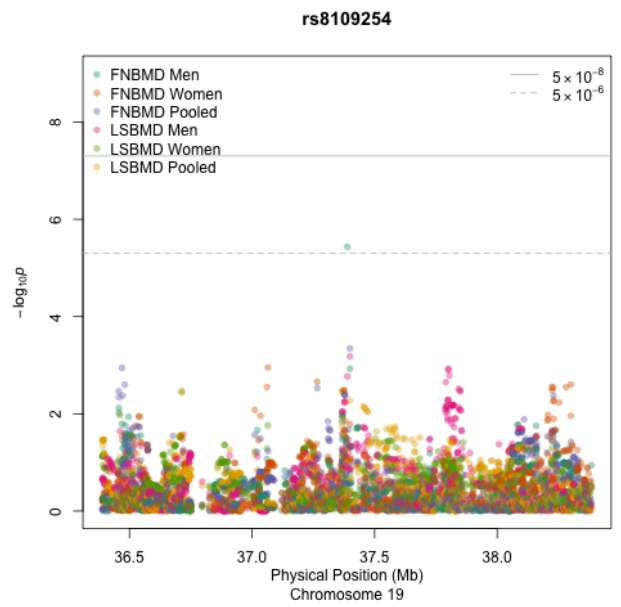


Figure G26: Eur. Am. BMD – *rs8109254*

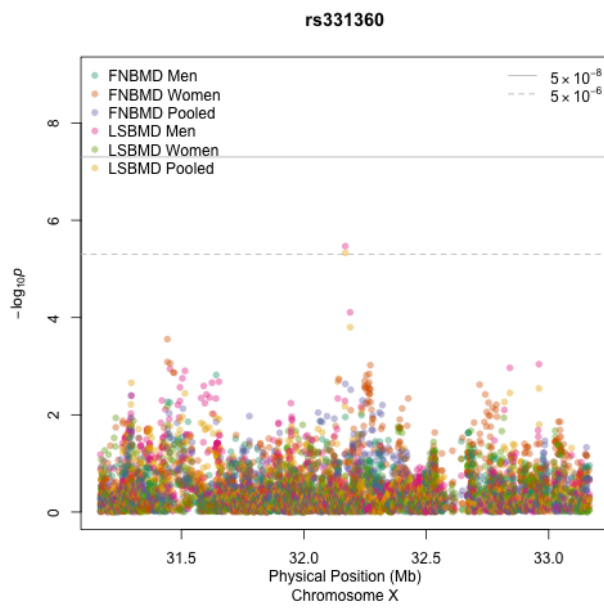


Figure G27: Eur. Am. BMD – *rs331360*

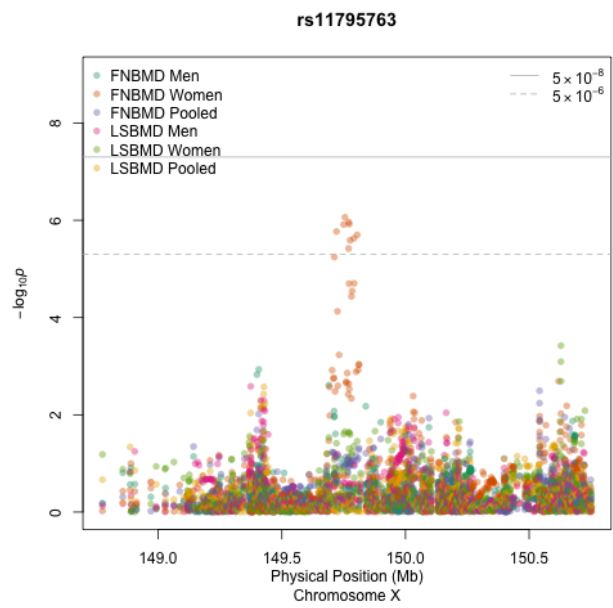


Figure G28: Eur. Am. BMD – *rs11795763*

APPENDIX H

LOCUS PLOTS OF FRACTURE RISK IN EUROPEAN AMERICANS

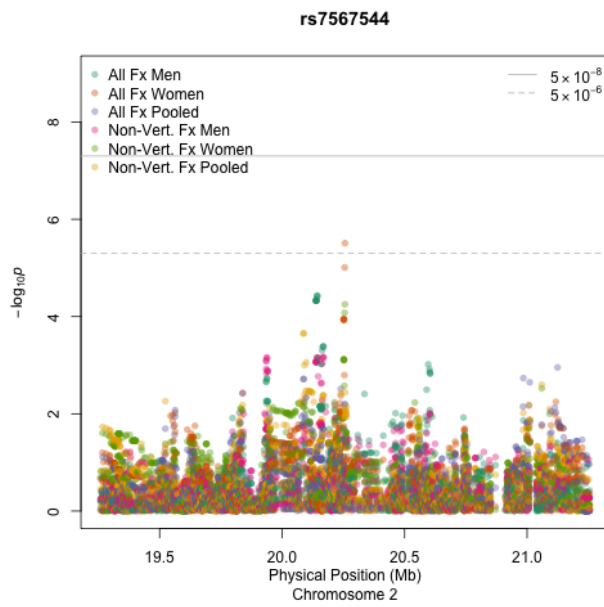


Figure H1: Eur. Am. Fx – *rs7567544*

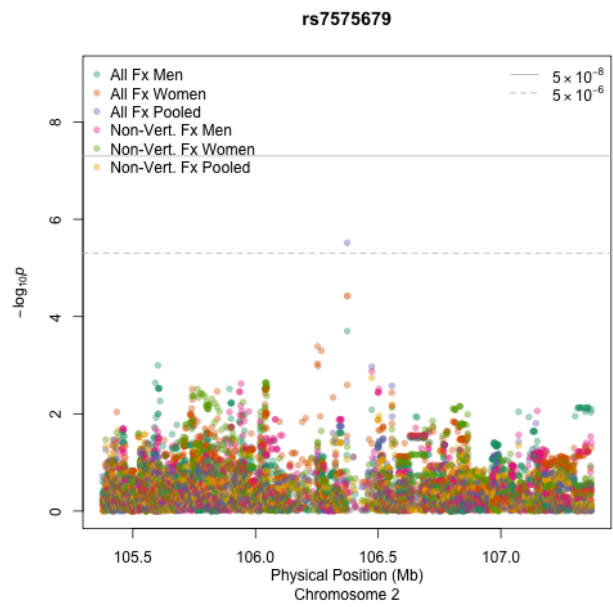


Figure H2: Eur. Am. Fx – *rs7575679*

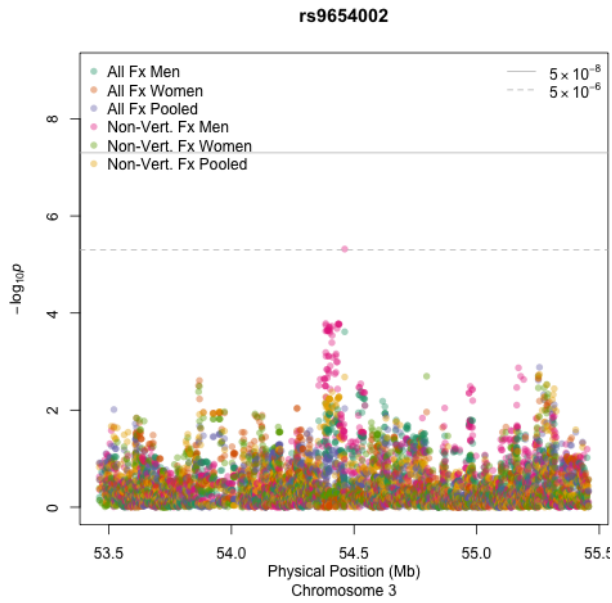


Figure H3: Eur. Am. Fx – *rs9654002*

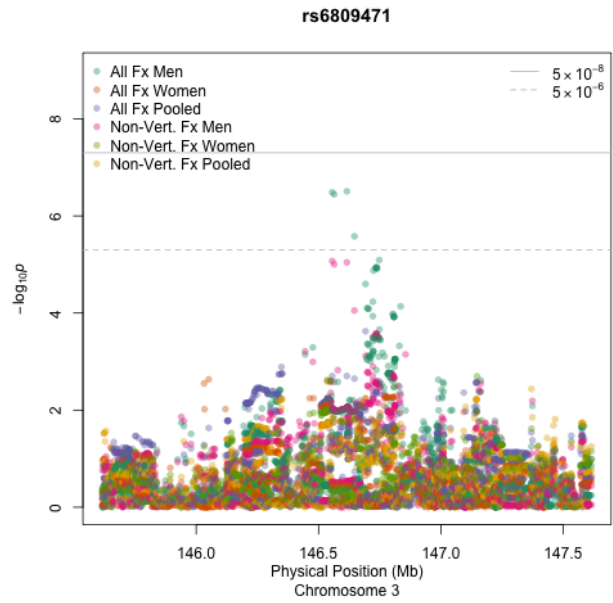


Figure H4: Eur. Am. Fx – *rs6809471*

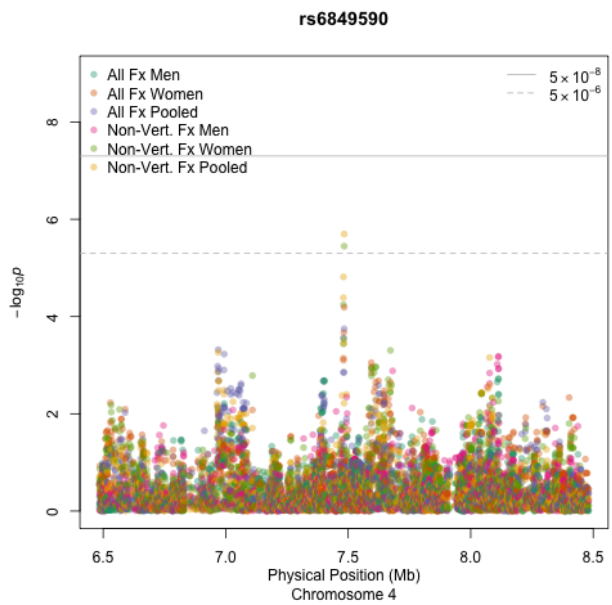


Figure H5: Eur. Am. Fx – *rs6849590*

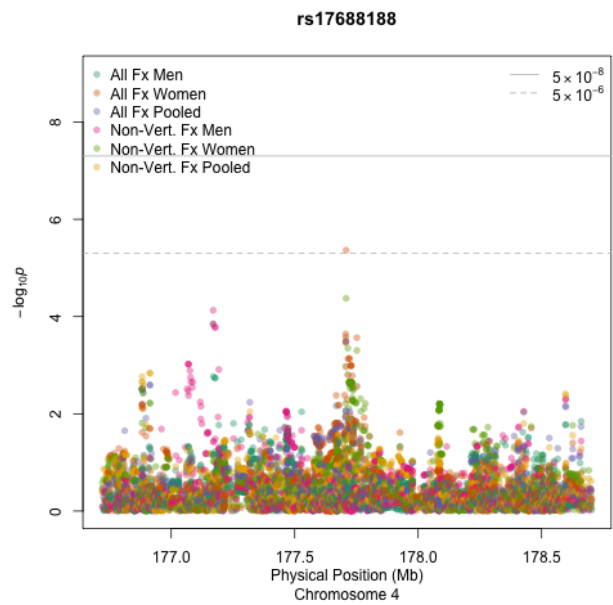


Figure H6: Eur. Am. Fx – *rs17688188*

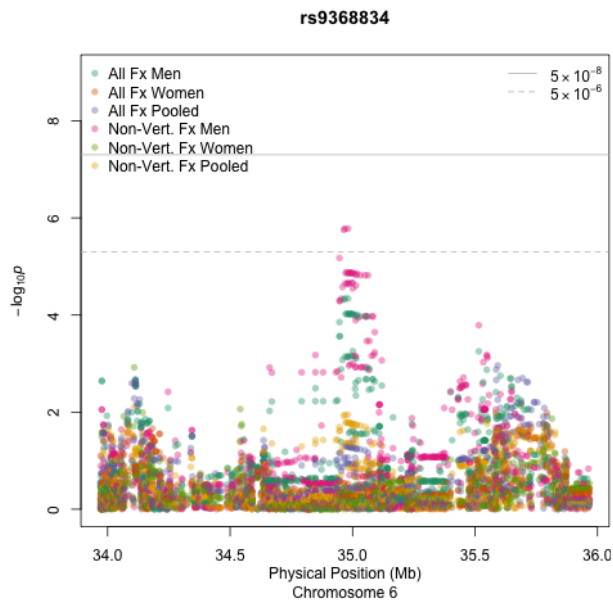


Figure H7: Eur. Am. Fx – *rs9368834*

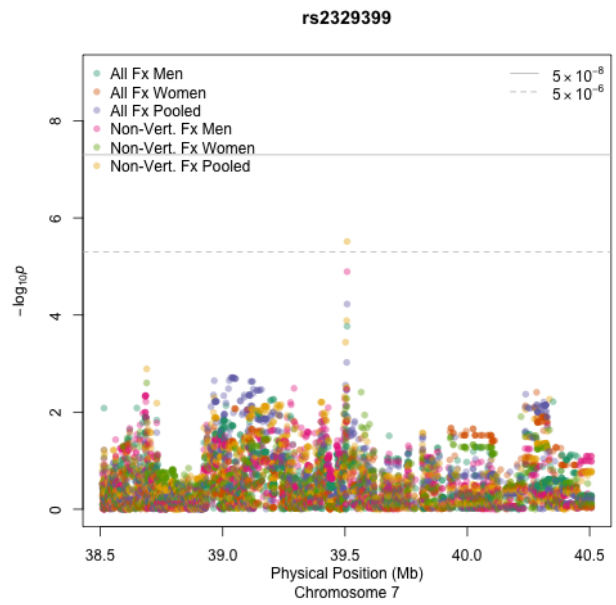


Figure H8: Eur. Am. Fx – *rs2329399*

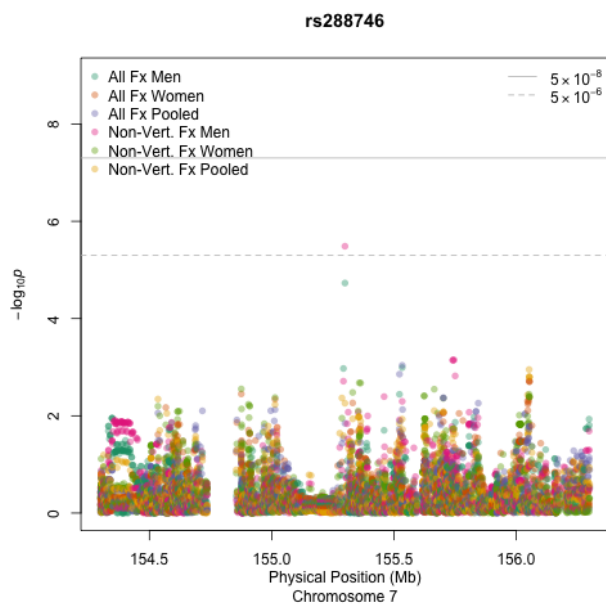


Figure H9: Eur. Am. Fx – *rs288746*

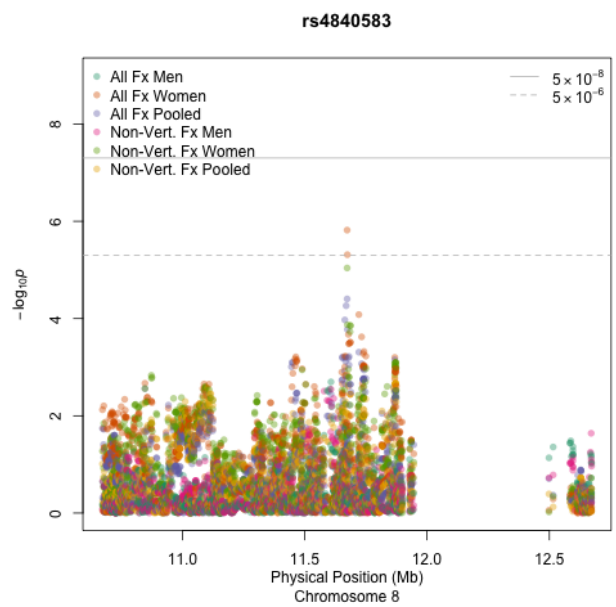


Figure H10: Eur. Am. Fx – *rs4840583*

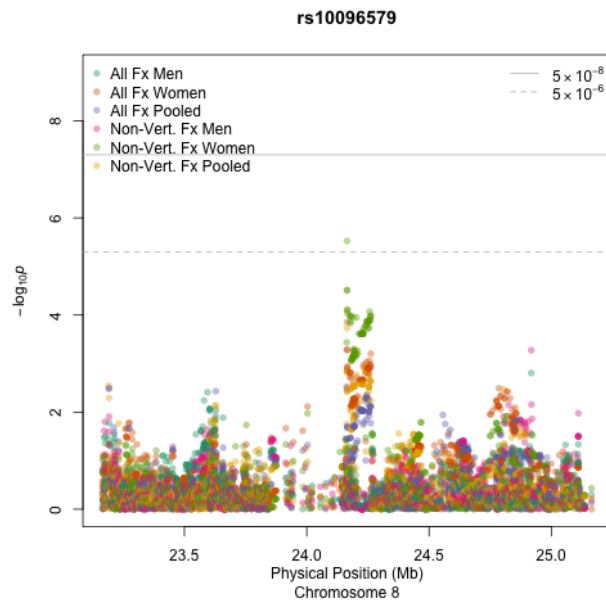


Figure H11: Eur. Am. Fx – *rs10096579*

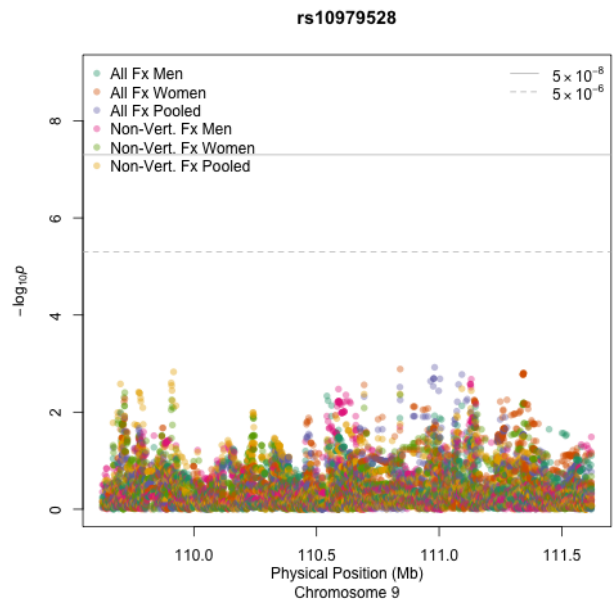


Figure H12: Eur. Am. Fx – *rs10979528*

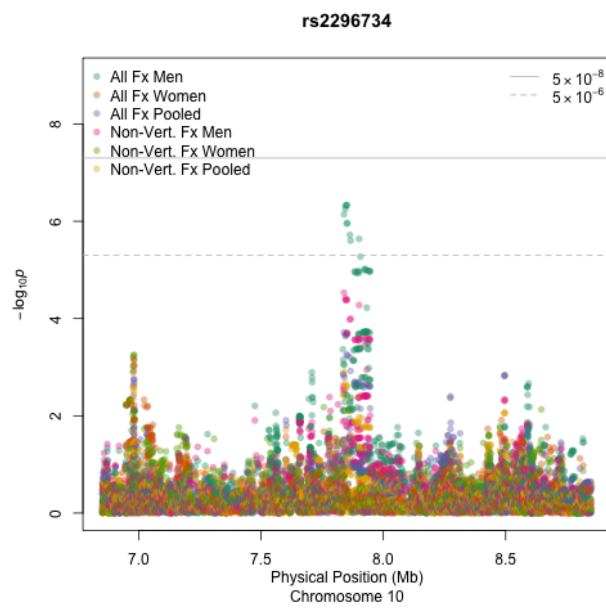


Figure H13: Eur. Am. Fx – *rs2296734*

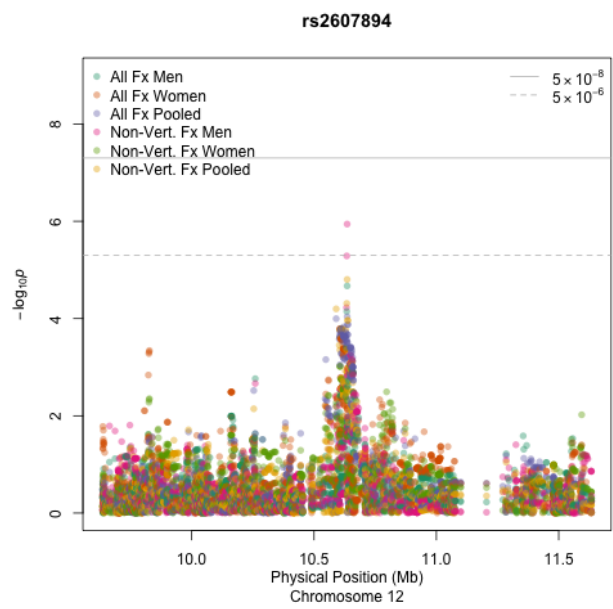


Figure H14: Eur. Am. Fx – *rs2607894*

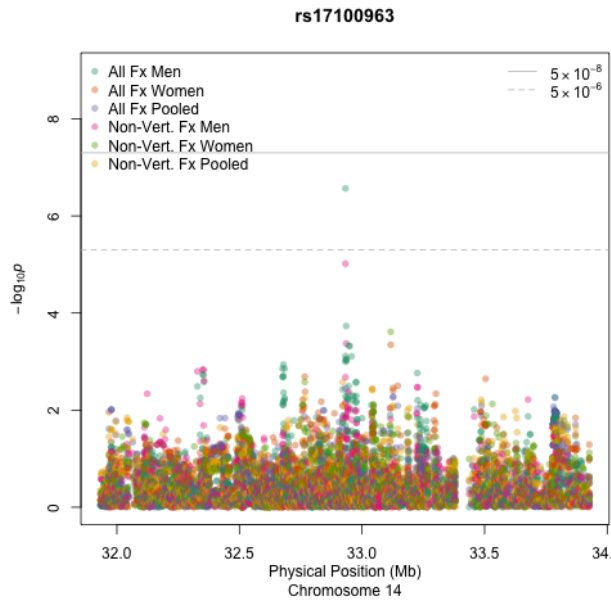


Figure H15: Eur. Am. Fx – *rs17100963*

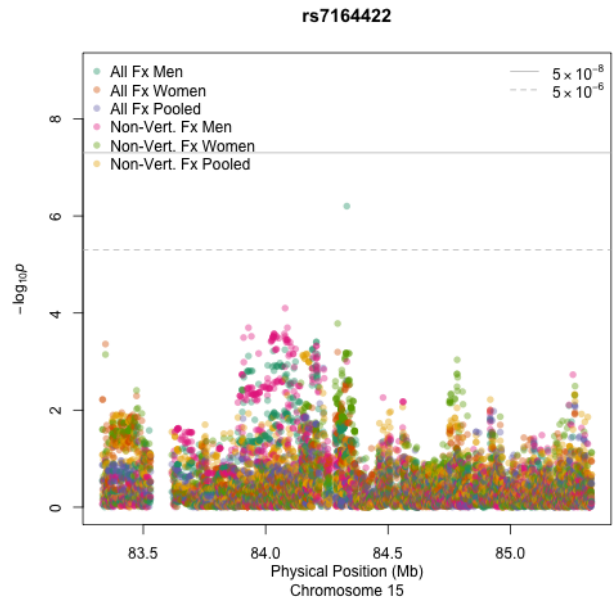


Figure H16: Eur. Am. Fx – *rs7164422*

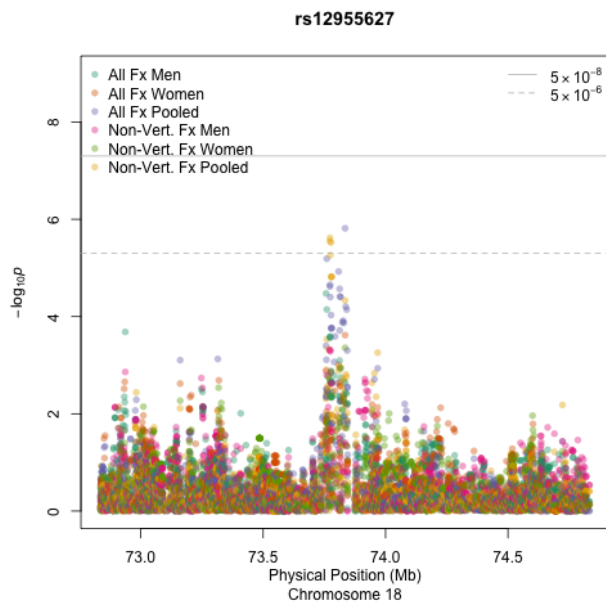


Figure H17: Eur. Am. Fx – *rs12955627*

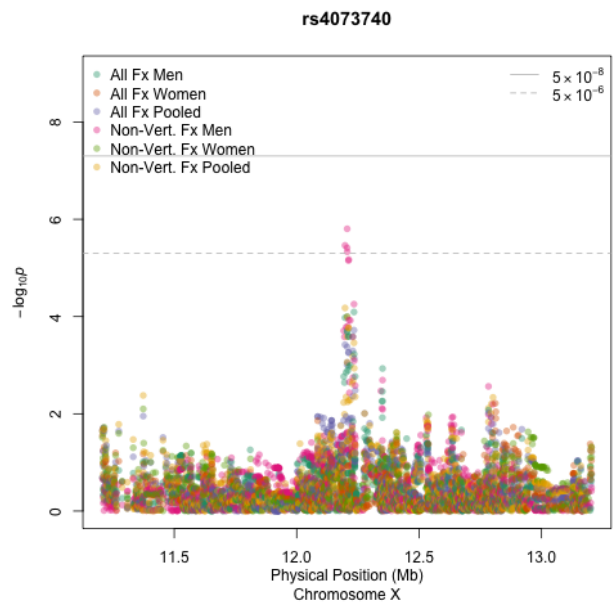


Figure H18: Eur. Am. Fx – *rs4073740*

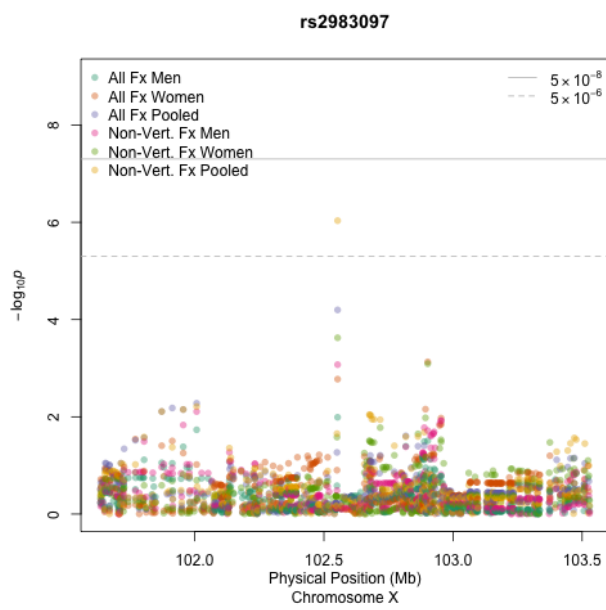


Figure H19: Eur. Am. Fx – *rs2983097*

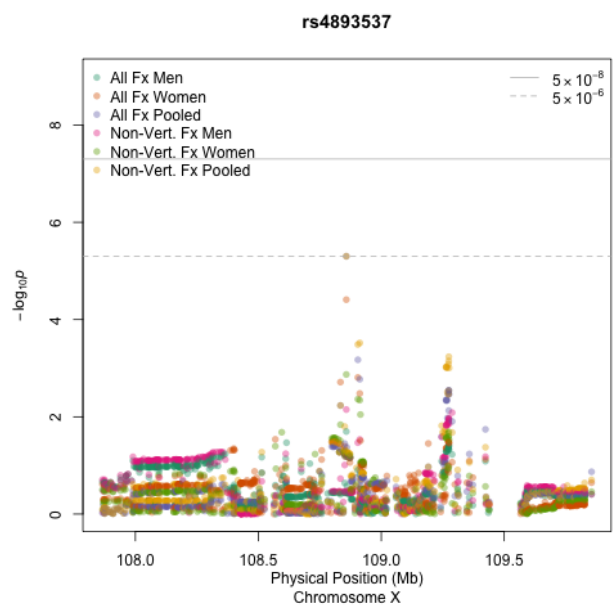


Figure H20: Eur. Am. Fx – *rs4893537*

APPENDIX I

LOCUS PLOTS OF 1000 GENOMES REPLICATION ANALYSIS

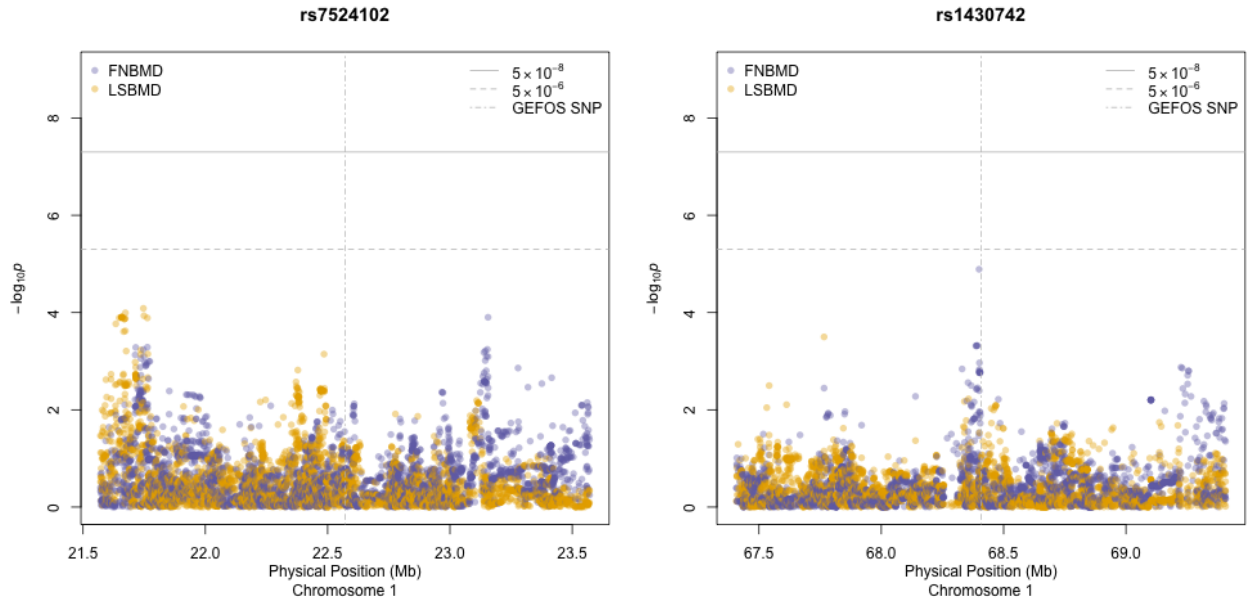


Figure I1: 1000 Genomes – *rs7524102* (*ZBTB40*)

Figure I2: 1000 Genomes – *rs1430742* (*GPR177*)

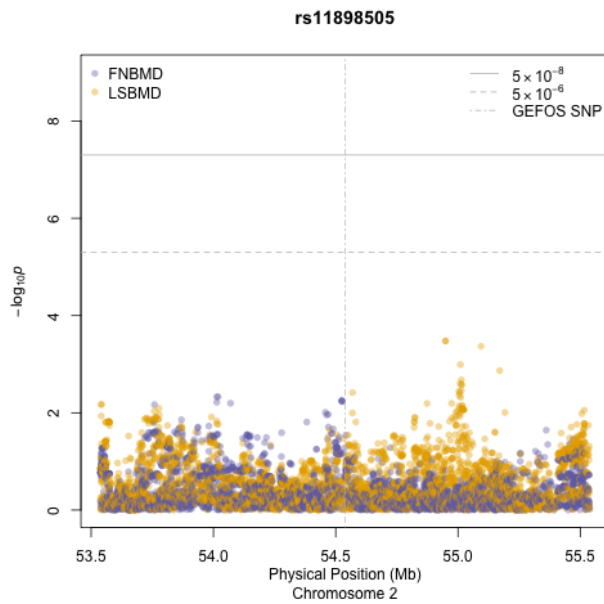


Figure I3: 1000 Genomes – *rs11898505* (*SPTBN1*)

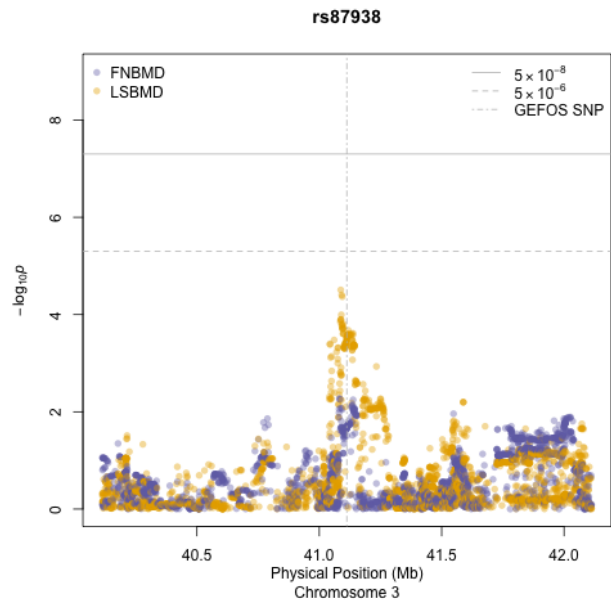


Figure I4: 1000 Genomes – *rs87938* (*CTNNB1*)

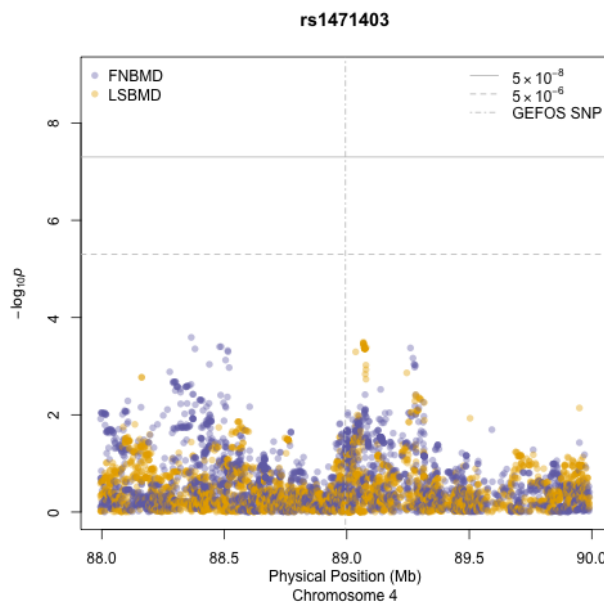


Figure I5: 1000 Genomes – *rs1471403* (*MEPE*)

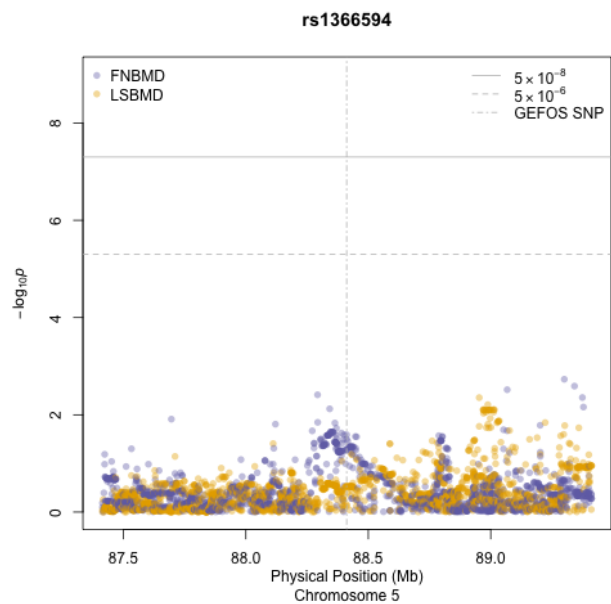


Figure I6: 1000 Genomes – *rs1366594* (*MEF2C*)

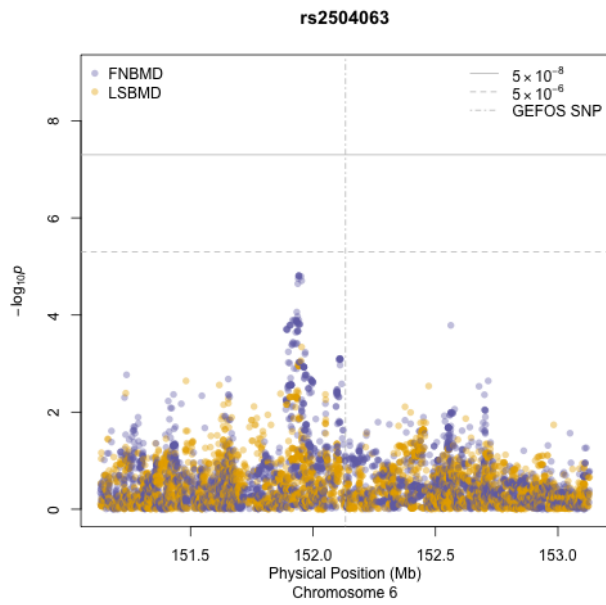


Figure I7: 1000 Genomes – *rs2504063* (*ESR1*)

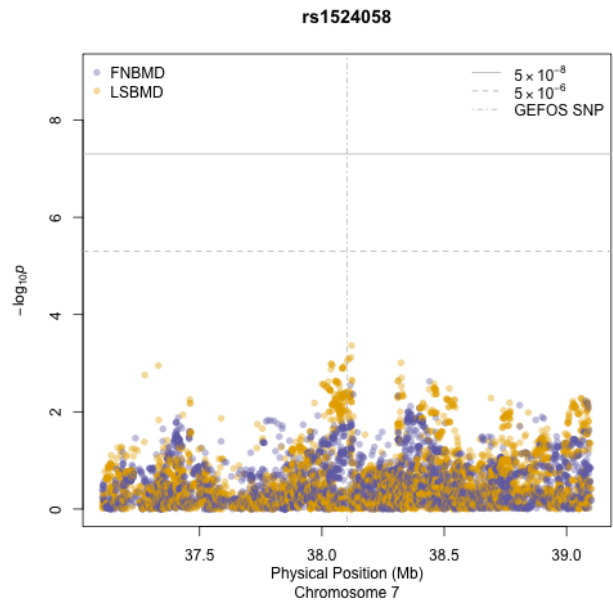


Figure I8: 1000 Genomes – *rs1524058* (*STARD3NL*)

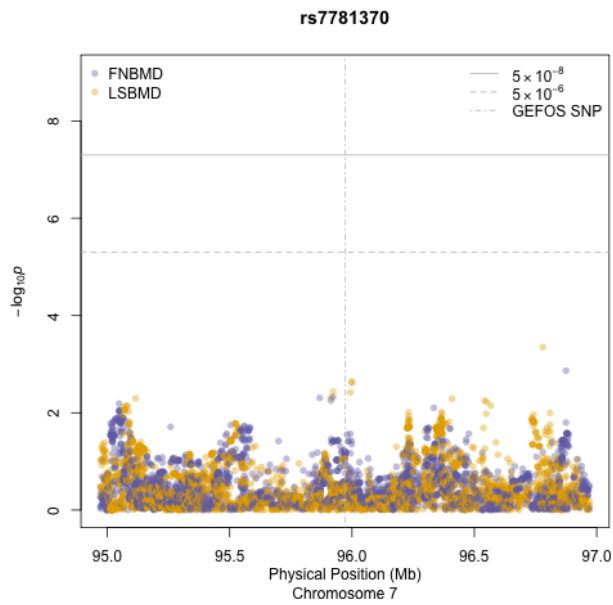


Figure I9: 1000 Genomes – *rs7781370* (*FLJ42280*)

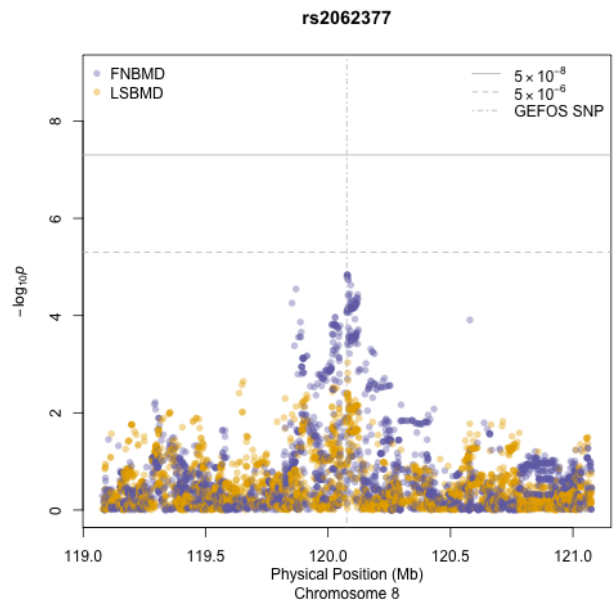


Figure I10: 1000 Genomes – *rs2062377* (*TNFRSF11B*)

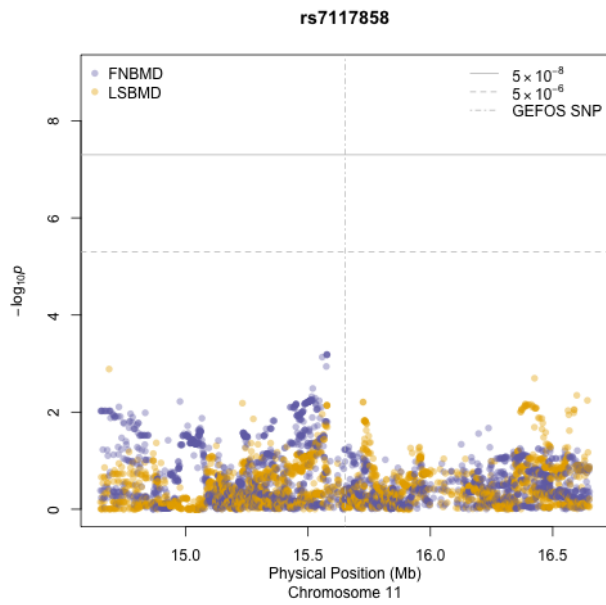


Figure I11: 1000 Genomes – *rs7117858* (*SOX6*)

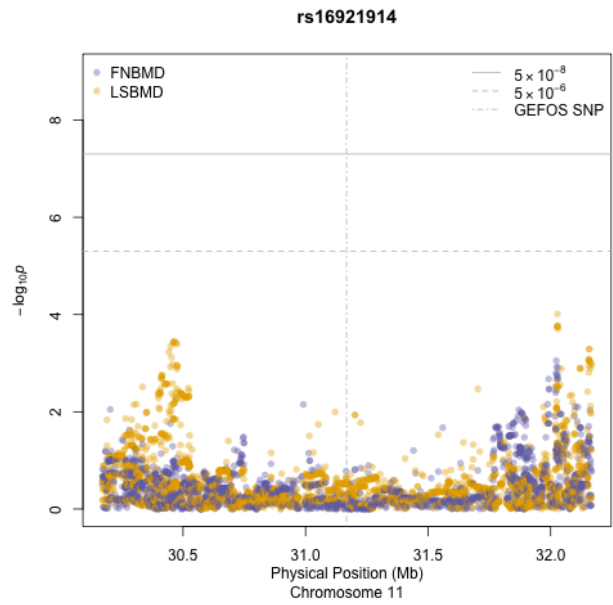


Figure I12: 1000 Genomes – *rs16921914* (*DCDC5*)

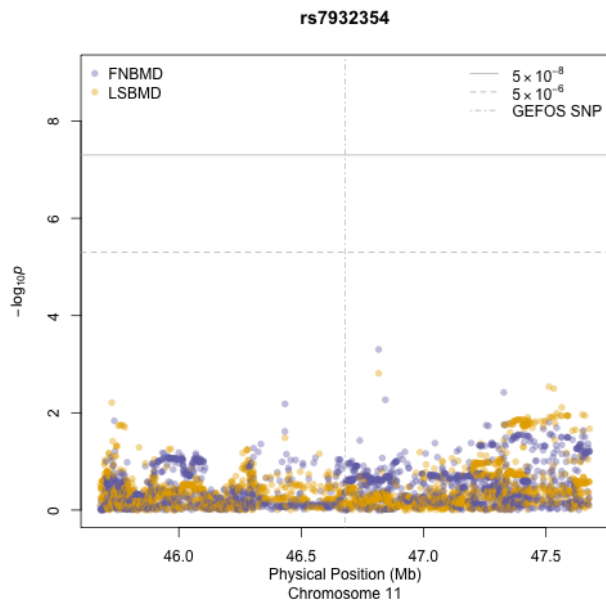


Figure I13: 1000 Genomes – *rs7932354* (*ARHGAP1*)

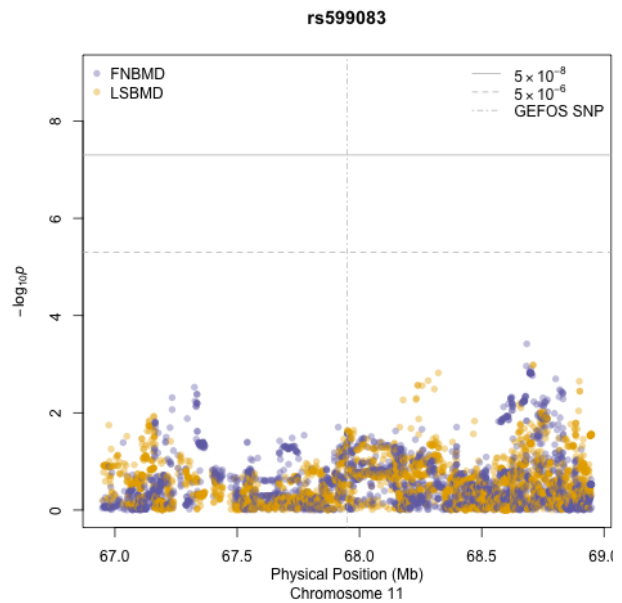


Figure I14: 1000 Genomes – *rs599083* (*LRP5*)

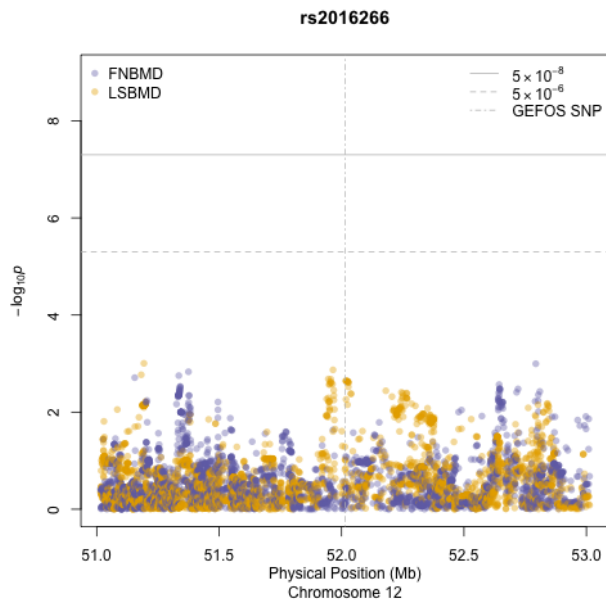


Figure I15: 1000 Genomes – *rs2016266* (*SP7*)

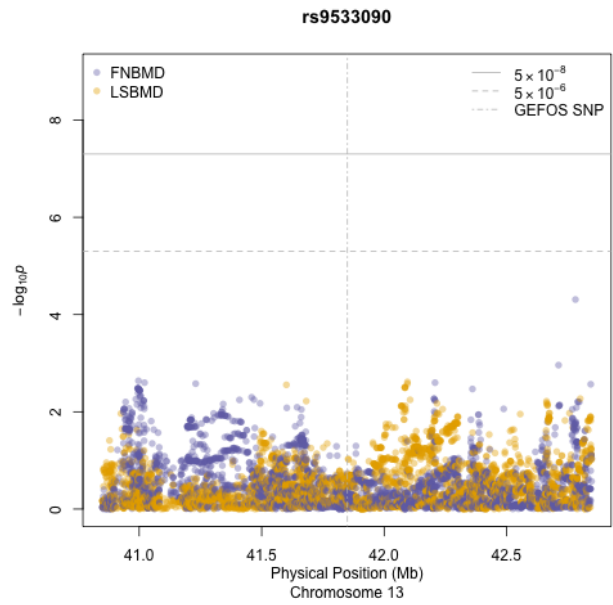


Figure I16: 1000 Genomes – *rs9533090* (*AKAP11*)

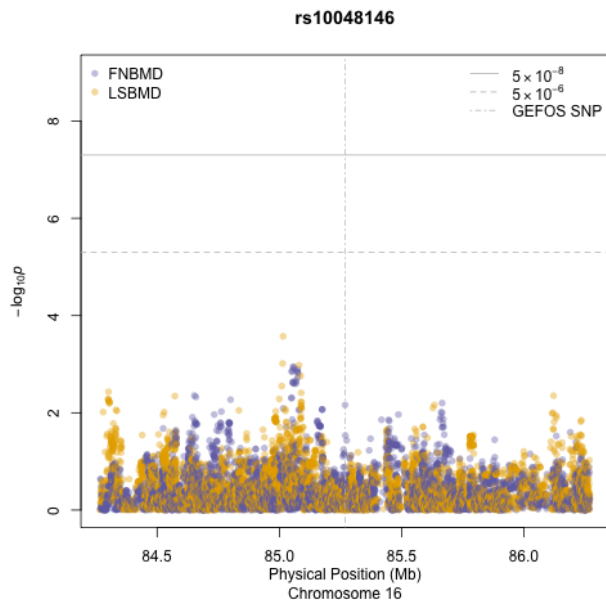


Figure I17: 1000 Genomes – *rs10048146* (*FOXL1*)

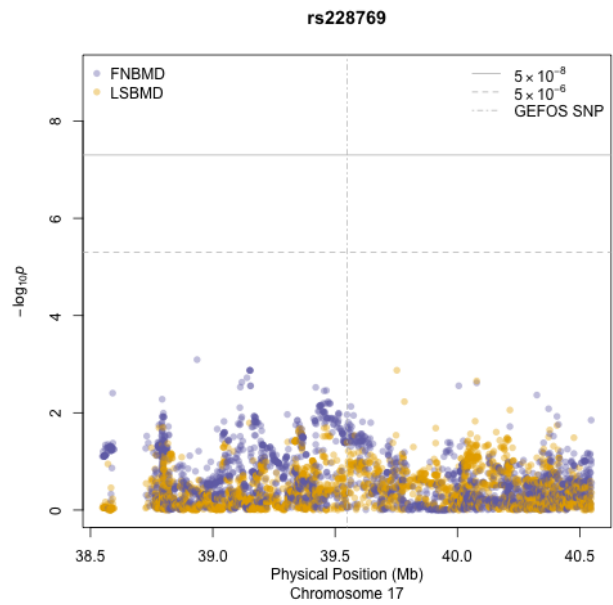


Figure I18: 1000 Genomes – *rs228769* (*HDAC5*)

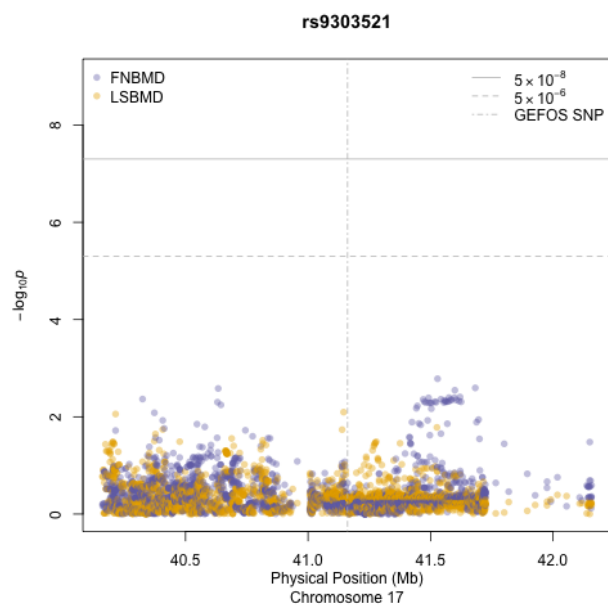


Figure I19: 1000 Genomes - *rs9303521* (*CRHR1*)

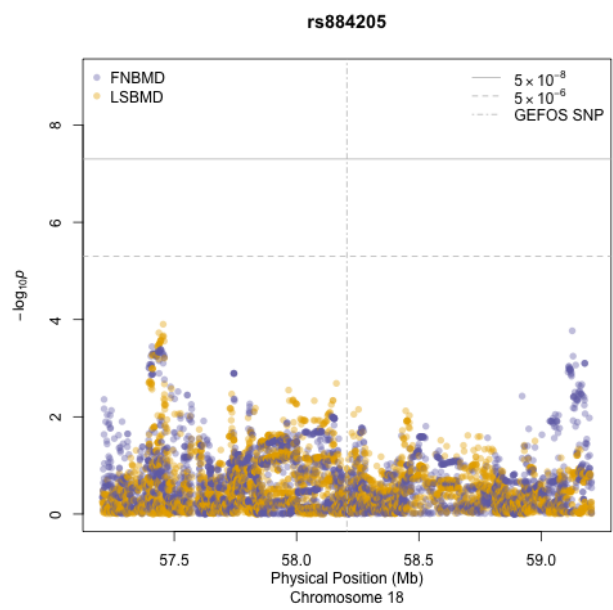


Figure I20: 1000 Genomes - *rs884205* (*TN-FRSF11A*)

APPENDIX J

LOCUS PLOTS OF BMD IN AFRICAN AMERICANS

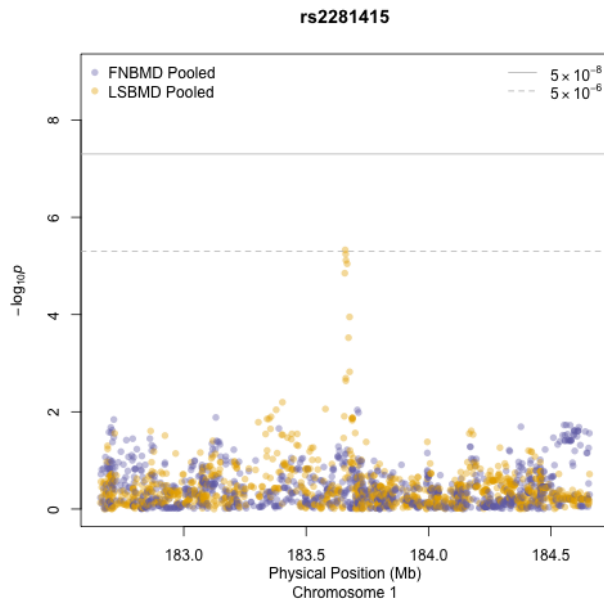


Figure J1: Afr. Am. BMD – *rs2281415*

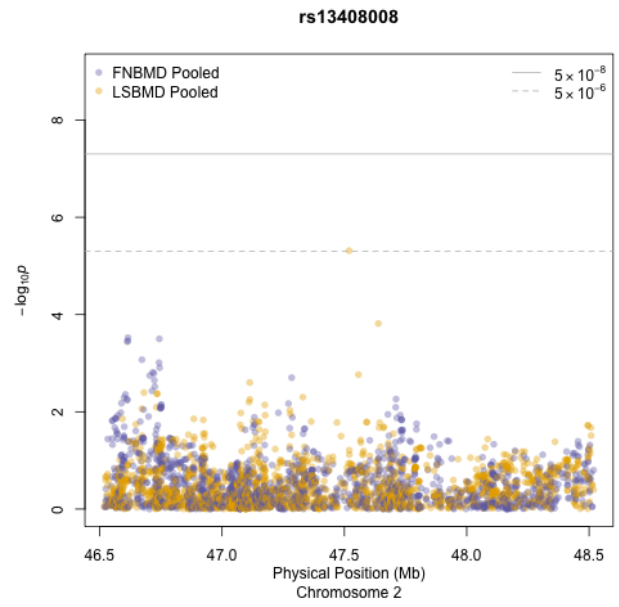


Figure J2: Afr. Am. BMD – *rs13408008*

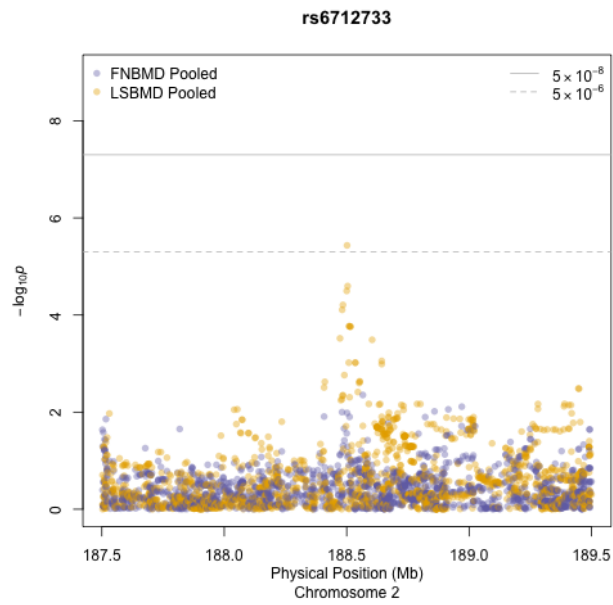


Figure J3: Afr. Am. BMD – *rs6712733*

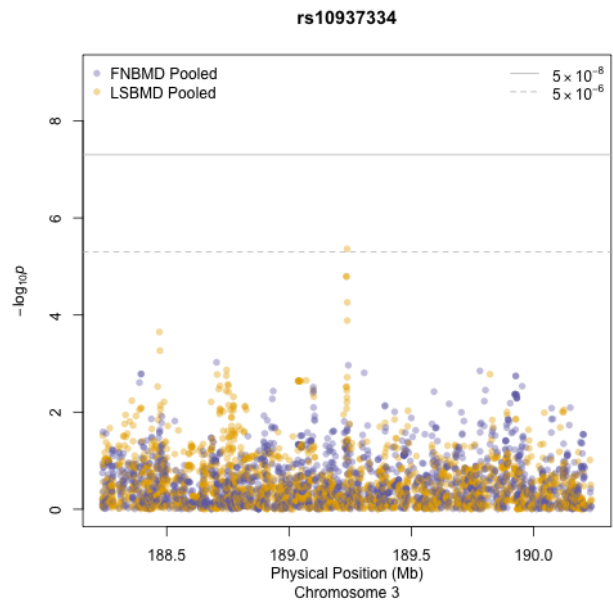


Figure J4: Afr. Am. BMD – *rs10937334*

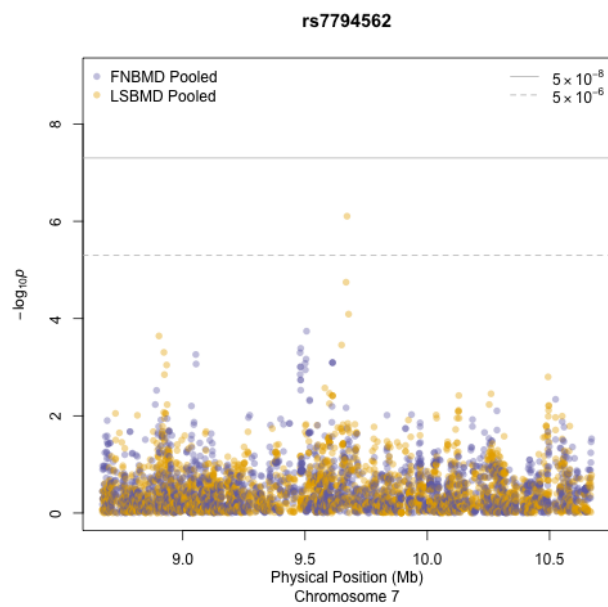


Figure J5: Afr. Am. BMD – *rs7794562*

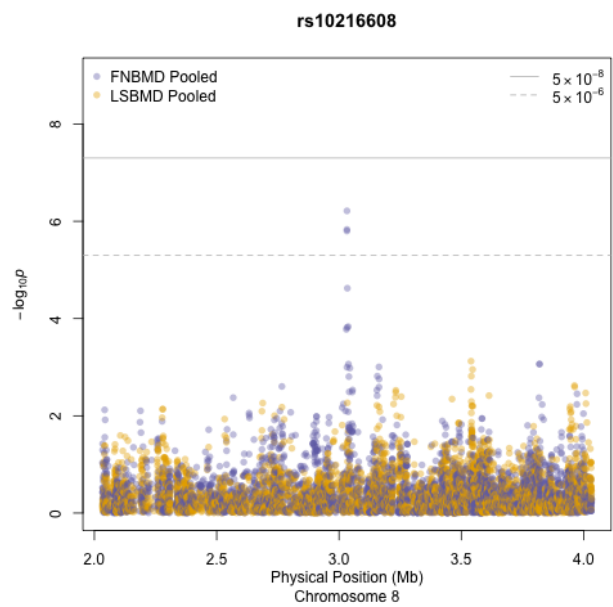


Figure J6: Afr. Am. BMD – *rs10216608*

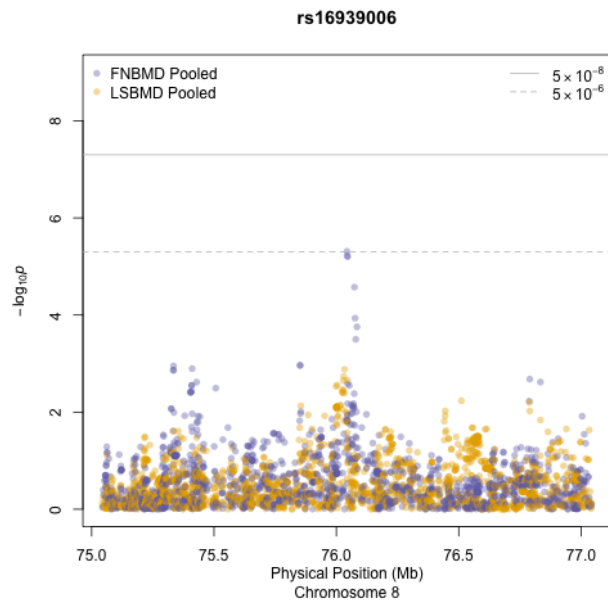


Figure J7: Afr. Am. BMD – *rs16939006*

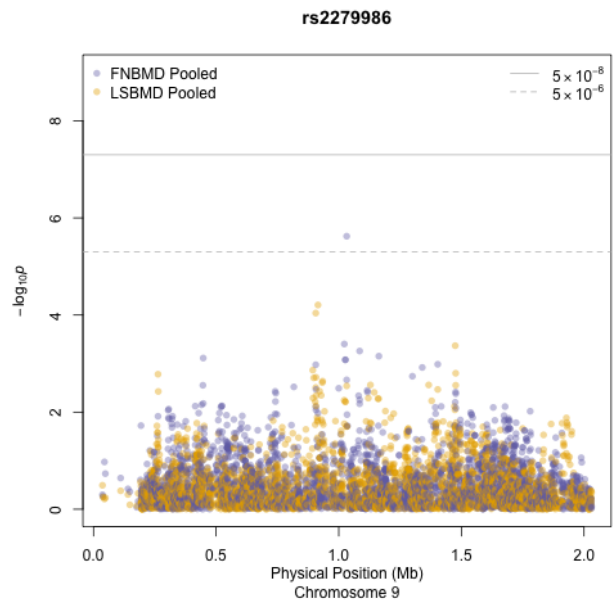


Figure J8: Afr. Am. BMD – *rs2279986*

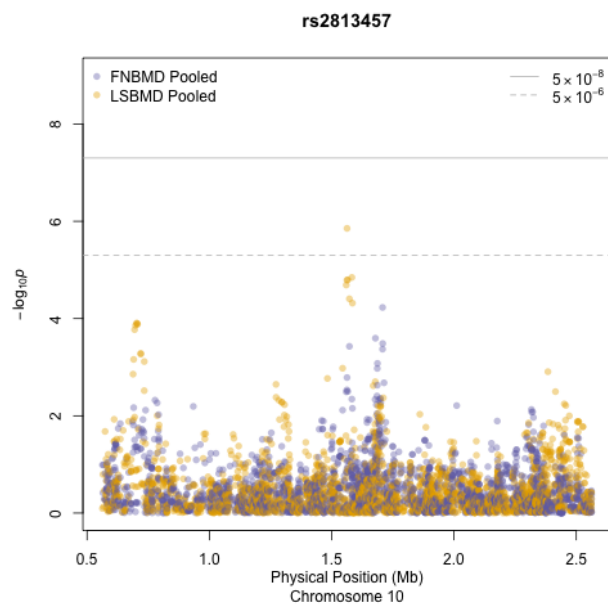


Figure J9: Afr. Am. BMD – *rs2813457*

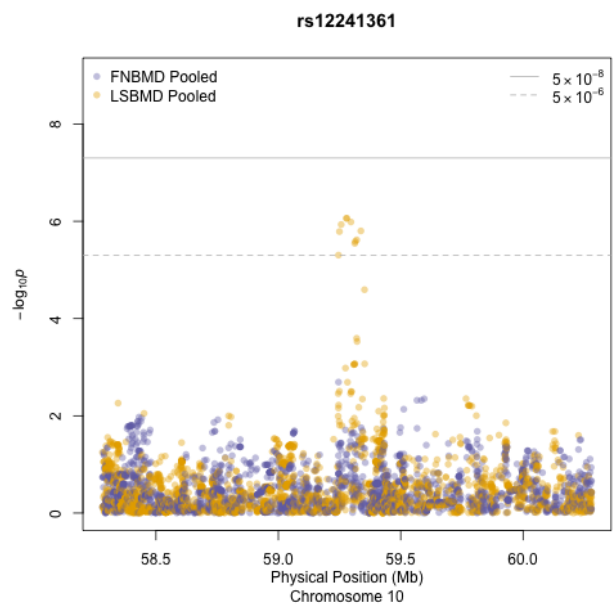


Figure J10: Afr. Am. BMD – *rs12241361*

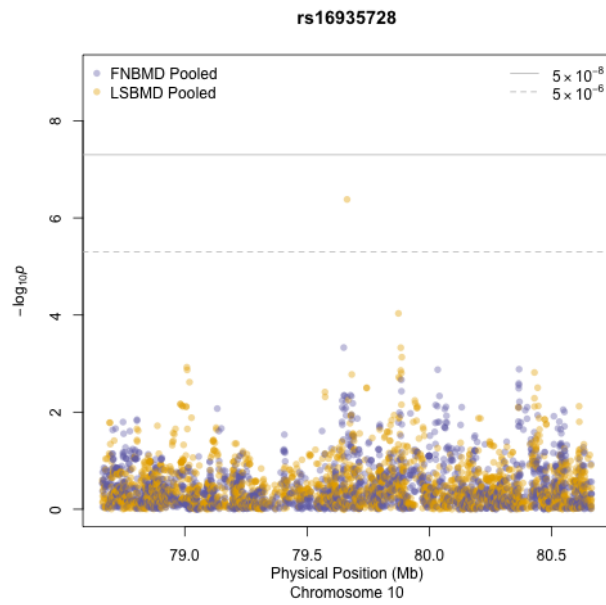


Figure J11: Afr. Am. BMD – *rs16935728*

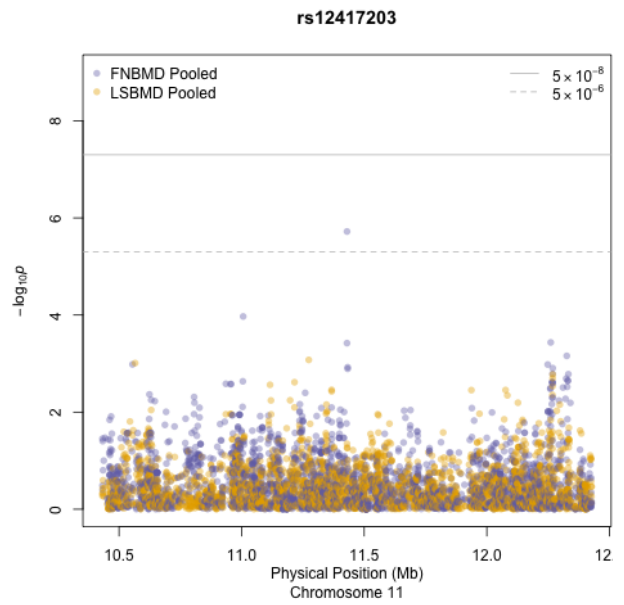


Figure J12: Afr. Am. BMD – *rs12417203*

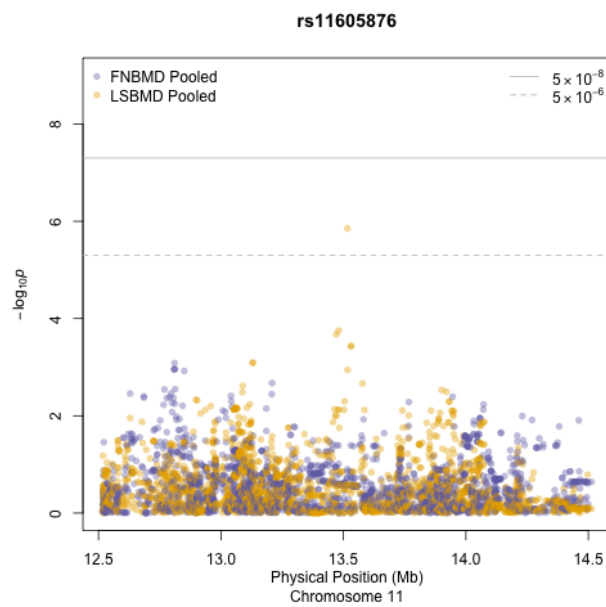


Figure J13: Afr. Am. BMD – *rs11605876*

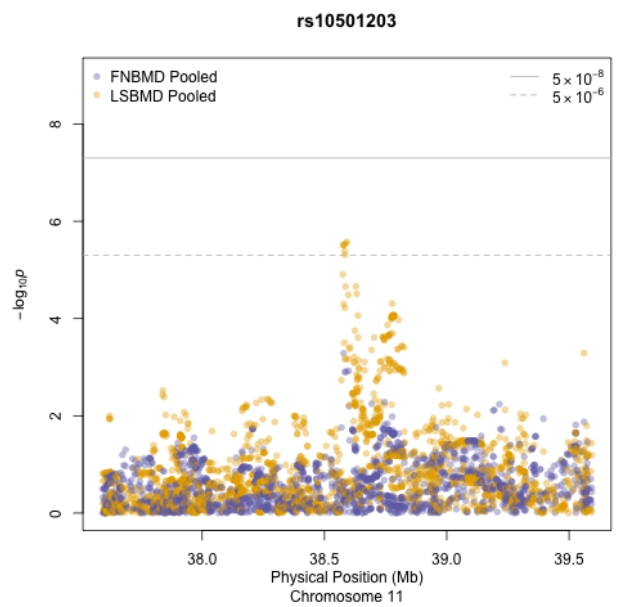


Figure J14: Afr. Am. BMD – *rs10501203*

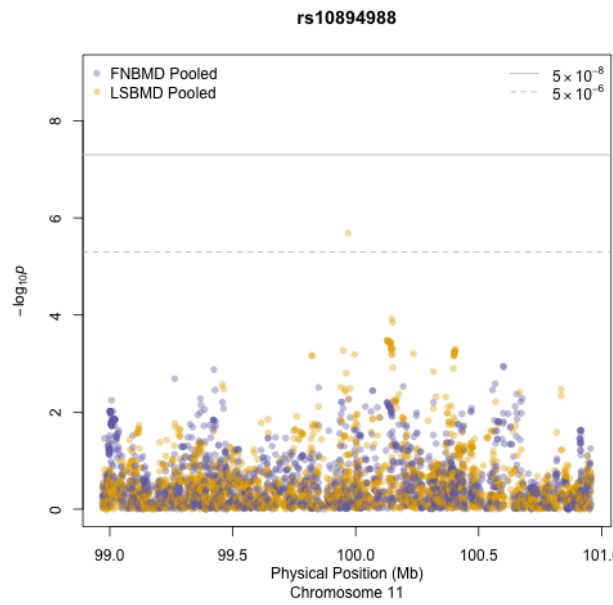


Figure J15: Afr. Am. BMD – *rs10894988*

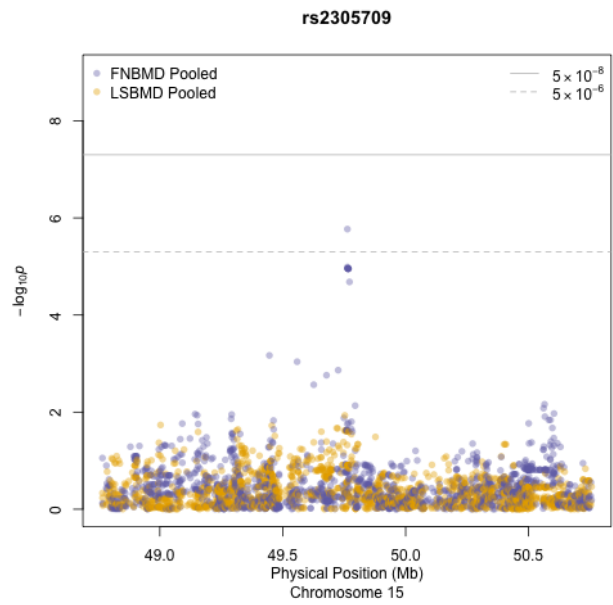


Figure J16: Afr. Am. BMD – *rs2305709*

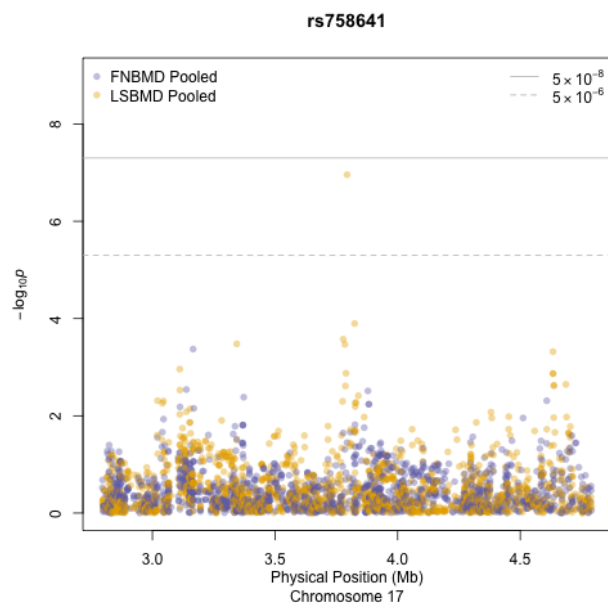


Figure J17: Afr. Am. BMD – *rs758641*

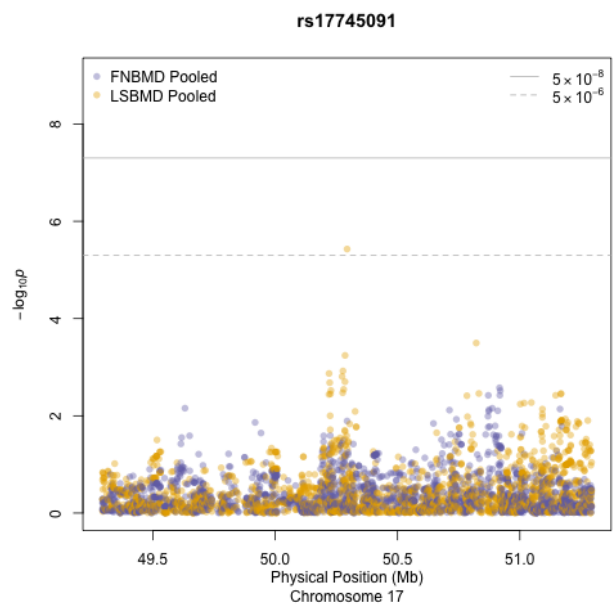


Figure J18: Afr. Am. BMD – *rs17745091*

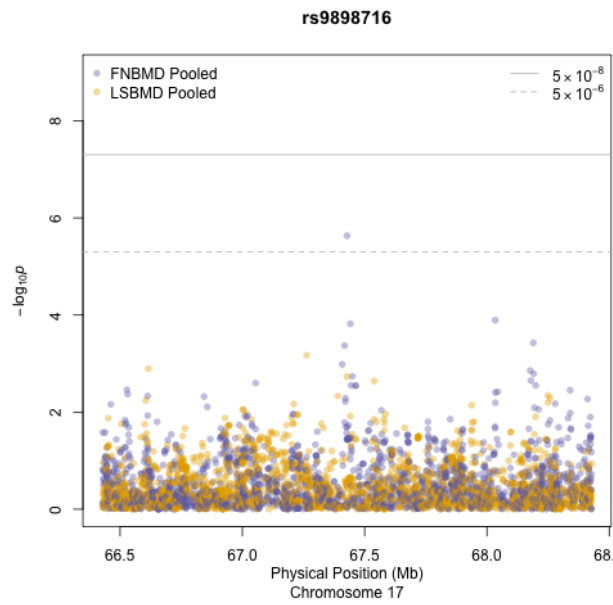


Figure J19: Afr. Am. BMD – *rs9898716*

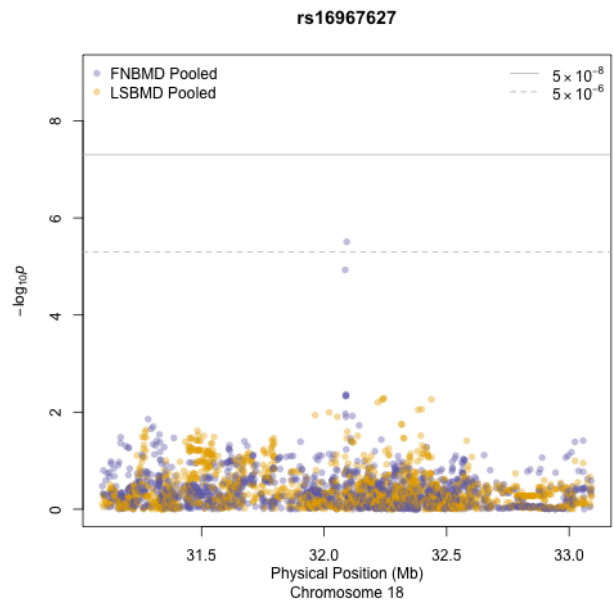


Figure J20: Afr. Am. BMD – *rs16967627*

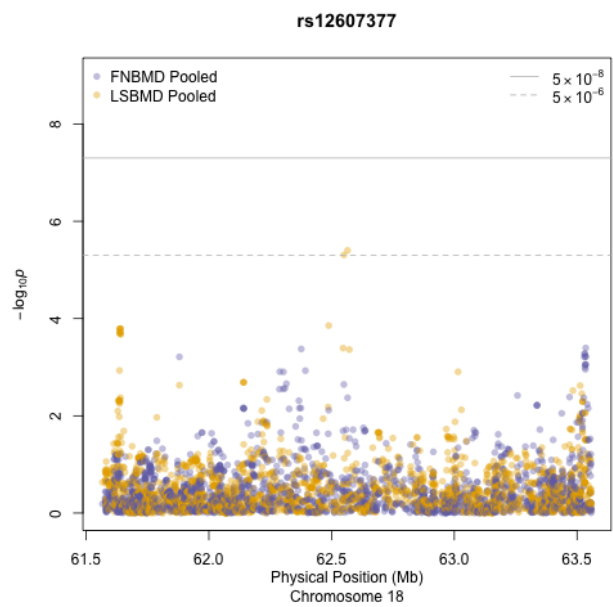


Figure J21: Afr. Am. BMD – *rs12607377*

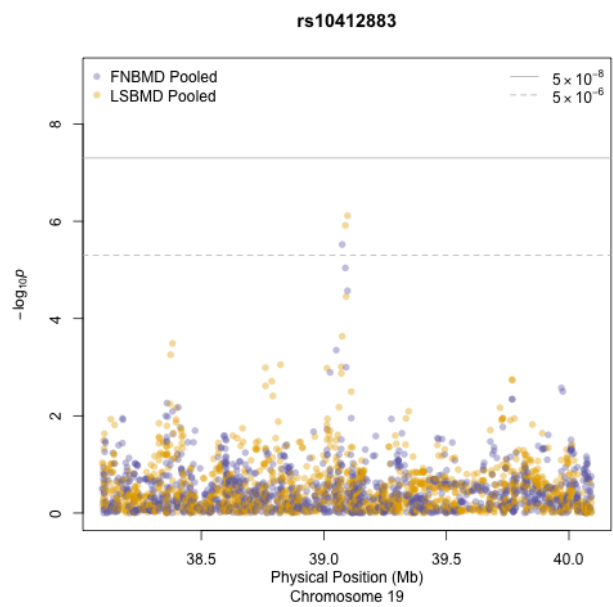


Figure J22: Afr. Am. BMD – *rs10412883*

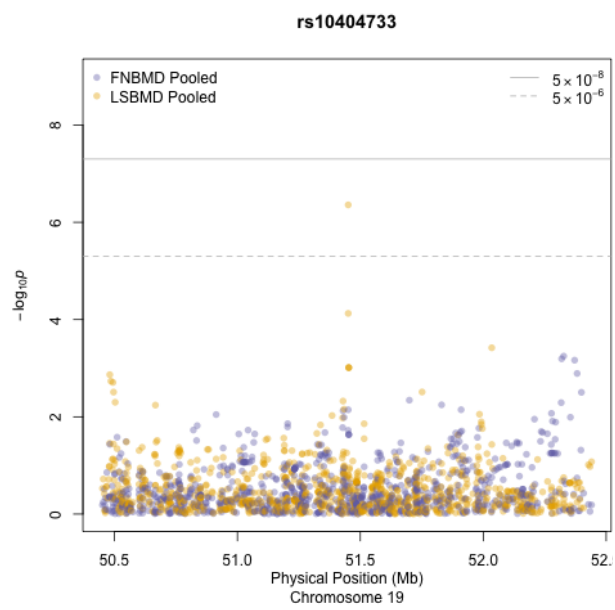


Figure J23: Afr. Am. BMD – *rs10404733*

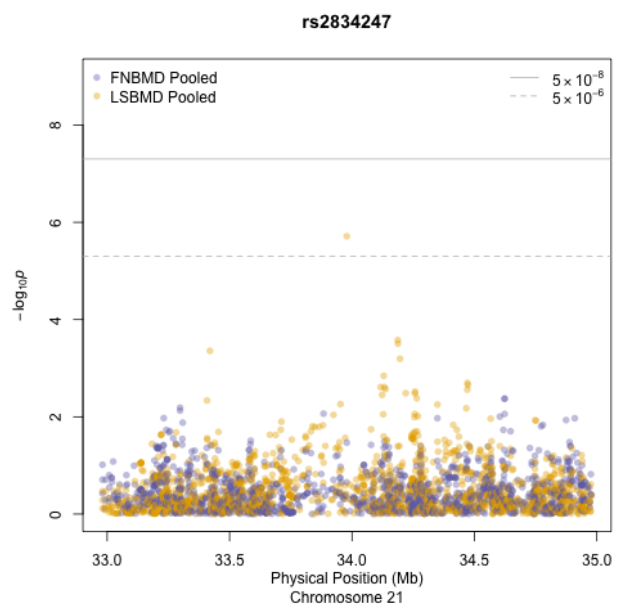


Figure J24: Afr. Am. BMD – *rs2834247*

BIBLIOGRAPHY

- C. Aalkjær and A. Hughes. Chloride and bicarbonate transport in rat resistance arteries. *J. Physiol. (Lond.)*, 436:57–73, 1991.
- G. R. Abecasis, D. L. Altshuler, A. Auton, L. D. Brooks, R. M. Durbin, R. A. Gibbs, M. E. Hurles, and G. A. McVean for the 1000 Genomes Project Consortium. A map of human genome variation from population-scale sequencing. *Nature*, 467:1061–73, 2010.
doi: 10.1038/nature09534.
- S. Ahmed, G. Thomas, M. Ghousaini, C. S. Healey, M. K. Humphreys, R. Platte, J. Morrison, M. Maranian, K. A. Pooley, R. Luben, D. Eccles, D. G. Evans, O. Fletcher, N. Johnson, I. dos Santos Silva, J. Peto, M. R. Stratton, N. Rahman, K. Jacobs, R. Prentice, G. L. Anderson, A. Rajkovic, J. D. Curb, R. G. Ziegler, C. D. Berg, S. S. Buys, C. A. McCarty, H. S. Feigelson, E. E. Calle, M. J. Thun, W. R. Diver, S. Bojesen, B. G. Nordestgaard, H. Flyger, T. Dörk, P. Schürmann, P. Hillemanns, J. H. Karstens, N. V. Bogdanova, N. N. Antonenkova, I. V. Zalutsky, M. Bermisheva, S. Fedorova, E. Khusnutdinova, D. Kang, K.-Y. Yoo, D. Y. Noh, S.-H. Ahn, P. Devilee, C. J. van Asperen, R. A. E. M. Tollenaar, C. Seynaeve, M. Garcia-Closas, J. Lissowska, L. Brinton, B. Peplonska, H. Nevanlinna, T. Heikkinen, K. Aittomäki, C. Blomqvist, J. L. Hopper, M. C. Southey, L. Smith, A. B. Spurdle, M. K. Schmidt, A. Broeks, R. R. van Hien, S. Cornelissen, R. L. Milne, G. Ribas, A. González-Neira, J. Benitez, R. K. Schmutzler, B. Burwinkel, C. R. Bartram, A. Meindl, H. Brauch, C. Justenhoven, U. Hamann, J. Chang-Claude, R. Hein, S. Wang-Gohrke, A. Lindblom, S. Margolin, A. Mannermaa, V.-M. Kosma, V. Kataja, J. E. Olson, X. Wang, Z. Fredericksen, G. G. Giles, G. Severi, L. Baglietto, D. R. English, S. E. Hankinson, D. G. Cox, P. Kraft, L. J. Vatten, K. Hveem, M. Kumle, A. Sigurdson, M. Doody, P. Bhatti, B. H. Alexander, M. J. Hooning, A. M. W. van den Ouweland, R. A. Oldenburg, M. Schutte, P. Hall, K. Czene, J. Liu, Y. Li, A. Cox, G. Elliott, I. Brock, M. W. R. Reed, C.-Y. Shen, J.-C. Yu, G.-C. Hsu, S.-T. Chen, H. Anton-Culver, A. Ziogas, I. L. Andrulis, J. A. Knight, J. Beesley, E. L. Goode, F. Couch, G. Chenevix-Trench, R. N. Hoover, B. A. J. Ponder, D. J. Hunter, P. D. P. Pharoah, A. M. Dunning, S. J. Chanock, and D. F. Easton. Newly discovered breast cancer susceptibility loci on 3p24 and 17q23.2. *Nat. Genet.*, 41:585–590, 2009.
doi: 10.1038/ng.354.
- M. Ainola, T.-F. Li, J. Mandelin, M. Hukkanen, S. J. Choi, J. Salo, and Y. T. Kontinen. Involvement of a disintegrin and a metalloproteinase 8 (ADAM8) in osteoclastogenesis and pathological bone destruction. *Ann. Rheum. Dis.*, 68:427–434, 2009.
doi: 10.1136/ard.2008.088260.
- D. B. Allison, M. C. Neale, R. Zannolli, N. J. Schork, C. I. Amos, , and J. Blangero. Testing the robustness of the likelihood-ratio test in a variance-component quantitative-trait loci-mapping procedure. *Am. J. Hum. Genet.*, 65:531–544, 1999.
doi: 10.1086/302487.
- L. Almasy and J. Blangero. Multipoint quantitative-trait linkage analysis in general pedigrees. *Am. J. Hum. Genet.*, 62: 1198–1211, 1998a.
doi: 10.1086/301844.

- L. Almasy and J. Blangero. Multipoint quantitative-trait linkage analysis in general pedigrees. *Am. J. Hum. Genet.*, 62: 1198–211, 1998b.
doi: 10.1086/301844.
- D. Altshuler, L. D. Brooks, A. Chakravarti, F. S. Collins, M. J. Daly, and P. Donnelly. A haplotype map of the human genome. *Nature*, 437:1299–1320, 2005.
doi: 10.1038/nature04226.
- C. I. Amos. Robust variance-components approach for assessing genetic linkage in pedigrees. *Am. J. Hum. Genet.*, 54: 535–43, 1994.
- N. K. Arden and T. D. Spector. Genetic influences on muscle strength, lean body mass, and bone mineral density: A twin study. *J. Bone Miner. Res.*, 12:2076–2081, 1997.
doi: 10.1359/jbmr.1997.12.12.2076.
- Y. S. Aulchenko, M. V. Struchalin, and C. M. van Duijn. ProbABEL package for genome-wide association analysis of imputed data. *BMC Bioinformatics*, 11:134, 2010.
doi: 10.1186/1471-2105-11-134.
- S.-A. Bacanu, B. Devlin, and K. Roeder. Association studies for quantitative traits in structured populations. *Genet. Epidemiol.*, 22:78–93, 2002.
doi: 10.1359/10.1002/gepi.1045.
- F. P. Barry and J. M. Murphy. Mesenchymal stem cells: clinical applications and biological characterization. *Int. J. Biochem. Cell Biol.*, 36:568–584, 2004.
doi: 10.1016/j.biocel.2003.11.001.
- R. N. Baumgartner, K. M. Koehler, D. Gallagher, L. Romero, S. B. Heymsfield, R. R. Ross, P. J. Garry, and R. D. Lindeman. Epidemiology of sarcopenia among the elderly in New Mexico. *Am. J. Epidemiol.*, 147:755–763, 1998.
- T. J. Beck, M. A. Petit, G. Wu, M. S. LeBoff, J. A. Cauley, and Z. Chen. Does obesity really make the femur stronger? BMD, geometry, and fracture incidence in the Women’s Health Initiative-Observational Study. *J. Bone Miner. Res.*, 24: 1369–1379, 2009.
doi: 10.1359/jbmr.090307.
- J. E. Below, E. R. Gamazon, J. V. Morrison, A. Konkashbaev, A. Pluzhnikov, P. M. McKeigue, E. J. Parra, S. C. Elbein, D. M. Hallman, D. L. Nicolae, G. I. Bell, M. Cruz, N. J. Cox, and C. L. Hanis. Genome-wide association and meta-analysis in populations from Starr County, Texas, and Mexico City identify type 2 diabetes susceptibility loci and enrichment for expression quantitative trait loci in top signals. *Diabetologia*, in press, 2011.
doi: 10.1007/s00125-011-2188-3.
- P. C. Billings, J. L. Fiori, J. L. Bentwood, M. P. O’Connell, X. Jiao, B. Nussbaum, R. J. Caron, E. M. Shore, and F. S. Kaplan. Dysregulated BMP signaling and enhanced osteogenic differentiation of connective tissue progenitor cells from patients with fibrodysplasia ossificans progressiva (FOP). *J. Bone Miner. Res.*, 23:305–313, 2007.
doi: 10.1359/jbmr.071030.
- D. M. Black, S. R. Cummings, H. K. Genant, M. C. Nevitt, L. Palermo, and W. Browner. Axial and appendicular bone density predict fractures in older women. *J. Bone Miner. Res.*, 7:633–638, 1992.
doi: 10.1002/jbmr.5650070607.
- H. Blain, A. Vuillemin, C. Jeandel, P. Jouanny, F. Guillemin, and E. Le Bihan. Lean mass plays a gender-specific role in familial resemblance for femoral neck bone mineral density in adult subjects. *Osteoporos. Int.*, 17:897–907, 2006.
doi: 10.1007/s00198-005-0062-1.

- J. Blangero, J. T. Williams, and L. Almasy. Robust LOD scores for variance component-based linkage analysis. *Genet. Epidemiol.*, 19(Suppl. 1):S8–S14, 2000.
doi: 10.1002/1098-2272(2000)19:1+<:aid-gepi2>3.0.co;2-y.
- J. Blangero, J. T. Williams, and L. Almasy. Variance component methods for detecting complex trait loci. *Adv. Genet.*, 42:151–181, 2001.
- M. Boehnke and N. J. Cox. Accurate inference of relationships in sib-pair linkage studies. *Am. J. Hum. Genet.*, 61:423–9, 1997.
doi: 10.1086/514862.
- D. Bok, G. Galbraith, I. Lopez, M. Woodruff, S. Nusinowitz, H. BeltrandelRio, W. Huang, S. Zhao, R. Geske, C. Montgomery, I. Van Sligtenhorst, C. Friddle, K. Platt, M. J. Sparks, A. Pushkin, N. Abuladze, A. Ishiyama, R. Dukkupati, W. Liu, and I. Kurtz. Blindness and auditory impairment caused by loss of the sodium bicarbonate cotransporter NBC3. *Nat. Genet.*, 34:313–319, 2003.
doi: 10.1038/ng1176.
- W. F. Boron and E. L. Boulpaep. Intracellular pH regulation in the renal proximal tubule of the salamander. Na–H exchange. *J. Gen. Physiol.*, 81:29–52, 1983.
- P. Bouyer, H. Sakai, T. Itokawa, T. Kawano, C. M. Fulton, W. F. Boron, and K. L. Insogna. Colony-stimulating Factor-1 increases osteoclast intracellular pH and promotes survival via the electroneutral Na/HCO₃ cotransporter NBCn1. *Endocrinology*, 148:831–840, 2006.
doi: 10.1210/en.2006-0547.
- J. Broadwin, D. Goodman-Gruen, and D. Slymen. Ability of fat and fat-free mass percentages to predict functional disability in older men and women. *J. Am. Geriatr. Soc.*, 49:1641–1645, 2001.
doi: 10.1111/j.1532-5415.2001.49273.x.
- C. H. Bunker, A. L. Patrick, B. R. Konety, R. Dhir, A. M. Brufsky, C. A. Vivas, M. J. Becich, D. L. Trump, and L. H. Kuller. High prevalence of screen-detected prostate cancer among Afro-Caribbeans: the Tobago Prostate Cancer Survey. *Cancer Epidemiol. Biomarkers Prev.*, 11:726–9, 2002.
- J. T. Burdick, W.-M. Chen, G. R. Abecasis, and V. G. Cheung. *In silico* method for inferring genotypes in pedigrees. *Nat. Genet.*, 38:1002–1004, 2006.
doi: 10.1038/ng1863.
- R. Burge, B. Dawson-Hughes, D. H. Solomon, J. B. Wong, A. King, and A. Tosteson. Incidence and economic burden of osteoporosis-related fractures in the United States, 2005–2025. *J. Bone Miner. Res.*, 22:465–75, 2007.
doi: 10.1359/jbmr.061113.
- D. R. Carter, M. L. Bouxsein, and R. Marcus. New approaches for interpreting projected bone densitometry data. *J. Bone Miner. Res.*, 7:137–145, 1992.
doi: 10.1002/jbmr.5650070204.
- J. A. Cauley, M. E. Danielson, R. M. Boudreau, K. Y. Z. Forrest, J. M. Zmuda, M. Pahor, F. A. Tylavsky, S. R. Cummings, T. B. Harris, and A. B. Newman. Inflammatory markers and incident fracture risk in older men and women: the Health Aging and Body Composition Study. *J. Bone Miner. Res.*, 22:1088–95, 2007.
doi: 10.1359/jbmr.070409.
- Y. Chen, H. Shen, F. Yang, P.-Y. Liu, N. Tang, R. R. Recker, and H.-W. Deng. Choice of study phenotype in osteoporosis genetic research. *J. Bone Miner. Metab.*, 27:121–126, 2009.
doi: 10.1007/s00774-008-0020-z.

- C. Chiang, Y. Litingtung, E. Lee, K. E. Young, J. L. Corden, H. Westphal, and P. A. Beachy. Cyclopia and defective axial patterning in mice lacking *Sonic hedgehog* gene function. *Nature*, 383:407–413, 1996.
doi: 10.1038/383407a0.
- M.-Y. Chien, T.-Y. Huang, and Y.-T. Wu. Prevalence of sarcopenia estimated using a bioelectrical impedance analysis prediction equation in community-dwelling elderly people in Taiwan. *J. Am. Geriatr. Soc.*, 56:1710–1715, 2008.
doi: 10.1111/j.1532-5415.2008.01854.x.
- U. Chinappen-Horsley, G. M. Blake, I. Fogelman, B. Kato, K. R. Ahmadi, and T. D. Spector. Quantitative trait loci for bone lengths on chromosome 5 using dual energy x-ray absorptiometry imaging in the twins uk cohort. *PLoS ONE*, 3: e1752, 2008.
doi: 10.1371/journal.pone.0001752.
- Y. S. Cho, M. J. Go, Y. J. Kim, J. Y. Heo, J. H. Oh, H.-J. Ban, D. Yoon, M. H. Lee, D.-J. Kim, M. Park, S.-H. Cha, J.-W. Kim, B.-G. Han, H. Min, Y. Ahn, M. S. Park, H. R. Han, H.-Y. Jang, E. Y. Cho, J.-E. Lee, N. H. Cho, C. Shin, T. Park, J. W. Park, J.-K. Lee, L. Cardon, G. Clarke, M. I. McCarthy, J.-Y. Lee, J.-K. Lee, B. Oh, and H.-L. Kim. A large-scale genome-wide association study of Asian populations uncovers genetic factors influencing eight quantitative traits. *Nat. Genet.*, 41: 527–534, 2009.
doi: 10.1038/ng.357.
- I. Choi, C. Aalkjaer, E. L. Boulpaep, and W. F. Boron. An electroneutral sodium/bicarbonate cotransporter NBCn1 and associated sodium channel. *Nature*, 405:571–575, 2000.
doi: 10.1038/35014615.
- S. J. Choi, J.-H. Han, and G. D. Roodman. ADAM8: A novel osteoclast stimulating factor. *J. Bone Miner. Res.*, 16:814–822, 2001.
doi: 10.1359/jbmr.2001.16.5.814.
- G. A. Churchill and R. W. Doerge. Empirical threshold values for quantitative trait mapping. *Genetics*, 138:963–971, 1994.
- S. E. Churchill. Particulate versus integrated evolution of the upper body in late Pleistocene humans: a test of two models. *Am. J. Phys. Anthropol.*, 100:559–583, 1996.
doi: 10.1002/(sici)1096-8644(199608)100:4<559::aid-ajpa9>3.0.co;2-l.
- B. C. Clark and T. M. Manini. Sarcopenia ≠ dynapenia. *J. Gerontol. A Biol. Sci. Med. Sci.*, 63:829–834, 2008.
- G. M. Clarke, K. W. Carter, L. J. Palmer, A. P. Morris, and L. R. Cardon. Fine mapping versus replication in whole-genome association studies. *Am. J. Hum. Genet.*, 81:995–1005, 2007.
doi: 10.1086/521952.
- C. Cotsapas, E. K. Speliotes, I. J. Hatoum, D. M. Greenawalt, R. Dobrin, P. Y. Lum, C. Suver, E. Chudin, D. Kemp, M. Reitman, B. F. Voight, B. M. Neale, E. E. Schadt, J. N. Hirschhorn, L. M. Kaplan, M. J. Daly, and GIANT consortium. Common body mass index-associated variants confer risk of extreme obesity. *Hum. Mol. Genet.*, 18:3502–3507, 2009.
doi: 10.1093/hmg/ddp292.
- N. Cox, E. Gamazon, S. Das, N. Rasouli, P. Kern, and S. Elbein. Looking for genes in all the wrong places? Platform presentation at the 60th Meeting of the American Society of Human Genetics, Washington, District of Columbia, November 2010.
- A. J. Cruz-Jentoft, J. P. Baeyens, J. M. Bauer, Y. Boirie, T. Cederholm, F. Landi, F. C. Martin, J.-P. Michel, Y. Rolland, S. M. Schneider, E. Topinková, M. Vandewoude, and M. Zamboni. Sarcopenia: European consensus on definition and diagnosis: Report of the European Working Group on Sarcopenia in Older People. *Age Ageing*, 39:412–423, 2010.
doi: 10.1093/ageing/afq034.

- T. F. Day, X. Guo, L. Garrett-Beal, and Y. Yang. Wnt/ β -catenin signaling in mesenchymal progenitors controls osteoblast and chondrocyte differentiation during vertebrate skeletogenesis. *Dev. Cell*, 8:739–750, 2005.
doi: 10.1016/j.devcel.2005.03.016.
- C. De Laet, J. A. Kanis, A. Odén, H. Johanson, O. Johnell, P. Delmas, J. A. Eisman, H. Kroger, S. Fujiwara, P. Garnero, E. V. McCloskey, D. Mellstrom, L. J. Melton, P. J. Meunier, H. A. P. Pols, J. Reeve, A. Silman, and A. Tenenhouse. Body mass index as a predictor of fracture risk: a meta-analysis. *Osteoporos. Int.*, 16:1330–1338, 2005.
doi: 10.1007/s00198-005-1863-y.
- S. Demissie, J. Dupuis, L. A. Cupples, T. J. Beck, D. P. Kiel, and D. Karasik. Proximal hip geometry is linked to several chromosomal regions: genome-wide linkage results from the Framingham Osteoporosis Study. *Bone*, 40:743–750, 2007.
doi: dx.doi.org/10.1016/j.bone.2006.09.020.
- H.-W. Deng, M. C. Mahaney, J. T. Williams, J. Li, T. Conway, K. M. Davies, J.-L. Li, H. Deng, and R. R. Recker. Relevance of the genes for bone mass variation to susceptibility to osteoporotic fractures and its implications to gene search for complex human diseases. *Genet. Epidemiol.*, 22:12–25, 2001.
doi: 10.1002/gepi.1040.
- H.-W. Deng, F.-H. Xu, Q.-Y. Huang, H. Shen, H. Deng, T. Conway, Y.-J. Liu, Y.-Z. Liu, J.-L. Li, H.-T. Zhang, K. M. Davies, and R. R. Recker. A whole-genome linkage scan suggests several genomic regions potentially containing quantitative trait loci for osteoporosis. *J. Clin. Endocrinol. Metab.*, 87:5151–5159, 2002.
doi: dx.doi.org/10.1210/jc.2002-020474.
- J. M. Devaney, L. L. Tosi, D. T. Fritz, H. A. Gordish-Dressman, S. Jiang, F. E. Orkunoglu-Suer, A. H. Gordon, B. T. Harmon, P. D. Thompson, P. M. Clarkson, T. J. Angelopoulos, P. M. Gordon, N. M. Moyna, L. S. Pescatello, P. S. Visich, R. F. Zoeller, C. Brandoli, E. P. Hoffman, and M. B. Rogers. Differences in fat and muscle mass associated with a functional human polymorphism in a post-transcriptional *BMP2* gene regulatory element. *J. Cell. Biochem.*, 107:1073–1082, 2009.
doi: 10.1002/jcb.22209.
- B. Devlin and K. Roeder. Genomic control for association studies. *Biometrics*, 55:997–1004, 1999.
doi: 10.1111/j.0006-341x.1999.00997.x.
- R. Dorajoo, A. I. F. Blakemore, X. Sim, R. T.-H. Ong, D. P. K. Ng, M. Seielstad, T.-Y. Wong, S.-M. Saw, P. Froguel, J. Liu, and E.-S. Tai. Replication of 13 obesity loci among Singaporean Chinese, Malay and Asian-Indian populations. *Int. J. Obes.* (London), in press, 2011.
doi: 10.1038/ijo.2011.86.
- E. L. Duncan, P. Danoy, J. P. Kemp, P. J. Leo, E. McCloskey, G. C. Nicholson, R. Eastell, R. L. Prince, J. A. Eisman, G. Jones, P. N. Sambrook, I. R. Reid, E. M. Dennison, J. Wark, J. B. Richards, A. G. Uitterlinden, T. D. Spector, C. Esapa, R. D. Cox, S. D. M. Brown, R. V. Thakker, K. A. Addison, L. A. Bradbury, J. R. Center, C. Cooper, C. Cremin, K. Estrada, D. Felsenberg, C.-C. Glüer, J. Hadler, M. J. Henry, A. Hofman, M. A. Kotowicz, J. Makovey, S. C. Nguyen, T. V. Nguyen, J. A. Pasco, K. Pryce, D. M. Reid, F. Rivadeneira, C. Roux, K. Stefansson, U. Styrkarsdottir, G. Thorleifsson, R. Tichawangana, D. M. Evans, and M. A. Brown. Genome-wide association study using extreme truncate selection identifies novel genes affecting bone mineral density and fracture risk. *PLoS Genet.*, 7:e1001372, 2011.
doi: 10.1371/journal.pgen.1001372.
- V. Dvornyk, X.-H. Liu, H. Shen, S. F. Lei, L. J. Zhao, Q.-R. Huang, Y.-J. Qin, D.-K. Jiang, J.-R. Long, Y.-Y. Zhang, G. Gong, R. R. Recker, and H. W. Deng. Differentiation of Caucasians and Chinese at bone mass candidate genes: implication for ethnic difference of bone mass. *Ann. Hum. Genet.*, 67:216–227, 2003.
doi: 10.1046/j.1469-1809.2003.00037.x.
- M. P. Epstein, W. L. Duren, and M. Boehnke. Improved inference of relationship for pairs of individuals. *Am. J. Hum. Genet.*, 67:1219–31, 2000.
doi: 10.1016/s0002-9297(07)62952-8.

K. Estrada, E. Evangelou, Y.-H. Hsu, U. Styrkársdóttir, C.-T. Liu, A. Moayyeri, S. Kaptoge, E. Duncan, N. Amin, D. Kiel, D. Karasik, O. Albagha, M. Brown, C. M. Kammerer, M. C. Zillikens, C. Ohlsson, G. Porleifsson, J. Reeve, L. Vandenput, R. L. Minster, A. G. Uitterlinden, L. M. Yerges-Armstrong, J. B. Richards, N. Glazer, A. Kung, D. Koller, K. Stefansson, J. Ioannidis, S. Ralston, and F. Rivadeneira for the GEFOS and AOGC Consortia. Meta-analysis of genome-wide association studies for bone-mineral-density (BMD) identifies 34 loci regulating BMD and a novel locus for fracture risk. Platform presentation at the 60th Annual Meeting of the American Society of Human Genetics, Washington, District of Columbia, November 2010a.

K. Estrada, G. Porleifsson, E. Evangelou, D. L. Koller, J. B. Richards, L. M. Yerges-Armstrong, L. Vandenput, N. Amin, N. Glazer, O. Albagha, R. L. Minster, S. Kaptoge, S. Xiao, Y.-H. Hsu, A. Uitterlinden, A. Kung, C. M. Kammerer, C. Ohlsson, C. M. van Duijn, D. Evans, D. Karasik, D. Kiel, E. Streeten, E. Duncan, J. Cauley, J. Wilson, J. Robbins, J. Reeve, M. C. Zillikens, M. Brown, M. Lorentzon, M. J. Eacons, M. Peacock, P. Sham, S. Ralston, T. Harris, T. Spector, U. Porsteinsdóttir, Y. Liu, J. Ioannidis, U. Styrkársdóttir, and F. Rivadeneira for the GEFOS and AOGC Consortia. Meta-analysis of genome-wide association studies identify 34 loci that regulate BMD with evidence of both site specific and generalized effects. Oral presentation at the 2010 Annual Meeting of the American Society for Bone and Mineral Research, Toronto, Ontario, October 2010b.

K. Estrada, E. Evangelou, Y.-H. Hsu, U. Styrkársdóttir, C.-T. Liu, A. Moayyeri, S. Kaptoge, E. Duncan, N. Amin, D. Kiel, D. Karasik, O. M. Albagha, M. Brown, T. D. Spector, M. C. Zillikens, C. Ohlsson, G. Porleifsson, J. Reeve, L. Vandenput, U. Pettersson, T. O'Neill, J. A. Riancho, O. Ljunggren, F. Rousseau, W. D. Leslie, B. Obermayer-Pietsch, N. Alonso, B. Langdahl, X. Nogués, R. Prince, P. Lips, S. Cheng, J. Marc, P. Kollia, M. L. Brandi, L. Hocking, E. Khusnutdina, C. Cooper, T. Lehtimäki, R. Jackson, J.-M. Koh, R. L. Minster, L. M. Yerges-Armstrong, B. Richards, N. Glazer, A. Kung, D. Koller, D. Evans, J. Ioannidis, S. H. Ralston, A. G. Uitterlinden, and F. Rivadeneira for the AOGC, GEFOS and GENOMOS Consortia. Association analyses of 47,500 individuals identifies six fracture loci and 82 bmd loci clustering in biological pathways that regulate osteoblast and osteoclast activity. Oral presentation at the 3rd Joint Meeting of the European Calcified Tissue Society and the International Bone and Mineral Society, Athens, Greece, May 2011.

B. S. Everitt, S. Landau, and M. Leese. *Cluster Analysis*. Arnold, London, 4th edition, 2001.

S. L. Ferrari, S. Deutsch, U. Choudhury, T. Chevalley, J.-P. Bonjour, E. T. Dermizakis, R. Rizzoli, and S. E. Antonarakis. Polymorphisms in the low-density lipoprotein receptor-related protein 5 (*LRP5*) gene are associated with variation in vertebral bone mass, vertebral bone size, and stature in whites. *Am. J. Hum. Genet.*, 74:866–875, 2004.
doi: [dx.doi.org/10.1086/420771](https://doi.org/10.1086/420771).

C. S. Fox, N. Heard-Costa, L. A. Cupples, J. Dupuis, R. S. Vasan, and L. D. Atwood. Genome-wide association to body mass index and waist circumference: the Framingham Heart Study 100K project. *BMC Med. Genet.*, 8(Suppl 1):S18, 2007.
doi: [10.1186/1471-2350-8-s1-s18](https://doi.org/10.1186/1471-2350-8-s1-s18).

T. M. Frayling, N. J. Timpson, M. N. Weedon, E. Zeggini, R. M. Freathy, C. M. Lindgren, J. R. B. Perry, K. S. Elliott, H. Lango, N. W. Rayner, B. Shields, L. W. Harries, J. C. Barrett, S. Ellard, C. J. Groves, B. Knight, A.-M. Patch, A. R. Ness, S. Ebrahim, D. A. Lawlor, S. M. Ring, Y. Ben-Shlomo, M.-R. Jarvelin, U. Sovio, A. J. Bennett, D. Melzer, L. Ferrucci, R. J. F. Loos, I. Barroso, N. J. Wareham, F. Karpe, K. R. Owen, L. R. Cardon, M. Walker, G. A. Hitman, C. N. A. Palmer, A. S. F. Doney, A. D. Morris, G. Davey Smith, A. T. Hattersley, and M. I. McCarthy. A common variant in the *FTO* gene is associated with body mass index and predisposes to childhood and adult obesity. *Science*, 316:889–894, 2007.
doi: [10.1126/science.1141634](https://doi.org/10.1126/science.1141634).

K. A. Frazer, D. G. Ballinger, D. R. Cox, D. A. Hinds, L. L. Stuve, R. A. Gibbs, J. W. Belmont, A. Boudreau, P. Hardenbol, S. M. Leal, S. Pasternak, D. A. Wheeler, T. D. Willis, F. Yu, H. Yang, C. Zeng, Y. Gao, H. Hu, W. Hu, C. Li, W. Lin, S. Liu, H. Pan, X. Tang, J. Wang, W. Wang, J. Yu, B. Zhang, Q. Zhang, H. Zhao, H. Zhao, J. Zhou, S. B. Gabriel, R. Barry, B. Blumenstiel, A. Camargo, M. Defelice, M. Faggart, M. Goyette, S. Gupta, J. Moore, H. Nguyen, R. C. Onofrio, M. Parkin, J. Roy, E. Stahl, E. Winchester, L. Ziaugra, D. Altshuler, Y. Shen, Z. Yao, W. Huang, X. Chu, Y. He, L. Jin, Y. Liu, Y. Shen, W. Sun, H. Wang, Y. Wang, Y. Wang, X. Xiong, L. Xu, M. M. Y. Waye, S. K. W. Tsui, H. Xue, J. T.-F. Wong, L. M. Galver, J.-B. Fan, K. Gunderson, S. S. Murray, A. R. Oliphant, M. S. Chee, A. Montpetit, F. Chagnon, V. Ferretti, M. Leboeuf, J.-F. Olivier, M. S. Phillips, S. Roumy, C. Sallée, A. Verner, T. J. Hudson, P.-Y. Kwok, D. Cai, D. C. Koboldt, R. D. Miller, L. Pawlikowska, P. Taillon-Miller, M. Xiao, L.-C. Tsui, W. Mak, Y.-Q. Song, P. K. H. Tam, Y. Nakamura, T. Kawaguchi, T. Kitamoto, T. Morizono, A. Nagashima, Y. Ohnishi, A. Sekine, T. Tanaka, T. Tsunoda, P. Deloukas, C. P. Bird, M. Delgado, E. T. Dermitzakis, R. Gwilliam, S. Hunt, J. Morrison, D. Powell, B. E. Stranger, P. Whittaker, D. R. Bentley, M. J. Daly, P. I. W. de Bakker, J. Barrett, Y. R. Chretien, J. Maller, S. McCarroll, N. Patterson, I. Peèr, A. Price, S. Purcell, D. J. Richter, P. Sabeti, R. Saxena, S. F. Schaffner, P. C. Sham, P. Varilly, D. Altshuler, L. D. Stein, L. Krishnan, A. V. Smith, M. K. Tello-Ruiz, G. A. Thorisson, A. Chakravarti, P. E. Chen, D. J. Cutler, C. S. Kashuk, S. Lin, G. R. Abecasis, W. Guan, Y. Li, H. M. Munro, Z. S. Qin, D. J. Thomas, G. McVean, A. Auton, L. Bottolo, N. Cardin, S. Eyheramendy, C. Freeman, J. Marchini, S. Myers, C. Spencer, M. Stephens, P. Donnelly, L. R. Cardon, G. Clarke, D. M. Evans, A. P. Morris, B. S. Weir, T. Tsunoda, J. C. Mullikin, S. T. Sherry, M. Feolo, A. Skol, H. Zhang, C. Zeng, H. Zhao, I. Matsuda, Y. Fukushima, D. R. Macer, E. Suda, C. N. Rotimi, C. A. Adebamowo, I. Ajayi, T. Aniagwu, P. A. Marshall, C. Nkwodimmah, C. D. M. Royal, M. F. Leppert, M. Dixon, A. Peiffer, R. Qiu, A. Kent, K. Kato, N. Niikawa, I. F. Adewole, B. M. Knoppers, M. W. Foster, E. W. Clayton, J. Watkin, R. A. Gibbs, J. W. Belmont, D. Muzny, L. Nazareth, E. Sodergren, G. M. Weinstock, D. A. Wheeler, I. Yakub, S. B. Gabriel, R. C. Onofrio, D. J. Richter, L. Ziaugra, B. W. Birren, M. J. Daly, D. Altshuler, R. K. Wilson, L. L. Fulton, J. Rogers, J. Burton, N. P. Carter, C. M. Clee, M. Griffiths, M. C. Jones, K. McLay, R. W. Plumb, M. T. Ross, S. K. Sims, D. L. Willey, Z. Chen, H. Han, L. Kang, M. Godbout, J. C. Wallenburg, P. L'Archevêque, G. Bellemare, K. Saeki, H. Wang, D. An, H. Fu, Q. Li, Z. Wang, R. Wang, A. L. Holden, L. D. Brooks, J. E. McEwen, M. S. Guyer, V. Ota Wang, J. L. Peterson, M. Shi, J. Spiegel, L. M. Sung, L. F. Zacharia, F. S. Collins, K. Kennedy, R. Jamieson, and J. Stewart for the International HapMap Consortium. A second generation human haplotype map of over 3.1 million SNPs. *Nature*, 449:851–861, 2007.
doi: 10.1038/nature06258.

H. M. Frost. Bone's mechanostat: a 2003 update. *Anat. Rec. A Discov. Mol. Cell Evol. Biol.*, 275:1081–1101, 2003.

H. M. Frost and E. Schönau. The “muscle-bone unit” in children and adolescents: a 2000 overview. *J. Pediatr. Endocrinol. Metab.*, 13:571–590, 2000.

W. J. Gauderman and J. M. Morrison. *QUANTO 1.1: A Computer Program for Power and Sample Size Calculations for Genetic-Epidemiology Studies*, 2006.
hydra.usc.edu/gxe.

E. Ginsburg, T. Škarić-Jurić, E. Kobylansky, I. Malkin, and P. Rudan. Evidence on major gene control of cortical index in pedigree data from Middle Dalmatia, Croatia. *Am. J. Hum. Biol.*, 13:398–408, 2001.
doi: 10.1002/ajhb.1064.

S. Giroux, L. Elfassihi, V. Clément, J. Bussièrès, A. Bureau, D. E. C. Cole, and F. Rousseau. High-density polymorphisms analysis of 23 candidate genes for association with bone mineral density. *Bone*, 47:975–981, 2010.
doi: 10.1016/j.bone.2010.06.030.

D. A. Glass, P. Bialek, J. D. Ahn, M. Starbuck, M. S. Patel, H. Clevers, M. M. Taketo, F. Long, A. P. McMahon, R. A. Lang, and G. Karsenty. Canonical Wnt signaling in differentiated osteoblasts controls osteoclast differentiation. *Dev. Cell*, 8: 751–764, 2005.
doi: 10.1016/j.devcel.2005.02.017.

H. S. Glauber, W. M. Vollmer, M. C. Nevitt, E. K. E, and E. S. Orwoll. Body weight versus body fat distribution, adiposity, and frame size as predictors of bone density. *J. Clin. Endocrinol. Metab.*, 80:1118–1123, 1995.
doi: 10.1210/jc.80.4.1118.

- Y. Gluzman. SV40-transformed simian cells support the replication of early SV40 mutants. *Cell*, 23:175–182, 1981.
- S. Gnudi, E. Sitta, and L. Lisi. Relationship of body mass index with main limb fragility fractures in postmenopausal women. *J. Bone Miner. Metab.*, 27:479–484, 2009.
doi: 10.1007/s00774-009-0056-8.
- B. H. Goodpaster, S. W. Park, T. B. Harris, S. B. Kritchevsky, M. Nevitt, A. V. Schwartz, E. M. Simonsick, F. A. Tylavsky, M. Visser, and A. B. Newman. The loss of skeletal muscle strength, mass, and quality in older adults: the Health, Aging and Body Composition Study. *J. Gerontol. A Biol. Sci. Med. Sci.*, 61:1059–1064, 2006.
- A. Graebe, E. L. Schuck, P. Lensing, L. Putcha, and H. Derendorf. Physiological, pharmacokinetic, and pharmacodynamic changes in space. *J. Clin. Pharmacol.*, 44:837–853, 2004.
doi: 10.1177/0091270004267193.
- S. Granholm, P. Lundberg, and U. H. Lerner. Calcitonin inhibits osteoclast formation in mouse haematopoietic cells independently of transcriptional regulation by receptor activator of NF- κ B and c-Fms. *J. Endocrinol.*, 195:415–427, 2007.
doi: 10.1677/joe-07-0338.
- L. Grgurevic, B. Macek, M. Mercep, M. Jelic, T. Smoljanovic, I. Erjavec, I. Dumic-Cule, S. Prgomet, D. Durdevic, D. Vnuk, M. Lipar, M. Stejskal, V. Kufner, J. Brkljacic, D. Maticic, and S. Vukicevic. Bone morphogenetic protein (BMP)1-3 enhances bone repair. *Biochem. Biophys. Res. Commun.*, 408:25–31, 2011.
doi: 10.1016/j.bbrc.2011.03.109.
- Y. Guo, L.-J. Tan, S.-F. Lei, T.-L. Yang, X.-D. Chen, F. Zhang, Y. Chen, F. Pan, H. Yan, X. Liu, Q. Tian, Z.-X. Zhang, Q. Zhou, C. Qiu, S.-S. Dong, X.-H. Xu, Y.-F. Guo, X.-Z. Zhu, S.-L. Liu, X.-L. Wang, X. Li, Y. Luo, L.-S. Zhang, M. Li, J.-T. Wang, T. Wen, B. Drees, J. Hamilton, C. J. Papasian, R. R. Recker, X.-P. Song, J. Cheng, and H.-W. Deng. Genome-wide association study identifies *ALDH7A1* as a novel susceptibility gene for osteoporosis. *PLoS Genet.*, 6:e1000806, 2010a.
doi: 10.1371/journal.pgen.1000806.
- Y. Guo, L.-S. Zhang, T.-L. Yang, Q. Tian, D.-H. Xiong, Y.-F. Pei, and H.-W. Deng. *IL21R* and *PTH* may underlie variation of femoral neck bone mineral density as revealed by a genome-wide association study. *J. Bone Miner. Res.*, 25:1042–1048, 2010b.
doi: 10.1359/jbmr.091040.
- M. Gupta, C. L. Cheung, Y. H. Hsu, S. Demissie, L. A. Cupples, D. P. Kiel, and D. Karasik. Identification of homogenous genetic architecture of multiple genetically correlated traits by block clustering of genome-wide associations. *J. Bone Miner. Res.*, 26:1261–1271, 2011.
doi: 10.1002/jbmr.333.
- R. Ha-Vinh, Y. Alanay, R. A. Bank, A. B. Campos-Xavier, A. Zankl, A. Superti-Furga, and L. Bonafé. Phenotypic and molecular characterization of Bruck syndrome (osteogenesis imperfecta with contractures of the large joints) caused by a recessive mutation in *PLOD2*. *Am. J. Med. Genet. A*, 131A:115–120, 2004.
doi: 10.1002/ajmg.a.30231.
- M. Harris, T. V. Nguyen, G. M. Howard, P. J. Kelly, and J. A. Eisman. Genetic determinants of bone mass in adults: a twin study. *Bone*, 22:141–145, 1998.
doi: 10.1016/s8756-3282(97)00252-4.

N. L. Heard-Costa, M. C. Zillikens, K. L. Monda, A. Johansson, T. B. Harris, M. Fu, T. Haritunians, M. F. Feitosa, T. Aspelund, G. Eiriksdottir, M. Garcia, L. J. Launer, A. V. Smith, B. D. Mitchell, P. F. McArdle, A. R. Shuldiner, S. J. Bielinski, E. Boerwinkle, F. Brancati, E. W. Demerath, J. S. Pankow, A. M. Arnold, Y.-D. I. Chen, N. L. Glazer, B. McKnight, B. M. Psaty, J. I. Rotter, N. Amin, H. Campbell, U. Gyllensten, C. Pattaro, P. P. Pramstaller, I. Rudan, M. Struchalin, V. Vitart, X. Gao, A. Kraja, M. A. Province, Q. Zhang, L. D. Atwood, J. Dupuis, J. N. Hirschhorn, C. E. Jaquish, C. J. O'Donnell, R. S. Vasan, C. C. White, Y. S. Aulchenko, K. Estrada, A. Hofman, F. Rivadeneira, A. G. Uitterlinden, J. C. M. Witteman, B. A. Oostra, R. C. Kaplan, V. Gudnason, J. R. O'Connell, I. B. Borecki, C. M. van Duijn, L. A. Cupples, C. S. Fox, and K. E. North. *NRXN3* is a novel locus for waist circumference: A genome-wide association study from the CHARGE Consortium. *PLoS Genet.*, 5:e1000539, 2009.
doi: 10.1371/journal.pgen.1000539.

S. C. Heath. Markov chain Monte Carlo segregation and linkage analysis for oligogenic models. *Am. J. Hum. Genet.*, 61: 748–60, 1997.
doi: 10.1086/515506.

T. Hill and P. Lewicki. *STATISTICS Methods and Applications*. StatSoft, Tulsa, 2007.
www.statsoft.com/textbook.

T. P. Hill, D. Später, M. M. Taketo, W. Birchmeier, and C. Hartmann. Canonical wnt/ β -catenin signaling prevents osteoblasts from differentiating into chondrocytes. *Dev. Cell*, 8:727–738, 2005.
doi: 10.1016/j.devcel.2005.02.013.

A. Hinney, T. T. Nguyen, A. Scherag, S. Friedel, G. Brönnner, T. D. Müller, H. Grallert, T. Illig, H.-E. Wichmann, W. Rief, H. Schäfer, and J. Hebebrand. Genome wide association (GWA) study for early onset extreme obesity supports the role of fat mass and obesity associated gene (*FTO*) variants. *PLoS ONE*, 2:e1361, 2007.
doi: 10.1371/journal.pone.0001361.

T. J. Hoffmann, N. J. Marini, and J. S. Witte. Comprehensive approach to analyzing rare genetic variants. *PLoS ONE*, 5: e13584, 2010.
doi: 10.1371/journal.pone.0013584.

P. Holmans, E. K. Green, J. Singh Pahwa, M. A. R. Ferreira, S. M. Purcell, P. Sklar, M. J. Owen, M. C. O'Donovan, and N. Craddock. Gene ontology analysis of GWA study data sets provides insights into the biology of bipolar disorder. *Am. J. Hum. Genet.*, 85:13–24, 2009.
doi: 10.1016/j.ajhg.2009.05.011.

D. R. Hopkins, S. Keles, and D. S. Greenspan. The bone morphogenetic protein 1/Tolloid-like metalloproteinases. *Matrix Biol.*, 26:508–523, 2007.
doi: 10.1016/j.matbio.2007.05.004.

F.-C. Hsu, L. Lenchik, B. J. Nicklas, K. Lohman, T. C. Register, J. Mychaleckyj, C. D. Langefeld, B. I. Freedman, D. W. Bowden, and J. J. Carr. Heritability of body composition measured by DXA in the Diabetes Heart Study. *Obesity*, 13: 312–319, 2005.
doi: 10.1038/oby.2005.42.

H. Hsu, M. C. Zillikens, S. G. Wilson, C. R. Farber, S. Demissie, N. Soranzo, E. N. Bianchi, E. Grundberg, L. Liang, J. B. Richards, K. Estrada, Y. Zhou, A. van Nas, M. F. Moffatt, G. Zhai, A. Hofman, J. B. van Meurs, H. A. P. Pols, R. I. Price, O. Nilsson, T. Pastinen, L. A. Cupples, A. J. Lusis, E. E. Schadt, S. Ferrari, A. G. Uitterlinden, F. Rivadeneira, T. D. Spector, D. Karasik, and D. P. Kiel. An integration of genome-wide association study and gene expression profiling to prioritize the discovery of novel susceptibility loci for osteoporosis-related traits. *PLoS Genet.*, 6:e1000977, 2010.
doi: 10.1371/journal.pgen.1000977.

M. R. Hughes, P. J. Malloy, D. G. Kieback, R. A. Kesterson, J. W. Pike, D. Feldman, and B. W. O'Malley. Point mutations in the human vitamin D receptor gene associated with hypocalcemic rickets. *Science*, 242:1702–1705, 1988.
doi: 10.1126/science.2849209.

W. Huygens, M. A. Thomis, M. W. Peeters, R. F. Vlietinck, and G. P. Beunen. Determinants and upper-limit heritabilities of skeletal muscle mass and strength. *Can. J. Appl. Physiol.*, 29:186–200, 2004.

M. Iannuzzi-Sucich, K. M. Prestwood, and A. M. Kenny. Prevalence of sarcopenia and predictors of skeletal muscle mass in healthy, older men and women. *J. Gerontol. A Biol. Sci. Med. Sci.*, 57:M772–M777, 2002.
doi: 10.1093/gerona/57.12.m772.

S. Ichikawa, D. L. Koller, L. R. Padgett, D. Lai, S. L. Hui, M. Peacock, T. Foroud, and M. J. Econs. Replication of previous genome-wide association studies of bone mineral density in premenopausal American women. *J. Bone Miner. Res.*, 25: 1821–1829, 2010.
doi: 10.1002/jbmr.62.

J. P. A. Ioannidis, I. Stavrou, T. A. Trikalinos, C. Zois, M. L. Brandi, L. Gennari, O. Albagha, S. H. Ralston, and A. Tsatsoulis. Association of polymorphisms of the estrogen receptor α gene with bone mineral density and fracture risk in women: A meta-analysis. *J. Bone Miner. Res.*, 17:2048–2060, 2002.
doi: 10.1359/jbmr.2002.17.11.2048.

J. P. A. Ioannidis, M. Y. Ng, P. C. Sham, E. Zintzaras, C. M. Lewis, H.-W. Deng, M. J. Econs, D. Karasik, M. Devoto, C. M. Kammerer, T. Spector, T. Andrew, L. A. Cupples, E. L. Duncan, T. Foroud, D. P. Kiel, D. Koller, B. Langdahl, B. D. Mitchell, M. Peacock, R. Recker, H. Shen, K. Sol-Church, L. D. Spotila, A. G. Uitterlinden, S. G. Wilson, A. W. C. Kung, and S. H. Ralston. Meta-analysis of genome-wide scans provides evidence for sex- and site-specific regulation of bone mass. *J. Bone Miner. Res.*, 22:173–183, 2007.
doi: 10.1359/jbmr.060806.

H. Ishizuka, V. García-Palacios, G. Lu, M. A. Subler, H. Zhang, C. S. Boykin, S. J. Choi, L. Zhao, K. Patrene, D. L. Galson, H. C. Blair, T. M. Hadi, J. J. Windle, N. Kurihara, and G. D. Roodman. ADAM8 enhances osteoclast precursor fusion and osteoclast formation in vitro and in vivo. *J. Bone Miner. Res.*, 26:169–181, 2010.
doi: 10.1002/jbmr.199.

F. C. Jensen, A. J. Girardi, R. V. Gilden, and H. Koprowski. Infection of human and simian tissue cultures with Rous sarcoma virus. *Proc. Natl Acad. Sci. U.S.A.*, 52:53–59, 1964.

O. Johnell and J. A. Kanis. An estimate of the worldwide prevalence and disability associated with osteoporotic fractures. *Osteoporos. Int.*, 17:1726–1733, 2006.
doi: 10.1007/s00198-006-0172-4.

M. L. Johnson, G. Gong, W. Kimberling, S. M. Reckér, D. B. Kimmel, and R. B. Recker. Linkage of a gene causing high bone mass to human chromosome 11 (11q12–13). *Am. J. Hum. Genet.*, 60:1326–1332, 1997.
doi: dx.doi.org/10.1086/515470.

J. A. Kanis, L. J. Melton, C. Christiansen, C. C. Johnston, and N. Khaltaev. The diagnosis of osteoporosis. *J. Bone Miner. Res.*, 9:1137–1141, 1994.
doi: 10.1002/jbmr.5650090802.

D. Karasik and D. P. Kiel. Genetics of the musculoskeletal system: a pleiotropic approach. *J. Bone Miner. Res.*, 23:788–802, 2008.
doi: 10.1359/jbmr.080218.

D. Karasik, E. Ginsburg, G. Livshits, O. Pavlovsky, and E. Kobylansky. Evidence of major gene control of cortical bone loss in humans. *Genet. Epidemiol.*, 19:410–421, 2000.
doi: 10.1002/1098-2272(200012)19:4<410::aid-gepi11>3.0.co;2-k.

D. Karasik, L. A. Cupples, M. T. Hannan, and D. P. Kiel. Genome screen for a combined bone phenotype using principal component analysis: the Framingham study. *Bone*, 34:547–556, 2004.
doi: 10.1016/j.bone.2003.11.017.

- D. Karasik, Y. Zhou, L. A. Cupples, M. T. Hannan, D. P. Kiel, and S. Demissie. Bivariate genome-wide linkage analysis of femoral bone traits and leg lean mass: Framingham Study. *J. Bone Miner. Res.*, 24:710–718, 2009.
doi: 10.1359/jbmr.081222.
- D. Karasik, Y.-H. Hsu, Y. Zhou, L. A. Cupples, D. P. Kiel, and S. Demissie. Genome-wide pleiotropy of osteoporosis-related phenotypes: the Framingham Study. *J. Bone Miner. Res.*, 25:1555–1563, 2010.
doi: 10.1002/jbmr.38.
- H. Z. Ke, H. Qi, A. F. Weidema, Q. Zhang, N. Panupinthu, D. T. Crawford, W. A. Grasser, V. M. Paralkar, M. Li, L. P. Audoly, C. A. Gabel, W. S. S. Jee, S. J. Dixon, S. M. Sims, and D. D. Thompson. Deletion of the P2X₇ nucleotide receptor reveals its regulatory roles in bone formation and resorption. *Mol. Endocrinol.*, 17(7):1356–1367, 2003.
doi: 10.1210/me.2003-0021.
- D. E. Kelley, B. S. Slasky, and J. Janosky. Skeletal muscle density: effects of obesity and non-insulin-dependent diabetes mellitus. *Am. J. Clin. Nutr.*, 54:509–515, 1991.
- D. P. Kiel, S. Demissie, J. Dupuis, K. L. Lunetta, J. M. Murabito, and D. Karasik. Genome-wide association with bone mass and geometry in the Framingham Heart Study. *BMC Med. Genet.*, 8(Suppl. 1):S14, 2007.
doi: 10.1186/1471-2350-8-s1-s14.
- K. Kim, B. Perroud, G. Espinal, D. Kachinskas, I. Austrheim-Smith, B. M. Wolfe, and C. H. Warden. Genes and networks expressed in perioperative omental adipose tissue are correlated with weight loss from Roux-en-Y gastric bypass. *Int. J. Obes. (London)*, 32:1395–1406, 2008.
doi: 10.1038/ijo.2008.106.
- M. A. Koay, P. Y. Woon, Y. Zhang, L. J. Miles, E. L. Duncan, S. H. Ralston, J. E. Compston, C. Cooper, R. Keen, B. L. Langdahl, A. MacLelland, J. O’Riordan, H. A. Pols, D. M. Reid, A. G. Uitterlinden, J. A. Wass, and M. A. Brown. Influence of *LRP5* Polymorphisms on Normal Variation in BMD. *J. Bone Miner. Res.*, 19:1619–1627, 2004.
doi: dx.doi.org/10.1359/jbmr.040704.
- D. L. Koller, L. A. Rodriguez, J. C. Christian, C. W. Slemenda, M. J. Econs, S. L. Hui, P. Morin, P. M. Conneally, G. Joslyn, M. E. Curran, M. Peacock, C. C. Johnston, and T. Foroud. Linkage of a QTL contributing to normal variation in bone mineral density to chromosome 11q12–13. *J. Bone Miner. Res.*, 13:1903–1908, 1998.
- D. L. Koller, M. J. Econs, P. A. Morin, J. C. Christian, S. L. Hui, P. Parry, M. E. Curran, L. A. Rodriguez, P. M. Conneally, G. Joslyn, M. Peacock, C. C. Johnston, and T. Foroud. Genome screen for QTLs contributing to normal variation in bone mineral density and osteoporosis. *J. Clin. Endocrinol. Metab.*, 85:3116–3120, 2000.
doi: dx.doi.org/10.1210/jc.85.9.3116.
- D. L. Koller, G. Liu, M. J. Econs, S. L. Hui, P. A. Morin, G. Joslyn, L. A. Rodriguez, P. M. Conneally, J. C. Christian, C. C. Johnston, T. Foroud, and M. Peacock. Genome screen for quantitative trait loci underlying normal variation in femoral structure. *J. Bone Miner. Res.*, 16:985–991, 2001.
doi: 10.1359/jbmr.2001.16.6.985.
- D. L. Koller, S. Ichikawa, D. Lai, L. R. Padgett, K. F. Doheny, E. Pugh, J. Paschall, S. L. Hui, H. J. Edenberg, X. Xuei, M. Peacock, M. J. Econs, and T. Foroud. Genome-wide association study of bone mineral density in premenopausal European-American women and replication in African-American women. *J. Clin. Endocrinol. Metab.*, 95:1802–1809, 2010.
doi: 10.1210/jc.2009-1903.
- M. Koš, G. Reid, S. Denger, and F. Gannon. Genomic organization of the human ERα gene promoter region. *Mol. Endocrinol.*, 15:2057–2063, 2001.

- K. Kristjansson, A. R. Rut, M. Hewison, J. L. O'Riordan, and M. R. Hughes. Two mutations in the hormone binding domain of the vitamin D receptor cause tissue resistance to 1,25 dihydroxyvitamin D₃. *J. Clin. Invest.*, 92:12–16, 1993. doi: 10.1172/jci116539.
- J. L. Kuk, T. J. Saunders, L. E. Davidson, and R. Ross. Age-related changes in total and regional fat distribution. *Ageing Res. Rev.*, 8:339–48, 2009. doi: 10.1016/j.arr.2009.06.001.
- M. H. Kung, K. Yukata, R. J. O'Keefe, , and M. J. Zuscik. Aryl hydrocarbon receptor-mediated impairment of chondrogenesis and fracture healing by cigarette smoke and benzo(α)pyrene. *J. Cell. Physiol.*, in press, 2011. doi: 10.1002/jcp.22819.
- T.-H. Kwon, C. Fulton, W. Wang, I. Kurtz, J. Frøkiær, C. Aalkjær, and S. Nielsen. Chronic metabolic acidosis upregulates rat kidney Na–HCO₃⁻ cotransporters NBCn1 and NBC3 but not NBC1. *Am. J. Physiol. Renal Physiol.*, 282:F341–F351, 2002. doi: 10.1152/ajprenal.00104.2001.
- M. M. L. Laaksonen, T. A. Outila, M. U. M. Kärkkäinen, V. E. Kemi, H. J. Rita, M. Perola, L. M. Valsta, and C. J. E. Lamberg-Allardt. Associations of vitamin D receptor, calcium-sensing receptor and parathyroid hormone gene polymorphisms with calcium homeostasis and peripheral bone density in adult Finns. *J. Nutrigenet. Nutrigenomics*, 2:55–63, 2009. doi: 10.1159/000204960.
- A. C. Lam, M. Schouten, Y. S. Aulchenko, C. S. Haley, and D.-J. de Koning. Rapid and robust association mapping of expression quantitative trait loci. *BMC Proc.*, 1:S144, 2007.
- J. D. Lampasso, W. Chen, and N. Marzec. The expression profile of PKC isoforms during MC3T3-E1 differentiation. *Int. J. Mol. Med.*, 17:1125–1131, 2006.
- E. S. Lander and N. J. Schork. Genetic dissection of complex traits. *Science*, 265:2037–2048, 1994. doi: 10.1126/science.8091226.
- K. Lange, R. Cantor, S. Horvath, M. Perola, C. Sabatti, J. Sinsheimer, and E. Sobel. Mendel version 4.0: a complete package for the exact genetic analysis of discrete traits in pedigree and population data sets. *Am. J. Hum. Genet.*, 69 (Suppl.):504, 2001.
- D.-Y. Lee, H. Kim, S. Y. Ku, S. H. Kim, Y. M. Choi, and J. G. Kim. Association between polymorphisms in wnt signaling pathway genes and bone mineral density in postmenopausal Korean women. *Menopause*, 17:1064–1070, 2010. doi: 10.1097/gme.0b013e3181da4da3.
- N. K. Lee, H. Sowa, E. Hinoi, M. Ferron, J. D. Ahn, C. Confavreux, R. Dacquin, P. J. Mee, M. D. McKee, D. Y. Jung, Z. Zhang, J. K. Kim, F. Mauvais-Jarvis, P. Ducy, and G. Karsenty. Endocrine regulation of energy metabolism by the skeleton. *Cell*, 130:456–469, 2007. doi: 10.1016/j.cell.2007.05.047.
- S. H. Lee, J. H. J. van der Werf, B. J. Hayes, M. E. Goddard, and P. M. Visscher. Predicting unobserved phenotypes for complex traits from whole-genome SNP data. *PLoS Genet.*, 4:e1000231, 2008. doi: 10.1371/journal.pgen.1000231.t006.
- Y. H. Lee, Y. H. Rho, S. J. Choi, J. D. Ji, and G. G. Song. Meta-analysis of genome-wide linkage studies for bone mineral density. *J. Hum. Genet.*, 51:480–486, 2006. doi: 10.1007/s10038-006-0390-9.
- V. Lefebvre, W. Huang, V. R. Harley, P. N. Goodfellow, and B. de Crombrughe. SOX9 is a potent activator of the chondrocyte-specific enhancer of the Proα1(II) collagen gene. *Mol. Cell Biol.*, 17:2336–2346, 1997.

M.-M. Lei, T.-F. Yang, Z.-Q. Tu, L. Liu, Y. Fang, and G.-L. Wang. Oestrogen receptor- α polymorphism and risk of fracture: a meta-analysis of 13 studies including 1279 cases and 6069 controls. *J. Int. Med. Res.*, 38:1575–1583, 2010.

S.-F. Lei, Y.-Y. Zhang, F.-Y. Deng, M.-Y. Liu, X.-H. Liu, X.-G. Zhou, and H.-W. Deng. Bone mineral density and five prominent candidate genes in Chinese men: associations, interaction effects and their implications. *Maturitas*, 51:199–206, 2005.

doi: 10.1016/j.maturitas.2004.08.001.

E. S. Leib, E. M. Lewiecki, N. Binkley, and R. C. Hamdy. Official positions of the International Society for Clinical Densitometry. *J. Clin. Densitom.*, 7:1–5, 2004.

doi: 10.1385/jcd:7:1:1.

B. Li and S. M. Leal. Methods for detecting associations with rare variants for common diseases: application to analysis of sequence data. *Am. J. Hum. Genet.*, 83:311–321, 2008.

doi: 10.1016/j.ajhg.2008.06.024.

M.-X. Li, P. C. Sham, S. S. Cherny, and Y.-Q. Song. A knowledge-based weighting framework to boost the power of genome-wide association studies. *PLoS ONE*, 5:e14480, 2010a.

doi: 10.1371/journal.pone.0014480.

Y. Li, C. J. Willer, J. Ding, P. Scheet, and G. R. Abecasis. MaCH: using sequence and genotype data to estimate haplotypes and unobserved genotypes. *Genet. Epidemiol.*, 34:816–34, 2010b.

doi: 10.1002/gepi.20533.

C. M. Lindgren, I. M. Heid, J. C. Randall, C. Lamina, V. Steinthorsdottir, L. Qi, E. K. Speliotes, G. Thorleifsson, C. J. Willer, B. M. Herrera, A. U. Jackson, N. Lim, P. Scheet, N. Soranzo, N. Amin, Y. S. Aulchenko, J. C. Chambers, A. Drong, J. Luan, H. N. Lyon, F. Rivadeneira, S. Sanna, N. J. Timpson, M. C. Zillikens, J. H. Zhao, P. Almgren, S. Bandinelli, A. J. Bennett, R. N. Bergman, L. L. Bonnycastle, S. J. Bumpstead, S. J. Chanock, L. Cherkas, P. Chines, L. Coin, C. Cooper, G. Crawford, A. Doering, A. Dominiczak, A. S. F. Doney, S. Ebrahim, P. Elliott, M. R. Erdos, K. Estrada, L. Ferrucci, G. Fischer, N. G. Forouhi, C. Gieger, H. Grallert, C. J. Groves, S. Grundy, C. Guiducci, D. Hadley, A. Hamsten, A. S. Havulinna, A. Hofman, R. Holle, J. W. Holloway, T. Illig, B. Isomaa, L. C. Jacobs, K. Jameson, P. Jousilahti, F. Karpe, J. Kuusisto, J. Laitinen, G. M. Lathrop, D. A. Lawlor, M. Mangino, W. L. McArdle, T. Meitinger, M. A. Morken, A. P. Morris, P. Munroe, N. Narisu, A. Nordström, P. Nordström, B. A. Oostra, C. N. A. Palmer, F. Payne, J. F. Peden, I. Prokopenko, F. Renström, A. Ruokonen, V. Salomaa, M. S. Sandhu, L. J. Scott, A. Scuteri, K. Silander, K. Song, X. Yuan, H. M. Stringham, A. J. Swift, T. Tuomi, M. Uda, P. Vollenweider, G. Waeber, C. Wallace, G. B. Walters, M. N. Weedon, J. C. M. Witteman, C. Zhang, W. Zhang, M. J. Caulfield, F. S. Collins, G. Davey Smith, I. N. M. Day, P. W. Franks, A. T. Hattersley, F. B. Hu, M.-R. Jarvelin, A. Kong, J. S. Kooner, M. Laakso, E. Lakatta, V. Mooser, A. D. Morris, L. Peltonen, N. J. Samani, T. D. Spector, D. P. Strachan, T. Tanaka, J. Tuomilehto, A. G. Uitterlinden, C. M. van Duijn, N. J. Wareham, H. Watkins, D. M. Waterworth, M. Boehnke, P. Deloukas, L. Groop, D. J. Hunter, U. Thorsteinsdottir, D. Schlessinger, H.-E. Wichmann, T. M. Frayling, G. R. Abecasis, J. N. Hirschhorn, R. J. F. Loos, K. Stefansson, K. L. Mohlke, I. Barroso, and M. I. McCarthy. Genome-wide association scan meta-analysis identifies three loci influencing adiposity and fat distribution. *PLoS Genet.*, 5:e1000508, 2009.

doi: 10.1371/journal.pgen.1000508.t001.

H. Ling, D. M. Waterworth, H. A. Stirnadel, T. I. Pollin, P. J. Barter, Y. A. Kesäniemi, R. W. Mahley, R. McPherson, G. Waeber, T. P. Bersot, J. C. Cohen, S. M. Grundy, V. E. Mooser, and B. D. Mitchell. Genome-wide linkage and association analyses to identify genes influencing adiponectin levels: The GEMS Study. *Obesity*, 17:737–744, 2009.

doi: 10.1038/oby.2008.625.

X.-G. Liu, L.-J. Tan, S.-F. Lei, Y.-J. Liu, H. Shen, L. Wang, H. Yan, Y.-F. Guo, D.-H. Xiong, X.-D. Chen, F. Pan, T.-L. Yang, Y.-P. Zhang, Y. Guo, N. L. Tang, X.-Z. Zhu, H.-Y. Deng, S. Levy, R. R. Recker, C. J. Papasian, and H.-W. Deng. Genome-wide association and replication studies identified *TRHR* as an important gene for lean body mass. *Am. J. Hum. Genet.*, 84:418–423, 2009a.

doi: 10.1016/j.ajhg.2009.02.004.

- Y.-J. Liu, F.-H. Xu, H. Shen, Y.-Z. Liu, H.-Y. Deng, L.-J. Zhao, Q.-Y. Huang, V. Dvornyk, T. Conway, K. M. Davies, J.-L. Li, R. R. Recker, and H.-W. Deng. A follow-up linkage study for quantitative trait loci contributing to obesity-related phenotypes. *J. Clin. Endocrinol. Metab.*, 89:875–882, 2004.
doi: 10.1210/jc.2003-030774.
- Y.-Z. Liu, Y.-F. Pei, J.-F. Liu, F. Yang, Y. Guo, L. Zhang, X.-G. Liu, H. Yan, L. Wang, Y.-P. Zhang, S. Levy, R. R. Recker, and H.-W. Deng. Powerful bivariate genome-wide association analyses suggest the *SOX6* gene influencing both obesity and osteoporosis phenotypes in males. *PLoS ONE*, 4:e6827, 2009b.
doi: 10.1371/journal.pone.0006827.
- K. J. Livak and T. D. Schmittgen. Analysis of relative gene expression data using real-time quantitative PCR and the $2^{-\Delta\Delta C_T}$ method. *Methods*, 25:402–408, 2001.
doi: 10.1006/meth.2001.1262.
- G. Livshits, B. S. Kato, S. G. Wilson, and T. D. Spector. Linkage of genes to total lean body mass in normal women. *J. Clin. Endocrinol. Metab.*, 92:3171–3176, 2007.
doi: dx.doi.org/10.1210/jc.2007-0418.
- R. W. Löbbert, A. Winterpacht, B. Seipel, and B. U. Zabel. Molecular cloning and chromosomal assignment of the human homologue of the rat cGMP-inhibited phosphodiesterase 1 (PDE3A)—a gene involved in fat metabolism located at 11p15.1. *Genomics*, 37:211–218, 1996.
doi: 10.1006/geno.1996.0544.
- A. C. Looker, E. S. Orwoll, C. C. Johnston, R. L. Lindsay, H. W. Wahner, W. L. Dunn, M. S. Calvo, T. B. Harris, and S. P. Heyse. Prevalence of low femoral bone density in older U.S. adults from NHANES III. *J. Bone Miner. Res.*, 12:1761–8, 1997.
doi: 10.1359/jbmr.1997.12.11.1761.
- R. J. F. Loos, C. M. Lindgren, S. Li, E. Wheeler, J. H. Zhao, I. Prokopenko, M. Inouye, R. M. Freathy, A. P. Attwood, J. S. Beckmann, S. I. Berndt, Prostate, Lung, Colorectal, and Ovarian (PLCO) Cancer Screening Trial, S. Bergmann, A. J. Bennett, S. A. Bingham, M. Bochud, M. Brown, S. Cauchi, J. M. Connell, C. Cooper, G. Davey Smith, I. Day, C. Dina, S. De, E. T. Dermizakis, A. S. F. Doney, K. S. Elliott, P. Elliott, D. M. Evans, I. S. Farooqi, P. Froguel, J. Ghorri, C. J. Groves, R. Gwilliam, D. Hadley, A. S. Hall, A. T. Hattersley, J. Hebebrand, I. M. Heid, KORA, B. Herrera, A. Hinney, S. E. Hunt, M.-R. Jarvelin, T. Johnson, J. D. M. Jolley, F. Karpe, A. Keniry, K. T. Khaw, R. N. Luben, M. Mangino, J. Marchini, W. L. McArdle, R. McGinnis, D. Meyre, P. B. Munroe, A. D. Morris, A. R. Ness, M. J. Neville, A. C. Nica, K. K. Ong, S. O’Rahilly, K. R. Owen, C. N. A. Palmer, K. Papadakis, S. Potter, A. Pouta, L. Qi, Nurses’ Health Study, J. C. Randall, N. W. Rayner, S. M. Ring, M. S. Sandhu, A. Scherag, M. A. Sims, K. Song, N. Soranzo, E. K. Speliotes, Diabetes Genetics Initiative, H. E. Syddall, S. A. Teichmann, N. J. Timpson, J. H. Tobias, M. Uda, SardiNIA Study, C. I. Ganz Vogel, C. Wallace, D. M. Waterworth, M. N. Weedon, Wellcome Trust Case Control Consortium, C. J. Willer, FUSION, Wraight, X. Yuan, E. Zeggini, J. N. Hirschhorn, D. P. Strachan, W. H. Ouwehand, M. J. Caulfield, N. J. Samani, T. M. Frayling, P. Vollenweider, G. Waeber, V. Mooser, P. Deloukas, M. I. McCarthy, N. J. Wareham, and I. Barroso. Common variants near *MC4R* are associated with fat mass, weight and risk of obesity. *Nat. Genet.*, 40:768–775, 2008.
doi: 10.1038/ng.140.
- B. E. Madsen and S. R. Browning. A groupwise association test for rare mutations using a weighted sum statistic. *PLoS Genet.*, 5:e1000384, 2009.
doi: 10.1371/journal.pgen.1000384.
- H. H. M. Maes, M. C. Neale, and L. J. Eaves. Genetic and environmental factors in relative body weight and human adiposity. *Behav. Genet.*, 27:325–351, 1997.
doi: 10.1023/a:1025635913927.
- V.-P. Mäkinen, M. Parkkonen, M. Wessman, P.-H. Groop, T. Kanninen, and K. Kaski. High-throughput pedigree drawing. *Eur. J. Hum. Genet.*, 13:987–989, 2005.
doi: 10.1038/sj.ejhg.5201430.

- S. C. Marks and P. W. Lane. Osteopetrosis, a new recessive skeletal mutation on chromosome 12 of the mouse. *J. Hered.*, 67:11–18, 1976.
- A. C. McDonald, J. A. Schuijers, P.-J. Shen, A. L. Gundlach, and B. L. Grills. Expression of galanin and galanin receptor-1 in normal bone and during fracture repair in the rat. *Bone*, 33:788–797, 2003.
doi: 10.1016/s8756-3282(03)00244-8.
- A. C. McDonald, J. A. Schuijers, A. L. Gundlach, and B. L. Grills. Galanin treatment offsets the inhibition of bone formation and downregulates the increase in mouse calvarial expression of TNF α and GalR2 mRNA induced by chronic daily injections of an injurious vehicle. *Bone*, 40:895–903, 2007.
doi: 10.1016/j.bone.2006.10.018.
- E. McPherson and M. Clemens. Bruck syndrome (osteogenesis imperfecta with congenital joint contractures): Review and report on the first North American case. *Am. J. Med. Genet.*, 70:28–31, 1997.
doi: 10.1002/(sici)1096-8628(19970502)70:1<28::aid-ajmg6>3.0.co;2-n.
- S. Mencej-Bedrač, J. Preželj, T. Kocjan, R. Komadina, and J. Marc. Analysis of association of *LRP5*, *LRP6*, *SOST*, *DKK1*, and *CTNNB1* genes with bone mineral density in a Slovenian population. *Calcif. Tissue Int.*, 85:501–506, 2009.
doi: 10.1007/s00223-009-9306-y.
- D. Meyre, J. Delplanque, J.-C. Chèvre, C. Lecoeur, S. Lobbens, S. Gallina, E. Durand, V. Vatin, F. Degraeve, C. Proença, S. Gaget, A. Körner, P. Kovacs, W. Kiess, J. Tichet, M. Marre, A.-L. Hartikainen, F. Horber, N. Potoczna, S. Hercberg, C. Levy-Marchal, F. Pattou, B. Heude, M. Tauber, M. I. McCarthy, A. I. F. Blakemore, A. Montpetit, C. Polychronakos, J. Weill, L. J. M. Coin, J. Asher, P. Elliott, M.-R. Järvelin, S. Visvikis-Siest, B. Balkau, R. Sladek, D. Balding, A. Walley, C. Dina, and P. Froguel. Genome-wide association study for early-onset and morbid adult obesity identifies three new risk loci in European populations. *Nat. Genet.*, 41:157–159, 2009.
doi: 10.1038/ng.301.
- I. Miljkovic-Gacic, R. E. Ferrell, A. L. Patrick, C. M. Kammerer, and C. H. Bunker. Estimates of African, European and Native American ancestry in Afro-Caribbean men on the island of Tobago. *Hum. Hered.*, 60:129–33, 2005.
doi: 10.1159/000089553.
- A. Moayyeri, S. Kaptoge, N. Dalzell, R. N. Luben, N. J. Wareham, S. Bingham, J. Reeve, and K. T. Khaw. The effect of including quantitative heel ultrasound in models for estimation of 10-year absolute risk of fracture. *Bone*, 45:180–184, 2009.
doi: 10.1016/j.bone.2009.05.001.
- L. S. Moniz and V. Stambolic. Nek10 mediates G₂/M cell cycle arrest and MEK autoactivation in response to UV irradiation. *Mol. Cell Biol.*, 31:30–42, 2010.
doi: 10.1128/mcb.00648-10.
- S. Morgenthaler and W. G. Thilly. A strategy to discover genes that carry multi-allelic or mono-allelic risk for common diseases: a cohort allelic sums test (CAST). *Mutat. Res.*, 615:28–56, 2007.
doi: 10.1016/j.mrfmmm.2006.09.003.
- National Osteoporosis Foundation. Fast Facts on Osteoporosis, 2008.
www.nof.org/osteoporosis/diseasefacts.htm.
- T. V. Nguyen, G. M. Howard, P. J. Kelly, and J. A. Eisman. Bone mass, lean mass, and fat mass: same genes or same environments? *Am. J. Epidemiol.*, 147:3–16, 1998.
- D. L. Nicolae, E. Gamazon, W. Zhang, S. Duan, M. E. Dolan, and N. J. Cox. Trait-associated SNPs are more likely to be eQTLs: annotation to enhance discovery from GWAS. *PLoS Genet.*, 6:e1000888, 2010.
doi: 10.1371/journal.pgen.1000888.

- J. M. Norris, C. D. Langefeld, M. E. Talbert, M. R. Wing, T. Haritunians, T. E. Fingerlin, A. J. G. Hanley, J. T. Ziegler, K. D. Taylor, S. M. Haffner, Y.-D. I. Chen, D. W. Bowden, and L. E. Wagenknecht. Genome-wide association study and follow-up analysis of adiposity traits in Hispanic Americans: the IRAS Family Study. *Obesity*, 17:1932–1941, 2009. doi: 10.1038/oby.2009.143.
- S. D. Ohlendorff, C. L. Tofteng, J.-E. B. Jensen, S. Petersen, R. Civitelli, M. Fenger, B. Abrahamsen, A. P. Hermann, P. Eiken, and N. R. Jørgensen. Single nucleotide polymorphisms in the P2X₇ gene are associated to fracture risk and to effect of estrogen treatment. *Pharmacogenet. Genomics*, 17:555–567, 2007.
- T. Okano, Y. Ishidou, M. Kato, T. Imamura, K. Yonemori, N. Origuchi, S. Matsunaga, H. Yoshida, P. ten Dijke, and T. Sakou. Orthotopic ossification of the spinal ligaments of Zucker fatty rats: A possible animal model for ossification of the human posterior longitudinal ligament. *J. Orthop. Res.*, 15:820–829, 1997. doi: 10.1002/jor.1100150606.
- V. Paracchini, P. Pedotti, and E. Taioli. Genetics of leptin and obesity: A HuGE review. *Am. J. Epidemiol.*, 162:101–114, 2005. doi: 10.1093/aje/kwi174.
- L. Paternoster, M. Lorentzon, L. Vandenput, M. K. Karlsson, Ö. Ljunggren, A. Kindmark, D. Mellstrom, J. P. Kemp, C. E. Jarett, J. M. P. Holly, A. Sayers, B. St. Pourcain, N. J. Timpson, P. Deloukas, G. Davey Smith, S. M. Ring, D. M. Evans, J. H. Tobias, and C. Ohlsson. Genome-wide association meta-analysis of cortical bone mineral density unravels allelic heterogeneity at the *RANKL* locus and potential pleiotropic effects on bone. *PLoS Genet.*, 6:e1001217, 2010. doi: 10.1371/journal.pgen.1001217.
- M. Peacock, D. L. Koller, D. Lai, S. Hui, T. Foroud, and M. J. Econs. Sex-specific quantitative trait loci contribute to normal variation in bone structure at the proximal femur in men. *Bone*, 37:467–473, 2005. doi: dx.doi.org/10.1016/j.bone.2005.05.005.
- O. M. Pearson and D. E. Lieberman. The aging of Wolff’s “Law”: ontogeny and responses to mechanical loading in cortical bone. *Am. J. Phys. Anthropol.*, 125(Suppl. 39):63–99, 2004. doi:10.1002/ajpa.20155.
- I. Peér, R. Yelensky, D. Altshuler, and M. J. Daly. Estimation of the multiple testing burden for genomewide association studies of nearly all common variants. *Genet. Epidemiol.*, 32:381–385, 2008. doi: 10.1002/gepi.20303.
- R. P. Peeters, A. W. van den Beld, H. van Toor, A. G. Uitterlinden, J. A. M. J. L. Janssen, S. W. J. Lamberts, and T. J. Visser. Increased expression of a novel osteoclast-stimulating factor, ADAM8, in interface tissue around loosened hip prostheses. *J. Rheumatol.*, 30:2033–2038, 2003.
- T. Peters, K. Ausmeier, and U. Rütter. Cloning of Fatso (*Fto*), a novel gene deleted by the Fused toes (*Ft*) mouse mutation. *Mamm. Genome*, 10:983–986, 1999.
- M. S. Phillips, Q. Liu, H. A. Hammond, V. Dugan, P. J. Hey, C. T. Caskey, and J. F. Hess. Leptin receptor missense mutation in the fatty Zucker rat. *Nat. Genet.*, 13:18–19, 1996. doi: 10.1038/ng0596-18.
- N. A. Pocock, J. A. Eisman, J. L. Hopper, M. G. Yeates, P. N. Sambrook, and S. Eberl. Genetic determinants of bone mass in adults: a twin study. *J. Clin. Invest.*, 80:706–710, 1987. doi: 10.1172/jci113125.

- O. Polašek, A. Marušić, K. Rotim, C. Hayward, V. Vitart, J. Huffman, S. Campbell, S. Janković, M. Boban, Z. Biloglav, I. Kolčić, V. Krželj, J. Terzić, L. Matec, G. Tometić, D. Nonković, J. Ninčević, M. Pehlić, J. Žedelj, V. Velagić, D. Juričić, I. Kirac, S. Belak Kovačević, A. F. Wright, H. Campbell, and I. Rudan. Genome-wide association study of anthropometric traits in Korčula Island, Croatia. *Croat. Med. J.*, 50:7–16, 2009.
doi: 10.3325/cmj.2009.50.7.
- K. E. S. Poole and J. Reeve. Parathyroid hormone—a bone anabolic and catabolic agent. *Curr. Opin. Pharmacol.*, 5: 612–617, 2005.
doi: 10.1016/j.coph.2005.07.004.
- R. L. Prince. Counterpoint: estrogen effects on calcitropic hormones and calcium homeostasis. *Endocr. Rev.*, 15:301–309, 1994.
doi: 10.1210/edrv-15-3-301.
- S. J. Prior, S. M. Roth, X. Wang, C. Kammerer, I. Miljkovic-Gacic, C. H. Bunker, V. W. Wheeler, A. L. Patrick, and J. M. Zmuda. Genetic and environmental influences on skeletal muscle phenotypes as a function of age and sex in large, multigenerational families of African heritage. *J. Appl. Physiol.*, 103:1121–1127, 2007.
doi: 10.1152/jappphysiol.00120.2007.
- R. J. Pruim, R. P. Welch, S. Sanna, T. M. Teslovich, P. S. Chines, T. P. Gliedt, M. Boehnke, G. R. Abecasis, and C. J. Willer. LocusZoom: regional visualization of genome-wide association scan results. *Bioinformatics*, 26:2336–2337, 2010.
doi: 10.1093/bioinformatics/btq419.
- S. M. Purcell, N. R. Wray, J. L. Stone, P. M. Visscher, M. C. O'Donovan, P. F. Sullivan, and P. Sklar. Common polygenic variation contributes to risk of schizophrenia and bipolar disorder. *Nature*, 460:748–752, 2009.
doi: 10.1038/nature08185.
- A. Pushkin, N. Abuladze, I. Lee, D. Newman, J. Hwang, and I. Kurtz. Cloning, tissue distribution, genomic organization, and functional characterization of NBC3, a new member of the sodium bicarbonate cotransporter family. *J. Biol. Chem.*, 274:16569–16575, 1999.
doi: 10.1074/jbc.274.23.16569.
- R Development Core Team. *R: A Language and Environment for Statistical Computing*, 2008.
www.r-project.org.
- T. Rankinen, A. Zuberi, Y. C. Chagnon, S. J. Weisnagel, G. Argyropoulos, B. Walts, L. Pérusse, and C. Bouchard. The human obesity gene map: the 2005 update. *Obesity*, 14:529–644, 2006.
doi: 10.1038/oby.2006.71.
- H. Rao, G. Lu, H. Kajiyama, V. Garcia-Palacios, N. Kurihara, J. Anderson, K. Patrene, D. Sheppard, H. C. Blair, J. J. Windle, S. J. Choi, and G. D. Roodman. $\alpha_9\beta_1$: a novel osteoclast integrin that regulates osteoclast formation and function. *J. Bone Miner. Res.*, 21:1657–1665, 2006.
doi: 10.1359/jbmr.060718.
- I. R. Reid, L. D. Plank, and M. C. Evans. Fat mass is an important determinant of whole body bone density in premenopausal women but not in men. *J. Clin. Endocrinol. Metab.*, 75:779–782, 1992.
doi: 10.1210/jc.75.3.779.
- J. B. Richards, F. Rivadeneira, M. Inouye, T. M. Pastinen, N. Soranzo, S. G. Wilson, T. Andrew, M. Falchi, R. Gwilliam, K. R. Ahmadi, A. M. Valdes, P. Arp, P. Whittaker, D. J. Verlaan, M. Jhamai, V. Kumanduri, M. Moorhouse, J. B. van Meurs, A. Hofman, H. A. P. Pols, D. Hart, G. Zhai, B. S. Kato, B. H. Mullin, F. Zhang, P. Deloukas, A. G. Uitterlinden, and T. D. Spector. Bone mineral density, osteoporosis, and osteoporotic fractures: a genome-wide association study. *Lancet*, 371:1505–1512, 2008.
doi: 10.1016/s0140-6736(08)60599-1.

- M. Riester, P. F. Stadler, and K. Klemm. FRANz: reconstruction of wild multi-generation pedigrees. *Bioinformatics*, 25: 2134–2139, 2009.
doi: 10.1093/bioinformatics/btp064.
- R. Riihonen, S. Nielsen, H. K. Väänänen, T. Laitala-Leinonen, and T.-H. Kwon. Degradation of hydroxyapatite *in vivo* and *in vitro* requires osteoclastic sodium-bicarbonate co-transporter NBCn1. *Matrix Biol.*, 29:287–294, 2010.
doi: 10.1016/j.matbio.2010.01.003.
- N. Risch and K. Merikangas. The future of genetic studies of complex human diseases. *Science*, 273:1516–7, 1996.
doi: 10.1126/science.273.5281.1516.
- F. Rivadeneira, U. Styrkársdóttir, K. Estrada, B. V. Halldórsson, Y.-H. Hsu, J. B. Richards, M. C. Zillikens, F. K. Kavvoura, N. Amin, Y. S. Aulchenko, L. A. Cupples, P. Deloukas, S. Demissie, E. Grundberg, A. Hofman, A. Kong, D. Karasik, J. B. van Meurs, B. Oostra, T. Pastinen, H. A. P. Pols, G. Sigurdsson, N. Soranzo, G. Thorleifsson, U. Thorsteinsdóttir, F. M. K. Williams, S. G. Wilson, Y. Zhou, S. H. Ralston, C. M. van Duijn, T. Spector, D. P. Kiel, K. Stefansson, J. P. A. Ioannidis, and A. G. Uitterlinden for the Genetic Factors for Osteoporosis (GEFOS) Consortium. Twenty bone-mineral-density loci identified by large-scale meta-analysis of genome-wide association studies. *Nat. Genet.*, 41:1199–1206, 2009.
doi: 10.1038/ng.446.
- G. D. Roodman. Regulation of osteoclast differentiation. *Ann. N. Y. Acad. Sci.*, 1068:100–109, 2006.
doi: 10.1196/annals.1346.013.
- A. S. Ryan and B. J. Nicklas. Age-related changes in fat deposition in mid-thigh muscle in women: relationships with metabolic cardiovascular disease risk factors. *Int. J. Obes. (London)*, 23:126–132, 1999.
doi: 10.1038/sj.ijo.0800777.
- P. Scheet and M. Stephens. A fast and flexible statistical model for large-scale population genotype data: applications to inferring missing genotypes and haplotypic phase. *Am. J. Hum. Genet.*, 78:629–644, 2006.
doi: 10.1086/502802.
- A. Scherag, C. Dina, A. Hinney, V. Vatin, S. Scherag, C. I. G. Vogel, T. D. Müller, H. Grallert, H.-E. Wichmann, B. Balkau, B. Heude, M.-R. Jarvelin, A.-L. Hartikainen, C. Levy-Marchal, J. Weill, J. Delplanque, A. Körner, W. Kiess, P. Kovacs, N. W. Rayner, I. Prokopenko, M. I. McCarthy, H. Schäfer, I. Jarick, H. Boeing, E. Fisher, T. Reinehr, J. Heinrich, P. Rzehak, D. Berdel, M. Borte, H. Biebermann, H. Krude, D. Rosskopf, C. Rimmbach, W. Rief, T. Fromme, M. Klingenspor, A. Schürmann, N. Schulz, M. M. Nöthen, T. W. Mühleisen, R. Erbel, K.-H. Jöckel, S. Moebus, T. Boes, T. Illig, P. Froguel, J. Hebebrand, and D. Meyre. Two new loci for body-weight regulation identified in a joint analysis of genome-wide association studies for early-onset extreme obesity in French and German study groups. *PLoS Genet.*, 6:e1000916, 2010.
doi: 10.1371/journal.pgen.1000916.
- A. Schindeler, R. Liu, and D. G. Little. The contribution of different cell lineages to bone repair: Exploring a role for muscle stem cells. *Differentiation*, 77:12–18, 2009.
doi: 10.1016/j.diff.2008.09.007.
- A. M. Schott, C. Cormier, D. Hans, F. Favier, E. Hausherr, P. Dargent-Molina, P. D. Delmas, C. Ribot, J. L. Sebert, G. Breart, and P. J. Meunier. How hip and whole-body bone mineral density predict hip fracture in elderly women: the EPIDOS Prospective Study. *Osteoporos. Int.*, 8:247–254, 1998.
- A. Scuteri, S. Sanna, W.-M. Chen, M. Uda, G. Albai, J. Strait, S. Najjar, R. Nagaraja, M. Orrú, G. Usala, M. Dei, S. Lai, A. Maschio, F. Busonero, A. Mulas, G. B. Ehret, A. A. Fink, A. B. Weder, R. S. Cooper, P. Galan, A. Chakravarti, D. Schlessinger, A. Cao, E. Lakatta, and G. R. Abecasis. Genome-wide association scan shows genetic variants in the *FTO* gene are associated with obesity-related traits. *PLoS Genet.*, 3:e115, 2007.
doi: 10.1371/journal.pgen.0030115.
- E. Seeman, J. L. Hopper, N. R. Young, C. Formica, P. Goss, and C. Tsalamandris. Do genetic factors explain associations between muscle strength, lean mass, and bone density? A twin study. *Am. J. Physiol.*, 270:E320–E327, 1996.

- J. R. Shaffer, C. M. Kammerer, D. Reich, G. McDonald, N. Patterson, B. Goodpaster, D. C. Bauer, J. Li, A. B. Newman, J. A. Cauley, T. B. Harris, F. Tyllavsky, R. E. Ferrell, J. M. Zmuda, and Health ABC Study. Genetic markers for ancestry are correlated with body composition traits in older African Americans. *Osteoporos. Int.*, 18:733–741, 2007.
doi: 10.1007/s00198-006-0316-6.
- M. S. Sheikh and A. J. Fornace. Death and decoy receptors and p53-mediated apoptosis. *Leukemia*, 14:1509–1513, 2000.
- H. Shen, J.-R. Long, D.-H. Xiong, Y.-J. Liu, Y.-Z. Liu, P. Xiao, L.-J. Zhao, V. Dvornyk, Y.-Y. Zhang, S. Rocha-Sanchez, P.-Y. Liu, J.-L. Li, and H.-W. Deng. Mapping quantitative trait loci for cross-sectional geometry at the femoral neck. *J. Bone Miner. Res.*, 20:1973–1982, 2005.
doi: dx.doi.org/10.1359/jbmr.050715.
- Y. Sheu, J. A. Cauley, V. W. Wheeler, A. L. Patrick, C. H. Bunker, C. M. Kammerer, and J. M. Zmuda. Natural history and correlates of hip BMD loss with aging in men of African ancestry: the Tobago Bone Health Study. *J. Bone Miner. Res.*, 24:1290–8, 2009.
doi: 10.1359/jbmr.090221.
- J. Shin, Y.-M. Kim, S.-Z. Li, S.-K. Lim, and W. Lee. Structure-function of the TNF receptor-like cysteine-rich domain of osteoprotegerin. *Mol. Cells*, 25:352–257, 2008.
- E. M. Shore, M. Xu, G. J. Feldman, D. A. Fenstermacher, T.-J. Cho, I. H. Choi, J. M. Connor, P. Delai, D. L. Glaser, M. LeMerrer, R. Morhart, J. G. Rogers, R. Smith, J. T. Triffitt, J. A. Urtizberea, M. Zasloff, M. A. Brown, and F. S. Kaplan. A recurrent mutation in the BMP type I receptor ACVR1 causes inherited and sporadic fibrodysplasia ossificans progressiva. *Nat. Genet.*, 38:525–527, 2006.
doi: doi:10.1038/ng1783.
- W. S. Simonet, D. L. Lacey, C. R. Dunstan, M. Kelley, M. S. Chang, R. Lüthy, H. Q. Nguyen, S. Wooden, L. Bennett, T. Boone, G. Shimamoto, M. DeRose, R. Elliott, A. Colombero, H. L. Tan, G. Trail, J. Sullivan, E. Davy, N. Bucay, L. Renshaw-Gegg, T. M. Hughes, D. Hill, W. Pattison, P. Campbell, S. Sander, G. Van, J. Tarpley, P. Derby, R. Lee, and W. J. Boyle. Osteoprotegerin: a novel secreted protein involved in the regulation of bone density. *Cell*, 89:309–319, 1997.
- T. Sørensen. A method of establishing groups of equal amplitude in plant sociology based on similarity of species and its application to analyses of the vegetation on Danish commons. *Biol. Skr.*, 5:1–34, 1948.

E. K. Speliotes, C. J. Willer, S. I. Berndt, K. L. Monda, G. Thorleifsson, A. U. Jackson, H. L. Allen, C. M. Lindgren, J. Luan, R. Mägi, J. C. Randall, S. Vedantam, T. W. Winkler, L. Qi, T. Workalemahu, I. M. Heid, V. Steinthorsdottir, H. M. Stringham, M. N. Weedon, E. Wheeler, A. R. Wood, T. Ferreira, R. J. Weyant, A. V. Segrè, K. Estrada, L. Liang, J. Nemes, J.-H. Park, S. Gustafsson, T. O. Kilpeläinen, J. Yang, N. Bouatia-Naji, T. Esko, M. F. Feitosa, Z. Kutalik, M. Mangino, S. Raychaudhuri, A. Scherag, A. V. Smith, R. Welch, J. H. Zhao, K. K. Aben, D. M. Absher, N. Amin, A. L. Dixon, E. Fisher, N. L. Glazer, M. E. Goddard, N. L. Heard-Costa, V. Hoesel, J.-J. Hottenga, A. Johansson, T. Johnson, S. Ketkar, C. Lamina, S. Li, M. F. Moffatt, R. H. Myers, N. Narisu, J. R. B. Perry, M. J. Peters, M. Preuss, S. Ripatti, F. Rivadeneira, C. Sandholt, L. J. Scott, N. J. Timpson, J. P. Tyrer, S. van Wingerden, R. M. Watanabe, C. C. White, F. Wiklund, C. Barlassina, D. I. Chasman, M. N. Cooper, J.-O. Jansson, R. W. Lawrence, N. Pellikka, I. Prokopenko, J. Shi, E. Thiering, H. Alavere, M. T. S. Alibrandi, P. Almgren, A. M. Arnold, T. Aspelund, L. D. Atwood, B. Balkau, A. J. Balmforth, A. J. Bennett, Y. Ben-Shlomo, R. N. Bergman, S. Bergmann, H. Biebermann, A. I. F. Blakemore, T. Boes, L. L. Bonnycastle, S. R. Bornstein, M. J. Brown, T. A. Buchanan, F. Busonero, H. Campbell, F. P. Cappuccio, C. Cavalcanti-Proença, Y.-D. I. Chen, C.-M. Chen, P. S. Chines, R. Clarke, L. Coin, J. Connell, I. N. M. Day, M. d. Heijer, J. Duan, S. Ebrahim, P. Elliott, R. Elosua, G. Eiriksdottir, M. R. Erdos, J. G. Eriksson, M. F. Facheris, S. B. Felix, P. Fischer-Posovszky, A. R. Folsom, N. Friedrich, N. B. Freimer, M. Fu, S. Gaget, P. V. Gejman, E. J. C. Geus, C. Gieger, A. P. Gjesing, A. Goel, P. Goyette, H. Grallert, J. Grässler, D. M. Greenawalt, C. J. Groves, V. Gudnason, C. Guiducci, A.-L. Hartikainen, N. Hassanali, A. S. Hall, A. S. Havulinna, C. Hayward, A. C. Heath, C. Hengstenberg, A. A. Hicks, A. Hinney, A. Hofman, G. Homuth, J. Hui, W. Igl, C. Iribarren, B. Isomaa, K. B. Jacobs, I. Jarick, E. Jewell, U. John, T. Jorgensen, P. Jousilahti, A. Jula, M. Kaakinen, E. Kajantie, L. M. Kaplan, S. Kathiresan, J. Kettunen, L. Kinnunen, J. W. Knowles, I. Kolcic, I. R. König, S. Koskinen, P. Kovacs, J. Kuusisto, P. Kraft, K. Kvaløy, J. Laitinen, O. Lantieri, C. Lanzani, L. J. Launer, C. Lecoeur, T. Lehtimäki, G. Lettre, J. Liu, M.-L. Lokki, M. Lorentzon, R. N. Luben, B. Ludwig, MAGIC, P. Manunta, D. Marek, M. Marre, N. G. Martin, W. L. McArdle, A. McCarthy, B. McKnight, T. Meitinger, O. Melander, D. Meyre, K. Midthjell, G. W. Montgomery, M. A. Morken, A. P. Morris, R. Mulic, J. S. Ngwa, M. Nelis, M. J. Neville, D. R. Nyholt, C. J. O'Donnell, S. O'Rahilly, K. K. Ong, B. Oostra, G. Paré, A. N. Parker, M. Perola, I. Pichler, K. H. Pietiläinen, C. G. P. Platou, O. Polašek, A. Pouta, S. Rafelt, O. Raitakari, N. W. Rayner, M. Ridderstrale, W. Rief, A. Ruukonen, and N. Robertson. Association analyses of 249,796 individuals reveal 18 new loci associated with body mass index. *Nat. Genet.*, 42:937–948, 2010.

doi: 10.1038/ng.686.

U. Styrkarsdottir, J.-B. Cazier, A. Kong, O. Rolfsson, H. Larsen, E. Bjarnadottir, V. D. Johannsdottir, M. S. Sigurdardottir, Y. Bagger, C. Christiansen, I. Reynisdottir, S. F. A. Grant, K. Jonasson, M. L. Frigge, J. R. Gulcher, G. Sigurdsson, and K. Stefansson. Linkage of osteoporosis to chromosome 20p12 and association to *BMP2*. *PLoS Biol.*, 1:351–360, 2003.

doi: 10.1371/journal.pbio.0000069.

U. Styrkarsdottir, B. V. Halldorsson, S. Gretarsdottir, D. F. Gudbjartsson, G. B. Walters, T. Ingvarsson, T. Jonsdottir, J. Saemundsdottir, J. R. Center, T. V. Nguyen, Y. Bagger, J. R. Gulcher, J. A. Eisman, C. Christiansen, G. Sigurdsson, A. Kong, U. Thorsteinsdottir, and K. Stefansson. Multiple genetic loci for bone mineral density and fractures. *N. Engl. J. Med.*, 358:2355–2365, 2008.

doi: 10.1056/nejmoa0801197.

U. Styrkarsdottir, B. V. Halldorsson, S. Gretarsdottir, D. F. Gudbjartsson, G. B. Walters, T. Ingvarsson, T. Jonsdottir, J. Saemundsdottir, S. Snorraddottir, J. R. Center, T. V. Nguyen, P. Alexandersen, J. R. Gulcher, J. A. Eisman, C. Christiansen, G. Sigurdsson, A. Kong, U. Thorsteinsdottir, and K. Stefansson. New sequence variants associated with bone mineral density. *Nat. Genet.*, 41:15–17, 2009.

doi: 10.1038/ng.284.

X. Sun, S.-F. Lei, F.-Y. Deng, S. Wu, C. Papacian, J. Hamilton, R. R. Recker, and H.-W. Deng. Genetic and environmental correlations between bone geometric parameters and body compositions. *Calcif. Tissue Int.*, 79:43–49, 2006.

doi: 10.1007/s00223-006-0041-3.

M. E. Tabangin, J. G. Woo, and L. J. Martin. The effect of minor allele frequency on the likelihood of obtaining false positives. *BMC Proc.*, 3:S41, 2009.

doi: 10.1186/1753-6561-3-s7-S41.

- M. Tahara, A. Aiba, M. Yamazaki, Y. Ikeda, S. Goto, H. Moriya, and A. Okawa. The extent of ossification of posterior longitudinal ligament of the spine associated with nucleotide pyrophosphatase gene and leptin receptor gene polymorphisms. *Spine*, 30:877–80, 2005.
- K. Takaya, Y. Ogawa, N. Isse, T. Okazaki, N. Satoh, H. Masuzaki, K. Mori, N. Tamura, K. Hosoda, and K. Nakao. Molecular cloning of rat leptin receptor isoform complementary DNAs—identification of a missense mutation in Zucker fatty (*fafa*) rats. *Biochem. Biophys. Res. Commun.*, 225:75–83, 1996.
doi: 10.1006/bbrc.1996.1133.
- P.-N. Tan, M. Steinbach, and V. Kumar. *Introduction to Data Mining*. Addison–Wesley, Boston, 2005.
- Z. H. Tang, P. Xiao, S. F. Lei, F. Y. Deng, L. J. Zhao, H. Y. Deng, L. J. Tan, H. Shen, D. H. Xiong, R. R. Recker, and H. W. Deng. A bivariate whole-genome linkage scan suggests several shared genomic regions for obesity and osteoporosis. *J. Clin. Endocrinol. Metab.*, 92:2751–2757, 2007.
doi: 10.1210/jc.2006-2607.
- M. Tenne, F. McGuigan, L. Jansson, P. Gerdhem, K. J. Obrant, H. Luthman, and K. Åkesson. Genetic variation in the PTH pathway and bone phenotypes in elderly women: Evaluation of *PTH*, *PTH1LH*, *PTHR1* and *PTHR2* genes. *Bone*, 42:719–727, 2008.
doi: 10.1016/j.bone.2007.12.005.
- M. Tenne, F. E. McGuigan, H. Ahlberg, P. Gerdhem, and K. Åkesson. Variation in the *PTH* gene, hip fracture, and femoral neck geometry in elderly women. *Calcif. Tissue Int.*, 86:359–366, 2010.
doi: 10.1007/s00223-010-9351-6.
- N. J. Timpson, C. M. Lindgren, M. N. Weedon, J. Randall, W. H. Ouwehand, D. P. Strachan, N. W. Rayner, M. Walker, G. A. Hitman, A. S. F. Doney, C. N. A. Palmer, A. D. Morris, A. T. Hattersley, E. Zeggini, T. M. Frayling, and M. I. McCarthy. Adiposity-related heterogeneity in patterns of type 2 diabetes susceptibility observed in genome-wide association data. *Diabetes*, 58:505–510, 2008.
doi: 10.2337/db08-0906.
- N. J. Timpson, J. H. Tobias, J. B. Richards, N. Soranzo, E. L. Duncan, A.-M. Sims, P. Whittaker, V. Kumanduri, G. Zhai, B. Glaser, J. Eisman, G. Jones, G. Nicholson, R. Prince, E. Seeman, T. D. Spector, M. A. Brown, L. Peltonen, G. Davey Smith, P. Deloukas, and D. M. Evans. Common variants in the region around *Osterix* are associated with bone mineral density and growth in childhood. *Hum. Mol. Genet.*, 18:1510–1517, 2009.
doi: 10.1093/hmg/ddp052.
- T. Thomas and B. Burguera. Is leptin the link between fat and bone mass? *J. Bone Miner. Res.*, 17:1563–1569, 2002.
doi: 10.1359/jbmr.2002.17.9.1563.
- G. Thorleifsson, G. B. Walters, D. F. Gudbjartsson, V. Steinthorsdottir, P. Sulem, A. Helgadóttir, U. Styrkarsdóttir, S. Gretarsdóttir, S. Thorlacius, I. Jonsdóttir, T. Jonsdóttir, E. J. Olafsdóttir, G. H. Olafsdóttir, T. Jonsson, F. Jonsson, K. Borch-Johnsen, T. Hansen, G. Andersen, T. Jorgensen, T. Lauritzen, K. K. Aben, A. L. Verbeek, N. Roeleveld, E. Kampman, L. R. Yanek, L. C. Becker, L. Tryggvadóttir, T. Rafnar, D. M. Becker, J. Gulcher, L. A. Kiemeny, O. Pedersen, A. Kong, U. Thorsteinsdóttir, and K. Stefansson. Genome-wide association yields new sequence variants at seven loci that associate with measures of obesity. *Nat. Genet.*, 41:18–24, 2008.
doi: 10.1038/ng.274.
- C. Thouverey, A. Malinowska, M. Balcerzak, A. Strzelecka-Kiliszek, R. Buchet, M. Dadlez, and S. Pikula. Proteomic characterization of biogenesis and functions of matrix vesicles released from mineralizing human osteoblast-like cells. *J. Proteomics*, 74:1123–1134, 2011.
doi: 10.1016/j.jprot.2011.04.005.

A. Torkamani and N. J. Schork. *Methods in Molecular Biology*, volume 563 of *Methods in Molecular Biology*. Humana Press, Totowa, NJ, 2009.

doi: 10.1007/978-1-60761-175-2_16.

R. C. Tryon. *Cluster Analysis*. McGraw-Hill, New York, 1939.

J. Y. Tung, C. B. Do, D. A. Hinds, A. K. Kiefer, J. M. Macpherson, A. B. Chowdry, U. Francke, B. T. Naughton, J. L. Mountain, A. Wojcicki, and N. Eriksson. Efficient replication of over 180 genetic associations with self-reported medical data. *Nat. Precedings*, preprint, 2011.

hdl: 10101/npre.2011.6014.2.

R. T. Turner, B. L. Riggs, and T. C. Spelsberg. Skeletal effects of estrogen. *Endocr. Rev.*, 15:275–300, 1994.

doi: 10.1210/edrv-15-3-275.

A. G. Uitterlinden, S. H. Ralston, M. L. Brandi, A. H. Carey, D. Grinberg, B. L. Langdahl, P. Lips, R. Lorenc, B. Obermayer-Pietsch, J. Reeve, D. M. Reid, A. Amedei, A. Amidei, A. Bassiti, M. Bustamante, L. B. Husted, A. Diez-Perez, H. Dobnig, A. M. Dunning, A. Enjuanes, A. Fahrleitner-Pammer, Y. Fang, E. Karczmarewicz, M. Kruk, J. P. T. M. van Leeuwen, C. Mavilia, J. B. J. van Meurs, J. Mangion, F. E. A. McGuigan, H. A. P. Pols, W. Renner, F. Rivadeneira, N. M. van Schoor, S. Scollen, R. E. Sherlock, and J. P. A. Ioannidis. The association between common vitamin D receptor gene variations and osteoporosis: a participant-level meta-analysis. *Ann. Intern. Med.*, 145:255–264, 2006.

S. E. Utvåg, K. B. Iversen, O. Grundnes, and O. Reikerås. Poor muscle coverage delays fracture healing in rats. *Acta Orthop. Scand.*, 73:471–474, 2002.

doi: 10.1080/00016470216315.

A. J. van der Slot, A.-M. Zuurmond, A. F. J. Bardoel, C. Wijmenga, H. E. H. Pruijs, D. O. Sillence, J. Brinckman, D. J. Abraham, C. M. Black, N. Verzijl, J. DeGroot, R. Hanemaaijer, J. M. TeKoppele, T. W. J. Huizinga, and R. A. Bank. Identification of *PLOD2* as telopeptide lysyl hydroxylase, an important enzyme in fibrosis. *J. Biol. Chem.*, 278:40967–40972, 2003.

doi: 10.1074/jbc.m307380200.

T. P. van Staa, E. M. Dennison, H. G. M. Leufkens, and C. Cooper. Epidemiology of fractures in England and Wales. *Bone*, 29:517–522, 2001.

doi: 10.1016/s8765-3282(01)00614-7.

T. Videman, E. Levälähti, M. C. Battié, R. Simonen, E. Vanninen, and J. Kaprio. Heritability of BMD of femoral neck and lumbar spine: A multivariate twin study of Finnish men. *J. Bone Miner. Res.*, 22:1455–1462, 2007. doi: 10.1359/jbmr.070606.

M. Visser, T. B. Harris, J. Langlois, M. T. Hannan, R. Roubenoff, D. T. Felson, P. W. Wilson, and D. P. Kiel. Body fat and skeletal muscle mass in relation to physical disability in very old men and women of the Framingham Heart Study. *J. Gerontol. A Biol. Sci. Med. Sci.*, 53:M214–M221, 1998a.

M. Visser, D. P. Kiel, J. Langlois, M. T. Hannan, D. T. Felson, P. W. Wilson, and T. B. Harris. Muscle mass and fat mass in relation to bone mineral density in very old men and women: the Framingham Heart Study. *Appl. Radiat. Isot.*, 49: 745–747, 1998b.

doi: 10.1016/s0969-8043(97)00101-2.

M. Visser, S. B. Kritchevsky, B. H. Goodpaster, A. B. Newman, M. Nevitt, E. Stamm, and T. B. Harris. Leg muscle mass and composition in relation to lower extremity performance in men and women aged 70 to 79: the Health, Aging and Body Composition Study. *J. Am. Geriatr. Soc.*, 50:897–904, 2002.

H. Vorum, T. H. Kwon, C. Fulton, B. Simonsen, I. Choi, W. Boron, A. B. Maunsbach, S. Nielsen, and C. Aalkjær. Immunolocalization of electroneutral Na–HCO₃ cotransporter in rat kidney. *Am. J. Physiol. Renal Physiol.*, 279:F901–F909, 2000.

E. S. Wan, M. H. Cho, N. Boutaoui, B. J. Klanderma, J. S. Sylvia, J. P. Ziniti, S. Won, C. Lange, S. G. Pillai, W. H. Anderson, X. Kong, D. A. Lomas, P. S. Bakke, A. Gulsvik, E. A. Regan, J. R. Murphy, B. J. Make, J. D. Crapo, E. F. Wouters, B. R. Celli, E. K. Silverman, and D. L. Demeo. Genome-wide association analysis of body mass in chronic obstructive pulmonary disease. *Am. J. Respir. Cell Mol. Biol.*, in press, 2010.
doi: 10.1165/rcmb.2010-0294oc.

K. Wang, M. Li, and M. Bucan. Pathway-based approaches for analysis of genomewide association studies. *Am. J. Hum. Genet.*, 81:1278–1283, 2007a.
doi: 10.1086/522374.

K. Wang, W.-D. Li, C. K. Zhang, Z. Wang, J. T. Glessner, S. F. A. Grant, H. Zhao, H. Hakonarson, and R. A. Price. A genome-wide association study on obesity and obesity-related traits. *PLoS ONE*, 6:e18939, 2011.
doi: 10.1371/journal.pone.0018939.

X. Wang, C. M. Kammerer, V. W. Wheeler, A. L. Patrick, C. H. Bunker, and J. M. Zmuda. Genetic and environmental determinants of volumetric and areal BMD in multi-generational families of African ancestry: the Tobago Family Health Study. *J. Bone Miner. Res.*, 22:527–36, 2007b.
doi: 10.1359/jbmr.070106.

X. Wang, C. M. Kammerer, V. W. Wheeler, A. L. Patrick, C. H. Bunker, and J. M. Zmuda. Pleiotropy and heterogeneity in the expression of bone strength-related phenotypes in extended pedigrees. *J. Bone Miner. Res.*, 22:1766–1772, 2007c.
doi: 10.1359/jbmr.070718.

X.-L. Wang, F.-Y. Deng, L.-J. Tan, H.-Y. Deng, Y.-Z. Liu, C. J. Papasian, R. R. Recker, and H.-W. Deng. Bivariate whole genome linkage analyses for total body lean mass and BMD. *J. Bone Miner. Res.*, 23:447–452, 2007d. doi: 10.1359/jbmr.071033.

F. W. Wehrli, J. A. Hopkins, S. N. Hwang, H. K. Song, P. J. Snyder, and J. G. Haddad. Cross-sectional study of osteopenia with quantitative MR imaging and bone densitometry. *Radiology*, 217:527–538, 2000.

C. J. Willer, E. K. Speliotes, R. J. F. Loos, S. Li, C. M. Lindgren, I. M. Heid, S. I. Berndt, A. L. Elliott, A. U. Jackson, C. Lamina, G. Lettre, N. Lim, H. N. Lyon, S. A. McCarroll, K. Papadakis, L. Qi, J. C. Randall, R. M. Roccasecca, S. Sanna, P. Scheet, M. N. Weedon, E. Wheeler, J. H. Zhao, L. C. Jacobs, I. Prokopenko, N. Soranzo, T. Tanaka, N. J. Timpson, P. Almgren, A. Bennett, R. N. Bergman, S. A. Bingham, L. L. Bonnycastle, M. Brown, N. P. Burtt, P. Chines, L. Coin, F. S. Collins, J. M. Connell, C. Cooper, G. Davey Smith, E. M. Dennison, P. Deodhar, P. Elliott, M. R. Erdos, K. Estrada, D. M. Evans, L. Gianniny, C. Gieger, C. J. Gillson, C. Guiducci, R. Hackett, D. Hadley, A. S. Hall, A. S. Havulinna, J. Hebebrand, A. Hofman, B. Isomaa, K. B. Jacobs, T. Johnson, P. Jousilahti, Z. Jovanovic, K. T. Khaw, P. Kraft, M. Kuokkanen, J. Kuusisto, J. Laitinen, E. G. Lakatta, J. Luan, R. N. Luben, M. Mangino, W. L. McArdle, T. Meitinger, A. Mulas, P. B. Munroe, N. Narisu, A. R. Ness, K. Northstone, S. O’Rahilly, C. Purmann, M. G. Rees, M. Ridderstråle, S. M. Ring, F. Rivadeneira, A. Ruokonen, M. S. Sandhu, J. Saramies, L. J. Scott, A. Scuteri, K. Silander, M. A. Sims, K. Song, J. Stephens, S. Stevens, H. M. Stringham, Y. C. L. Tung, T. T. Valle, C. M. van Duijn, K. S. Vimalaswaran, P. Vollenweider, G. Waeber, C. Wallace, R. M. Watanabe, D. M. Waterworth, N. Watkins, J. C. M. Witteman, E. Zeggini, G. Zhai, M. C. Zillikens, D. Altshuler, M. J. Caulfield, S. J. Chanock, I. S. Farooqi, L. Ferrucci, J. M. Guralnik, A. T. Hattersley, F. B. Hu, M.-R. Jarvelin, M. Laakso, V. Mooser, K. K. Ong, W. H. Ouwehand, V. Salomaa, N. J. Samani, T. D. Spector, T. Tuomi, J. Tuomilehto, M. Uda, A. G. Uitterlinden, N. J. Wareham, P. Deloukas, T. M. Frayling, L. C. Groop, R. B. Hayes, D. J. Hunter, K. L. Mohlke, L. Peltonen, D. Schlessinger, D. P. Strachan, H.-E. Wichmann, M. I. McCarthy, M. Boehnke, I. Barroso, G. R. Abecasis, and J. N. Hirschhorn. Six new loci associated with body mass index highlight a neuronal influence on body weight regulation. *Nat. Genet.*, 41:25–34, 2008.
doi: 10.1038/ng.287.

World Health Organization. Assessment of fracture risk and its application to screening for postmenopausal osteoporosis. Technical Report Series No. 843, WHO, Geneva, Switzerland, 1994.

- J. M. Wozney, V. Rosen, A. J. Celeste, L. M. Mitsock, M. J. Whitters, R. W. Kriz, R. M. Hewick, and E. A. Wang. Novel regulators of bone formation: molecular clones and activities. *Science*, 242:1528–1534, 1988.
doi: 10.1126/science.3201241.
- D.-H. Xiong, F.-H. Xu, P.-Y. Liu, H. Shen, J.-R. Long, L. Elze, R. R. Recker, and H.-W. Deng. Vitamin D receptor gene polymorphisms are linked to and associated with adult height. *J. Med. Genet.*, 42:228–234, 2005.
- D.-H. Xiong, H. Shen, P. Xiao, Y.-F. Guo, J.-R. Long, L.-J. Zhao, Y.-Z. Liu, H.-Y. Deng, J.-L. Li, R. R. Recker, and H.-W. Deng. Genome-wide scan identified QTLs underlying femoral neck cross-sectional geometry that are novel studied risk factors of osteoporosis. *J. Bone Miner. Res.*, 21:424–437, 2006.
doi: 10.1359/jbmr.051202.
- D.-H. Xiong, X.-G. Liu, Y.-F. Guo, L.-J. Tan, L. Wang, B.-Y. Sha, Z.-H. Tang, F. Pan, T.-L. Yang, X.-D. Chen, S.-F. Lei, L. M. Yerges, X.-Z. Zhu, V. W. Wheeler, A. L. Patrick, C. H. Bunker, Y. Guo, H. Yan, Y.-F. Pei, Y.-P. Zhang, S. Levy, C. J. Papasian, P. Xiao, Y. W. Lundberg, R. R. Recker, Y.-Z. Liu, Y.-J. Liu, J. M. Zmuda, and H.-W. Deng. Genome-wide association and follow-up replication studies identified *ADAMTS18* and *TGFBR3* as bone mass candidate genes in different ethnic groups. *Am. J. Hum. Genet.*, 84:388–398, 2009.
doi: 10.1016/j.ajhg.2009.01.025.
- L. M. Yerges, L. Klei, J. A. Cauley, K. Roeder, C. M. Kammerer, S. P. Moffett, K. E. Ensrud, C. S. Nestlerode, L. M. Marshall, A. R. Hoffman, C. Lewis, T. F. Lang, E. Barrett-Connor, R. E. Ferrell, E. S. Orwoll, and J. M. Zmuda. High-density association study of 383 candidate genes for volumetric BMD at the femoral neck and lumbar spine among older men. *J. Bone Miner. Res.*, 24:2039–2049, 2009.
doi: 10.1359/jbmr.090524.
- H. Yoshida, S.-I. Hayashi, T. Kunisada, M. Ogawa, S. Nishikawa, H. Okamura, T. Sudo, L. D. Shultz, and S.-I. Nishikawa. The murine mutation osteopetrosis is in the coding region of the macrophage colony stimulating factor gene. *Nature*, 345:442–444, 1990.
doi: 10.1038/345442a0.
- W. Yu, M. Gwinn, M. Clyne, A. Yesupriya, and M. J. Khoury. A navigator for human genome epidemiology. *Nat. Genet.*, 40:124–125, 2008.
doi: 10.1038/ng0208-124.
- Q. Zhang, R. Guo, Y. Lu, L. Zhao, Q. Zhou, E. M. Schwarz, J. Huang, D. Chen, Z.-G. Jin, B. F. Boyce, and L. Xing. VEGF-C, a lymphatic growth factor, is a RANKL target gene in osteoclasts that enhances osteoclastic bone resorption through an autocrine mechanism. *J. Biol. Chem.*, 283:13491–13499, 2008.
doi: 10.1074/jbc.m708055200.
- Y.-Y. Zhang, P.-Y. Liu, Y. Lu, P. Xiao, Y.-J. Liu, J.-R. Long, H. Shen, L.-J. Zhao, L. Elze, R. R. Recker, and H.-W. Deng. Tests of linkage and association of *PTH/PTHrP* receptor type 1 gene with bone mineral density and height in Caucasians. *J. Bone Miner. Metab.*, 24:36–41, 2005.
doi: 10.1007/s00774-005-0643-2.
- J. Zhao, P. Xiao, Y. Guo, Y.-J. Liu, Y.-F. Pei, T.-L. Yang, F. Pan, Y. Chen, H. Shen, L.-J. Zhao, C. J. Papasian, B. M. Drees, J. J. Hamilton, H.-Y. Deng, R. R. Recker, and H.-W. Deng. Bivariate genome linkage analysis suggests pleiotropic effects on chromosomes 20p and 3p for body fat mass and lean mass. *Genet. Res.*, 90:259–268, 2008.
doi: 10.1017/s0016672308009257.
- J. M. Zmuda, L. M. Yerges-Armstrong, S. P. Moffett, L. Klei, C. M. Kammerer, K. Roeder, J. A. Cauley, A. Kuipers, K. E. Ensrud, C. S. Nestlerode, A. R. Hoffman, C. E. Lewis, T. F. Lang, E. Barrett-Connor, R. E. Ferrell, and E. S. Orwoll for the Osteoporotic Fractures in Men (MrOS) Study Group. Genetic analysis of vertebral trabecular bone density and cross-sectional area in older men. *Osteoporos. Int.*, 22:1079–1090, 2010.
doi: 10.1007/s00198-010-1296-0.